

STRUCTURE MODIFICATION TO ENHANCE PULSE PROTEIN FUNCTIONALITIES
AND FLAVOR PROFILE: OPPORTUNITIES IN SACCHARIDE MEDIATED
GLYCATION VIA MAILLARD-DRIVEN CHEMISTRY

A Dissertation
Submitted to the Graduate Faculty
of the
North Dakota State University
of Agriculture and Applied Science

By

Fengchao Zha

In Partial Fulfillment of the Requirements
for the Degree of
DOCTOR OF PHILOSOPHY

Major Program:
Cereal Science

July 2020

Fargo, North Dakota

North Dakota State University
Graduate School

Title

STRUCTURE MODIFICATION TO ENHANCE PULSE PROTEIN
FUNCTIONS AND FLAVOR PROFILE: OPPORTUNITIES IN
SACCHARIDE MEDIATED GLYCATION VIA MAILLARD-
DRIVEN CHEMISTRY

By

Fengchao Zha

The Supervisory Committee certifies that this *disquisition* complies with North Dakota
State University's regulations and meets the accepted standards for the degree of

DOCTOR OF PHILOSOPHY

SUPERVISORY COMMITTEE:

Dr. Bingcan Chen

Chair

Dr. Frank Manthey

Dr. Clifford Hall

Dr. Zhongyu Yang

Approved:

7/11/2020

Date

Dr. Richard D. Horsley

Department Chair

ABSTRACT

Owing to the combined characteristics of low allergens and lipids, as well as high versatility and abundance, eco-friendly pulse-based protein has served as a critical contender to supplement animal protein. The inferior solubility and off-flavor, however, place a practical restriction on its application. Glycation via Maillard-driven reaction is a potential green chemistry to modulate protein structure and functions. The various types of protein, saccharides with different molecular mass and structural characteristics, and two reaction systems (dry and wet heating) were applied to synthesize protein-saccharides conjugates. The aims were to investigate (i) the effect of glycation on functionalities and flavor of pulse-based protein using above-mentioned elements, and (ii) mechanisms by which glycation affects the protein architectures and modulates its functionalities. SDS-PAGE, SEM and FTIR-ATR were applied to confirm the successful development of protein-saccharide conjugates. The extent of glycation was time-dependent, and 11S and 7S globulin were mainly responsible for conjugation with gum Arabic (GA) under dry heating conditions (60°C, 79% relative humidity, pH 7.0). Glycation significantly improved protein solubility at neutral pH, whereas such effect varied depending on the protein source and reaction time. The stability of emulsion against environment stress and lipid oxidation gained a significant improvement, which was attributed to electrostatic interactions and stronger steric hindrance of protein-GA conjugates. HS-SPME-GC-MS analysis indicated glycation is a promising approach to mitigate the beany flavor, presumably because of the alterations in protein structure resulting in release of unpleasant odorants. The solubility of pea protein was sufficiently improved after glycation, while its thermal stability was remarkably lowered under wet heating conditions (80°C, pH 10.0). The proposed principle involved glycation via Maillard-driven chemistry enhanced the surface hydrophilicity of protein and unfolded its spatial architectures.

ACKNOWLEDGMENTS

I would like to acknowledge numerous people for their assistance and support during my doctoral program. My deep gratitude goes first to my advisor, Dr. Bingcan Chen for furnishing the invaluable opportunity and his expert guidance and patience. His unwavering enthusiasm for scientific research kept me constantly engaged with my study, and his personal generosity helped make my time at the research group enjoyable. I am also grateful to my other graduate committee members: Dr. Frank Manthey, Dr. Clifford Hall, and Dr. Zhongyu Yang, and deeply appreciate their continuous assistance and guidance.

My appreciation also extends to my laboratory colleagues: Allen Peckrul, Minwei Xu, Jing Wan, and Yang Lan for their kind assistance through the whole experiments; Thanks also go to Dr. Richard Horsley, Dr. Paul Schwarz, Dr. Senay Simsek, and Dr. Anuradha Vegi, for their invaluable academical enlightenment and instruction; Dr. Jiajia Rao and Dr. Jae Ohm for their kind support to the utilization of instruments in their laboratories; all Cereal Science Faculty and other faculties for teaching invaluable courses and knowledge that help me overcome many difficulties on the way to success. I really appreciate the China Scholarship Council (CSC) for funding to support my life.

I would like to express my sincere gratitude to my family for their endless love and support though we are far apart; to my friends the couple of Yuxiang Yuan and Xiaoyan Zhu, the couple of Minwei Xu and Zhao Jin, Dianhui Wu, Jing Wan, Zixuan Gu, Serap Vatansever and all other friends, for giving me words of encouragement; to my roommates Yang Lan and Chang Liu for their kind support and attention; to my soccer-playing buddies for helping me survive all the stress and making my life enjoyable; to myself for the persistence of a dream at many sleepless nights. It is not that I stay up late, but that the night needs my bright star. If memory is a square city, then, I would like to paint the earth as a prison and trap myself in it.

DEDICATION

This work is wholeheartedly dedicated to my advisor and my family:

To my advisor, Bingcan Chen, without your fruitful guidance and supervision, the work
would not be accomplished.

To my beloved parents, elder brother and sister, whose affection, love, and spiritual
encouragement make me able to get such achievements and honors

TABLE OF CONTENTS

ABSTRACT.....	iii
ACKNOWLEDGEMENTS.....	iv
DEDICATION.....	v
LIST OF TABLES.....	xi
LIST OF FIGURES.....	xii
1. GENERAL INTRODUCTION.....	1
1.1. Introduction.....	1
1.2. Objectives and Hypotheses.....	4
1.3. References.....	5
2. LITERATURE REVIEW.....	11
2.1. Pulse Protein Structure 1°–4° and Classification of Storage Proteins.....	11
2.1.1. 2S albumin storage proteins.....	11
2.1.2. 7S and 11S globulin storage proteins.....	13
2.2. Chemical Modification of Proteins.....	15
2.2.1. Acylation.....	17
2.2.2. Phosphorylation.....	20
2.2.3. Amidation and esterification.....	23
2.3. Non-enzymatic Glycation.....	25
2.3.1. Structure modification of protein by non-enzymatic glycation.....	25
2.3.2. Maillard-flavor formation.....	30
2.4. References.....	34
3. PEA PROTEIN ISOLATE-GUM ARABIC MAILLARD CONJUGATES IMPROVES PHYSICAL AND OXIDATIVE STABILITY OF OIL-IN-WATER EMULSIONS.....	50
3.1. Abstract.....	50
3.2. Introduction.....	50
3.3. Materials and Methods.....	52

3.3.1. Materials	52
3.3.2. Preparation of PPI-GA conjugates.....	53
3.3.3. Amadori compounds and melanoidins formation.....	53
3.3.4. Measurement of free amino groups	53
3.3.5. Color development.....	54
3.3.6. Sodium dodecyl sulphate-polyacrylamide gel electrophoresis (SDS-PAGE).....	54
3.3.7. Relative solubility of PPI-GA conjugates.....	55
3.3.8. Scanning electron microscopy	55
3.3.9. Preparation of corn oil-in-water emulsions with PPI-GA conjugates	55
3.3.10. Particle size & zeta potential measurement	56
3.3.11. Physical stability of emulsions against environment stresses.....	56
3.3.12. Lipid oxidation kinetics of emulsions.....	57
3.3.13. Statistical analysis.....	57
3.4. Results and Discussion.....	58
3.4.1. Impact of incubation time on chemical properties of PPI-GA conjugates	58
3.4.1.1. SDS-PAGE profile of PPI and PPI-GA conjugates	58
3.4.1.2. Non-specific markers and free amino groups in PPI-GA conjugates	59
3.4.1.3. Changes of browning index	61
3.4.2. Impact of incubation time on the solubility of PPI-GA conjugates.....	62
3.4.3. Impact of incubation time on the emulsifying property of PPI-GA conjugates ...	64
3.4.4. Physical stability of oil-in-water emulsions stabilized by PPI-GA conjugates	65
3.4.4.1. Influence of pH on physical stability of emulsions.....	66
3.4.4.2. Influence of thermal processing on physical stability of emulsions	68
3.4.4.3. Influence of ionic strength on physical stability of emulsions.....	69
3.4.5. Oxidative stability of oil-in-water emulsions stabilized by PPI-GA conjugates ..	71
3.5. Conclusion.....	72
3.6. References	73

4. THE STRUCTURAL MODIFICATION OF PEA PROTEIN CONCENTRATE WITH GUM ARABIC BY CONTROLLED MAILLARD REACTION ENHANCES ITS FUNCTIONAL PROPERTIES AND FLAVOR ATTRIBUTES	79
4.1. Abstract	79
4.2. Introduction	80
4.3. Materials and Methods	82
4.3.1. Materials	82
4.3.2. Preparation of PPC-GA conjugates	82
4.3.3. Amadori compounds and melanoidins formation.....	82
4.3.4. Free amino groups	83
4.3.5. Color development.....	83
4.3.6. Sodium dodecyl sulphate-polyacrylamide gel electrophoresis (SDS-PAGE).....	83
4.3.7. Fourier transform infrared spectroscopy-attenuated total reflection	83
4.3.8. Scanning electron microscopy	83
4.3.9. Relative solubility of PPC-GA conjugates	83
4.3.10. Preparation of corn oil-in-water emulsions with PPC-GA conjugates.....	83
4.3.11. Particle size & zeta potential measurement.....	84
4.3.12. Physical stability of emulsions against environment stresses.....	84
4.3.13. Volatile compounds measurements	84
4.3.14. Statistical analysis.....	85
4.4. Results and Discussion.....	85
4.4.1. Structure characterization of PPC and PPC-GA conjugates.....	85
4.4.2. Determination of degree of PPC-GA conjugation.....	88
4.4.3. Impact of incubation time on the solubility of PPC-GA conjugates	91
4.4.4. Impact of incubation time on the emulsifying property of PPC-GA conjugates..	94
4.4.5. Physical stability of oil-in-water emulsions stabilized by PPC-GA conjugates...	95
4.4.5.1. Influence of pH on physical stability of emulsions.....	95
4.4.5.2. Influence of thermal processing on physical stability of emulsions	97

4.4.5.3. Influence of ionic strength on physical stability of emulsions.....	99
4.4.6. Impact of conjugation on the flavor attributes of PPC	101
4.5. Conclusion.....	105
4.6. References	106
5. GUM ARABIC-MEDIATED SYNTHESIS OF GLYCO-PEA PROTEIN HYDROLYSATE VIA MAILLARD REACTION IMPROVES SOLUBILITY, FLAVOR PROFILE, AND FUNCTIONALITY OF PEA PROTEIN	112
5.1. Abstract	112
5.2. Introduction	112
5.3. Materials and Methods	115
5.3.1. Materials	115
5.3.2. Gum Arabic-mediated synthesis of glyco-pea protein hydrolysate.....	115
5.3.3. Characterization of structure and degree of conjugation	116
5.3.4. Determination of molecular weight by size exclusion chromatography with multiangle laser light scattering (SEC-MALLS) detector	116
5.3.5. Volatile substances in glyco-pea protein hydrolysate	117
5.3.6. Relative solubility of glyco-pea protein hydrolysate.....	117
5.3.7. Corn oil-in-water emulsion prepared by glyco-PPH	118
5.3.8. Physical stability of emulsions against pH changes	118
5.3.9. Lipid oxidation kinetics of emulsions.....	118
5.3.10. Statistical analysis.....	119
5.4. Results and Discussion.....	119
5.4.1. Structure characterization of glyco-pea protein hydrolysate	119
5.4.2. Molecular parameters of glyco-pea protein hydrolysate	124
5.4.3. Degree of conjugation in glyco-PPH.....	129
5.4.4. Volatile substances in glycoprotein	131
5.4.5. Solubility and emulsification properties of glyco-PPH.....	137
5.4.6. Oxidative stability of oil-in-water emulsions stabilized by glyco-PPH	140

5.5. Conclusion.....	142
5.6. References	142
6. CONJUGATION OF PEA PROTEIN ISOLATE VIA MAILLARD-DRIVEN CHEMISTRY WITH SACCHARIDES OF DIVERSE MOLECULAR MASS: MOLECULAR INTERACTION CAUSING AGGREGATION OR GLYCATION? ...	150
6.1. Abstract	150
6.2. Introduction	150
6.3. Materials and Methods	153
6.3.1. Extraction of pea protein isolate.....	153
6.3.2. Saccharides-mediated synthesis of glyco-pea protein isolate.....	153
6.3.3. Characterization and degree of glycosylated proteins	154
6.3.4. Size exclusion-high performance liquid chromatography (SEC-HPLC)	154
6.3.5. Relative solubility of glyco-pea protein isolate	155
6.3.6. Differential scanning calorimetry (DSC).....	155
6.3.7. Volatile substances in glyco-pea protein isolate.....	155
6.3.8. Statistical analysis.....	156
6.4. Results and Discussion.....	156
6.4.1. Characterization of formation and conjugation extent in glyco-PPI	156
6.4.2. Molecular parameters of glyco-pea protein isolate	163
6.4.3. Solubility and thermal stability of glyco-pea protein isolate.....	168
6.4.4. Volatiles substances in glycoprotein	172
6.5. Conclusion.....	176
6.6. References	177
7. OVERALL SUMMARY AND CONCLUSION.....	183
7.1. Conclusions	183
7.2. Future Research.....	184

LIST OF TABLES

<u>Table</u>	<u>Page</u>
5.1. Molecular mass parameters of various glyco-PPH determined by SEC-MALLS.	128
5.2. The level of selected off-flavor volatiles in various glyco-PPH conjugates (n = 3)	136
6.1. Percentage of integrated area from SEC-HPLC spectra at 280 nm, of glyco-PPI conjugates incubated in an aqueous system (80°C, pH 10.0).	166
6.2. Thermal parameters of various heat-treated glyco-PPI conjugates (n = 3)	172

LIST OF FIGURES

<u>Figure</u>	<u>Page</u>
1.1. Schematic illustration of opportunities for flavor to interact with protein molecules, adapted from Reineccius (2005).....	3
2.1. (A) Schematic representation of the disulfide bond patterns formed between the 8 conserved cysteine residues in the 2S albumin family, adapted from Morenno & Clemente, (2008); (B) Schematic ribbon representation of the 2S albumin storage protein from <i>Moringa oleifera</i> seed protein Mo-CBP3-4 (PDB entry:6S3F).....	12
2.2. (A) Monomers of adzuki bean (<i>Vigna angularis</i>) 7S globulin-1 (adapted from Fukuda et al., 2008). The broken line in the figure is the pseudo-dyad axis of the N- and C- terminal modules. (B) Stereo view of ribbon diagram of the trimeric protein along threefold axis of symmetry showing the crystal structure of adzuki bean 7S globulin-1 (PDB entry: 2EA7). The three subunits are shown in magenta, cyan, and green, respectively; (C) The trimer is shown in the orthogonal view..	12
2.3. (A) Pseudoradial-symmetrical arrangement of 11S globulin subunits where the domains are arranged radial-symmetrically by Plietz et al. (1987). Hypothetical arrangement of α and β chains in each subunit within the hexameric molecule is shown. N and C designate the N- and C- terminal regions, respectively, of α and β chains. The twofold pseudosymmetry axes are indicated by “x”; (B) Monomers of pea prolegumin (<i>Pisum sativum</i>) 11S globulin (PDB entry: 3KSC). The broken line in the figure is the pseudosymmetry axis of the acidic (α) and basic subunit (β); the disulfide linkages are displayed as spheres. (C) Stereo view of ribbon diagram of the hexameric molecule along twofold axis of symmetry showing the crystal structure of pea 11S globulin (PDB entry: 3KSC). The six subunits are shown in yellow, grey, dark salmon, cyan, magenta, and green, respectively; (D) The hexamer is viewed after 90° rotation. (E) Schematic model for the quaternary structure association-dissociation phenomena of legumin- and vicilin-type globulins.....	14
2.4. Scheme of various chemical modification of a protein.....	17
2.5. Schematic presentation of Maillard reaction	26
2.6. (A) Aroma and structure classification of flavor compounds resulting during the Maillard reaction or caramelization (adapted from Hodge et al., 1972); (B) common Maillard reaction compounds responsible for flavor in dairy products	33
3.1. SDS-PAGE patterns of PPI and PPI-GA conjugates at different incubation time.....	58
3.2. The absorbance of non-specific Maillard markers at 304 nm and 420 nm as a function of incubation time.	61
3.3. The brown index (BI) and available free amino groups of PPI and PPI-GA conjugates during the course of incubation (0, 1, 3, and 5 days) at 60°C and 79% relative humidity.....	61

3.4. The color development of PPI and PPI-GA conjugates during the course of incubation (0, 1, 3, and 5 days) at 60°C and 79% relative humidity.....	61
3.5. Solubility of PPI and PPI-GA conjugates during the course of incubation (0, 1, 3, and 5 days) at 60°C and 79% relative humidity	63
3.6. SEM (Magnification 1000×; scale bar =10µm) for surface characteristics of PPI and PPI-GA conjugates during the course of incubation (0, 1, 3, and 5 days) at 60°C and 79% relative humidity	64
3.7. Particle size (d_{32} and d_{43}) (A); particle size distribution (B) of corn oil-in water emulsions (pH 7.0) stabilized by PPI, PPI-GA mixture, and PPI-GA conjugates formed with different incubation time (1, 3, and 5 days).....	65
3.8. Influence of pH on particle size (A), real figures (B) and ζ -potential (C) of emulsions (pH 7.0) stabilized by PPI, PPI-GA mixture, and PPI-GA conjugates incubated for 1 day... ..	66
3.9. Influence of thermal treatment on particle size (A), real figures (B) and ζ -potential (C) of emulsions (pH 7.0) stabilized by PPI, PPI-GA mixture, and PPI-GA conjugates incubated for 1 day... ..	68
3.10. Influence of salt concentration on particle size (A), real figures (B) and ζ -potential (C) of emulsions (pH 7.0) stabilized by PPI, PPI-GA mixture, and PPI-GA conjugates incubated for 1 day... ..	70
3.11. The formation of lipid hydroperoxides (A) and hexanal (B) in corn oil-in-water emulsions (pH 7.0) stabilized by PPI, PPI-GA mixture, and PPI-GA conjugates incubated for 1 day during storage at 37°C	71
4.1. SDS-PAGE patterns for different PPC-GA conjugates: lane M for protein markers; lanes 1-7 for PPC-0 day; PPC-1 day, PPC-3 day, PPC-5 day, PPC-GA conjugates-1 day, PPC-GA conjugates-3 day, PPC-GA conjugates-5 day, respectively	86
4.2. The characteristic structure of PPC-GA conjugate by Fourier transform infrared spectroscopy-attenuated total reflection (FTIR-ATR).	88
4.3. Changes in absorbance at 304 nm and 420 nm in mixture of PPC and GA incubated at 60°C and 79% relative humidity for 0-5 day.....	89
4.4. Changes of free amino groups (A) as a function of incubation time during glycation of PPC and GA at 60°C and 79% relative humidity; The real figures of samples (B). ..	90
4.5. Color development in samples incubated at different times of 0, 1, 3, 5 day, respectively, under 60°C and 79% relative humidity conditions.	91
4.6. Relative protein solubility of different PPC-GA conjugates incubated at different times of 1, 3, 5 day, respectively.....	92

4.7. SEM for surface characters profiles of PPC-GA conjugates: 1-3 for GA, PPC, mixture of PPC and gum Arabic, 4-6 for PPC-GA conjugates incubated at different times of 1, 3, 5 day, respectively.....	93
4.8. (A) Changes of particle size (d_{32} and d_{43}) at different incubation times for emulsions stabilized with PPC alone, mixture of PPC and gum Arabic and PPC-GA conjugates; (B) Changes of size distribution for emulsions stabilized with PPC alone, mixture of PPC and gum Arabic and PPC-GA conjugates.....	94
4.9. Changes of particle size (A), real figures (B) and ζ -potential (C) for emulsions stabilized with PPC alone, mixture of PPC with GA and PPC-GA conjugates against different pHs.....	97
4.10. Changes of particle size (A), real figures (B) and ζ -potential (C) for emulsions stabilized with PPC alone, mixture of PPC with GA and PPC-GA conjugates against thermal temperature.....	99
4.11. Changes of particle size (A), real figures (B) and ζ -potential (C) for emulsions stabilized with PPC alone, mixture of PPC with GA and PPC-GA conjugates against ionic strengths.....	100
4.12. Principal component analysis (PCA) of identified flavor compositions by GC-MS, (A) the loadings of different PPC-GA conjugates; (B) the scores of various identified volatile compounds.	103
4.13. The impacts of incubation time on the selected off-flavors in different PPC-GA conjugates.	104
5.1. SDS-PAGE patterns for different glyco-PPH: lane M for protein markers; lanes 1-8 for pea protein isolate (PPI), PPH-0 day, PPH-1 day, PPH-3 day, PPH-5 day, glyco-PPH-1 day, glyco-PPH-3 day, and glyco-PPH-5 day, respectively.	119
5.2. The characteristic structure of glyco-PPH (1 day) by Fourier transform infrared spectroscopy-attenuated total reflection (FTIR-ATR).	121
5.3. SEM for surface characters profiles of glyco-PPH: 1-3 for PPH, GA, mixture of PPH and gum arabic, 4-6 for glyco-PPH with different times of 1, 3, 5 day, respectively.....	123
5.4. (A-H) A range of selected samples were characterized by a size-exclusion chromatography with multiangle laser light scattering (SEC-MALLS)..	125
5.5. Changes in absorbance at 304 nm and 420 nm in the mixture of PPH and GA reacted at 60°C and 79% relative humidity for 0-5 day.....	129
5.6. Changes of free amino groups as a function of reaction time during cross-linking of PPH and GA at 60°C and 79% relative humidity.....	130
5.7. Color development (A) and real figures (B) of samples reacted at 0, 1, 3, and 5 days, respectively.....	131

5.8. Principal component analysis (PCA) (A) loading plot (B) score plot of identified flavor compositions in different glyco-PPH.....	134
5.9. Chromatograms of beany flavor markers.....	135
5.10. Relative protein solubility of different glyco-PPH cross-linked at 1, 3, and 5 days, respectively.....	137
5.11. Changes of particle size (d_{43}) for emulsions stabilized with pea protein hydrolysate (PPH) alone, mixture of PPH and gum Arabic (GA), and various glyco-PPH.....	138
5.12. Changes of particle size (d_{43}) and ζ -potential for emulsions stabilized with pea protein hydrolysate (PPH) alone, mixture of PPH with gum Arabic (GA), and glyco-PPH with 1 day reaction against different pHs.	139
5.13. The formation of (A) lipid hydroperoxides and (B) hexanal in corn oil-in-water emulsions (pH 7.0) stabilized by pea protein hydrolysate (PPH), mixture of PPH with gum Arabic (GA), and glyco-PPH for 1 day during storage at 37°C.....	141
6.1. Color development in samples incubated for various time, where a and b-value mean redness and yellowness, respectively.	157
6.2. Schematic illustration of heat induced pea protein isolate denaturation and aggregation and of the Maillard-driven glycation reaction.	159
6.3. Changes in absorbance at 304 nm in the mixture of PPI and diverse saccharides reacted at 80°C, which is associated with Amadori compounds development.	160
6.4. SDS-PAGE patterns for different glyco-PPI.	162
6.5. Changes of free amino groups as a function of reaction time during glycation of PPI with saccharides at 80°C.	163
6.6. The elution profiles monitored by UV at 280 nm for a range of selected samples, characterized by a size-exclusion chromatography (SEC-HPLC)	164
6.7. Typical calibration curve obtained with proteins from the MWGF1000 Kit run on Yarra™ SEC-4000 LC column; V_e and V_o mean elution volume and void volume, respectively.....	165
6.8. Schematic ribbon diagram of the 11S globulin (PDB entry: 3FZ3); 7S globulin-1 (PDB entry: 2EA7), and 2S albumin (PDB entry: 6S3F), and the association-dissociation phenomena of legumin- and vicilin-type globulins.....	167
6.9. Relative protein solubility of different glyco-PPI conjugates at 12 and 24 hour (n = 6), respectively, at neutral pH (7.0).	169
6.10. DSC thermograms of glyco-PPI conjugates incubating pea protein isolate with diverse saccharides at a scan rate 10°C/min.....	171
6.11. Gas chromatograms of a set of selected samples.	173

6.12. Hierarchical cluster analysis and heat map of various glyco-PPI conjugates.	174
6.13. Principal component analysis (PCA) (A) loading plot (B) score plot of identified flavor compositions in different glyco-PPI.	175
6.14. The level of selected off-flavor volatiles in various heat-treated glyco-PPI conjugates (n = 3).	176

1. GENERAL INTRODUCTION

1.1. Introduction

Pulse crops are narrowly defined by the United Nations' Food and Agriculture Organization (FAO) as legume crops that are harvested solely for the dry seeds. Proteins from pulse seeds (200–250 g kg⁻¹), combined with being cholesterol-free, low allergenicity and non-GMO status (Abeysekara, Chilibeck, Vatanparast, & Zello, 2012; McCrory, Hamaker, Lovejoy, & Eichelsdoerfer, 2010; Schuster-gajzágó, 2004; Stone, Karalash, Tyler, Warkentin, & Nickerson, 2015), makes pulse protein a serious plant-derived contender. The trend toward more well-balanced and health-benefiting diet also predictably divert the trajectory of protein-based foodstuffs and challenge the animal-derived protein consumption (Schneider, 2002). Therapeutic pulse-based proteins have proven invaluable in campaigns against coronary heart diseases and diabetes (Abeysekara et al., 2012; McCrory, Hamaker, Lovejoy, & Eichelsdoerfer, 2010). The nutritional and functional benefits of relatively inexpensive pulse proteins and their environmental benefits like nitrogen-fixing ability provide consumers a potential dietary transition opportunity (Klupšaitė & Juodeikienė, 2015; Schneider, 2002). Nevertheless, pulse proteins still have remained underexploited or largely been dampened in food applications. The poor functionality and unacceptable sensory characteristics are limiting factors preventing widespread adoption of pulse protein.

Alkaline extraction followed by acid (isoelectric) precipitation has been performed commercially when it comes to preparation of pulse proteins. Such process could give rise to the lower solubility of end products (Lam, Can Karaca, Tyler, & Nickerson, 2018). The protein functionalities that are highly associated with solubility like emulsification, foaming and gelling, are then impaired (Chéreau et al., 2016; Lam et al., 2018). Over the last several decades, modification in protein structure and thereby mediating macromolecular function has been proven to be a promising initiative to improve the functionality of proteins (Baslé, Joubert,

& Pucheault, 2010; Spicer & Davis, 2014). Such structural alterations have been traditionally accomplished through chemical and enzymatic treatments that in turn modulate protein activity (Baslé et al., 2010; Mohammadinejad et al., 2019; Powell et al., 2001; Spicer & Davis, 2014; Walsh, 2001). Through these initiatives, developing value-added commodity and specialty products with increased protein levels, especially those of 7S and 11S globulins lowering levels of lipoxygenase, and improving protein functionalities might match the intended use (Tandang-Silvas, Tecson-Mendoza, Mikami, Utsumi, & Maruyama, 2011). Functional properties, such as solubility, water-holding capacity, gel-formation, viscosity, emulsification, and foaming, serve as the basis of end-product performance (Kester & Richardson, 1984; Klupšaitė & Juodeikienė, 2015; Singhal, Karaca, Tyler, & Nickerson, 2016). Such functionalities are governed by intrinsic physicochemical characteristics, namely, amino acid composition and sequence, spatial conformation, net surface charge, hydrophobicity/hydrophilicity, and molecular flexibility/rigidity. (Kester & Richardson, 1984; Klupšaitė & Juodeikienė, 2015). A desired functionality by virtue of protein structure modification may involve intentional alteration of one or more of above-mentioned characteristics.

Flavor profile, a more pronounced consideration, has been discovered to exhibit taste modulatory function and is deemed critical to consumer's acceptability. Indeed, the perceived taste or palatability of pulse ingredients containing products are not well accepted by the Western palate, with reproaches including bitterness and green/beany odor (Roland, Pouvreau, Curran, Van De Velde, & De Kok, 2017). Particularly, indigenous odorants of pulse proteins arising from oxidative degradation of unsaturated fatty acid in protein-bound lipids catalyzed by lipoxygenase (LOX), have proved problematic upon subsequent application (Kalbrenner, Warner, & Eldridge, 1974; Rackis, Honig, Sessa, & Moser, 1972; Rackis, Sessa, & Honig, 1979; Sessa & Rackis, 1977; Whitfield & Shipton, 1966; Zha, Yang, Rao, & Chen, 2019). Therefore, to address objectionable flavors residing in pulse proteins is of great urgency. In

general, chemical interactions and mass transfer effects are responsible for the flavor release and thereby influence the perception of flavor profiles (Carr et al., 1996; Goubet, Le Quéré, Sémon, Seuvre, & Voilley, 2000; Reineccius, & Peppard, 2003; Roberts, Elmore, Langley, & Bakker, 1996). Chemical interactions between flavors and protein molecules has been documented (Reineccius, 2005; **Figure 1.1**);). These interactions involve hydrophobic interactions, hydrogen bonds, ionic bonds, and covalent bonds, which are in turn influenced by amino acid composition, protein tertiary structure and conformation (Fischer & Widder, 1997; Mottram & Nobrega, 2000; O'Neill, 1996). With respect to the mass transfer effects, one must consider both the viscosity and gel structures are generally associated with proteins, which serves as a physical barrier in odorant transmission (Carr et al., 1996; Roberts et al., 1996) and signifies an alteration of functional performance of proteins which would in turn lead to a far-reaching impact on its flavor profiles.

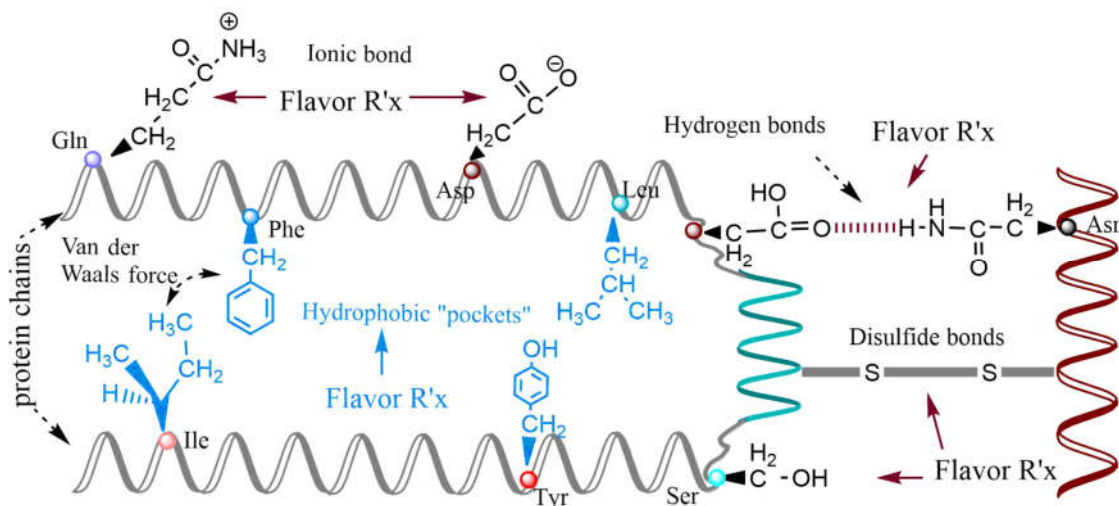


Figure 1.1. Schematic illustration of opportunities for flavor to interact with protein molecules, adapted from Reineccius (2005). Note: the chemical structures in the figure indicate amino acid residues. Gln, glutamine; Phe, phenylalanine; Asp, aspartic acid; Leu, leucine; Asn, asparagine; Ile, isoleucine; Tyr, tyrosine; Ser, serine.

Numerous attempts have been conducted to modify protein structure and further improve nutritional, functional, and sensory properties of proteins through physical, chemical, and enzymatic treatments (Kester & Richardson, 1984; Mirmoghtadaie, Shojaee Aliabadi, &

Hosseini, 2016). Some of these methods involve noxious chemical reagents, which limits the usage of modified proteins as food ingredients (Jiménez-Castaño, Villamiel, & López-Fandiño, 2007). Glycation, through attaching a carbonyl-containing moiety of carbohydrate to the protein in the early stage of Maillard reaction (MR), is an effective alternative for improving the functional properties without involving a chemical catalysis (de Oliveira, Coimbra, de Oliveira, Zuñiga, & Rojas, 2016; Oliver, Melton, & Stanley, 2006). However, advanced stage of Maillard reaction should be controlled under certain conditions since it will inevitably result in undesirable outcomes such as toxic compounds, off-flavor, and discoloration (Hellwig & Henle, 2014; Martins, Jongen, & Van Boekel, 2000). Therefore, the present work aims at producing the partially glycated pulse proteins via Maillard-driven chemistry, with enhanced functional properties mainly solubility, physical stability, antioxidant activity, and emulsifying properties, and elimination of the off-flavor. The impact of types of pulse proteins and carbohydrate with diverse molecular weight, and then the environmental factors, including pH, incubation time and relative humidity, on functional properties of pulse proteins will be investigated. Ultimately, the mechanisms of the enhanced functional properties and flavor profiles alteration will be elucidated, in the context of the well-documented structure–function studies.

1.2. Objectives and Hypotheses

Modifying pulse proteins through Maillard-induced glycation is an approach to reconstruct its microstructures and alter its functional properties. The proposed research will provide important knowledge to promote the industrial and commercial application of pulse proteins. The objectives of this research were, therefore, to investigate:

Objective 1: How glycation of pea protein isolate with gum Arabic impacts physical and oxidative stability of oil-in-water emulsions

Objective 2: How glycation of pea protein concentrates with gum Arabic via controlled Maillard reaction impacts protein structure, its functional properties and flavor attributes.

Objective 3: How gum Arabic-mediated glycation via Maillard reaction using dry-heating means alters the solubility, flavor profile, and functionality of pea protein hydrolysate.

Objective 4: Characterize the molecular interactions in conjugation of pea protein isolate via Maillard-driven chemistry with saccharides of diverse molecular mass in aqueous systems

It is hypothesized that the examined functional properties of pulse-based proteins are improved, the off-flavors of pulse-based proteins are ameliorated, and the relevant mechanisms of structure-function are elaborated

1.3. References

- Abeyssekara, S., Chilibeck, P. D., Vatanparast, H., & Zello, G. A. (2012). A pulse-based diet is effective for reducing total and LDL-cholesterol in older adults. *British Journal of Nutrition*, *108*(SUPPL. 1). <https://doi.org/10.1017/S0007114512000748>
- Baslé, E., Joubert, N., & Pucheault, M. (2010). Protein chemical modification on endogenous amino acids. *Chemistry and Biology*, *17*(3), 213–227. <https://doi.org/10.1016/j.chembiol.2010.02.008>
- Carr, J., Baloga, D., Guinard, J. X., Lawter, L., Marty, C., & Squire, C. (1996). The effect of gelling agent type and concentration on flavor release in model systems. *ACS Symposium Series*, *633*, 98–108. <https://doi.org/10.1021/bk-1996-0633.ch009>
- Chéreau, D., Videcoq, P., Ruffieux, C., Pichon, L., Motte, J. C., Belaid, S., Ventureira, J., & Lopez, M. (2016). Combination of existing and alternative technologies to promote oilseeds and pulses proteins in food applications. *OCL - Oilseeds and Fats, Crops and Lipids*, *41*(1). <https://doi.org/10.1051/ocl/2016020>

- de Oliveira, F. C., Coimbra, J. S. dos R., de Oliveira, E. B., Zuñiga, A. D. G., & Rojas, E. E. G. (2016). Food protein-polysaccharide conjugates obtained via the Maillard reaction: A Review. *Critical Reviews in Food Science and Nutrition*, *56*(7), 1108–1125.
<https://doi.org/10.1080/10408398.2012.755669>
- Fischer, N., & Widder, S. (1997). How proteins influence food flavor. *Food Technology*, *51*(1), 68–70. Retrieved from <http://agris.fao.org/agris-search/search.do?recordID=US9719377>
- Goubet, I., Le Quéré, J. L., Sémon, E., Seuvre, A. M., & Voilley, A. (2000). Competition between aroma compounds for the binding on β -cyclodextrins: Study of the nature of interactions. *ACS Symposium Series*, *763*, 246–259. <https://doi.org/10.1021/bk-2000-0763.ch020>
- Hellwig, M., & Henle, T. (2014). Baking, ageing, diabetes: A short history of the Maillard reaction. *Angewandte Chemie International Edition*, *53*(39), 10316–10329.
<https://doi.org/10.1002/anie.201308808>
- Jiménez-Castaño, L., Villamiel, M., & López-Fandiño, R. (2007). Glycosylation of individual whey proteins by Maillard reaction using dextran of different molecular mass. *Food Hydrocolloids*, *21*(3), 433–443. <https://doi.org/10.1016/j.foodhyd.2006.05.006>
- Kalbrenner, J. E., Warner, K., & Eldridge, A. C. (1974). Flavors derived from linoleic and linolenic acid hydroperoxides. *Cereal Chemistry*, *51*, 406–416. Retrieved from https://www.aaccnet.org/publications/cc/backissues/1974/Documents/chem51_406.pdf
- Kester, J. J., & Richardson, T. (1984). Modification of whey proteins to improve functionality. *Journal of Dairy Science*, *67*(11), 2757–2774.
[https://doi.org/10.3168/jds.S0022-0302\(84\)81633-1](https://doi.org/10.3168/jds.S0022-0302(84)81633-1)

- Klupšaitė, D., & Juodeikienė, G. (2015). Legume: composition, protein extraction and functional properties. A review. *Chemical Technology*, 66(1), 5-12.
<https://doi.org/10.5755/j01.ct.66.1.12355>
- Lam, A. C. Y., Can Karaca, A., Tyler, R. T., & Nickerson, M. T. (2018). Pea protein isolates: Structure, extraction, and functionality. *Food Reviews International*, 34(2), 126–147.
<https://doi.org/10.1080/87559129.2016.1242135>
- Martins, S. I. F. S., Jongen, W. M. F., & Van Boekel, M. A. J. S. (2000). A review of Maillard reaction in food and implications to kinetic modelling. *Trends in Food Science and Technology*, 11(9-10), 364–373. [https://doi.org/10.1016/S0924-2244\(01\)00022-X](https://doi.org/10.1016/S0924-2244(01)00022-X)
- McCrary, M. A., Hamaker, B. R., Lovejoy, J. C., & Eichelsdoerfer, P. E. (2010). Pulse consumption, satiety, and weight management. *Academic.Oup.Com*, 1(1), 17–33.
Retrieved from <https://academic.oup.com/advances/article-abstract/1/1/17/4591548>
- Mirmoghtadaie, L., Shojaee Aliabadi, S., & Hosseini, S. M. (2016). Recent approaches in physical modification of protein functionality. *Food Chemistry*, 199, 619–627.
<https://doi.org/10.1016/j.foodchem.2015.12.067>
- Mohammadinejad, R., Shavandi, A., Raie, D. S., Sangeetha, J., Soleimani, M., Hajibehzad, S. S., Thangadurai, D., Hospet., R., Popoola, J. O., Arzani, A., & Gómez-Lim, M. A. (2019). Plant molecular farming: Production of metallic nanoparticles and therapeutic proteins using green factories. *Green Chemistry*. 21(8), 1845-1865.
<https://doi.org/10.1039/c9gc00335e>
- Mottram, D. S., & Nobrega, I. C. C. (2000). Interaction between sulfur-containing flavor compounds and proteins in foods. *ACS Symposium Series*, 763, 274–281.
<https://doi.org/10.1021/bk-2000-0763.ch022>
- O'Neill, T. E. (1996). Flavor binding by food proteins: An Overview. *ACS Symposium Series*, 633, 59–74. <https://doi.org/10.1021/bk-1996-0633.ch006>

- Oliver, C. M., Melton, L. D., & Stanley, R. A. (2006). Creating proteins with novel functionality via the Maillard reaction: A Review. *Critical Reviews in Food Science and Nutrition*, 46(4), 337–350. <https://doi.org/10.1080/10408690590957250>
- Powell, K. A., Ramer, S. W., Del Cardayr, S. B., Stemmer, W. P. C., Tobin, M. B., Longchamp, P. F., & Huisman, G. W. (2001). Directed evolution and biocatalysis. *Angewandte Chemie International Edition*, 40(21), 3948–3959. [https://doi.org/10.1002/1521-3773\(20011105\)40:21<3948::AID-ANIE3948>3.0.CO;2-N](https://doi.org/10.1002/1521-3773(20011105)40:21<3948::AID-ANIE3948>3.0.CO;2-N)
- Rackis, J., Honig, D., Sessa, D., & Moser, H. A. (1972). Lipoxygenase and peroxidase activities of soybeans as related to the flavor profile during maturation. *Cereal Chemistry*, 49, 586-597. Retrieved from https://www.aaccnet.org/publications/cc/backissues/1972/Documents/Chem49_586.pdf
- Rackis, J. J., Sessa, D. J., & Honig, D. H. (1979). Flavor problems of vegetable food proteins. *Journal of the American Oil Chemists' Society*, 56(3), 262–271. <https://doi.org/10.1007/BF02671470>
- Reineccius, G. (2005). Flavor release from foods. In *Flavor Chemistry and Technology* (Second Edi, 139–155). <https://doi.org/10.1007/978-94-011-9759-5>
- Reineccius, T.A., & Peppard, T. L (2003). Comparison of flavor release from alpha-, beta-and gamma-cyclodextrins. *Experts.Umn.Edu*, 68, 1234–1239. Retrieved from <https://experts.umn.edu/en/publications/comparison-of-flavor-release-from-alpha-beta-and-gamma-cyclodextr>
- Roberts, D. D., Elmore, J. S., Langley, K. R., & Bakker, J. (1996). Effects of sucrose, guar gum, and carboxymethylcellulose on the release of volatile flavor compounds under dynamic conditions. *Journal of Agricultural and Food Chemistry*, 44(5), 1321–1326. <https://doi.org/10.1021/jf950567c>

- Roland, W. S. U., Pouvreau, L., Curran, J., Van De Velde, F., & De Kok, P. M. T. (2017). Flavor aspects of pulse ingredients. *Cereal Chemistry*, *94*(1), 58–65.
<https://doi.org/10.1094/CCHEM-06-16-0161-FI>
- Schneider, A. V. C. (2002). Overview of the market and consumption of pulses in Europe. *British Journal of Nutrition*, *88*(S3), 243–250. <https://doi.org/10.1079/bjn2002713>
- Schuster-gajzágó, I. (2004). Nutritional aspects of legumes. *Cultivated Plants, Primarily as Food Sources*, *1*, 1–7. Retrieved from <http://www.eolss.net/sample-chapters/c10/e5-02-02.pdf>
- Sessa, D. J., & Rackis, J. J. (1977). Lipid-derived flavors of legume protein products. *Journal of the American Oil Chemists' Society*, *54*(10), 468–473.
<https://doi.org/10.1007/BF02671039>
- Singhal, A., Karaca, A. C., Tyler, R., & Nickerson, M. (2016). Pulse proteins: from processing to structure-function relationships. In *Grain Legumes*.
<https://doi.org/10.5772/64020>
- Spicer, C. D., & Davis, B. G. (2014). Selective chemical protein modification. *Nature Communications*, *5*(1), 4740–4754. <https://doi.org/10.1038/ncomms5740>
- Stone, A. K., Karalash, A., Tyler, R. T., Warkentin, T. D., & Nickerson, M. T. (2015). Functional attributes of pea protein isolates prepared using different extraction methods and cultivars. *Food Research International*, *76*(P1), 31–38.
<https://doi.org/10.1016/j.foodres.2014.11.017>
- Tandang-Silvas, M. R. G., Tecson-Mendoza, E. M., Mikami, B., Utsumi, S., & Maruyama, N. (2011). Molecular design of seed storage proteins for enhanced food physicochemical properties. *Annual Review of Food Science and Technology*, *2*(1), 59–73.
<https://doi.org/10.1146/annurev-food-022510-133718>

Walsh, C. (2001). Enabling the chemistry of life. *Nature*, 409(6817), 226–231.

<https://doi.org/10.1038/35051697>

Whitfield, F. B., & Shipton, J. (1966). Volatile carbonyls in stored unblanched frozen peas.

Journal of Food Science, 31(3), 328–331. <https://doi.org/10.1111/j.1365->

2621.1966.tb00501.x

Zha, F., Yang, Z., Rao, J., & Chen, B. (2019). Gum Arabic-mediated synthesis of glyco-pea

protein hydrolysate via Maillard reaction improves solubility, flavor profile, and

functionality of plant protein. *Journal of Agricultural and Food Chemistry*, 67(36),

10195–10206. <https://doi.org/10.1021/acs.jafc.9b04099>

2. LITERATURE REVIEW

2.1. Pulse Protein Structure 1°–4° and Classification of Storage Proteins

Four different levels of structures, including primary (1°), secondary (2°), tertiary (3°), and quaternary (4°) are well-defined in three-dimensional functional structure of protein. The primary structure is constructed by peptide bonds between amino acids (Silva et al., 2014). Other advanced structures are assembled based on the primary structure by hydrogen bonds, non-specific hydrophobic interactions, salt bridges, and disulfide bonds (Silva et al., 2014). The structural characters of proteins impart their particular nutritional and functional properties (Radivojac et al., 2013). Seed storage proteins were empirically classified based on their solubility and can be divided into water soluble albumins, dilute salt soluble globulins, alcohol soluble prolamins, and dilute acid/alkaline soluble glutelins (Osborne, 1924). Accurately and conveniently, seed proteins can be further divided into 2S, 7S, and 11/12S based on their sedimentation coefficients (Mandal & Mandal, 2000). In general, seed storage proteins of pulses are mainly composed of 2S albumins and 7S or 11S globulins (Chéreau et al., 2016; Tandang-Silvas, Tecson-Mendoza, Mikami, Utsumi, & Maruyama, 2011).

2.1.1. 2S albumin storage proteins

The 2S albumins are compact globular unit that are rich in sulphur-containing amino acids, especially cysteine. It commonly consists of two polypeptide chains with molecular mass values of ~9 kDa and ~4 kDa (**Fig. 2.1A**), respectively, which are linked by disulfide linkages (Moreno & Clemente, 2008; Shewry, Napier, & Tatham, 1995). Typically, they are synthesized as single precursor protein that are proteolytically cleaved with the loss of a linker peptide and short peptides form both N- and C- terminus (Shewry et al., 1995). 2S albumins are characterized by the presence of a well-conserved skeleton of 8 cysteine residues and a three-dimensional structure enriched in α -helices (Moreno & Clemente, 2008), as shown in **Figure 2.1 A&B**. Several linear IgE-binding epitopes of 2S albumins have been described to highlight

its allergenicity in seeds of many mono- and di-cotyledonous plants (Moreno & Clemente, 2008).

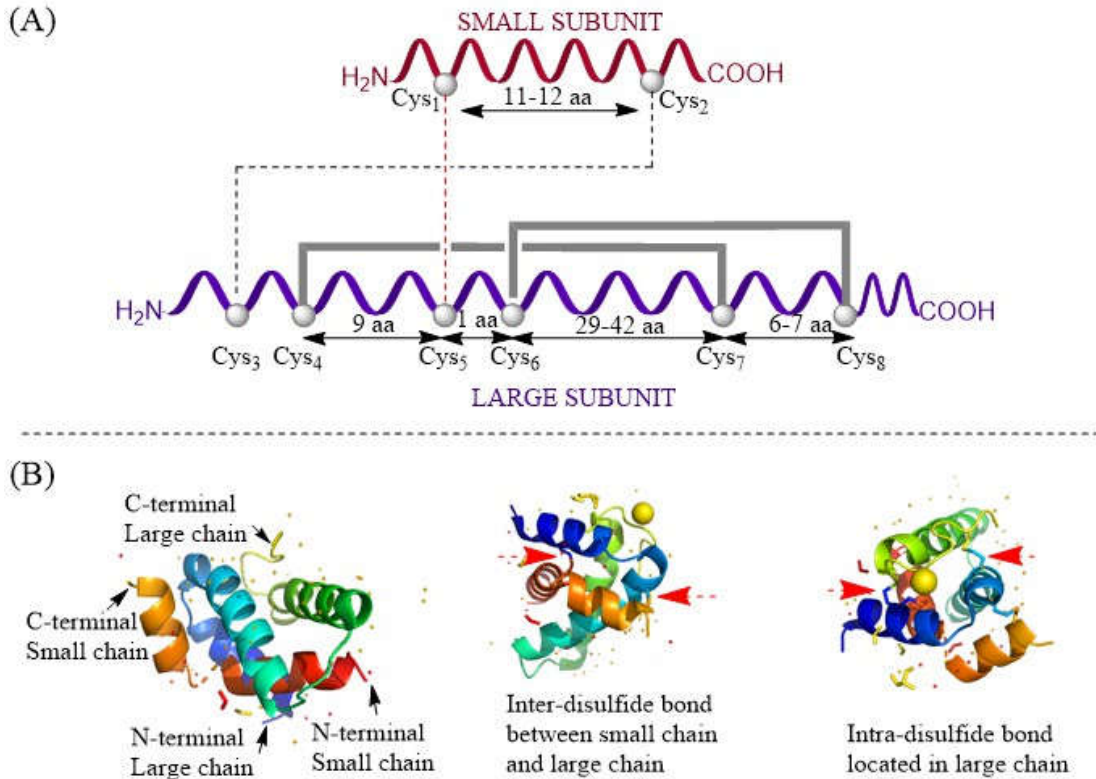


Figure 2.1. (A) Schematic representation of the disulfide bond patterns formed between the 8 conserved cysteine residues in the 2S albumin family, adapted from Moreno & Clemente, (2008); (B) Schematic ribbon representation of the 2S albumin storage protein from *Moringa oleifera* seed protein Mo-CBP3-4 (PDB entry: 6S3F). The disulfide bridges are represented by sticks and the interactions with inter- and intra-chains.

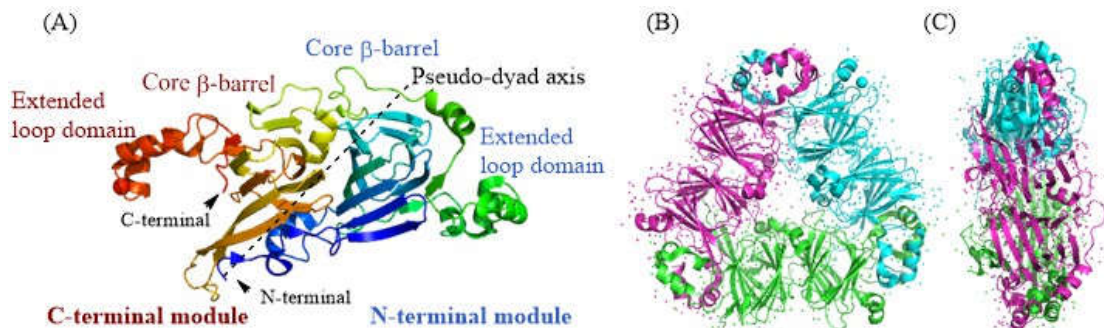


Figure 2.2. (A) Monomers of adzuki bean (*Vigna angularis*) 7S globulin-1 (adapted from Fukuda et al., 2008). The broken line in the figure is the pseudo-dyad axis of the N- and C-terminal modules. (B) Stereo view of ribbon diagram of the trimeric protein along threefold axis of symmetry showing the crystal structure of adzuki bean 7S globulin-1 (PDB entry: 2EA7). The three subunits are shown in magenta, cyan, and green, respectively; (C) The trimer is shown in the orthogonal view.

2.1.2. 7S and 11S globulin storage proteins

Globulin proteins are dominant in seed storage proteins of pulses. 7S vicilin-like globulins are structured principally by non-covalent interactions, which are trimeric molecules with molecular masses ranging from 150 to 200 kDa (Jain, Kumar, & Salunke, 2016; Tandang-Silvas et al., 2011). The lack of cysteine and methionine residues contributes to the absence of disulfide linkages. Comparative structural proteomics throw light on potential physiological functions of vicilins or vicilin-like proteins. A case in point, the monomer of adzuki bean (*Vigna angularis*) vicilins is in the asymmetric unit, which consists of α -helices, β -sheets, and flexible loops (**Fig. 2.2A**). A monomer can be split across a pseudo-dyad axis into two similar constituents; wherein a core region and extended arms exist, constructing N- and C-terminal domains (Fukuda et al., 2008; Jain et al., 2016). Core regions of each domain are created by β -barrels while the extended arms consist of α -helices. Each monomer also consists of a core region structured by pair of β -barrels and α -helices protruding outward from each core resulting in a linkage with the adjacent monomers, giving rise to the construction of a trimer (Jain et al., 2016). The trimeric architectures around the threefold crystallographic axis are displayed in ribbon diagram (**Fig. 2.2B&C**). The trimerization of 7S confers thermostability to pulse protein (Jain et al., 2016). Electrostatic and hydrophobic interactions at each monomer–monomer interface play pivotal roles in consolidation of tertiary conformation of vicilins (Jain et al., 2016).

11S legumin-like globulins are hexamer ($M_w \sim 300\text{--}400$ kDa) that consist of six subunit pairs that interact non-covalently, which are further assembled via two trimeric intermediates (Shewry et al., 1995; Tandang-Silvas et al., 2010; Utsumi, 1992). The prevalently established model for the quaternary structure of 11S globulins (**Fig. 2.3A**) is an assembly of six spherical subunits into a trigonal antiprism with a maximum dimension of 11 nm (Plietz, Drescher, & Damaschun, 1987). Each subunit pairs ($M_w \sim 50\text{--}60$ kDa) contains two conserved disulfide

bonds (**Fig. 2.3B**), and further consists of a heavy α -acidic chain of Mw~30–40 kDa and a light β -basic chain of Mw~20 kDa linked with a single disulfide bond (Tandang-Silvas et al., 2010; Wanasundara, 2011). These features give rise to the hexameric crystal structure of pea 11S globulin (**Figure 2.3C&D**).

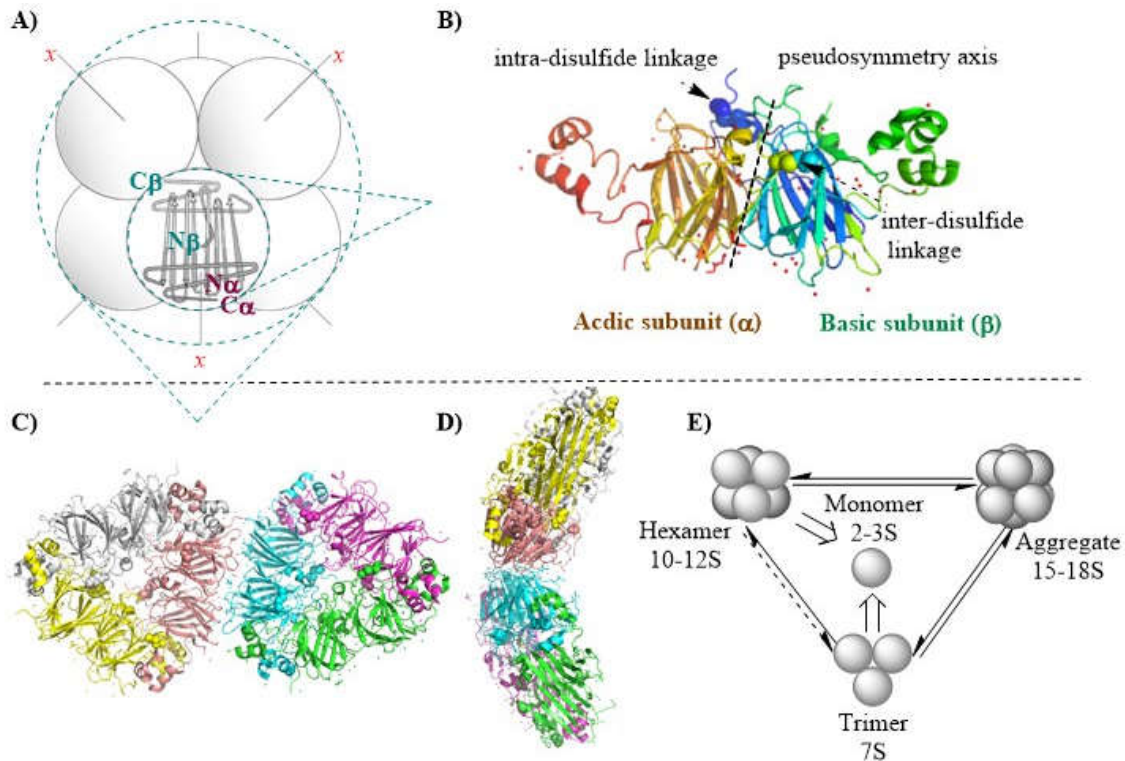


Figure 2.3. (A) Pseudoradial-symmetrical arrangement of 11S globulin subunits where the domains are arranged radial-symmetrically by Plietz et al. (1987). Hypothetical arrangement of α and β chains in each subunit within the hexameric molecule is shown. N and C designate the N- and C- terminal regions, respectively, of α and β chains. The twofold pseudosymmetry axes are indicated by “x”; (B) Monomers of pea prolegumin (*Pisum sativum*) 11S globulin (PDB entry: 3KSC). The broken line in the figure is the pseudosymmetry axis of the acidic (α) and basic subunit (β); the disulfide linkages are displayed as spheres. (C) Stereo view of ribbon diagram of the hexameric molecule along twofold axis of symmetry showing the crystal structure of pea 11S globulin (PDB entry: 3KSC). The six subunits are shown in yellow, grey, dark salmon, cyan, magenta, and green, respectively; (D) The hexamer is viewed after 90° rotation. (E) Schematic model for the quaternary structure association-dissociation phenomena of legumin- and vicilin-type globulins.

Globulins are synthesized and accumulated during legume seed development. Their detailed subunit compositions vary considerably because of differences in post-translational processing. A notable similarity among legume seed globulins lies in their reversible and

irreversible association–dissociation phenomena (**Fig. 2.3E**), which is modulated by both ionic strength (I) and pH (Shewry et al., 1995; Wanasundara, 2011). The hexameric assembly of 11S cruciferin of rapeseed exists under $I > 0.5$, and then dissociates into 7S trimers with a decline of I in medium (Schwenke, Raab, Plietz, & Damaschun, 1983). Dissociated trimers are capable of reassembling upon elevating I (Schwenke & Linow, 1982). Cruciferin would initiate irreversible dissociation under acidic conditions with the presence of 4.0 M urea. It was noted that the native structure of mustard 12S globulins unfolded between pH 5.0 and 3.0 and reassembled beyond pH 3.0 (Murthy & Rao, 1984). Such re-association depends on entropically driven hydrophobic interaction of non-polar residues. The somewhat easy association–dissociation confirms that monomer interactions are non-covalent in nature. Still, future research on elucidating the structure variations and dynamics of pulse protein subunits during storage and processing is required as this could help design pertinent strategies for structure modification.

2.2. Chemical Modification of Proteins

Chemical modification is an unambiguous means to modulate protein functionalities in scientific and industrial communities. In general, chemical modification selectively incorporate functional groups on proteins via the active residues of interest which yields customizable properties and activities (Baslé, Joubert, & Pucheault, 2010; Spicer & Davis, 2014). Two critical features would be needed for chemical modification of a protein, an attachable molecule of interest and a practical reaction (Baslé et al., 2010). The molecule should endow a protein with some specific functions desirable in food application, while the reaction serves to provide the vehicles of yielding the well-defined protein constructs in high efficiency and functional form. In general, the reactions for protein modification utilizes the inherent reactivity of certain amino acid side chains that are commonly referred to as amino, carboxyl, disulfide, imidazole, indole, phenolic, sulfhydryl, and thioether (Baslé et al., 2010; Chalker, Bernardes, Lin, &

Davis, 2009; Spicer & Davis, 2014). These reactions do not only involve in the development of covalent linkage but in alteration of noncovalent forces including van der Waals forces, electrostatic interactions, hydrophobic interactions, and hydrogen bonds, and thereby leading to molecular conformation changes followed by intentional functional outcomes (Baslé et al., 2010; Chalker et al., 2009; Kester & Richardson, 1984).

The modification susceptibility of the amino acid side chains closely relates to its chemical reactivity and affinity, polarity and electric charge of the adjacent residues, external conditions (pH, temperature, etc.), and nucleophilicity of the reagent applied (Feeney, 1977; Klupšaitė & Juodeikienė, 2015; Spicer & Davis, 2014). In essence, incorporation of molecule of interest (**Fig. 2.4**) into protein moiety commonly induces the alteration of the surface charge and hydrophobicity of a protein, with subsequent transformation of isoelectric point (IEP) and spatial conformation, which in turn leads to profound variation in functional behaviors of a protein (Kester & Richardson, 1984; Klupšaitė & Juodeikienė, 2015; Lam, Can Karaca, Tyler, & Nickerson, 2018). Some typical chemical derivatizations to be of general use in protein modification are outlined below.

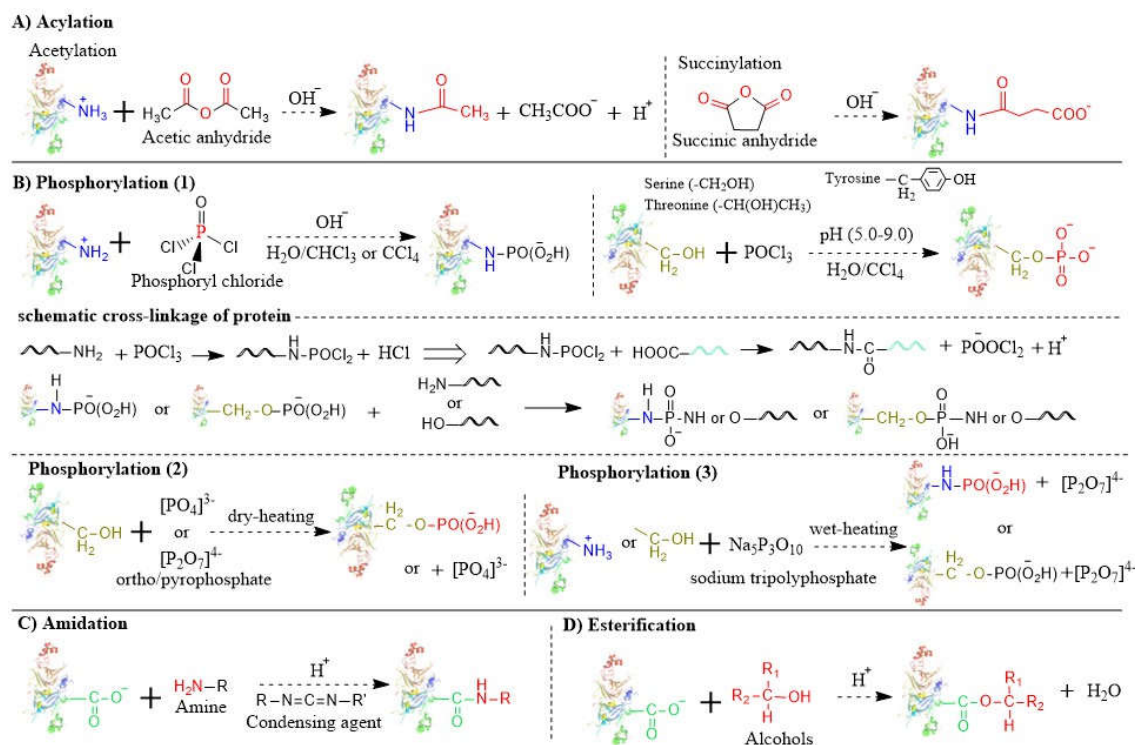


Figure 2.4. Scheme of various chemical modification of a protein. (A) acylation, including acetylation and succinylation, with ϵ -amino group of lysine residue in proteins; (B) three variant of protein phosphorylation using different phosphorylating reagents; (C) amidation with the carboxyl group of amino acid residues in proteins; (D) protein esterification with the aid of acid catalysis.

2.2.1. Acylation

Nucleophilic amino acid residues are required for a protein acylation with activated acid anhydrides (Baslé et al., 2010; Franzen & Kinsella, 1976). In particular, cationic ϵ -amino group of lysine is most readily accessible among such residues that might be ascribed to its relatively low acid dissociation constants (pka) and steric availability for approaching to the acylating agents (Franzen & Kinsella, 1976). Reactions with acetic and succinic anhydrides (**Fig. 2.4A**) are involved in the introduction of neutral acetyl moiety and anionic succinate residues, respectively (Franzen & Kinsella, 1976; Kester & Richardson, 1984; Yin, Tang, Wen, Yang, & Yuan, 2010). Acetylation and succinylation have been applied with some success to various proteins (Kester & Richardson, 1984).

Upon acetylation the IEP of protein shifts toward a more acidic pH reflecting an increase in the electronegativity of acetylated proteins since the unshielding of carboxylate groups by neutralization of the protonated amino groups occurs (Franzen & Kinsella, 1976; Johnson & Brekke, 1983; Krause, 2002). This resulting decrease in electrostatic attractions tends to provoke a partial unfolding of the polypeptide chains with subsequent conformational transition into a relatively expanded structural state (Franzen & Kinsella, 1976; Johnson & Brekke, 1983; Krause, 2002; Ponnampalam, Goulet, Amiot, Chamberland, & Brisson, 1988; Yin et al., 2010). It was clearly documented that acetylation of faba bean protein resulted in partial dissociation of 11S globulin into 3S subunits, and a significant decline in α -helical structure (Schwenke, Knopfe, Seifert, Görnitz, & Zirwer, 2001). Analogously, structural unfolding and 2° and 3° conformational changes of 7S vicilin also have been observed in acetylated kidney bean proteins (Yin et al., 2010). Notably, the conformation and association–dissociation state of proteins seems to be closely associated with the extent of acetylation (Ponnampalam et al., 1988; Schwenke et al., 2001).

Unlike acetylation, the succinylated proteins render the juxtaposition of negatively charged carboxyl groups in amino acid residues which yields higher net negative charge (Franzen & Kinsella, 1976). The resulting electrostatic repulsion between juxtaposed carboxyl groups indeed brings about a stepwise dissociation of the protein and further into more extensive unfolding state (Achouri & Zhang, 2001; Franzen & Kinsella, 1976). It has been reported that 11S globulins of pea protein dissociate gradually into 3S subunits via a trimeric 7S intermediate after successive succinylation (Schwenke et al., 1990). Yin et al noted succinylation of 7S vicilin from kidney bean resulted in a distinct change in tertiary conformation, and further a progressive transformation of the β -sheet into α -helix or random coil (Yin et al., 2010). Although the 2° conformation of wheat gluten was altered after succinylation, β -turn was converted into β -sheet and random coil but negligible changes in the

level of α -helix (Liu et al., 2018). It thereby appeared to imply that practical effects of succinylation on protein structure were related to the type of proteins modified.

Upon acylation the aforementioned variations in physical/structure characters of a protein consequentially lead to certain alterations in its functionalities. Undoubtedly, aqueous solubility of acylated proteins is enhanced at the pH ranging from IEP of native protein to alkaline (Dua, Mahajan, & Mahajan, 1996; Kester & Richardson, 1984; Yin, Tang, Wen, & Yang, 2009). This is facilitated by protein–water interaction upon protein structural unfolding, and the effect seems to be more pronounced with succinylation. Interestingly, numerous conflicting literatures can be found on emulsification and foaming properties of acylated proteins. An improvement in emulsification and foaming properties was achieved after acylation for wheat gluten (Liu et al., 2018), cowpea protein (Mune Mune, Minka, & Mbome, 2011), milk (Shilpashree, Arora, Chawla, & Tomar, 2015), mung bean protein (Charoensuk, Brannan, Chanasattru, & Chaiyasit, 2018); bambarra groundnut (Lawal, Adebawale, & Adebawale, 2007); yet adverse impacts on their activity or stability were also revealed (Dua et al., 1996; Miedzianka, Pęksa, & Aniołowska, 2012; Mohamed, Biresaw, Xu, Hojilla-Evangelista, & Rayas-Duarte, 2009). The justification for individual conclusion is likewise not quite conclusive and sometimes even antithetical in the activity or stability aspects, which manifest that the effects of acylation is somewhat uncertain and may be variable. Such discrepancy seems to hint that emulsification and foaming properties of protein are not necessarily improved with the increase of its solubility, albeit both are associated with protein solubility. It has been postulated that changes in net charge and structural unfolding of a protein causes the buried hydrophobic residues to become exposed to the solution, and which alters the hydrophilic–hydrophobic balance and, in essence, is ultimately responsible for protein modification (Dua et al., 1996; Lawal et al., 2007; Sosulski & Fleming, 1977; Yin et al., 2010). Hence, it can be inferred that the degree of acylation, anhydride to protein ration, and protein

type/composition and structure would also contribute to the final functionalities (Yin et al., 2010; Ponnampalam et al., 1988; Achouri & Zhang, 2001; Charoensuk et al., 2018).

Franzen and Kinsella (1976) pointed out that succinylation led to an improvement in flavor of leaf protein. Nevertheless, due to substantially no odors nor flavors being imparted, there is comparatively little to signify whether some specific desirable modified proteins were developed via succinylation. Means and Feeney (1971) also reported that using coffee whiteners with acylated soybean protein endowed end-products with good flavor. It is reasonable to anticipate that acetylation and succinylation of pulse proteins, owing to an alteration in protein inherent structure, may give varied effects on protein–odorants binding affinities, and thus result in retention or release of different flavor compounds (Wang & Arntfield, 2016). Further attempts are needed to unearth specific effects of acylation on flavor formation in pulse proteins.

2.2.2. Phosphorylation

An alternative chemical modification is to synthesize phosphoproteins through introduction of acidic phosphoryl groups into specific active-center residues (**Fig. 2.4B**), primarily covering hydroxyl oxygen, and amino or imidazole nitrogen (Baslé et al., 2010; Matheis, Penner, Feeney, & Whitaker, 1983; Mayer & Heidelberger, 1946). In comparison with extremely acid labile N-bound phosphates that liberate its phosphorus spontaneously in aqueous systems, O-bound ones are more acceptable for incorporation into liquid food systems (Matheis et al., 1983; Matheis & Whitaker, 1984). However, one assumption is N-phospho-amino derivatives may be somewhat superior in terms of digestibility and availability of amino acids (Woo, Creamer, & Richardson, 1982). Its acid lability renders N–P bonds easily to be cleaved during digestion and thus should furnish the same bioavailability as normal amino acids (Woo et al., 1982). Various chemical reagents offering protein phosphorylation have been summarized previously (Frank & Goldwhite, 1984; Kester & Richardson, 1984; Matheis &

Whitaker, 1984). Among them, phosphorus oxychloride (POCl_3) was frequently selected as a phosphorylating donor on a practical and economical basis (**Fig. 2.4B-1**). Some requisite functionality of protein were indeed ameliorated after phosphorylation even in the occurrence of intermolecular polymerization of proteins (Kester & Richardson, 1984; Matheis, 1991). The postulated mechanism of intermolecular cross-linking is shown in **Figure 2.4B** (Matheis, 1991; Matheis & Whitaker, 1984).

More recently, another feasible mean has been portrayed, namely, phosphorylating reactive hydroxylated amino acid residues by dry-heating the homogeneous mixture of proteins and orthophosphate or pyrophosphate (**Fig. 2.4B-2**) (Li, Enomoto, Hayashi, Zhao, & Aoki, 2010; Li et al., 2005; Li, Salvador, Ibrahim, Sugimoto, & Aoki, 2003). Whereas it has been extensively applied into the modification of animal proteins; this approach garners limited investigation for pulse proteins. It was concluded that dry-heating poly-L-lysine hydrobromide in the presence of pyrophosphate introduced an N–P bond; while no N–P bond was formed in the protein employed by this means (Li et al., 2009). Accumulated evidences have indicated that phosphorylation leads to changes in the architecture of proteins, legitimately ascribing to the electrostatic repulsion from incorporated phosphate groups (Li, Enomoto, et al., 2010; Li et al., 2005; Li, Ibrahim, Sugimoto, Hatta, & Aoki, 2004). Accordingly, protein functionalities such as heat stability (Li et al., 2009, 2004, 2003), emulsification (Li, Chen, et al., 2010), foaming (Hayashi et al., 2009), and gelling properties (Chen et al., 2019) were improved with the exception of a slight decrease in water solubility (Li et al., 2005). Basic proteins appeared to be more conveniently phosphorylated rather than acidic ones in the presence of pyrophosphate (Li et al., 2009). With regarding to phosphorylation site, tryptic phosphopeptides was characterized from phosphorylated ovalbumin and identified the development of O–P linkages at threonine 136 and tyrosine 125 residues (Li et al., 2009). It was, however, identified that specific reactive sites in phosphorylated ovalbumin were only

serine residues, including serine 48, 103, 147, 151, 221, 224 and 384 (Wang, Tu, Liu, Zhang, & Chen, 2016). Future study should be focused on elucidating the nature of phosphate linkages and phosphorylation sites on pulse proteins.

In general, phosphorus content that can be introduced in protein is low, with less than 1g/100 g protein can be achieved by dry-heating (85°C and different pHs) (Li, Enomoto, et al., 2010). Proteins firstly being conjugated with maltopentose via glycation, followed by subsequent phosphorylation by dry heating in the presence of pyrophosphate appeared to be an efficient approach to improve the phosphorus level in protein (Enomoto et al., 2009; Hirofumi Enomoto et al., 2007). The complicated procedure, with an attendant limited improvement in phosphorus level, is unwarranted for a large-scale application on a practical and economical basis. Compared to the long incubation (≥ 24 h) of dry-heating phosphorylation where relatively high temperature (usually $\geq 85^\circ\text{C}$) may exceed the thermal denaturation range of some proteins, wet-heating phosphorylation in the presence of sodium tripolyphosphate (**Fig. 2.4B-3**) seems to be more applicable for industrial application (Sheng et al., 2019). Accordingly, some literature have thrown light on the conformational changes in proteins after phosphorylation (Li, Enomoto, et al., 2010; Sheng et al., 2019; Yang et al., 2019). Some researchers claimed that the application of sodium tripolyphosphate allows the phosphate groups to be covalently attached to the $-\text{OH}$ or $-\text{NH}_2$ of amino acid residues, regardless of the dry- or wet-heating systems (Wang, Zhang, Fan, Yang, & Chen, 2019; Xiong, Zhang, & Ma, 2016). However, It was argued that all possible vulnerable phosphate sites from ovalbumin were merely located on serine 221, 269, 281 residues and tyrosine 281 under wet-heating conditions (Sheng et al., 2019). They further pointed out phosphorylation rendered ovalbumin to become more flexible and disordered, which is consistent with the research conducted by Tang, Yu, Lu, Fu, & Cai (2019). Considering protein functionalities, such as solubility, thermal stability, apparent viscosity, emulsification and foaming properties, the hydrophilic phosphorylation of a protein

results in distinctly enhancement in such intriguing properties (Hao et al., 2019; Sheng et al., 2019; Tang et al., 2019; Wang et al., 2019; Xiong et al., 2016; Yang et al., 2019).

2.2.3. Amidation and esterification

Derivatization of non-essential amino acid residues such as aspartic and glutamic acids may afford a more worthwhile approach to the nutritional quality of modified proteins compared to modification of essential amino acid residues, like $-\text{NH}_2$ of lysine or $-\text{OH}$ of threonine (Howell & Taylor, 1991; Mattarella & Richardson, 1983). Numerous proteins whose IEP approximate to pH 5.0 are negatively charged in neutral environment (Kester & Richardson, 1984; Malamud & Drysdale, 1978). Either amidation or esterification of the β - and γ -carboxyl groups of aspartate and glutamate (**Fig. 2.4C&D**) may convert negatively charged amino acids into positively charged derivatives, and thus modulate acidic proteins into basic ones accordingly (Kester & Richardson, 1984; Mattarella, Creamer, & Richardson, 1983).

Performing protein amidation (**Fig. 2.4C**) through a carbodiimide-mediated condensation with ammonium ion as the nucleophile has been documented (Howell & Taylor, 1991; Mattarella et al., 1983; Mattarella & Richardson, 1983). Amidated β -lactoglobulin possessed a more random structure than native protein as evidenced by the raised protein hydrophobicity, due to a change in the distribution of electrostatic interactions (Mattarella et al., 1983; Mattarella & Richardson, 1983). The study from Mattarella et al lent credence to the molten conformation of amidated β -lactoglobulin, which led to an increase in aperiodic structure as well as a remarkable decrease in β -sheet (Mattarella et al., 1983). These resultant alterations were reflected in different functionalities. Aqueous solubility of amidated β -lactoglobulin was improved at very acidic pH 3.0 and then gradually decreased when increasing pH; whereas its emulsification activity was less than that of native proteins (Mattarella & Richardson, 1983). Howell & Taylor (1991) reported foaming properties of bovine serum

albumin were enhanced after amidation. Recently, Sabatini et al proposed an operationally novel protocol for direct amidation utilizing borate esters as catalysts, with a visible improvement in terms of efficiency and sustainability (Sabatini, Boulton, & Sheppard, 2017). With a view to the efficient conversion of readily available amino acids into active pharmaceuticals through the amidation procedure (Sabatini et al., 2017), pulse protein may be amidated by adopting this protocol. Intriguingly, it is worthwhile to investigate whether such novel approach could bring about desirable alterations in protein functionalities.

In general, a protein is esterified when its exposed carboxyl groups are susceptible to nucleophilic attack by alcohols with the aid of hydrochloric acid as a catalyst (**Fig. 2.4D**). Sitohy et al sought to exploit the optimum esterification parameters, and concluded the extent of esterification closely associated with the level of acidic amino acid side chain of proteins, moisture content and the type of alcohol employed (Sitohy, Chobert, & Haertle, 2000). Esterification may facilitate structural unfolding of a protein, and consequently impact its functionalities (Briand, Chobert, & Haertlé, 1995; Mattarella et al., 1983; Mattarella & Richardson, 1983; Wang, Sun, & Wang, 2006). Briand et al identified 22 pepsin cleavage sites in esterified β -lactoglobulin that were partly derived from esterification-enhanced peptide bond accessibility, implying a potential improvement in peptic digestibility (Briand et al., 1995). Esterified soy protein gave a marked promotion in adhesive performance than native proteins, especially in water resistance, which may boost the application of a pulse protein based adhesive in green and sustainable chemical industry (Wang, Sun, & Wang, 2006). The increase in the amount of exposed hydrophobic groups stemming from the molten structural state was supposed to account for the elevated water resistance. Sitohy and Osman noticed that the solubility of three pulse proteins (soybean, broad bean, and chickpea) was improved to a certain extent at the pH range of 2.0–5.0 after esterification (Sitohy & Osman, 2010). Meanwhile,

emulsification and foaming properties of these esterified pulse proteins at the acidic pH range of 2.0–6.0 were superior than the corresponding native proteins (Osman, 2015).

2.3. Non-enzymatic Glycation

Of these chemical modifications, non-enzymatic glycation via Maillard reaction is one primary route for both function alteration and flavor development. This reaction occurs between carbonyls and amines is responsible for the aromas and flavors enjoyed by consumers; it, however, is simultaneously accompanied by the potential occurrence of off-flavors (Hellwig & Henle, 2014). The hitherto known concept of natural has been deeply rooted in the public mind (Feeney, 1977), with their fear for the word “chemical”. It is quite conceivable that non-enzymatic glycation via Maillard reaction, as characterized by spontaneous and natural without extraneous chemicals (de Oliveira, Coimbra, de Oliveira, Zuñiga, & Rojas, 2016; Oliver, Melton, & Stanley, 2006), shall be the most promising means for protein modification with a view to “green chemistry”. Hence, it is worth to review this reaction separately with the aforementioned chemical reactions.

2.3.1. Structure modification of protein by non-enzymatic glycation

The Maillard reaction, a thermally driven reaction between amino groups and carboxyl-containing moiety, inevitably triggered an alteration in protein charge and/or conformation with subsequent protein functionalities (de Oliveira et al., 2016; Oliver et al., 2006). The potential active amino acid residues including ϵ -amino group of lysine and the guanidino group of arginine in proteins are the primary sites of reaction (**Fig. 2.5A**) (Hellwig & Henle, 2014). Noteworthy, apart from attractive taste, appearance and pleasant aromas, Maillard reaction could also generate off-flavors and potentially deleterious substances (Hellwig & Henle, 2014; Newton, Fairbanks, Golding, Andrewes, & Gerrard, 2012). Hence, depending on the desired product features, designing the progress of Maillard reaction is of practical interest to food manufacturers (Newton et al., 2012; Martins, Jongen, & Van Boekel, 2000). A simplified

overview of Maillard reaction process is depicted in **Figure 2.5B**, which is divided into three phases (Hodge, 1953). The documented beneficial outcomes of Maillard reaction arise primarily at the initial and advanced phase (de Oliveira et al., 2016; Oliver et al., 2006). Particularly, the glycated protein conjugates functioning as an enhancer in protein functionalities are originated from Amadori rearrangement steps (**Figure 2.5B**) (Liu, Ru, & Ding, 2012; Zha, Yang, Rao, & Chen, 2019). Polysaccharides appear to be a better choice for controlling the extent of Maillard reaction, whose low reactivity and steric hindrance could block excessive color development and protein polymerization (de Oliveira et al., 2016).

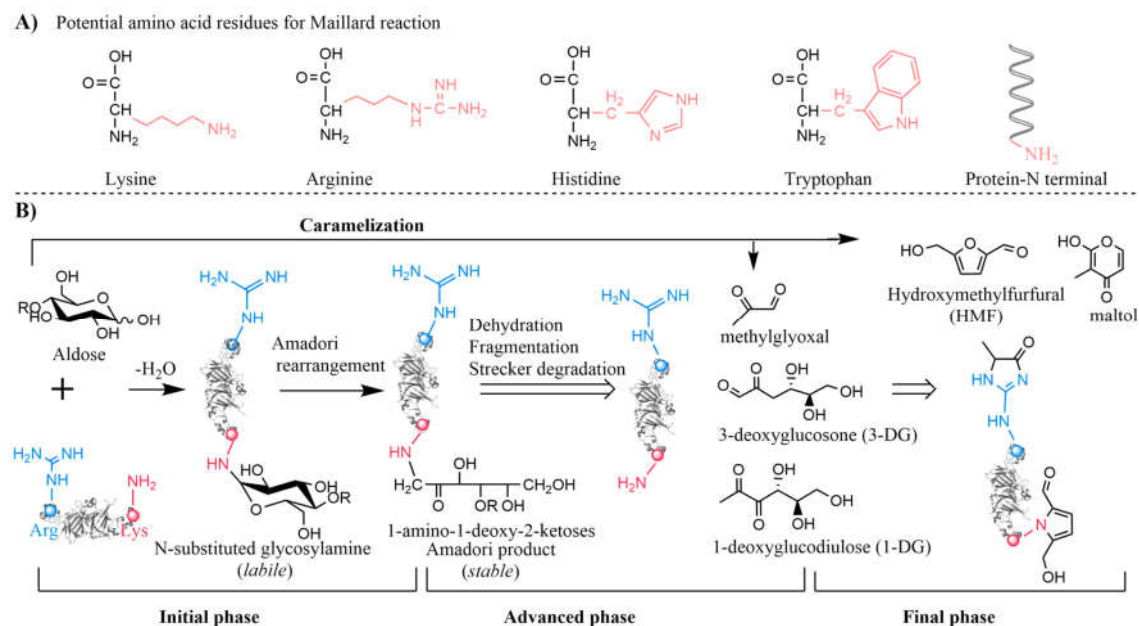


Figure 2.5. Schematic presentation of Maillard reaction. (A) potential amino acid residues for Maillard; (B) Maillard reaction on proteins (adapted from Hellwig & Henle, 2014).

Performing non-enzymatic glycation via Maillard reaction either dry-heating or wet-heating in buffer solution is mainstream. A dry-heating reaction is initiated by lyophilizing a solution of protein–saccharide (carbonyl donor) complexes, and thereafter incubating the homogenous dispersion under given temperature and relative humidity (de Oliveira et al., 2016; Oliver et al., 2006). The homogenous state, however, is very relative, particularly in the case of globular or rigid proteins (de Oliveira et al., 2016; Li et al., 2013; Zhuo et al., 2013). One

significant challenge of dry-heating lies in long incubation time that can go up from days or weeks in order to achieve sufficient level of glycation (de Oliveira et al., 2016; Oliver et al., 2006). Undeniably, dry reactants possess longer stability and is more ease of manipulation and preservation than that in an aqueous system (Oliver et al., 2006). Wet-heating on the other hand is characterized as shorter incubation time and more homogenous dispersion of reactants; however, it could simultaneously increase risk of protein denaturation and polymerization at elevated temperature (de Oliveira et al., 2016). In contrast, glycation in the dry condition does not significantly alter the native-like behavior of a protein (Oliver et al., 2006). New non-thermal techniques, such as pulsed electric fields and ultrasound, are applied to assist the glycation, and succeed in creating novel functional properties (Fu et al., 2019; Guan et al., 2010).

Processing parameters, such as the ratio of reactants, incubation time, protein structure (rigid or flexible), and carbohydrate chain length/structure (branched or straight chain) intervening in the synthesis of glycated protein have been concretely addressed in several critical reviews (de Oliveira et al., 2016; Oliver et al., 2006; Liu et al., 2012). Among most of the carbohydrates, gum Arabic is a popular candidate to conjugate with a wide variety of proteins via Maillard-driven chemistry. This is because gum Arabic is a highly branched complex polysaccharide whose main chain consists of 1,3-linked β -D-galactopyranosyl units (Sanchez et al., 2008). In addition, it contains ~2% of a polypeptide and is referred to as a heteropolysaccharide, bearing good functionalities. It has been broadly utilized in food systems as functional ingredients, such as emulsifier, texturizer, flavor-stabilizing agents, etc (de Oliveira et al., 2015). The main source of commercial gum Arabic is from *Acacia senegal* and *Acacia seyal* (Sanchez et al., 2008).

The structural consequences of such a modification are of practical interest since protein functionalities are profoundly influenced by its conformation and dissociation–

association state. Covalently grafting hydrophilic carbohydrate residues to a protein is expected to induce an increment in net negative charge; thus reducing IEP followed by conformational changes. The reality may differ considerably according to the literature. Du et al (2013) pointed out dry-heating glycation of rice dreg glutelin with κ -carrageenan lowered amounts of α -helix and β -sheet of glutelin concomitant with the raise in β -turns and random coil. It has been appraised that the β -sheet structures (“trains”) are relatively stable, while the α -helix, β -turn, and random coil structures (“loops”) are somewhat flexible and open (Xu et al., 2016; Yong, Yamaguchi, & Matsumura, 2006). Hence, this implies that dry-heating glycation with κ -carrageenan rendered the secondary structure of rice dreg glutelin to be a more extended form. Similarly, incorporation of glucose moieties into β -casein by glycation in wet-heating mitigated the degree of helicity of β -casein and probably resulted in β -turns formation (Darewicz & Dziuba, 2001). Guan et al also reported that grafting dextran to bovine serum albumin through pulsed electric field treatment caused a reduction in the level of α -helix and random coil, with a distinct increase in β -sheet and β -turns (Guan et al., 2010). Fu et al revealed ultrasound-assisted glycation of ovalbumin with xylose caused a distinct reduction in the level of α -helix and random coil, while increased in β -sheet and β -turn. The consequence of such structural modification rendered greater flexibility and loosening in tertiary structure of ovalbumin (Fu et al., 2019). In contrast, Niu et al noted that conjugating wheat germ protein with dextran under wet-heating led to a significant reduction of random coil and β -sheet while increment in α -helix (Niu, Jiang, Pan, & Zhai, 2011).

Interestingly, dry-heating glycation with low molecular weight carbohydrates appeared to show minimum effect on protein conformational changes. It was reported that the attachment of maltopentaose (~830 Da) to β -lactoglobulin under a restricted water environment did not incur a distinct change to the protein secondary structure (Enomoto et al., 2007). Additionally, glucose or maltodextrins (1 kDa), low molecular weight carbohydrate moieties, covalently

anchored to the protein insufficiently impacted the secondary structure of the protein (Wong, Day, McNaughton, & Augustin, 2009). Nevertheless, the structural alterations were reported in deamidated wheat protein upon conjugation with larger molecular weight maltodextrins (1.9 kDa or 4.3 kDa) in a dry state (Wong et al., 2009). The functionalities of glycated protein could also be regarded as an indirect evidence to hint the role of carbohydrate molar mass on protein conformation changes. Shu et al noted that emulsification properties of glycated lysozyme enhanced with increment in galactomannan molar mass (6–24 kDa); while glycation with the low molar mass of xyloglucan (1.4 kDa) and galactomannan (3.5–6 kDa) did not (Shu, Sahara, Nakamura, & Kato, 1996).

A question arises as to whether it is the heating method rather than carbohydrate molecular weight that regulates conformational changes of glycated protein. Morgan et al reported that conformation of globular β -lactoglobulin was drastically modified as glycation was performed with lactose in an aqueous wet-heating condition; while dry-heating did not significantly alter the native-like behaviors of the protein although it had higher degree of glycation (Morgan et al., 1999). They further noted that wet-heating glycation of dimeric β -lactoglobulin with lactose allowed the protein dissociated into structural unfolded monomer, that was then covalently linked by the free thiol groups to generate homodimers. Finally, non-covalent association between the unfolded homodimers underwent substantial aggregation resulting in the formation of polymers. The findings imply that protein structure seems to be more susceptible for modification under wet-heating conditions.

It is plausible that the number of carbohydrate moieties anchored to proteins may also influence the protein structures as well as the functionalities. A distinct structural unfolding occurred when whey protein isolate was glycated with 5 dextran moieties per molar of protein under a restricted wet-heating condition, but negligible alterations for 1 dextran moiety/protein (Wooster & Augustin, 2007). Shu et al also noted that 2 molar of galactomannan grafted to,

when attached to N-terminal and 97-lysine of one molar lysozyme in a dry-heating, gave excellent emulsification properties superior to those of 1 galactomannan/molar of protein (Shu et al., 1996). A challenge is to determine how to overcome the steric hindrance of the grafted saccharides and further boost the number of saccharides during protein glycation.

Admittedly, most of the reported fundamental research on protein non-enzymatic glycation was conducted using animal proteins. The far-reaching insights into changes of animal protein functionalities after controlled glycation gained, such as improved protein solubility, enhanced emulsification activity, upgraded foaming properties, reinforced thermal stability, and advanced antioxidant activity have shed light to the glycation of pulse proteins. In research reported in this dissertation, it was observed a darker color accompanied by interfacial and morphological microstructure alterations of yellow pea proteins when extending glycation with gum Arabic (Zha, Dong, Rao, & Chen, 2019a, 2019b; Zha, Yang, et al., 2019). In addition, the functionalities of glycated yellow pea protein including solubility, emulsification stability, and antioxidant activity were improved accordingly. The improvement of pea protein functionality was mainly attributed to increased steric hindrance rather than electrostatic repulsion generated by the grafted polysaccharide.

2.3.2. Maillard-flavor formation

Non-enzymatic glycation via Maillard reaction possess incomparable potency to modulate flavor profiles of a protein. Volatiles derived from the reaction with low chemosensory thresholds can act as exceptionally key contributors to food aroma (Hofmann, Krautwurst, & Schieberle, 2018). Cutting-edge flavor chemistry research has purveyed a toolkit to bridge the molecular structure with flavor characteristics, as well as elucidate avenues of flavor generation during glycation reaction (Hofmann, Krautwurst, & Schieberle, 2018). Principal pathways for the development of flavor compounds are outlined below.

Amadori compounds (1-amino-1-deoxy-2-ketoses) are critical non-volatile flavoring precursors (Hodge et al., 1972). Their degradation products *vic*-dicarbonyl compounds have an indispensable role in flavor development (Hellwig & Henle, 2014). Amadori compounds via 1,2- or 2,3-enolization and deamination produce *vic*-dicarbonyl compounds, e.g., 1-deoxyglucodiulose (1-DG) and 3-deoxyglucosone (3-DG), which further react with primary amines or hydrogen sulfide to form heterocyclic derivatives (Hellwig & Henle, 2014; Reineccius, 2005; Nursten, 2005). Alternatively, Amadori or *vic*-dicarbonyl compounds fragment into short-chain carboxylic acids and aldehydes through retro-aldolization or oxidative fission, of which can be aroma-active (Hellwig & Henle, 2014; Reineccius, 2005; Nursten, 2005). Strecker degradation of dicarbonyl compounds and their vinylogues also is a prime avenue, where they deaminate and decarboxylate to gain the corresponding aldehydes (Hellwig & Henle, 2014; Reineccius, 2005; **Fig.2.6**).

Five categories of structures as characteristic flavor generators during Maillard reaction are illustrated in **Figure 2.6A**. Caramel aroma-active components are labelled with cyclic enolones that give *O*-heterocyclic structures. Some specific *O*-heterocyclic and alicyclic caramel-like aroma compounds are listed in **Figure 2.6B**. Maltol (**1**) and ethyl maltol (2-ethyl-3-hydroxy-4(4H)-pyranone, **2**) have been identified in foods to perceive a caramel-like odor (Newton et al., 2012; Hodge et al., 1972; Reineccius, 2005). Furaneol (4-hydroxy-2,5-dimethyl-3(2H) furanone, **3**) has a burnt pineapple, strawberry-like aroma, and acts as a flavor enhancer for sweet products (Hellwig & Henle, 2014; Reineccius, 2005). Cyclotene (**4**) has a characteristic sweet maple odor, and its derivative 3-ethyl-2-hydroxy-2-cyclopenten-1-one (**5**) also gives nutty, maple and caramel flavors (Hellwig & Henle, 2014; Reineccius, 2005). The structural characteristics insofar as corny, nutty, bready, and roasted odorants (**Figure 2.6A**) are *N*-heterocyclic ring with 1 or 2 nitrogen atoms (Hodge et al., 1972). Of which this class of flavors, partially saturated *N*-heterocyclic derivatives (dotted portion) substituted with *C*-alkyl

or acetyl groups (R_1 in **Fig. 2.6A**) are dominant (Hodge et al., 1972). The characteristic aroma-structure correlation for *N*-heterocyclic compounds is shown in **Figure 2.6B**. The *C*-alkyl pyrazines foster roasted, nut-like aromas whereas methoxypyrazines generally have earthy, vegetable odors (Ohloff & Flament, 1979). 2-isobutyl-3-methoxy pyrazine (freshly green pepper aroma, **6**), acetyl pyrazines (popcorn character, **7**), and 2-acetyl pyrazine (roasted or burnt flavor, **8**) have been identified as prominent flavors in foods (Reineccius, 2005). As two most abundant pyrroles in foods, 2-formyl pyrrole (**9**) and 2-acetyl pyrrole (**10**) have been registered as sweet corny aroma and caramel-like odor, respectively (Ohloff & Flament, 1979; Reineccius, 2005). Despite pyridine compounds carry a broad array of chemical flavors, green odors are rather ordinary (Pittet & Hruza, 1974). 3-methylpyridine (green odor, **11**), 2-acetylpyridine (tobacco-like odor, **12**), and 3-methyl-4-ethyl pyridine (sweet and nutty, **13**) are singled out as exclusive Maillard reaction flavors in dairy products (Reineccius, 2005). Pyrrolines, such as 2-acetyl-1-pyrroline (popcorn-like odor, **14**), generally contribute to cereal or roasted notes (Hodge et al., 1972; Reineccius, 2005; Schieberle & Grosch, 1987).

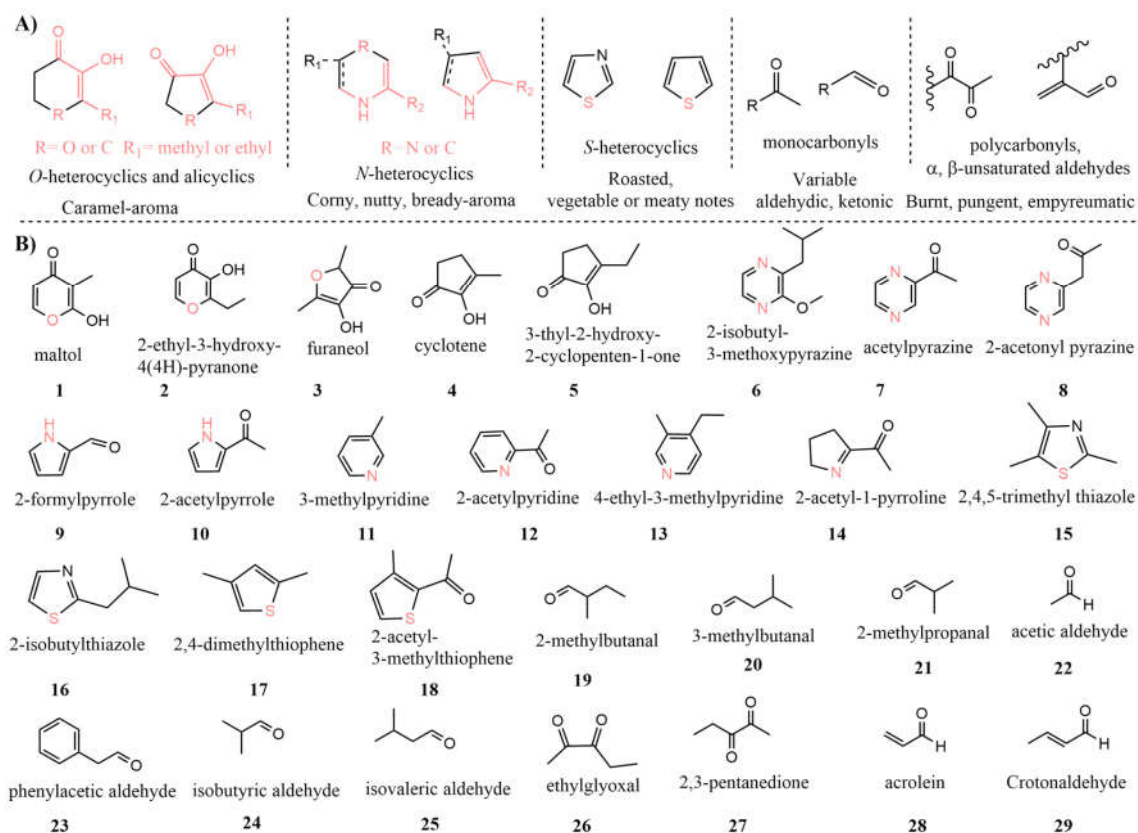


Figure 2.6. (A) Aroma and structure classification of flavor compounds resulting during the Maillard reaction or caramelization (adapted from Hodge et al., 1972); (B) common Maillard reaction compounds responsible for flavor in dairy products.

The thiazoles and thiophenes give nutty, roasted, vegetable, or meaty notes, whose structures are characterized as *S*-heterocyclic ring in nature (Reineccius, 2005). Some *S*-heterocyclics, like trimethyl thiazole (cocoa, nutty character, **15**), 2-isobutyl thiazole (green odor of tomato leaf, **16**), 2,4-dimethyl thiophene (fried onions, **17**), and 2-acetyl-3-methyl thiophene (honey-like, **18**), typical Maillard reaction products (**Fig. 2.6B**) (Reineccius, 2005). The monocarbonyl structures (**Fig. 2.6A**) register as variable aldehydes or ketone aromas, a selection of which are listed in **Figure 2.6B**. 2-methylbutanal (**19**), 3-methylbutanal (**20**), and 2-methylpropanal (**21**) are responsible for characteristic roasted aroma of kilned barley (Hodge et al., 1972; Wang, Kato, & Fujimaki, 1968). Acetic (**22**), phenylacetic (**23**), isobutyric (**24**), and isovaleric (**25**) aldehydes also contribute to bread, malt, peanut, and cocoa aromas (Hodge et al., 1972). A myriad of vicinal polycarbonyl structures and α , β -unsaturated aldehydes (**Fig.**

2.6A) are generally described as pungent, burnt aromas in character, such as ethylglyoxal (26), 2,3-pentanedione (27), acrolein (28), and crotonaldehyde (29) (Hodge et al., 1972). And these burnt-like flavor intermediates tend to condense readily for the development of melanoidins when the progress of this reaction proceeds to the final stage (Hodge et al., 1972). The flavor improvement of glycated pulse protein has yet to be broadly investigated.

2.4. References

- Achouri, A., & Zhang, W. (2001). Effect of succinylation on the physicochemical properties of soy protein hydrolysate. *Food Research International*, 34(6), 507–514.
[https://doi.org/10.1016/S0963-9969\(01\)00063-1](https://doi.org/10.1016/S0963-9969(01)00063-1)
- Baslé, E., Joubert, N., & Pucheault, M. (2010). Protein chemical modification on endogenous amino acids. *Chemistry and Biology*, 17(3), 213–227.
<https://doi.org/10.1016/j.chembiol.2010.02.008>
- Briand, L., Chobert, J. -M., & Haertlé, T. (1995). Peptic proteolysis of esterified β -casein and β -lactoglobulin. *International Journal of Peptide and Protein Research*, 46(1), 30–36.
<https://doi.org/10.1111/j.1399-3011.1995.tb00579.x>
- Chalker, J. M., Bernardes, G. J. L., Lin, Y. A., & Davis, B. G. (2009). Chemical modification of proteins at cysteine: Opportunities in chemistry and biology. *Chemistry - An Asian Journal*, 4(5), 630–640. <https://doi.org/10.1002/asia.200800427>
- Charoensuk, D., Brannan, R. G., Chanasattru, W., & Chaiyasit, W. (2018). Physicochemical and emulsifying properties of mung bean protein isolate as influenced by succinylation. *International Journal of Food Properties*, 21(1), 1633–1645.
<https://doi.org/10.1080/10942912.2018.1502200>
- Chen, J., Ren, Y., Zhang, K., Qu, J., Hu, F., & Yan, Y. (2019). Phosphorylation modification of myofibrillar proteins by sodium pyrophosphate affects emulsion gel formation and

- oxidative stability under different pH conditions. *Food and Function*, 10(10), 6568–6581. <https://doi.org/10.1039/c9fo01397k>
- Chéreau, D., Videcoq, P., Ruffieux, C., Pichon, L., Motte, J. C., Belaid, S., Ventureira, J., & Lopez, M. (2016). Combination of existing and alternative technologies to promote oilseeds and pulses proteins in food applications. *OCL - Oilseeds and Fats, Crops and Lipids*, 41(1). <https://doi.org/10.1051/ocl/2016020>
- Darewicz, M., & Dziuba, J. (2001). The effect of glycosylation on emulsifying and structural properties of bovine β -casein. *Nahrung - Food*, 45(1), 15–20. [https://doi.org/10.1002/1521-3803\(20010101\)45:1<15::AID-FOOD15>3.0.CO;2-Y](https://doi.org/10.1002/1521-3803(20010101)45:1<15::AID-FOOD15>3.0.CO;2-Y)
- de Oliveira, F. C., Coimbra, J. S. dos R., de Oliveira, E. B., Zuñiga, A. D. G., & Rojas, E. E. G. (2016). Food protein-polysaccharide conjugates obtained via the Maillard reaction: A review. *Critical Reviews in Food Science and Nutrition*, 56(7), 1108–1125. <https://doi.org/10.1080/10408398.2012.755669>
- de Oliveira, F. C., Dos Reis Coimbra, J. S., de Oliveira, E. B., Rodrigues, M. Q. R. B., Sabioni, R. C., De Souza, B. W. S., & Santos, I. J. B. (2015). Acacia gum as modifier of thermal stability, solubility and emulsifying properties of α -lactalbumin. *Carbohydrate Polymers*, 119, 210–218. <https://doi.org/10.1016/j.carbpol.2014.11.060>
- Du, Y., Shi, S., Jiang, Y., Xiong, H., Woo, M. W., Zhao, Q., Bai, C., Zhou, Q., & Sun, W. (2013). Physicochemical properties and emulsion stabilization of rice dreg glutelin conjugated with κ -carrageenan through Maillard reaction. *Journal of the Science of Food and Agriculture*, 93(1), 125–133. <https://doi.org/10.1002/jsfa.5739>
- Dua, S., Mahajan, A., & Mahajan, A. (1996). Improvement of functional properties of rapeseed (*Brassica campestris* var. Toria) preparations by chemical modification. *Journal of Agricultural and Food Chemistry*, 44(3), 706–710. <https://doi.org/10.1021/jf950289h>

- Enomoto, H., Hayashi, Y., Li, C. P., Ohki, S., Ohtomo, H., Shiokawa, M., & Aoki, T. (2009). Glycation and phosphorylation of α -lactalbumin by dry heating: Effect on protein structure and physiological functions. *Journal of Dairy Science*, *92*(7), 3057–3068. <https://doi.org/10.3168/jds.2009-2014>
- Enomoto, Hirofumi, Li, C. P., Morizane, K., Ibrahim, H. R., Sugimoto, Y., Ohki, S., Ohtomo, H., & Aoki, T. (2007). Glycation and phosphorylation of β -lactoglobulin by dry-heating: Effect on protein structure and some properties. *Journal of Agricultural and Food Chemistry*, *55*(6), 2392–2398. <https://doi.org/10.1021/jf062830n>
- Feeney, R. E. (1977). Chemical modification of food proteins. *In Food Proteins* (3–36). <https://doi.org/10.1021/ba-1977-0160.ch001>
- Frank, A. W., & Goldwhite, H. (1984). Synthesis and properties of N-, O-, and S-phospho derivatives of amino acids, peptides, and protein. *Critical Reviews in Biochemistry and Molecular Biology*, *16*(1), 51–101. <https://doi.org/10.3109/10409238409102806>
- Franzen, K. L., & Kinsella, J. E. (1976). Functional properties of succinylated and acetylated leaf protein. *Journal of Agricultural and Food Chemistry*, *24*(5), 914–919. <https://doi.org/10.1021/jf60207a041>
- Fu, X., Liu, Q., Tang, C., Luo, J., Wu, X., Lu, L., & Cai, Z. (2019). Study on structural, rheological and foaming properties of ovalbumin by ultrasound-assisted glycation with xylose. *Ultrasonics Sonochemistry*, *58*. 104644 <https://doi.org/10.1016/j.ultsonch.2019.104644>
- Fukuda, T., Maruyama, N., Salleh, M. R. M., Mikami, B., & Utsumi, S. (2008). Characterization and crystallography of recombinant 7S globulins of Adzuki bean and structure-function relationships with 7S globulins of various crops. *Journal of Agricultural and Food Chemistry*, *56*(11), 4145–4153. <https://doi.org/10.1021/jf072667b>

- Guan, Y. G., Lin, H., Han, Z., Wang, J., Yu, S. J., Zeng, X. A., Liu, YY., & Sun, W. W. (2010). Effects of pulsed electric field treatment on a bovine serum albumin-dextran model system, a means of promoting the Maillard reaction. *Food Chemistry*, *123*(2), 275–280. <https://doi.org/10.1016/j.foodchem.2010.04.029>
- Hao, L., Lin, G., Chen, C., Zhou, H., Chen, H., & Zhou, X. (2019). Phosphorylated zein as biodegradable and aqueous nanocarriers for pesticides with sustained-release and anti-UV properties. *Journal of Agricultural and Food Chemistry*, *67*(36), 9989–9999. <https://doi.org/10.1021/acs.jafc.9b03060>
- Hayashi, Y., Nagano, S., Enomoto, H., Li, C. P., Sugimoto, Y., Ibrahim, H. R., Hatta, H., Takeda, C., & Aoki, T. (2009). Improvement of foaming property of egg white protein by phosphorylation through dry-heating in the presence of pyrophosphate. *Journal of Food Science*, *74*(1), 68–72. <https://doi.org/10.1111/j.1750-3841.2008.01019.x>
- Hellwig, M., & Henle, T. (2014). Baking, ageing, diabetes: A short history of the Maillard reaction. *Angewandte Chemie International Edition*, *53*(39), 10316–10329. <https://doi.org/10.1002/anie.201308808>
- Hodge, J. E. (1953). Dehydrated foods, chemistry of browning reactions in model systems. *Journal of Agricultural and Food Chemistry*, *1*(15), 928–943. <https://doi.org/10.1021/jf60015a004>
- Hodge, J. E., Mills, F. D., & Fisher, B. E. (1972). Compounds of browned flavor derived from sugar-amine reactions I aromas: Structures: classes of compounds: caramel cyclic enolones. *Cereal Science Today*, *17*(2), 34–40.
- Hofmann, T., Krautwurst, D., & Schieberle, P. (2018). Current status and future perspectives in flavor research: Highlights of the 11th Wartburg symposium on flavor chemistry & biology. *Journal of Agricultural and Food Chemistry*, *66*(10), 2197–2203. <https://doi.org/10.1021/acs.jafc.7b06144>

- Howell, N. K., & Taylor, C. (1991). Effect of amidation on the foaming and physico-chemical properties of bovine serum albumin. *International Journal of Food Science & Technology*, 26(4), 385–395. <https://doi.org/10.1111/j.1365-2621.1991.tb01981.x>
- Jain, A., Kumar, A., & Salunke, D. M. (2016). Crystal structure of the vicilin from *Solanum melongena* reveals existence of different anionic ligands in structurally similar pockets. *Scientific Reports*, 6, 23600. <https://doi.org/10.1038/srep23600>
- Johnson, E. A., & Brekke, C. J. (1983). Functional properties of acylated pea protein isolates. *Journal of Food Science*, 48(3), 722–725. <https://doi.org/10.1111/j.1365-2621.1983.tb14883.x>
- Kester, J. J., & Richardson, T. (1984). Modification of whey proteins to improve functionality. *Journal of Dairy Science*, 67(11), 2757–2774. [https://doi.org/10.3168/jds.S0022-0302\(84\)81633-1](https://doi.org/10.3168/jds.S0022-0302(84)81633-1)
- Klupšaitė, D., & Juodeikienė, G. (2015). Legume: composition, protein extraction and functional properties. A review. *Chemical Technology*, 66(1). <https://doi.org/10.5755/j01.ct.66.1.12355>
- Krause, J. P. (2002). Comparison of the effect of acylation and phosphorylation on surface pressure, surface potential and foaming properties of protein isolates from rapeseed (*Brassica napus*). *Industrial Crops and Products*, 15(3), 221–228. [https://doi.org/10.1016/S0926-6690\(01\)00117-0](https://doi.org/10.1016/S0926-6690(01)00117-0)
- Lam, A. C. Y., Can Karaca, A., Tyler, R. T., & Nickerson, M. T. (2018). Pea protein isolates: Structure, extraction, and functionality. *Food Reviews International*, 34(2), 126–147. <https://doi.org/10.1080/87559129.2016.1242135>
- Lawal, O. S., Adebawale, K. O., & Adebawale, Y. A. (2007). Functional properties of native and chemically modified protein concentrates from bambarra groundnut. *Food Research International*, 40(8), 1003–1011. <https://doi.org/10.1016/j.foodres.2007.05.011>

- Li, C. P., Chen, D., Peng, J., Enomoto, H., Hayashi, Y., Li, C., Ou, L., & Aoki, T. (2010). Improvement of functional properties of whey soy protein phosphorylated by dry-heating in the presence of pyrophosphate. *LWT - Food Science and Technology*, *43*(6), 919–925. <https://doi.org/10.1016/j.lwt.2010.01.027>
- Li, C. P., Enomoto, H., Hayashi, Y., Zhao, H., & Aoki, T. (2010). Recent advances in phosphorylation of food proteins: A review. *LWT - Food Science and Technology*, *43*(9), 1295–1300. <https://doi.org/10.1016/j.lwt.2010.03.016>
- Li, C. P., Hayashi, Y., Enomoto, H., Hu, F., Sawano, Y., Tanokura, M., & Aoki, T. (2009). Phosphorylation of proteins by dry-heating in the presence of pyrophosphate and some characteristics of introduced phosphate groups. *Food Chemistry*, *114*(3), 1036–1041. <https://doi.org/10.1016/j.foodchem.2008.10.066>
- Li, C. P., Hayashi, Y., Shinohara, H., Ibrahim, H. R., Sugimoto, Y., Kurawaki, J., Matsudomi, N., & Aoki, T. (2005). Phosphorylation of ovalbumin by dry-heating in the presence of pyrophosphate: Effect on protein structure and some properties. *Journal of Agricultural and Food Chemistry*, *53*(12), 4962–4967. <https://doi.org/10.1021/jf047793j>
- Li, C. P., Ibrahim, H. R., Sugimoto, Y., Hatta, H., & Aoki, T. (2004). Improvement of functional properties of egg white protein through phosphorylation by dry-heating in the presence of pyrophosphate. *Journal of Agricultural and Food Chemistry*, *52*(18), 5752–5758. <https://doi.org/10.1021/jf0498259>
- Li, C. P., Salvador, A. S., Ibrahim, H. R., Sugimoto, Y., & Aoki, T. (2003). Phosphorylation of egg white proteins by dry-heating in the presence of phosphate. *Journal of Agricultural and Food Chemistry*, *51*(23), 6808–6815. <https://doi.org/10.1021/jf030043+>
- Li, Y., Zhong, F., Ji, W., Yokoyama, W., Shoemaker, C. F., Zhu, S., & Xia, W. (2013). Functional properties of Maillard reaction products of rice protein hydrolysates with

mono-, oligo- and polysaccharides. *Food Hydrocolloids*, 30(1), 53–60.

<https://doi.org/10.1016/j.foodhyd.2012.04.013>

Liu, J., Ru, Q., & Ding, Y. (2012). Glycation a promising method for food protein

modification: Physicochemical properties and structure, a review. *Food Research*

International, 49(1), 170–183. <https://doi.org/10.1016/j.foodres.2012.07.034>

Liu, Y., Zhang, L., Li, Y., Yang, Y., Yang, F., & Wang, S. (2018). The functional properties

and structural characteristics of deamidated and succinylated wheat gluten. *International Journal of Biological Macromolecules*, 109, 417–423.

<https://doi.org/10.1016/j.ijbiomac.2017.11.175>

Malamud, D., & Drysdale, J. W. (1978). Isoelectric points of proteins: A table. *Analytical*

Biochemistry, 86(2), 620–647. [https://doi.org/10.1016/0003-2697\(78\)90790-X](https://doi.org/10.1016/0003-2697(78)90790-X)

Mandal, S., & Mandal, R. K. (2000). Seed storage proteins and approaches for improvement

of their nutritional quality by genetic engineering. *Current Science*, 79, 576–589.

Martins, S. I. F. S., Jongen, W. M. F., & Van Boekel, M. A. J. S. (2000). A review of

Maillard reaction in food and implications to kinetic modelling. *Trends in Food Science*

and Technology, 11(9-10), 364–373. [https://doi.org/10.1016/S0924-2244\(01\)00022-X](https://doi.org/10.1016/S0924-2244(01)00022-X)

Matheis, G. (1991). Phosphorylation of food proteins with phosphorus oxychloride-

Improvement of functional and nutritional properties: A review. *Food Chemistry*, 39(1),

13–26. [https://doi.org/10.1016/0308-8146\(91\)90081-X](https://doi.org/10.1016/0308-8146(91)90081-X)

Matheis, Günter, Penner, M. H., Feeney, R. E., & Whitaker, J. R. (1983). Phosphorylation of

casein and lysozyme by phosphorus oxychloride. *Journal of Agricultural and Food*

Chemistry, 31(2), 379–387. <https://doi.org/10.1021/jf00116a049>

Matheis, Günter, & Whitaker, J. R. (1984). Chemical phosphorylation of food proteins: An

Overview and a Prospectus. *Journal of Agricultural and Food Chemistry*, 32(4), 699–

705. <https://doi.org/10.1021/jf00124a002>

- Mattarella, N. L., Creamer, L. K., & Richardson, T. (1983). Amidation or esterification of bovine β -Lactoglobulin to form positively charged proteins. *Journal of Agricultural and Food Chemistry*, 31(5), 968–972. <https://doi.org/10.1021/jf00119a012>
- Mattarella, N. L., & Richardson, T. (1983). Physicochemical and functional properties of positively charged derivatives of bovine β -lactoglobulin. *Journal of Agricultural and Food Chemistry*, 31(5), 972–978. <https://doi.org/10.1021/jf00119a013>
- Mayer, M., & Heidelberger, M. (1946). Physical, chemical and immunological properties of phosphorylated crystalline horse serum albumin. *Journal of the American Chemical Society*, 68(1), 18–25. <https://doi.org/10.1021/ja01205a007>
- Means, G E., & Feeney, R. E. (1971). Chemical modification of proteins. *Current Protocols in Protein Science*. 57(1), 15-0. <https://doi.org/10.1002/0471140864.ps1500s57>
- Miedzianka, J., Pęksa, A., & Aniołowska, M. (2012). Properties of acetylated potato protein preparations. *Food Chemistry*, 133(4), 1283–1291. <https://doi.org/10.1016/j.foodchem.2011.08.080>
- Mohamed, A., Biresaw, G., Xu, J., Hojilla-Evangelista, M. P., & Rayas-Duarte, P. (2009). Oats protein isolate: Thermal, rheological, surface and functional properties. *Food Research International*, 42(1), 107–114. <https://doi.org/10.1016/j.foodres.2008.10.011>
- Moreno, F. J., & Clemente, A. (2008). 2S albumin storage proteins: What makes them food allergens? *The Open Biochemistry Journal*, 2, 16–28. <https://doi.org/10.2174/1874091x00802010016>
- Morgan, F., Mollé, D., Henry, G., Vénien, A., Léonil, J., Peltre, G., Levieux, D., Maubois, J. L., & Bouhallab, S. (1999). Glycation of bovine β -lactoglobulin: Effect on the protein structure. *International Journal of Food Science and Technology*, 34(5–6), 429–435. <https://doi.org/10.1046/j.1365-2621.1999.00318.x>

- Mune, M. A., Minka, S. R., & Mbome, I. L. (2011). Functional properties of acetylated and succinylated cowpea protein concentrate and effect of enzymatic hydrolysis on solubility. *International Journal of Food Sciences and Nutrition*, 62(4), 310–317. <https://doi.org/10.3109/09637486.2010.538670>
- Murthy, N. V. K. K., & Rao, M. S. N. (1984). Acid denaturation of mustard 12S protein. *International Journal of Peptide and Protein Research*, 23(1), 94–103. <https://doi.org/10.1111/j.1399-3011.1984.tb02697.x>
- Newton, A. E., Fairbanks, A. J., Golding, M., Andrewes, P., & Gerrard, J. A. (2012). The role of the Maillard reaction in the formation of flavour compounds in dairy products - Not only a deleterious reaction but also a rich source of flavour compounds. *Food and Function*, 3(12), 1231–1241. <https://doi.org/10.1039/c2fo30089c>
- Niu, L. Y., Jiang, S. T., Pan, L. J., & Zhai, Y. S. (2011). Characteristics and functional properties of wheat germ protein glycosylated with saccharides through Maillard reaction. *International Journal of Food Science and Technology*, 46(10), 2197–2203. <https://doi.org/10.1111/j.1365-2621.2011.02737.x>
- Nursten, H. E. (2005). The chemistry of nonenzymic browning. In *The Maillard reaction: chemistry, biochemistry, and implications* (5–26). Royal Society of Chemistry.
- Ohloff, G., & Flament, I. (1979). The role of heteroatomic substances in the aroma compounds of foodstuffs. *Fortschritte Der Chemie Organischer Naturstoffe/Progress in the Chemistry of Organic Natural Products*, 36, 231–283. https://doi.org/10.1007/978-3-7091-3265-4_2
- Oliver, C. M., Melton, L. D., & Stanley, R. A. (2006). Creating proteins with novel functionality via the Maillard reaction: A review. *Critical Reviews in Food Science and Nutrition*, 46(4), 337–350. <https://doi.org/10.1080/10408690590957250>

- Osborne, T. B. (1924). The vegetable proteins. In *The vegetable proteins*. (Second Edi, 16–35). <https://doi.org/10.5962/bhl.title.28342>
- Osman, A. (2015). Esterification of legume proteins for enhancing functional properties. In Aberdos (Ed.). LAP LAMBERT Academic Publishing.
- Pittet, A. O., & Hruza, D. E. (1974). Comparative study of flavor properties of thiazole derivatives. *Journal of Agricultural and Food Chemistry*, 22(2), 264–269. <https://doi.org/10.1021/jf60192a009>
- Plietz, P., Drescher, B., & Damaschun, G. (1987). Relationship between the amino acid sequence and the domain structure of the subunits of the 11S seed globulins. *International Journal of Biological Macromolecules*, 9(3), 161–165. [https://doi.org/10.1016/0141-8130\(87\)90045-6](https://doi.org/10.1016/0141-8130(87)90045-6)
- Ponnampalam, R., Goulet, G., Amiot, J., Chamberland, B., & Brisson, G. J. (1988). Some functional properties of acetylated and succinylated oat protein concentrates and a blend of succinylated oat protein and whey protein concentrates. *Food Chemistry*, 29(2), 109–118. [https://doi.org/10.1016/0308-8146\(88\)90093-3](https://doi.org/10.1016/0308-8146(88)90093-3)
- Radivojac, P., Clark, W.T., Oron, T.R., Schnoes, A.M., Wittkop, T., Sokolov, A., Graim, K., Funk, C., Verspoor, K., Ben-Hur, A. & Pandey, G. (2013). A large-scale evaluation of computational protein function prediction. *Nature Methods*, 10(3), 221–227. <https://doi.org/10.1038/nmeth.2340>
- Reineccius, G. (2005). Changes in food flavor due to processing. In *Flavor chemistry and technology* (second edi, 103–132). Retrieved from <https://content.taylorfrancis.com/books/download?dac=C2009-0-19840-3&isbn=9780429204845&format=googlePreviewPdf>

- Sabatini, M. T., Boulton, L. T., & Sheppard, T. D. (2017). Borate esters: Simple catalysts for the sustainable synthesis of complex amides. *Science Advances*, 3(9).
<https://doi.org/10.1126/sciadv.1701028>
- Sanchez, C., Schmitt, C., Kolodziejczyk, E., Lapp, A., Gaillard, C., & Renard, D. (2008). The acacia gum arabinogalactan fraction is a thin oblate ellipsoid: A new model based on small-angle neutron scattering and ab initio calculation. *Biophysical Journal*, 94(2), 629–639. <https://doi.org/10.1529/biophysj.107.109124>
- Schieberle, P., & Grosch, W. (1987). Quantitative analysis of aroma compounds in wheat and rye bread crusts using a stable isotope dilution assay. *Journal of Agricultural and Food Chemistry*, 35(2), 252–257. <https://doi.org/10.1021/jf00074a021>
- Schwenke, K. D., & Linow, K. J. (1982). A reversible dissociation of the 12 S globulin from rapeseed (*Brassica napus* L.) depending on ionic strength. *Food / Nahrung*, 26(1), K5–K6. <https://doi.org/10.1002/food.19820260139>
- Schwenke, K. D., Raab, B., Plietz, P., & Damaschun, G. (1983). The structure of the 12 S globulin from rapeseed (*Brassica napus* L.). *Food / Nahrung*, 27(2), 165–175.
<https://doi.org/10.1002/food.19830270208>
- Schwenke, K. D., Knopfe, C., Seifert, A., Görnitz, E., & Zirwer, D. (2001). Acetylation of faba bean legumin: Conformational changes and aggregation. *Journal of the Science of Food and Agriculture*, 81(1), 126–134. [https://doi.org/10.1002/1097-0010\(20010101\)81:1<126::AID-JSFA788>3.0.CO;2-Y](https://doi.org/10.1002/1097-0010(20010101)81:1<126::AID-JSFA788>3.0.CO;2-Y)
- Schwenke, K. D., Zirwer, D., Gast, K., Görnitz, E., Linow, K. -J, & Gueguen, J. (1990). Changes of the oligomeric structure of legumin from pea (*Pisum sativum* L.) after succinylation. *European Journal of Biochemistry*, 194(2), 621–627.
<https://doi.org/10.1111/j.1432-1033.1990.tb15661.x>

- Sheng, L., Ye, S., Han, K., Zhu, G., Ma, M., & Cai, Z. (2019). Consequences of phosphorylation on the structural and foaming properties of ovalbumin under wet-heating conditions. *Food Hydrocolloids*, *91*, 166–173. <https://doi.org/10.1016/j.foodhyd.2019.01.023>
- Shewry, P. R., Napier, J. A., & Tatham, A. S. (1995). Seed storage proteins: structures and biosynthesis. *The Plant Cell*, *7*(7), 945–956.
- Shilpashree, B. G., Arora, S., Chawla, P., & Tomar, S. K. (2015). Effect of succinylation on physicochemical and functional properties of milk protein concentrate. *Food Research International*, *72*, 223–230. <https://doi.org/10.1016/j.foodres.2015.04.008>
- Shu, Y. W., Sahara, S., Nakamura, S., & Kato, A. (1996). Effects of the length of polysaccharide chains on the functional properties of the Maillard-type lysozyme-polysaccharide Conjugate. *Journal of Agricultural and Food Chemistry*, *44*(9), 2544–2548. <https://doi.org/10.1021/jf950586m>
- Silva, N. H. C. S., Vilela, C., Marrucho, I. M., Freire, C. S. R., Pascoal Neto, C., & Silvestre, A. J. D. (2014). Protein-based materials: From sources to innovative sustainable materials for biomedical applications. *Journal of Materials Chemistry B*, *2*(24), 3715–3740. <https://doi.org/10.1039/c4tb00168k>
- Sitohy, M., Chobert, J. M., & Haertle, T. (2000). Study of factors influencing protein esterification using β -lactoglobulin as a model. *Journal of Food Biochemistry*, *24*(5), 381–398. <https://doi.org/10.1111/j.1745-4514.2000.tb00708.x>
- Sitohy, M., & Osman, A. (2010). Antimicrobial activity of native and esterified legume proteins against Gram-negative and Gram-positive bacteria. *Food Chemistry*, *120*(1), 66–73. <https://doi.org/10.1016/j.foodchem.2009.09.071>

- Sosulski, F., & Fleming, S. E. (1977). Chemical, functional, and nutritional properties of sunflower protein products. *Journal of the American Oil Chemists' Society*, *54*(2).
<https://doi.org/10.1007/BF02912382>
- Spicer, C. D., & Davis, B. G. (2014). Selective chemical protein modification. *Nature Communications*, *5*, 4740–4754. <https://doi.org/10.1038/ncomms5740>
- Tandang-Silvas, M. R. G., Fukuda, T., Fukuda, C., Prak, K., Cabanos, C., Kimura, A., Itoh, T., Mikami, B., Utsumi, S., & Maruyama, N. (2010). Conservation and divergence on plant seed 11S globulins based on crystal structures. *Biochimica et Biophysica Acta Proteins and Proteomics*, *1804*(7), 1432–1442.
<https://doi.org/10.1016/j.bbapap.2010.02.016>
- Tandang-Silvas, M. R. G., Tecson-Mendoza, E. M., Mikami, B., Utsumi, S., & Maruyama, N. (2011). Molecular design of seed storage proteins for enhanced food physicochemical properties. *Annual Review of Food Science and Technology*, *2*(1), 59–73.
<https://doi.org/10.1146/annurev-food-022510-133718>
- Tang, S., Yu, J., Lu, L., Fu, X., & Cai, Z. (2019). Interfacial and enhanced emulsifying behavior of phosphorylated ovalbumin. *International Journal of Biological Macromolecules*, *131*, 293–300. <https://doi.org/10.1016/j.ijbiomac.2019.03.076>
- Utsumi, S. (1992). Plant food protein engineering. *Advances in Food and Nutrition Research*, *36*(C), 89–208. [https://doi.org/10.1016/S1043-4526\(08\)60105-9](https://doi.org/10.1016/S1043-4526(08)60105-9)
- Wanasundara, J. P. D. (2011). Proteins of brassicaceae oilseeds and their potential as a plant protein source. *Critical Reviews in Food Science and Nutrition*, *51*(7), 635–677.
<https://doi.org/10.1080/10408391003749942>
- Wang, Y., Sun, X. S., Wang, D. (2006). Performance of soy protein adhesive enhanced by esterification. *Transactions of the ASABE*, *49*(3), 713–719.
<https://doi.org/10.13031/2013.20469>

- Wang, H., Tu, Z. C., Liu, G. X., Zhang, L., & Chen, Y. (2016). Identification and quantification of the phosphorylated ovalbumin by high resolution mass spectrometry under dry-heating treatment. *Food Chemistry*, *210*, 141–147.
<https://doi.org/10.1016/j.foodchem.2016.04.082>
- Wang, K., & Arntfield, S. D. (2016). Modification of interactions between selected volatile flavour compounds and salt-extracted pea protein isolates using chemical and enzymatic approaches. *Food Hydrocolloids*, *61*, 567–577.
<https://doi.org/10.1016/j.foodhyd.2016.05.040>
- Wang, P. shui, Kato, H., & Fujimaki, M. (1968). Studies on flavor components of roasted barley. *Agricultural and Biological Chemistry*, *32*(4), 501–506.
<https://doi.org/10.1080/00021369.1968.10859083>
- Wang, Y. R., Zhang, B., Fan, J. L., Yang, Q., & Chen, H. Q. (2019). Effects of sodium tripolyphosphate modification on the structural, functional, and rheological properties of rice glutelin. *Food Chemistry*, *281*, 18–27.
<https://doi.org/10.1016/j.foodchem.2018.12.085>
- Wong, B. T., Day, L., McNaughton, D., & Augustin, M. A. (2009). The effect of maillard conjugation of deamidated wheat proteins with low molecular weight carbohydrates on the secondary structure of the protein. *Food Biophysics*, *4*(1), 1–12.
<https://doi.org/10.1007/s11483-008-9096-1>
- Woo, S. L., Creamer, L. K., & Richardson, T. (1982). Chemical phosphorylation of bovine β -lactoglobulin. *Journal of Agricultural and Food Chemistry*, *30*(1), 65–70.
<https://doi.org/10.1021/jf00109a013>
- Wooster, T. J., & Augustin, M. A. (2007). Rheology of whey protein-dextran conjugate films at the air/water interface. *Food Hydrocolloids*, *21*(7), 1072–1080.
<https://doi.org/10.1016/j.foodhyd.2006.07.015>

- Xiong, Z., Zhang, M., & Ma, M. (2016). Emulsifying properties of ovalbumin: Improvement and mechanism by phosphorylation in the presence of sodium tripolyphosphate. *Food Hydrocolloids*, *60*, 29–37. <https://doi.org/10.1016/j.foodhyd.2016.03.007>
- Xu, X., Liu, W., Liu, C., Luo, L., Chen, J., Luo, S., McClements, D. J., & Wu, L. (2016). Effect of limited enzymatic hydrolysis on structure and emulsifying properties of rice glutelin. *Food Hydrocolloids*, *61*, 251–260. <https://doi.org/10.1016/j.foodhyd.2016.05.023>
- Yang, S., Dai, L., Mao, L., Liu, J., Yuan, F., Li, Z., & Gao, Y. (2019). Effect of sodium tripolyphosphate incorporation on physical, structural, morphological and stability characteristics of zein and gliadin nanoparticles. *International Journal of Biological Macromolecules*, *136*, 653–660. <https://doi.org/10.1016/j.ijbiomac.2019.06.052>
- Yin, S. W., Tang, C. H., Wen, Q. B., & Yang, X. Q. (2009). Effects of acylation on the functional properties and in vitro trypsin digestibility of red kidney bean (*Phaseolus vulgaris* L.) protein isolate. *Journal of Food Science*, *74*(9). <https://doi.org/10.1111/j.1750-3841.2009.01349.x>
- Yin, S. W., Tang, C. H., Wen, Q. B., Yang, X. Q., & Yuan, D. B. (2010). The relationships between physicochemical properties and conformational features of succinylated and acetylated kidney bean (*Phaseolus vulgaris* L.) protein isolates. *Food Research International*, *43*(3), 730–738. <https://doi.org/10.1016/j.foodres.2009.11.007>
- Yong, Y. H., Yamaguchi, S., & Matsumura, Y. (2006). Effects of enzymatic deamidation by protein-glutaminase on structure and functional properties of wheat gluten. *Journal of Agricultural and Food Chemistry*, *54*(16), 6034–6040. <https://doi.org/10.1021/jf060344u>

- Zha, F., Dong, S., Rao, J., & Chen, B. (2019a). Pea protein isolate-gum Arabic Maillard conjugates improves physical and oxidative stability of oil-in-water emulsions. *Food Chemistry*, 285, 130–138. <https://doi.org/10.1016/j.foodchem.2019.01.151>
- Zha, F., Dong, S., Rao, J., & Chen, B. (2019b). The structural modification of pea protein concentrate with gum Arabic by controlled Maillard reaction enhances its functional properties and flavor attributes. *Food Hydrocolloids*, 92, 30–40. <https://doi.org/10.1016/j.foodhyd.2019.01.046>
- Zha, F., Yang, Z., Rao, J., & Chen, B. (2019). Gum Arabic-mediated synthesis of glyco-pea protein hydrolysate via Maillard reaction improves solubility, flavor profile, and functionality of plant protein. *Journal of Agricultural and Food Chemistry*, 67(36), 10195–10206. <https://doi.org/10.1021/acs.jafc.9b04099>
- Zhuo, X. Y., Qi, J. R., Yin, S. W., Yang, X. Q., Zhu, J. H., & Huang, L. X. (2013). Formation of soy protein isolate-dextran conjugates by moderate Maillard reaction in macromolecular crowding conditions. *Journal of the Science of Food and Agriculture*, 93(2), 316–323. <https://doi.org/10.1002/jsfa.5760>

3. PEA PROTEIN ISOLATE-GUM ARABIC MAILLARD CONJUGATES IMPROVE PHYSICAL AND OXIDATIVE STABILITY OF OIL-IN-WATER EMULSIONS¹

3.1. Abstract

The present work investigated the impact of incubation time (0, 1, 3, and 5 day) on the properties and functionalities of conjugates formed between pea protein isolate (PPI) and gum Arabic (GA). The participation of both 11S and 7S to form conjugates with GA was proved by SDS-PAGE. The degree of conjugation reaction was characterized by measuring the formation of Maillard reaction products, the loss of free amino groups, and color changes. Surface structure of conjugated PPI was characterized through scanning electron microscope. The results suggested that PPI intimately incorporated into GA after 1 day incubation, giving a non-homogeneous microstructure, resulting in a reduction of nearly 18 % available free amino and increasing solubility to 15.5%. Additionally, emulsion stabilized by PPI-GA conjugates had smaller particle size, higher surface charge, and stronger steric hindrance to stabilize the emulsion droplets against environmental stresses and lipid oxidation.

3.2. Introduction

World protein requirements remain an ongoing challenge with heightened concerns about protein malnutrition and unbalanced essential amino acid profiles (Boye, Zare, & Pletch, 2010). In light of its relatively inexpensive and more sustainable source as compared to animal proteins, plant derived proteins are of tremendous interest for applications in food industry in recent years. Pea protein, as a potential alternative protein source for human foods, complies

¹ Based on the article of Fengchao Zha, Shiyuan Dong, Jijia Rao & Bingcan Chen published in Food Chemistry online Jan. 2019 (DOI:10.1016/j.foodchem.2019.01.151). Fengchao Zha was responsible for methodology, data collection and analysis, was the primary developer of the conclusions advanced here, and drafted and revised all versions of this chapter. Shiyuan Dong assisted with reviewing the draft. Jijia Rao assisted with instruments. Bingcan Chen was primary responsible for resources, reviewing and editing, supervising.

well with market expectations because of its nutritional value and many beneficial effects on human health (Boye et al., 2010; Roy, Boye, & Simpson, 2010). However, the commercial development of pea protein especially in beverages as functional ingredients has been largely dampened by both its low water solubility and poor functionalities. High proportion of globulin fraction (~70 %) in pea protein is the major reason for its poor solubility. Additionally, the commonly adapted procedures to isolate pea protein from flour by direct alkaline extraction followed by acid precipitation can further decrease the solubility of globulin fraction. The functional properties of isolated pea proteins, such as emulsification, foaming, and gelation, are limited since they are closely associated with pea protein solubility (Pirestani, Nasirpour, Keramat, & Desobry, 2017; Yoshie-Stark, Wada, & Wäsche, 2008). For instance, a recent study by Gumus et al has found that emulsions stabilized by pea protein showed extensive droplet aggregation and creaming in a wide range of pH (3 to 6) indicating its poor functionality (Gumus, Decker, & McClements, 2017a).

Accumulated evidences have shown that the conjugation of protein-polysaccharide by means of Maillard reaction (MR) is a promising approach to improve the functional properties of protein (de Oliveira, Coimbra, de Oliveira, Zuñiga, & Rojas, 2016; Liu et al., 2017; Oliver, Melton, & Stanley, 2006; Ozturk & McClements, 2016). Nevertheless, scarce study has been made specially to modify the structure of pea protein isolate and improve its functionality via MR. The conjugation between protein and polysaccharide originates from the Amadori rearrangement of Schiff base compounds that formed via the condensation of carbonyl-containing moieties with available ϵ -amino groups at the initial stage of MR (Martinez-Alvarenga et al., 2013; Pirestani, Nasirpour, Keramat, Desobry, & Jasniewski, 2018). Among most of the polysaccharides, gum Arabic (GA) is a popular one to be conjugated with proteins since it has been extensively applied in food industry to stabilize flavors and essential oils. The food emulsions produced by the conjugated protein (e.g., soy whey protein isolate, canola

protein isolate, and α -lactalbumin) with gum Arabic have been shown to be physically stable against environmental stress including pH changes, ionic strength, and thermal processing (de Oliveira et al., 2015; Pirestani, Nasirpour, Keramat, & Desobry, 2017; Pirestani et al., 2018; Yang et al., 2015)

Previous researchers have shown that protein conjugates formed via MR possess greater antioxidant activity and can effectively decrease the oxidative rancidity of oil-in-water emulsions (Dong et al., 2012; Dong, Wei, Chen, McClements, & Decker, 2011). A recent study by Gumus et al. examined the antioxidant activity of pea protein to inhibit fish oil-in-water emulsions and concluded that pea protein was more effective than whey proteins in preventing the oxidation of washed emulsions. The stronger iron binding capacity of pea protein than that of whey protein suggested that pea protein might be a potential antioxidant (Gumus, Decker, & McClements, 2017b). However, little is known if the formation of conjugates would impact the antioxidant activity of PPI against emulsion oxidation.

Therefore, the purpose of the current study was to investigate the role of Maillard reaction on the structure and functional properties of PPI-GA conjugates, with a particular emphasis on their ability to enhance physical and oxidative stabilities of corn oil-in-water emulsions. We hypothesized that the functionality of PPI could be appreciably improved by forming conjugates with GA via time controlled Maillard reaction.

3.3. Materials and Methods

3.3.1. Materials

Pea protein isolate (PPI, Cargill & PURIS, moisture ~6%, protein ~80%, crude ash ~5%, and carbohydrate 9%) was kindly donated by Cargill (Minneapolis, MN, USA). Spray dried gum Arabic powder (GA, TIC Pretested®, moisture ~6.7%, polysaccharide ~90%, protein ~3.2%, and minerals ~ 0.2%) with a molecular weight of 0.25-2.5×10⁶ Da was kindly provided by TIC Gums (Belcamp, MD, USA). Mazola® corn oil was purchased locally. All

other chemicals used in this study were of analytical grade. Specification values of each commercial ingredient were obtained from manufacturers. All bulk samples were used as received. Deionized water of 18.2 M Ω .cm resistivity obtained from Barnstead GenPure PRO Standard (Thermo Fisher Scientific, Inc., Waltham, MA, USA) was used to prepare the solutions and emulsions.

3.3.2. Preparation of PPI-GA conjugates

Pea protein isolate (PPI) and gum Arabic (GA) were hydrated at a mass ratio of 1:4 in twice amount of deionized water overnight on a stir plate operating at 300 rpm under room temperature (RT, 22 °C). The mixture was carefully adjusted to pH 7.0 with 1.0 N NaOH and freeze-dried for 48 h (Lyophilizer, SP scientific, Gardiner, New York). Five grams of resultant powder was transferred in a 60 mL clear glass straight-sided jar. The uncovered jar was then placed on a perforated plate in an empty desiccator. Maillard reaction was performed in a closed desiccator maintained at relative humidity of 79% by saturated KBr solution and at 60°C by a pre-heated incubator (Heratherm IMH180, Thermo Fisher Scientific, Inc., USA). The reaction time was set at 0, 1, 3, and 5 day, respectively.

3.3.3. Amadori compounds and melanoidins formation

UV-Vis absorbance of the conjugates at 304 nm and 420 nm were used as an indicator for the formation of Amadori compounds and final high molecular weight compounds melanoidins, respectively (Wang & Ismail, 2012; Yadav, Strahan, Mukhopadhyay, Hotchkiss, & Hicks, 2012; Zhu, Damodaran, & Lucey, 2010). All measurements were performed using a Shimadzu UV-1100 PC model spectrophotometer (Shimadzu Corp., Kyoto, Japan) with deionized water as a blank reference.

3.3.4. Measurement of free amino groups

Free amino groups were quantified as described by Habeeb (Habeeb, 1966) with a slight modification. Briefly, both 1 mL of 4% NaHCO₃ (pH 8.5) and 1 mL of 0.1% 2,4,6-

trinitrobenzenesulfonic acid (TNBS) were transferred to 1 mL of PPI-GA conjugate solution (5 mg/mL), followed by mixing and incubating at 40°C for 2 h in a covered water bath to avoid light. Then, 10 % (w/v) sodium dodecyl sulfate was added prior to terminating the reaction by adding 0.5 mL HCl (1.0 N). The samples were then set at room temperature for 15 min before recording the absorbance at 340 nm using a Shimadzu UV-1100 PC model spectrophotometer (Shimadzu Corp., Kyoto, Japan). The free amino group was quantified using a calibration curve of L-leucine (0–2.0 mM).

3.3.5. Color development

The color of samples was measured using a Minolta Chroma Meter (Model CR-310, Japan) with a diffuse illumination/0-degree viewing geometry to obtain CIE L* a* b* values. The chromameter was calibrated with a standard white tile (Y=92.2, x=0.3162, and y=0.3324). Browning index (BI) was calculated using the following equations (Dadali, Apar, & Özbek, 2007).

$$BI = \frac{[100 \times (x - 0.31)]}{0.17} \quad (3.1)$$

$$x = \frac{(a^* + 1.75 \times L^*)}{(5.645 \times L^* + a^* - 3.012 \times b^*)} \quad (3.2)$$

3.3.6. Sodium dodecyl sulphate-polyacrylamide gel electrophoresis (SDS-PAGE)

SDS-PAGE was performed according to the method of Laemmli (Laemmli, 1970). Mini-PROTEAN TGX precast gel (Cat #456-8084) containing a separating gel of 15% and a stacking gel of 4% was applied in a Bio-Rad Mini-Protein apparatus III. Five microliter of 5 mg/mL PPI-GA conjugate solution was mixed with 4.75 µL 2×Laemmli sample buffer (Cat #161-0737) and 0.25 µL β-mercaptoethanol (Cat #161-0710), followed by heating sample at 90°C for 5 min. Electrophoresis was carried out in 1×Laemmli SDS-PAGE running buffer prepared by diluting 100 mL 10× Tris/Glycine/SDS buffer (Cat #161-0732, pH 8.3) with deionized water. Fifteen microliter samples were loaded on the gel after which was run by a

constant voltage (200V) for 30–40 min until the dye front reaches the reference line. A blue prestained protein standard (Cat #161-0373) was used to monitor the molecular weight changes. After gel electrophoresis, the gel was stained with 0.05% (w/v) Coomassie Brilliant Blue R-250 in 15% (v/v) methanol and 5% (v/v) acetic acid and destained with 3% (v/v) methanol and 10% (v/v) acetic acid. All chemicals involved were purchased from Bio-Rad Laboratories Inc (Hercules, CA, USA).

3.3.7. Relative solubility of PPI-GA conjugates

Protein solubility was determined according to the method of Bradford (Bradford, 1976). The unmodified and the conjugated samples were dispersed in 10 mM phosphate buffer pH 7.0 (1 mg/mL), and stirred for 30 min at room temperature to obtain uniform dispersions. Then the samples were filtered through Whatman Qualitative Filter Paper (Cat #1003-090). The absorbance of the resulting protein solutions was recorded at 595 nm and the protein concentration was calculated using a standard curve. The solubility was expressed as the percentage of the initial PPI concentration.

3.3.8. Scanning electron microscopy

Dried powder sample was directly applied to a double sided carbon tape on a cylindrical aluminum mount. Samples were then sputter coated with a conductive layer of gold (Cressington 108, Ted Pella Inc., CA, USA). Surface morphology of the samples was obtained using a JEOL JSM-6490LV scanning electron microscope (JEOL USA, Peabody MA, USA) at an accelerating voltage of 15 kV.

3.3.9. Preparation of corn oil-in-water emulsions with PPI-GA conjugates

An emulsifier solution was prepared by dispersing 0.20 wt% PPI-GA conjugates in phosphate buffer (10 mM, pH 7.0) and stirring for 3 h at room temperature. The supernatant solution was obtained after centrifugation at 2000 rpm for 30 min. Emulsions were prepared by blending 2 wt% corn oil with 98 wt% emulsifier solution in a high-speed blender

(M133/128-0, Biospec Products, Inc., ESGC, Switzerland) for 2 min. This coarse emulsion was then passed through a two-stage high-pressure valve homogenizer: 5000 psi first stage; 500 psi second stage (LAB 2000, APV-Gaulin, Wilmington, MA) for three times. Sodium azide (0.04 wt%) was added to prevent microbial growth. The pH of the emulsions was adjusted to pH 7.0 if required. The emulsions were kept on ice over the whole procedure to minimize oxidation. Emulsion stabilized by the same amount of PPI alone or the mixture of PPI-GA was used controls.

3.3.10. Particle size & zeta potential measurement

The emulsion particle size and size distributions were directly measured using a laser light scattering instrument (Mastersizer 3000, Malvern Instruments Ltd., Malvern, U.K.). Measurements were reported as the surface-weighted ($d_{32} = \sum n_i d_i^3 / \sum n_i d_i^2$) mean diameter and volume-weight mean diameter ($d_{43} = \sum n_i d_i^4 / \sum n_i d_i^3$), where n_i was the number of droplets of diameter d_i . The ζ -potential (mV) of emulsion droplets was measured using a micro-electrophoresis device (Nano-ZS, Malvern Instruments, Worcestershire, UK).

3.3.11. Physical stability of emulsions against environment stresses

To evaluate the stability of emulsions against pH changes, the emulsions were adjusted to different pH (2.0–8.0) using 1N HCl or NaOH, and left quiescently at room temperature for 30 min. To examine the stability of emulsions against thermal processing, emulsion samples (10 mL, pH 7.0) were transferred into glass test tubes, which were then incubated in a pre-heated incubator for 24 h at different temperatures (25, 37, and 72°C). After incubation, the emulsions were immediately cooled at room temperature. To assess the stability of emulsions against ionic stress, the emulsions (10 mL, pH 7.0) were adjusted to various desired salt concentrations (0, 100, 300, and 500 mM), and left quiescently at room temperature for 30 min. Changes in particle size and ζ -potential of emulsions were recorded.

3.3.12. Lipid oxidation kinetics of emulsions

Lipid hydroperoxides were measured as the primary oxidation product using a method adapted from Chen et al. (Chen, McClements, & Decker, 2010). Absorbance of emulsions was recorded at 510 nm, and lipid hydroperoxides values of emulsions were calculated from a cumene hydroperoxide standard curve. Secondary oxidation product marker hexanal was quantified using an Agilent 7890B gas chromatograph bundled with a PAL RSI 85 autosampler. Emulsion subsamples (1 mL) in 20 mL capped GC glass vials were preheated at 55°C for 15 min in an auto-sampler heating block. A 50/30 μm Divinylbenzene/Carboxen/Polydimethylsiloxane solid-phase microextraction (SPME) fiber needle (Supelco, Bellefonte, PA) was injected into the vial absorbing volatiles for 2 min, and then was transferred to the injector port (250°C) for 3 min. Split mode was selected at the ratio of 1:50 for the injection port. Volatiles were identified on a ZB-Wax column (60 m \times 0.25 mm i.d. \times 0.25 μm film thickness). Oven temperature program set as: Initial temp 35 °C, hold 3 min, to 80 °C at 20 °C/min, hold 4 min. The carrier gas was high purity helium (99.9995%) and the flow rate was 1.5 mL/min. A flame ionization detector (FID) was set at a temperature of 250°C. The concentration of hexanal was calculated from its peak areas using a standard curve prepared from an authentic standard (LOD: 82.3 ng/ml). The lag phase is defined as the time required for observing a sudden increase of hexanal formation.

3.3.13. Statistical analysis

Data were expressed as the mean \pm standard deviation of triplicate measurements. The data were statistically analyzed using statistical software, SAS version 9.4 (SAS institute Inc. Cary, NC). One-way analysis of variance (ANOVA) was conducted, and significant difference was defined at $p < 0.05$ by Tukey's test.

3.4. Results and Discussion

3.4.1. Impact of incubation time on chemical properties of PPI-GA conjugates

It is important to confirm both the formation and the extent of PPI-GA conjugation during the course of incubation so that one can control the reaction and attain the conjugates with desirable properties. In this section, three methods were employed to verify the formation of conjugates between the two polymers during incubation.

3.4.1.1. SDS-PAGE profile of PPI and PPI-GA conjugates

The molecular weight changes of PPI and PPI-GA system during incubation were monitored using SDS-PAGE (**Fig. 3.1**). Pea protein is mainly composed of albumins and globulins, accounting for nearly 10-20 % and 70-80 % of the total protein, respectively (Lam, Can Karaca, Tyler, & Nickerson, 2018). The characteristic bands of pea protein profile were observed in **Figure 3.1** (lane 1), which include a distinctive acidic subunit (~40 kDa) of 11S globulins and a 2S albumin with a heavy (~10 kDa) polypeptide chain.

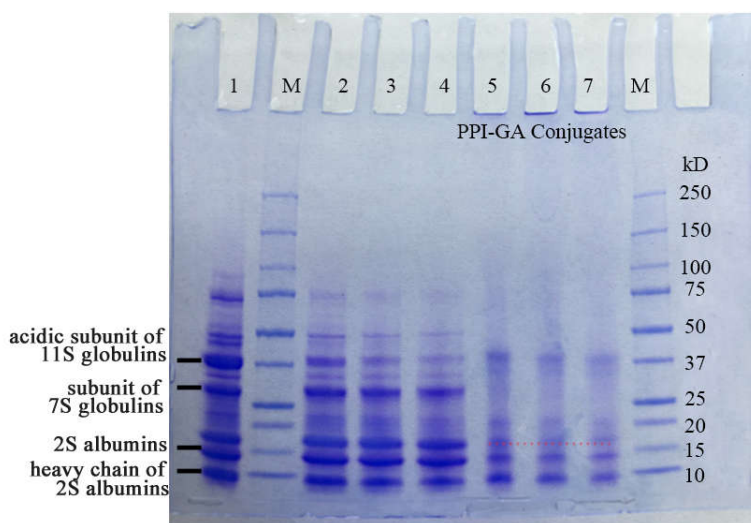


Figure 3.1. SDS-PAGE patterns of PPI and PPI-GA conjugates at different incubation time. (lane M for protein markers; lanes 1-4 representing PPI incubating for 0, 1, 3, and 5 days, respectively; lanes 5-7 representing PPI-GA incubating for 1, 3, and 5 days, respectively)

On a fundamental level, the occurrence of conjugation reaction in PPI-GA system through the covalent-linking should result in an increase in the molecular weight of resultant

conjugates concomitant with the disappearance or reduction of certain PPI subunits. This was corroborated by the formation of a new band near the loading end of PPI-GA conjugation systems (**Fig. 3.1**, lane 5, 6, & 7) which was unable to migrate into the separating gel due to the large molecular weights (Pirestani, Nasirpour, Keramat, & Desobry, 2017). The band, however, was not found in PPI alone during the entire course of incubation (**Fig. 3.1**, lanes 2, 3, & 4), confirming the formation of PPI-GA conjugates to be responsible for the newly formed band. The SDS-PAGE profile was in line with the report by Pirestani (Pirestani, Nasirpour, Keramat, & Desobry, 2017). Moreover, two strong bands (~15 kDa and ~28 kDa) presented in PPI (**Fig. 3.1**, lanes 1, 2, 3, and 4) with various incubation time was receded in PPI-GA conjugates (**Fig. 3.1**, dash-dot line highlighted). These results implied that both 11S and 7S are the major polypeptide units participating the conjugation reaction with GA, as those two bands were assigned to an acidic subunit of 11S and a subunit of 7S, respectively. The intensity of these polypeptides bands (**Fig. 3.1**, lane 5) dropped remarkably as the conjugation reaction proceeded for 1 day at 60 °C, and then less changes in the intensity (**Fig. 3.1**, lane 6 & 7) was found with the extension of incubation time, which again confirms the formation of conjugates between PPI and GA during incubation.

3.4.1.2. Non-specific markers and free amino groups in PPI-GA conjugates

The UV-VIS absorbance of Maillard reaction products (MRPs) solution at 304 nm and 420 nm have been widely accepted as non-specific markers to monitor the development of early-intermediate stage Amadori compounds and final stage melanoidins, respectively. As can be seen in **Figure 3.2**, a dramatic increase ($p < 0.05$) in the absorbance at 304 nm was displayed as PPI-GA mixture was incubated for 1 day. It was slowly raised and gradually leveled off as the increase of incubation time up to 5 day, suggesting a minuscule amount of Amadori compounds formed thereafter. A similar trend was established in measuring the absorbance of PPI-GA conjugates at 420 nm (**Fig. 3.2**). Conversely, no significant changes of the non-specific

markers for PPI alone were occurred during incubation, again reflecting the success conjugation of PPI-GA. Meanwhile, the absorbance values of all the PPI-GA conjugates recorded at 304 nm were higher than those at 420 nm, which coincides with another report (Delgado-Andrade, Morales, Seiquer, & Pilar Navarro, 2010). These results indicate that the formation of intermediate Amadori compounds is prior to the colored melanoidins under the mild incubation conditions. Besides, most Amadori compounds in PPI-GA systems were generated within the first day of incubation. Subsequently, these intermediate substances might undergo irreversible degradation and polymerization to form the colored and high molecular weight melanoidins with the extension of incubation time.

To further track the extent of PPI-GA conjugation, the free amino groups, major moieties of PPI to react with GA, as a function of incubation time was measured (**Fig. 3.3**). Obviously, available free amino groups in PPI-GA system rapidly decreased after 1 day incubation by diminution of nearly 18 %. However, only 4.5% reduction of free amino groups was obtained in PPI alone after a same incubation time period. Thus, it was concluded that the covalent binding of PPI to GA contributed to the reduction of available amino groups in conjugates. Further extending the incubation time slightly decreased the free amino groups in PPI-GA system. The reactivity reduction of GA subjected to longer incubation time has been previously reported which is linked with a number of factors, such as the flexibility, solubility, steric hindrance effects, and high molecular weight of GA (Pirestani, Nasirpour, Keramat, & Desobry, 2017).

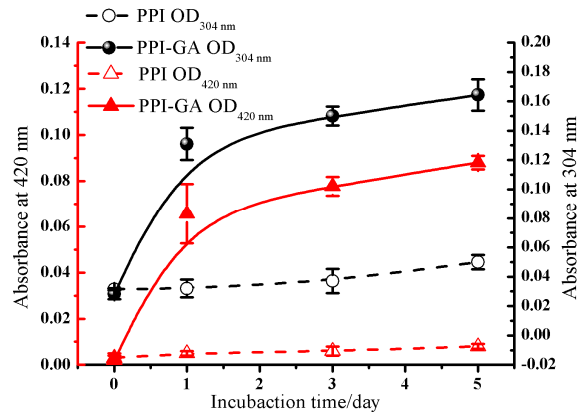


Figure 3.2. The absorbance of non-specific Maillard markers at 304 nm and 420 nm as a function of incubation time.

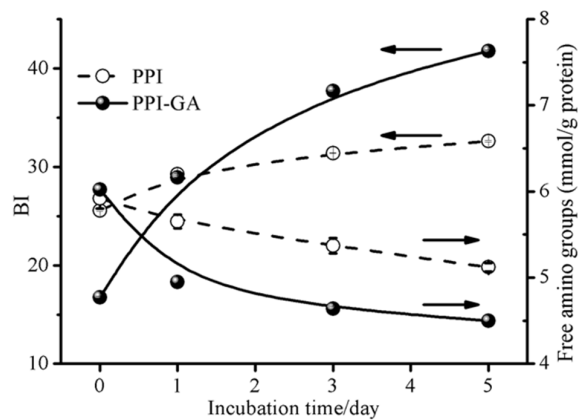


Figure 3.3. The brown index (BI) and available free amino groups of PPI and PPI-GA conjugates during the course of incubation (0, 1, 3, and 5 days) at 60°C and 79% relative humidity.

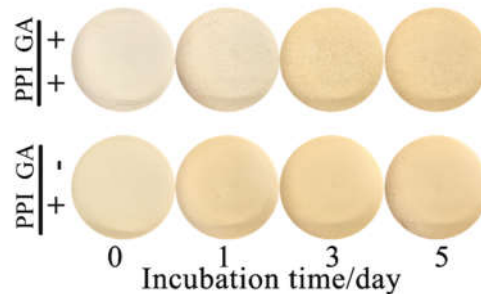


Figure 3.4. The color development of PPI and PPI-GA conjugates during the course of incubation (0, 1, 3, and 5 days) at 60°C and 79% relative humidity.

3.4.1.3. Changes of browning index

Browning index (BI) calculated by CIE Lab parameters has been applied as a clear indicator of color development in the course of MR (Martinez-Alvarenga et al., 2013). In general, BI of conjugates increased as the incubation time extended, which was in agreement

with the visual observation of the samples (**Fig. 3.4**). A considerable difference of ~12.15 units was shown between PPI-GA systems incubated for 0 day and for 1 day. The highest BI values (41.76 ± 0.12) was reached in PPI-GA system after up to 5 day incubation (**Eq. 3.1&3.2**). Considering the difference in BI value after 1 day incubation, the rate of Maillard reaction gradually decreased and then leveled off, which were in accordance with the evidences from absorbance at 304 and 420 nm. A statistical negative correlation was obtained between available free amino groups and BI ($r = -0.8944$, $p = 0.0027$). Such correlation can be selected as an indicator to predict the extent of PPI-GA conjugation over incubation time.

3.4.2. Impact of incubation time on the solubility of PPI-GA conjugates

Solubility is one of the most important properties of proteins and low solubility remains the greatest obstacles for PPI to be utilized as functional ingredients in food industry. **Fig. 3.5** presented the changes in solubility of PPI and PPI-GA conjugates incubated at a various time point. The solubility of PPI decreased substantially after 1 day of incubation, after which remained constant upon further incubation to 3 days. The loss of its solubility is associated with protein denaturation caused by thermal processing. The solubility of PPI-GA mixture (day 0) was similar as that of PPI itself ($p > 0.05$) denoting that physically presented GA is unable to increase the solubility of PPI. However, the solubility of PPI was significantly improved after conjugating with GA for 1 day. This can be explained by the involvement of poorly water soluble 11S and 7S subunits to form conjugates with hydrophilic GA which improve the overall water solubility of the system (**Fig. 3.1**).

Interestingly, longer incubation time had an adverse impact on the solubility of PPI-GA conjugates as revealed by the decline of solubility after 5 days of incubation. Since the interfacial and morphological properties of biopolymers can greatly impact their solubility, the surface morphology of PPI-GA conjugates was examined by scanning electron microscopy and taken at $1000\times$ magnification. Irregular polygonal (**Fig. 3.6-1**) and globular (**Fig. 3.6-2**)

morphological structures were primarily presented in GA and PPI, respectively. With respect to the mixture of PPI-GA (Fig. 3.6-3) without subjecting to incubation, the coexistence of both globular and polygonal implicated the physical mixing matrix of two biopolymers. A non-homogeneous hybrid network structure was established in PPI-GA conjugates after 1 day of incubation at 60°C, which can be explained by the intimate attachment of GA to the surface of PPI (Fig. 3.6-4). Such surface morphology may facilitate the interaction between conjugates and waters, thus increasing the solubility of PPI. Similar SEM morphology was reported previously after conjugation of corn fiber gum with milk protein (Yadav et al., 2012). As the incubation time increased, a more flattened and compressed surface was observed in PPI-GA conjugates (Fig. 3.6-4&5), which may give rise to the decreased solubility.

The SEM results, combined with SDS-PAGE profile described *vide supra*, confirm that the conjugated PPI with GA with controlled incubation time could significantly increase solubility by attaching hydrophilic GA to the surface of PPI. The hydrogen bonding capacity of hydroxyl groups on the attached GA could improve conjugates-water interactions.

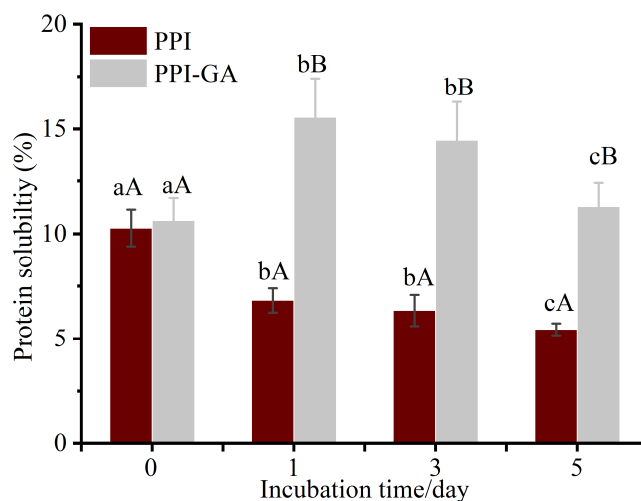


Figure 3.5. Solubility of PPI and PPI-GA conjugates during the course of incubation (0, 1, 3, and 5 days) at 60°C and 79% relative humidity. The lowercase is for comparison among groups at the same treatments; the uppercase is for comparison in groups at different treatments; different letters indicated significance at $p < 0.05$.

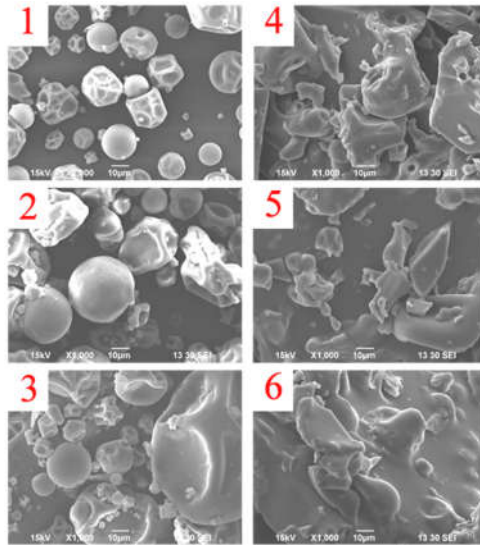


Figure 3.6. SEM (Magnification 1000×; scale bar =10μm) for surface characteristics of PPI and PPI-GA conjugates during the course of incubation (0, 1, 3, and 5 days) at 60°C and 79% relative humidity. 1, gum Arabic (GA); 2, pea protein isolate (PPI); 3, the mixture of GA and PPI; 4-6, PPI-GA-1, 3, 5, respectively.

3.4.3. Impact of incubation time on the emulsifying property of PPI-GA conjugates

The particle size and size distributions of emulsions stabilized by PPI-GA conjugates with different incubation time (0, 1, 3, and 5 day) were measured to determine the influence of this processing on conjugates emulsification property (**Fig. 3.7**). Like most of the previous studies using pea protein to form oil-in-water emulsions, the droplet size of PPI stabilized emulsions ($d_{32}=1.29 \mu\text{m}$; $d_{43}=1.43 \mu\text{m}$) was bigger than the preferred size ($d<0.5 \mu\text{m}$) in commercially fortified emulsions to reduce creaming and increase bioavailability (Walker, Decker, & McClements, 2015). Physically mixed PPI-GA reduced the size of emulsion droplet to a lesser extent ($d_{43}=1.17 \mu\text{m}$), which might be due to the inherent emulsification property of GA. The size of emulsions prepared by PPI-GA conjugates with shorter incubation time (1 and 3 day) was significantly lower ($d_{32}=0.60 \mu\text{m}$; $d_{43}=0.80 \mu\text{m}$) indicating the enhanced emulsification property of PPI derived from the covalent bonding with GA (rather than physical mixing). Conversely, such ability disappeared as the biopolymers were incubated for a longer time (5 days), presumably because of the excessive reactions between PPI and GA as indicated by the decrease of solubility (**Fig. 3.7A**).

The emulsions prepared from both PPI alone and the mixture of PPI-GA had a broad monomodal distribution, with a single peak around 1.28 and 1.13 μm , respectively (**Fig. 3.7B**). Conversely, a narrow monomodal distribution with a peak around 0.5 μm was observed in the emulsion prepared using PPI-GA conjugates after both 1 and 3 days incubation. Interestingly, further extend the incubation to 5 days, the conjugates rendered a bimodal distribution for the emulsion droplets it stabilized, which suggest that extensive reaction can reduce the emulsification property of conjugates.

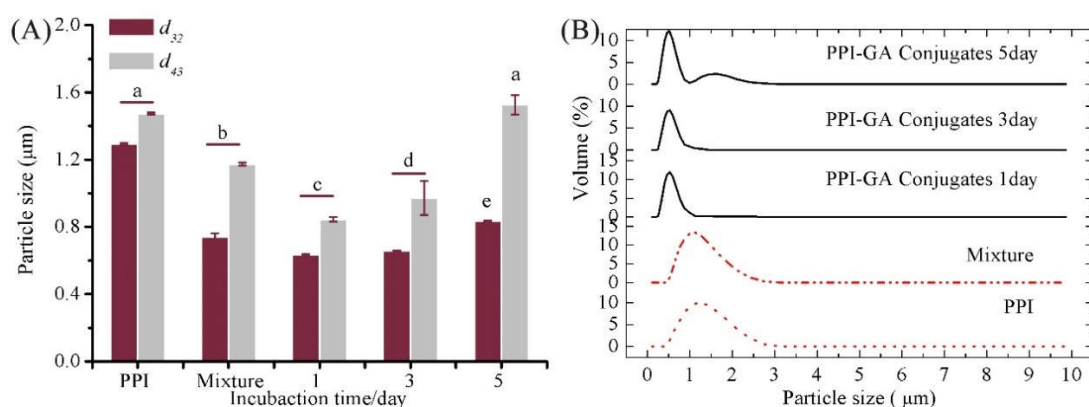


Figure 3.7. Particle size (d_{32} and d_{43}) (A); particle size distribution (B) of corn oil-in water emulsions (pH 7.0) stabilized by PPI, PPI-GA mixture, and PPI-GA conjugates formed with different incubation time (1, 3, and 5 days). The different lowercase indicated significance at $p < 0.05$.

3.4.4. Physical stability of oil-in-water emulsions stabilized by PPI-GA conjugates

A previous study has shown that pea protein stabilized oil droplets in oil-in-water emulsions are unstable to various kinds of environmental stresses, including pH changes, high ionic strengths, and thermal processing (Gumus et al., 2017a). A major objective of the present study was to determine if the physical stability of PPI-GA conjugates stabilized emulsions could be improved under environmental stresses. The conjugates developed after 1 day incubation were selected to prepare corn oil-in-water emulsion since they can form the smallest droplets with less final stage MRPs.

3.4.4.1. Influence of pH on physical stability of emulsions

The pH-tolerance (pH 2–8) of the emulsions stabilized by PPI-GA conjugates was investigated and compared with that of both PPI and PPI-GA mixture (Fig. 3.8A, B&C).

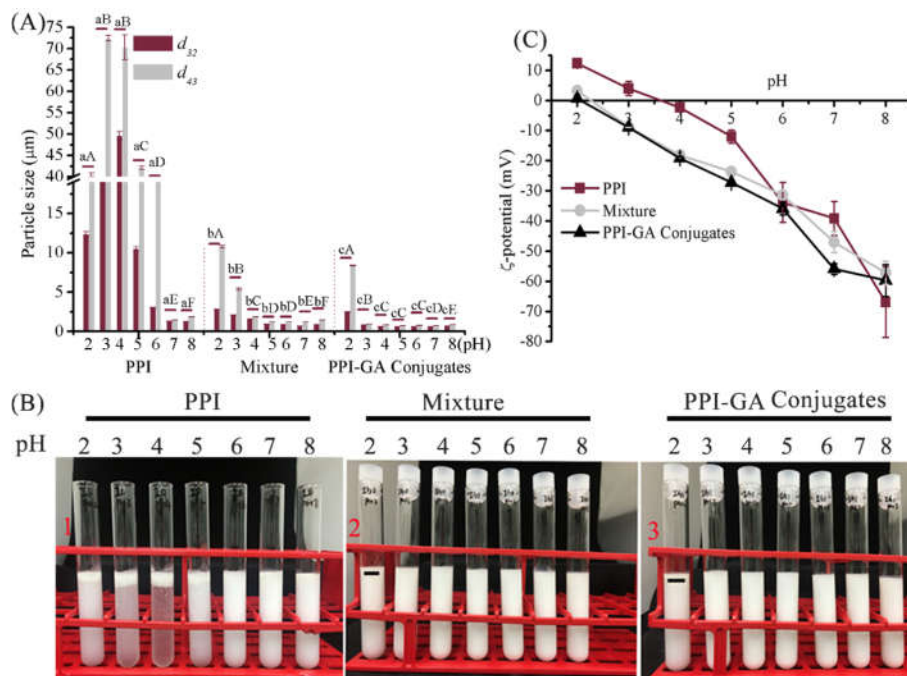


Figure 3.8. Influence of pH on particle size (A), real figures (B) and ζ -potential (C) of emulsions (pH 7.0) stabilized by PPI, PPI-GA mixture, and PPI-GA conjugates incubated for 1 day. The lowercase is for comparison among groups at the same treatments; the uppercase is for comparison in groups at different treatments; different letters indicated significance at $p < 0.05$.

PPI alone did not provide enough emulsion stability against pH, especially at acidic conditions. A phase separation with a transparent serum layer occurred in PPI stabilized emulsions at pH 2–6, but not in those prepared by PPI-GA conjugates and mixture with the exception of a slightly coalescence at pH 2 (Fig. 3.6B). This was further supported by particle size analysis where the mean particle size of PPI stabilized emulsion was significantly larger than those prepared by PPI-GA conjugates and mixture under the whole pH range. Meanwhile, the particle size of the emulsions prepared by PPI-GA conjugates and mixture was comparable in the pH range of 4–8, but an appreciable size increase was found in PPI-GA mixture stabilized emulsions as pH dropped to 3 and below. It has been reported that GA ineffectively stabilizes

emulsions at low pH (Nakauma et al., 2008). The well-maintained small particle size of emulsions prepared by PPI-GA conjugates, irrespective of the pH, suggests that the enhanced pH-tolerance of the emulsions was ascribed to the presence of GA that is covalently bound to PPI. The conjugation of GA to PPI would create an amphiphilic molecule with higher emulsifying potential, likely owing the inhibition of the unfolded protein–protein interaction and aggregation from the attached polysaccharide (Pirestani, Nasirpour, Keramat, Desobry, & Jasniewski, 2017).

To provide some insight into the origin of emulsion stability, the electrical charge of the oil droplets as a function of pH was measured (**Fig. 3.6C**). For PPI stabilized emulsions, the electrical charge was highly negative well above the isoelectric point ($\text{IEP} \approx 4$) and slightly positive well below it. The strong electrostatic repulsion of emulsion droplets stabilized by PPI at pH 5 and 6 cannot maintain the good physical stability, which suggests the poor functionality of PPI. An increase in the magnitude of the droplet charge was observed in both PPI-GA conjugates and mixture stabilized emulsions when pH was below 6. This can be attributed to the deprotonated carboxylic acid groups (COO^-) on GA that behaves as a buffer to compensate the increased amount of H^+ upon pH drop. Additionally, the electrical charge of the emulsion stabilized by PPI-GA conjugates was slightly higher than that of mixture when pH is above 5, which can be interpreted by the reduction of available free amino groups (NH_4^+) upon conjugation. The greater stability of emulsion stabilized by PPI-GA mixture at pH 4-8 is due to the strong steric repulsions from thick GA molecule layers (Ozturk, Argin, Ozilgen, & McClements, 2015). The improved stability of emulsion prepared by PPI-GA conjugates at lower pH (2–3) might be due to the greater steric repulsions between the droplets, which counteracts the van der Waals attraction in the case of decreased electrostatic repulsions around IEP and thereby prevents flocculation (Delahaije, Gruppen, Van Nieuwenhuijzen, Giuseppin, & Wierenga, 2013).

3.4.4.2. Influence of thermal processing on physical stability of emulsions

Emulsions stabilized by proteins alone are susceptible to thermal treatment, advancing a rapid phase separation into two immiscible phases by venture of protein denaturation at interface (Bi, Yang, Fang, Nishinari, & Phillips, 2017). The impact of thermal treatment (25, 37, and 72°C) on the stability of emulsions prepared by PPI-GA conjugates at pH 7.0 was investigated by measuring particle size and ζ -potential (Fig. 3.9A, B&C).

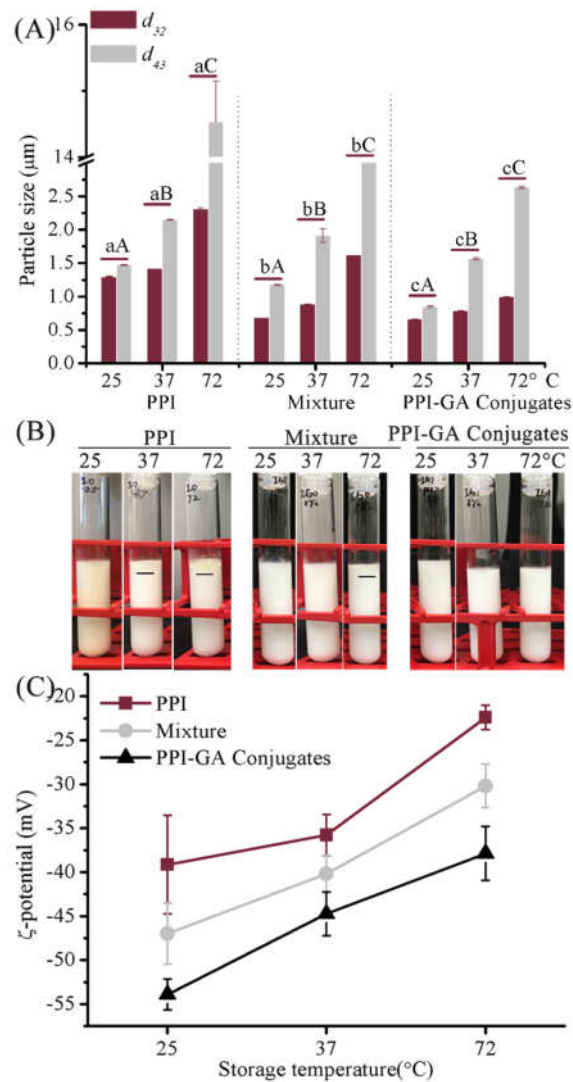


Figure 3.9. Influence of thermal treatment on particle size (A), real figures (B) and ζ -potential (C) of emulsions (pH 7.0) stabilized by PPI, PPI-GA mixture, and PPI-GA conjugates incubated for 1 day. The lowercase is for comparison among groups at the same treatments; the uppercase is for comparison in groups at different treatments; different letters indicated significance at $p < 0.05$.

As indicated in **Figure 3.9A**, emulsions stabilized by PPI-GA conjugates had much smaller mean particle size compared to the others at any given temperature. Mean particle size of emulsion ($d_{43}=2.64\ \mu\text{m}$) produced by PPI-GA conjugates increased slightly as temperature went up to 72°C ; whereas a dramatic increase was observed in the droplet coated by PPI-GA mixture ($d_{43}=5.37\ \mu\text{m}$). A considerable increase in mean particle size of emulsion prepared by PPI and mixture was observed as temperature rose up to 72°C , which suggests the tendency of emulsions to coalescence (**Fig. 3.9B**). The net ζ -potential of PPI-GA conjugate stabilized emulsions was much higher than the other two (**Fig. 3.9C**). This is not surprising as the conjugation could block the ionized amine groups at pH 7, which converts cationic amino groups to anionic GA residues. The increase in net negative charges surrounding the protein molecules along with the thicker layers of conjugates would promote both electrostatic and steric repulsions between the droplets, resulting in the improvement of emulsion stability upon thermal treatment.

3.4.4.3. Influence of ionic strength on physical stability of emulsions

The impact of various salt concentrations (0, 100, 300, and 500 mM NaCl) on particle size and ζ -potential of emulsions stabilized by PPI-GA conjugates at pH 7.0 was investigated (**Fig. 3.10A, B&C**).

PPI stabilized emulsion was relatively stable when 100 mM NaCl was introduced with d_{43} raised from 1.48 to 8.13 μm , yet no phase separation was noticed (**Fig. 3.10B**). In addition to the drastic increase of particle size and the decrease of ζ -potential when the concentration of NaCl was higher than 100 mM, a cream layer was also exhibited. The electrostatic repulsion, the dominant force to stabilize the emulsion in this case, was screened by the addition of salt which increases Van der Waals attractive interactions between droplets, causing the aggregation of emulsions (Bi et al., 2017). The changes of both particle size and ζ -potential of the emulsions prepared by PPI-GA mixture shared a similar pattern to that stabilized by PPI,

but with a lesser extent. Additionally, no phase separation was observed which indicates its greater stability than that prepared by PPI. Conversely, the PPI-GA conjugates stabilized emulsions were still homogeneous with a small particle size ($d_{43}=2.14 \mu\text{m}$) even when 500 mM salt was presented. These results indicated that conjugated PPI-GA effectively improved the salinity-tolerance of the emulsion it stabilized, which is on account of the enhanced electrostatic repulsion and steric hindrance.

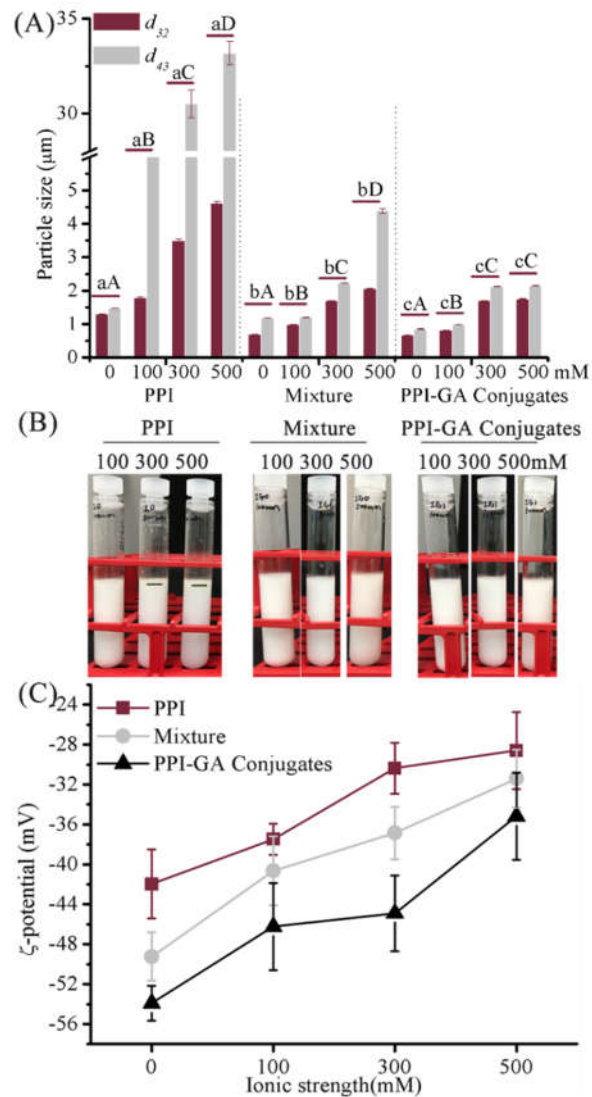


Figure 3.10. Influence of salt concentration on particle size (A), real figures (B), and ζ -potential (C), and of emulsions (pH 7.0) stabilized by PPI, PPI-GA mixture, and PPI-GA conjugates incubated for 1 day. The lowercase letters are for comparison among groups at the same treatments; the uppercase letters are for comparison in groups at different treatments; different letters indicated significance at $p < 0.05$.

3.4.5. Oxidative stability of oil-in-water emulsions stabilized by PPI-GA conjugates

Anionic polysaccharides in the aqueous phase of emulsions may retard lipid oxidation due to their iron binding capacity (Chen et al., 2010). However, when they serve as a coating for emulsions, anionic droplets can attract cationic transition metals (e.g., Fe^{2+}) to their surfaces, where lipid hydroperoxides are decomposed to promote lipid oxidation. This was a big concern in the current study since PPI-GA stabilized emulsions had the highest net negative surface charge. Therefore, the oxidative stability of emulsions stabilized by PPI-GA conjugates with 1 day incubation was investigated by determining the formation of both lipid hydroperoxides and hexanal during storage at 37°C (Fig. 3.11A&B).

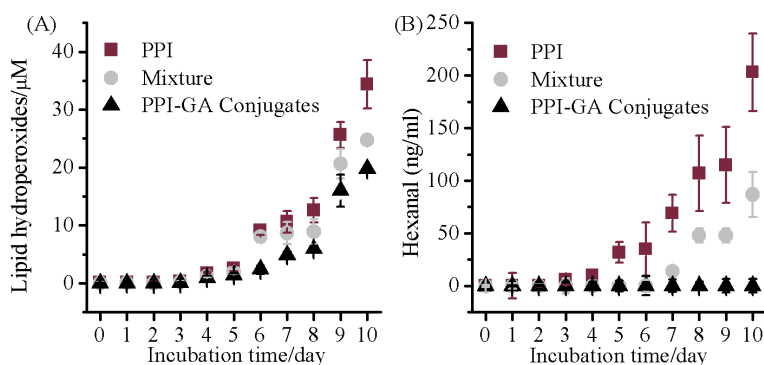


Figure 3.11. The formation of lipid hydroperoxides (A) and hexanal (B) in corn oil-in-water emulsions (pH 7.0) stabilized by PPI, PPI-GA mixture, and PPI-GA conjugates incubated for 1 day during storage at 37°C

A sudden increase in lipid hydroperoxides was observed in emulsions stabilized by PPI after 6 days of storage, which was in line with the formation of hexanal (Fig. 3.9A & B). Similarly, the formation of lipid hydroperoxides in the emulsions formed by PPI-GA was boosted after the same time of storage. However, the formation of hexanal lagged for 1 day and significant increase was observed after 7 days of storage. On the contrary to accelerate emulsion oxidation by attracting transition metals, the presence of GA in PPI-GA mixture stabilized emulsion extended the lag phase in terms of the formation of hexanal. In other words, steric hindrance derived from the thicker layer of GA on the droplet surface played a critical

role to hinder the transition metal ions from reaching the core lipids. When it came to the emulsion stabilized by PPI-GA conjugates, a slight increase of lipid hydroperoxides occurred after 7 days of storage while a sharp increase appeared after 9 days. These results indicate that PPI-GA conjugates could delay the development of lipid hydroperoxides. Surprisingly, the level of hexanal in PPI-GA conjugates-based emulsions was still lower than LOD even after subjecting to 10 days of storage. This result implied that PPI-GA conjugates can prevent the formation of hexanal, a chief marker of vegetable oil rancidity.

It has been previously reported that protein-polysaccharide conjugates developed by controlled Maillard reaction possess good antioxidant activity against lipid oxidation (Dong et al., 2012, 2011). The enhanced activities including radical scavenging activity, metal chelating activity, and scavenging of active oxygen species are proposed for the improved antioxidant activity of conjugates. In general, lipid hydroperoxides formed in the oil core of emulsion droplets will be transited to oil–water interface where they are decomposed by transition metal to form secondary oxidation products. In the current emulsion system, a slight inhibition of PPI-GA conjugates on lipid hydroperoxides formation with the concurrence of the greatest inhibitory activity against hexanal production was observed. It was therefore inferred that the conjugates formed barrier prevents the transition metal from interacting with hydroperoxides, rather than being as a scavenger to quench free radicals generated during storage.

3.5. Conclusion

The present research demonstrated the impact of incubation time on the properties and functionalities of PPI-GA conjugates. The conjugates formed by incubating pea protein isolate with hydrophilic gum Arabic (1:4) for 1 day not only restrained the production of final stage MRPs, but also effectively enhanced the solubility of the protein. The corn oil-in-water emulsions stabilized by the PPI-GA conjugates produced with a 1-day incubation had greater stability against environmental stresses than those prepared by PPI alone or PPI-GA mixture.

The improved stability of emulsions, especially at acidic pH, high temperature treatment, and high salt concentration, is primarily caused by steric hindrance effects of the conjugates. PPI-GA conjugates, formed through the controlled MR, can also inhibit the formation of volatile compounds and prevent emulsion oxidation.

3.6. References

- Bi, B., Yang, H., Fang, Y., Nishinari, K., & Phillips, G. O. (2017). Characterization and emulsifying properties of β -lactoglobulin-gum Acacia Seyal conjugates prepared via the Maillard reaction. *Food Chemistry*, *214*, 614–621.
<https://doi.org/10.1016/J.FOODCHEM.2016.07.112>
- Boye, J., Zare, F., & Pletch, A. (2010). Pulse proteins: Processing, characterization, functional properties and applications in food and feed. *Food Research International*, *43*, 414–431. <https://doi.org/10.1016/j.foodres.2009.09.003>
- Bradford, M. M. (1976). A rapid and sensitive method for the quantitation of microgram quantities of protein utilizing the principle of protein-dye binding. *Analytical Biochemistry*, *72*(1–2), 248–254. [https://doi.org/10.1016/0003-2697\(76\)90527-3](https://doi.org/10.1016/0003-2697(76)90527-3)
- Chen, B., McClements, D. J., & Decker, E. A. (2010). Role of continuous phase anionic polysaccharides on the oxidative stability of menhaden oil-in-water emulsions. *Journal of Agricultural and Food Chemistry*, *58*(6), 3779–3784.
<https://doi.org/10.1021/jf9037166>
- Dadali, G., Apar, D. K., & Özbek, B. (2007). Color change kinetics of okra undergoing microwave drying. *Drying Technology*, *25*(5), 925–936.
<https://doi.org/10.1080/07373930701372296>
- de Oliveira, F. C., Coimbra, J. S. dos R., de Oliveira, E. B., Zuñiga, A. D. G., & Rojas, E. E. G. (2016). Food protein-polysaccharide conjugates obtained via the Maillard reaction: A

review. *Critical Reviews in Food Science and Nutrition*, 56, 1108–1125.

<https://doi.org/10.1080/10408398.2012.755669>

de Oliveira, F. C., dos Reis Coimbra, J. S., de Oliveira, E. B., Rodrigues, M. Q. R. B., Sabioni, R. C., de Souza, B. W. S., & Santos, I. J. B. (2015). Acacia gum as modifier of thermal stability, solubility and emulsifying properties of α -lactalbumin. *Carbohydrate Polymers*, 119, 210–218. <https://doi.org/10.1016/J.CARBPOL.2014.11.060>

Delahaije, R. J. B. M., Gruppen, H., Van Nieuwenhuijzen, N. H., Giuseppin, M. L. F., & Wierenga, P. A. (2013). Effect of glycation on the flocculation behavior of protein-stabilized oil-in-water emulsions. *Langmuir*, 29(49), 15201–15208.

<https://doi.org/10.1021/la403504f>

Delgado-Andrade, C., Morales, F. J., Seiquer, I., & Pilar Navarro, M. (2010). Maillard reaction products profile and intake from Spanish typical dishes. *Food Research International*, 43(5), 1304–1311. <https://doi.org/10.1016/j.foodres.2010.03.018>

Dong, S., Panya, A., Zeng, M., Chen, B., McClements, D. J., & Decker, E. A. (2012). Characteristics and antioxidant activity of hydrolyzed β -lactoglobulin-glucose Maillard reaction products. *Food Research International*, 46(1).

<https://doi.org/10.1016/j.foodres.2011.11.022>

Dong, S., Wei, B., Chen, B., McClements, D. J., & Decker, E. A. (2011). Chemical and antioxidant properties of casein peptide and its glucose Maillard reaction products in fish oil-in-water emulsions. *Journal of Agricultural and Food Chemistry*, 59(24).

<https://doi.org/10.1021/jf203778z>

Gumus, C. E., Decker, E. A., & McClements, D. J. (2017a). Formation and stability of ω -3 oil emulsion-based delivery systems using plant proteins as emulsifiers: Lentil, pea, and faba bean proteins. *Food Biophysics*, 12(2), 186–197. <https://doi.org/10.1007/s11483-017-9475-6>

- Gumus, C. E., Decker, E. A., & McClements, D. J. (2017b). Impact of legume protein type and location on lipid oxidation in fish oil-in-water emulsions: Lentil, pea, and faba bean proteins. *Food Research International*, *100*, 175–185.
<https://doi.org/10.1016/j.foodres.2017.08.029>
- Habeeb, A. F. S. A. (1966). Determination of free amino groups in proteins by trinitrobenzenesulfonic acid. *Analytical Biochemistry*, *14*(3), 328–336.
[https://doi.org/10.1016/0003-2697\(66\)90275-2](https://doi.org/10.1016/0003-2697(66)90275-2)
- Laemmli, U. K. (1970). Cleavage of structural proteins during the assembly of the head of bacteriophage T4. *Nature*, *227*(5259), 680–685. <https://doi.org/10.1038/227680a0>
- Lam, A. C. Y., Can Karaca, A., Tyler, R. T., & Nickerson, M. T. (2018). Pea protein isolates: Structure, extraction, and functionality. *Food Reviews International*, *34*, 126–147.
<https://doi.org/10.1080/87559129.2016.1242135>
- Liu, S., Zhao, P., Zhang, J., Xu, Q., Ding, Y., & Liu, J. (2017). A comparative study of physicochemical and functional properties of silver carp myofibrillar protein glycosylated with glucose and maltodextrin. *RSC Advances*, *7*(2), 1008–1015.
<https://doi.org/10.1039/C6RA25088B>
- Martinez-Alvarenga, M., Martinez-Rodriguez, E. Y., Garcia-Amezquita, L. E., Olivas, G. I., Zamudio-Flores, P. B., Acosta-Muniz, C. H., & Sepulveda, D. R. (2013). Effect of Maillard reaction conditions on the degree of glycation and functional properties of whey protein isolate – Maltodextrin conjugates. *Food Hydrocolloids*, *38*, 110–118.
<https://doi.org/10.1016/j.foodhyd.2013.11.006>
- Nakauma, M., Funami, T., Noda, S., Ishihara, S., Al-Assaf, S., Nishinari, K., & Phillips, G. O. (2008). Comparison of sugar beet pectin, soybean soluble polysaccharide, and gum arabic as food emulsifiers. 1. Effect of concentration, pH, and salts on the emulsifying

- properties. *Food Hydrocolloids*, 22(7), 1254–1267.
<https://doi.org/10.1016/J.FOODHYD.2007.09.004>
- Nursten, H. (2005). *The Maillard Reaction: Chemistry, Biochemistry, and Implications*. Royal Society of Chemistry.
- Oliver, C. M., Melton, L. D., & Stanley, R. A. (2006). Creating proteins with novel functionality via the Maillard reaction: A review. *Critical Reviews in Food Science and Nutrition*, 46(4), 337–350. <https://doi.org/10.1080/10408690590957250>
- Ozturk, B., Argin, S., Ozilgen, M., & McClements, D. J. (2015). Formation and stabilization of nanoemulsion-based vitamin E delivery systems using natural biopolymers: Whey protein isolate and gum arabic. *Food Chemistry*, 188, 256–263.
<https://doi.org/10.1016/J.FOODCHEM.2015.05.005>
- Ozturk, B., & McClements, D. J. (2016). Progress in natural emulsifiers for utilization in food emulsions. *Current Opinion in Food Science*, 7, 1–6.
<https://doi.org/10.1016/J.COFS.2015.07.008>
- Pirestani, S., Nasirpour, A., Keramat, J., & Desobry, S. (2017). Preparation of chemically modified canola protein isolate with gum Arabic by means of Maillard reaction under wet-heating conditions. *Carbohydrate Polymers*, 155, 201–207.
<https://doi.org/10.1016/j.carbpol.2016.08.054>
- Pirestani, S., Nasirpour, A., Keramat, J., Desobry, S., & Jasniewski, J. (2017). Effect of glycosylation with gum Arabic by Maillard reaction in a liquid system on the emulsifying properties of canola protein isolate. *Carbohydrate Polymers*, 157, 1620–1627. <https://doi.org/10.1016/J.CARBPOL.2016.11.044>
- Pirestani, S., Nasirpour, A., Keramat, J., Desobry, S., & Jasniewski, J. (2018). Structural properties of canola protein isolate-gum Arabic Maillard conjugate in an aqueous model

- system. *Food Hydrocolloids*, 79, 228–234.
<https://doi.org/10.1016/j.foodhyd.2018.01.001>
- Roy, F., Boye, J. I., & Simpson, B. K. (2010). Bioactive proteins and peptides in pulse crops: Pea, chickpea and lentil. *Food Research International*, 43, 432–442.
<https://doi.org/10.1016/j.foodres.2009.09.002>
- Su, J. F., Huang, Z., Yuan, X. Y., Wang, X. Y., & Li, M. (2010). Structure and properties of carboxymethyl cellulose/soy protein isolate blend edible films crosslinked by Maillard reactions. *Carbohydrate Polymers*, 79(1), 145–153.
<https://doi.org/10.1016/J.CARBPOL.2009.07.035>
- Walker, R., Decker, E. A., & McClements, D. J. (2015). Development of food-grade nanoemulsions and emulsions for delivery of omega-3 fatty acids: opportunities and obstacles in the food industry. *Food & Function*, 6(1), 41–54.
<https://doi.org/10.1039/C4FO00723A>
- Wang, Q., & Ismail, B. (2012). Effect of Maillard-induced glycosylation on the nutritional quality, solubility, thermal stability and molecular configuration of whey protein. *International Dairy Journal*, 25(2), 112–122.
<https://doi.org/10.1016/j.idairyj.2012.02.009>
- Yadav, M. P., Strahan, G. D., Mukhopadhyay, S., Hotchkiss, A. T., & Hicks, K. B. (2012). Formation of corn fiber gum–milk protein conjugates and their molecular characterization. *Food Hydrocolloids*, 26(2), 326–333.
<https://doi.org/10.1016/J.FOODHYD.2011.02.032>
- Yang, Y., Cui, S. W., Gong, J., Guo, Q., Wang, Q., & Hua, Y. (2015). A soy protein-polysaccharides Maillard reaction product enhanced the physical stability of oil-in-water emulsions containing citral. *Food Hydrocolloids*, 48, 155–164.
<https://doi.org/10.1016/J.FOODHYD.2015.02.004>

- Yoshie-Stark, Y., Wada, Y., & Wäsche, A. (2008). Chemical composition, functional properties, and bioactivities of rapeseed protein isolates. *Food Chemistry*, *107*(1), 32–39. <https://doi.org/10.1016/J.FOODCHEM.2007.07.061>
- Zhu, D., Damodaran, S., & Lucey, J. A. (2010). Physicochemical and emulsifying properties of whey protein isolate (WPI)–dextran conjugates produced in aqueous solution. *Journal of Agricultural and Food Chemistry*, *58*(5), 2988–2994. <https://doi.org/10.1021/jf903643p>

4. THE STRUCTURAL MODIFICATION OF PEA PROTEIN CONCENTRATE WITH GUM ARABIC BY CONTROLLED MAILLARD REACTION ENHANCES ITS FUNCTIONAL PROPERTIES AND FLAVOR ATTRIBUTES²

4.1. Abstract

The aim of this research was to investigate the impact of conjugation with gum Arabic (GA) on the functional properties and flavor profile of pea protein concentrate (PPC). The PPC-GA conjugates were prepared by incubating the mixture at a mass ratio of 1:4 at 60 °C and 79 % relative humidity with variable times (0, 1, 3, and 5 days). The grafting of GA to PPC was confirmed using SDS-PAGE and Fourier transform infrared-attenuated total reflection spectra. The degree of conjugation between PPC and GA over the course of incubation was determined by non-specific Maillard reaction markers, the loss of free amino groups, and color development. The results suggested that the solubility and emulsification properties of PPC-GA conjugates was remarkably improved after 3 days of incubation and further extending incubation time deteriorated the functionalities. Surface morphology modifications of the conjugates revealed by scanning electron microscope may explain the enhanced functionality. The corn oil-in-water emulsions stabilized by PPC-GA conjugates of 3 days incubation also showed great physical stabilities against pH (2–8), thermal processing (25, 37, and 72 °C), and ionic strength (0, 100, 300, and 500 mM), as compared to PPC alone or the mixture of PPC and GA. HS-SPME-GC-MS analysis and quantification of beany flavor markers in PPC-GA conjugates indicated that the beany flavors markers were remarkably diminished after 1 day incubation.

² Based on the article of Fengchao Zha, Shiyuan Dong, Jijia Rao & Bingcan Chen published in Food Hydrocolloids online Jan. 2019 (DOI:10.1016/j.foodhyd.2019.01.046). Fengchao Zha was responsible for methodology, data collection and analysis, was the primary developer of the conclusions advanced here, and drafted and revised all versions of this chapter. Shiyuan Dong assisted with reviewing the draft. Jijia Rao assisted with instruments. Bingcan Chen was primary responsible for resources, reviewing and editing, supervising.

4.2. Introduction

The continuous world population growth accompanied by the increasing demand for protein induces a strong challenge on market supply and results in a market price multiplied by 4 over the last 15 years (Chéreau et al., 2016). Pea, the naturally dried seeds of *Pisum sativum* L, has gained significant interests for many reasons. The significant nutritional properties and potential health benefits associated with pea consumption, such as reducing LDL-cholesterol, weight management, the prevention of selenium and folate deficiency related diseases, lowering the incidence of type-2 diabetes mellitus and colon cancer, have been demonstrated extensively (Abeysekara, Chilibeck, Vatanparast, & Zello, 2012; Dahl, Foster, & Tyler, 2012).

Although the consumption of pea products is associated with all kinds of health benefits, the weekly average intake of beans and peas for adult males is less than 1 cup-equivalents (~ 180 g), which is far less than the recommended serving of 3 cup-equivalents (U.S. Department of Health and Human Services, 2015). In the meantime, the utilization of pea as functional food ingredients has also been limited. Two major factors limiting the consumption of pea and the application of pea protein have been identified. First, commercial pea proteins are commonly extracted by aqueous alkaline and isoelectric point precipitation resulting in the deterioration of functional properties, such as the lower solubility of final products (Lam, Can Karaca, Tyler, & Nickerson, 2018). Other functional properties associated with protein solubility like emulsification, foaming, and gelation, are impaired accordingly, which inevitably constrain its application as a food ingredient (Chéreau et al., 2016; Lam et al., 2018). Second, unpalatable flavors of pea proteins also impose restrictions on the consumer acceptance of pea protein enriched products (Ma et al., 2011). Such flavors, commonly described as grassy and beany flavors, arise from oxidative deterioration of unsaturated fatty acid in pea protein-bound lipids during pea seed storage and processing into protein concentrates.

Extensive reliable evidences have shown that the conjugation of protein-polysaccharide through Maillard reaction (MR) is a potential solution to improve the functional properties of protein (de Oliveira, Coimbra, de Oliveira, Zuñiga, & Rojas, 2016; Oliver, Melton, & Stanley, 2006). The conjugation between protein and polysaccharide originates from the Amadori rearrangement of Schiff base compounds that formed via the condensation of carbonyl-containing moieties with available ϵ -amino groups at the initial stage of MR (Martinez-Alvarenga et al., 2014; Pirestani, Nasirpour, Keramat, Desobry, & Jasniewski, 2018). The formation of conjugates makes proteins with low initial solubility by covalently linking with hydrophilic polysaccharides, improves emulsification properties and solubility (particularly at pH values below and around the isoelectric point) of the protein, and heat stability compared to original protein. Gum Arabic (GA), a highly branched polysaccharide, has been selected to be conjugated with proteins since it has been extensively applied into food industry to stabilize flavors and essential oils (de Oliveira et al., 2015; Martinez-Alvarenga et al., 2014). Furthermore, a substantial role of Maillard reaction in contributing to off-flavor removal and aroma flavor generation of processed foodstuffs also has been widely reported (Christoph Cerny & Davidek, 2003; Liu, Liu, He, Song, & Chen, 2015). Specifically, the Amadori rearrangement and the Strecker degradation in relation to flavor formation are of utmost importance, where available ϵ -amino groups are degraded by dicarbonyls formed in the Maillard reaction, leading to deamination and decarboxylation of the ϵ -amino groups (Van Boekel, 2006).

Therefore, the objective of this research was to investigate the impact of pea protein concentrates (PPC) conjugated with GA on functional properties and flavor attributes of PPC, with a particular emphasis on their ability to enhance physical stabilities of corn oil-in-water emulsions.

4.3. Materials and Methods

4.3.1. Materials

Pea protein concentrate (PPC, moisture ~6%, protein ~55%, lipid ~1-2%) was kindly donated by Ingredion Incorporated (Bridgewater, New Jersey). gum Arabic (GA, moisture ~6.7%, polysaccharide ~90%, protein ~3.2%, and minerals ~ 0.2%) with a molecular weight (M.W.) 0.25×10^6 - 2.5×10^6 Da was kindly provided by TIC Gums (Belcamp, MD). Mazola[®] Corn oil (refractive index ~1.47) was purchased locally. All other chemicals used in this study were of analytical grade. Specification values of each commercial ingredient were obtained from manufacturers. All bulk samples were used as received. Deionized water of 18.2 MΩ.cm resistivity obtained from Barnstead GenPure PRO Standard (Thermo Fisher Scientific, Inc., Waltham, MA) was used to prepare all solutions and emulsions.

4.3.2. Preparation of PPC-GA conjugates

The preparation of PPC-GA conjugates followed the procedure described in **Section 3.3.2.**

4.3.3. Amadori compounds and melanoidins formation

According to a reported method (Delgado-Andrade, Morales, Seiquer, & Pilar Navarro, 2010), UV-Vis absorbance of the conjugates at 304 nm and 420 nm was used as an indication of Amadori compounds formation (Wang & Ismail, 2012; Zhu, Damodaran, & Lucey, 2010), and high molecular weight melanoidins formation (Martinez-Alvarenga et al., 2014), respectively. When carrying out the measurements with quartz cuvettes (10 mm path length × 2 mm width × 45 mm height), appropriate dilutions to give an absorbance value of < 1.0 were prepared using deionized water, and all samples were of the same dilution for comparison. All measurements were performed using a Shimadzu UV-1100 PC model spectrophotometer (Shimadzu Corp., Kyoto, Japan) with deionized water as a blank reference.

4.3.4. Free amino groups

The measurement of free amino groups of PPC-GA conjugates followed the procedure described in **Section 3.3.4**.

4.3.5. Color development

The color of samples was measured using a Minolta Chroma Meter (Model CR-310, Japan) with a diffuse illumination/0-degree viewing geometry to obtain CIE L* a* b* values. The chromameter was calibrated with a standard white tile (Y=92.2, x=0.3162, and y=0.3324).

4.3.6. Sodium dodecyl sulphate-polyacrylamide gel electrophoresis (SDS-PAGE)

SDS-PAGE was performed according to the **Section 3.3.6**.

4.3.7. Fourier transform infrared spectroscopy-attenuated total reflection

Fourier transform infrared spectroscopy-attenuated total reflection (FTIR-ATR) spectra were recorded using a Varian 600-IR series spectrometer (Varian, Palo Alto, CA, USA) equipped with a high-sensitivity mercury cadmium telluride (MCT) detector and a Pike Miracle three-bounce Germanium crystal ATR accessory (PIKE technologies, Madison, WI). An absorbance spectrum of air as background was recorded prior to the measurement and automatically subtracted from the spectra of samples. The spectroscopy measurements were performed using dried fine powders (~10 mg) in the frequency range of 4000-800 cm^{-1} at a resolution of 4 cm^{-1} and 32 scans. The data was collected and processed through Varian Resolutions ProTM software.

4.3.8. Scanning electron microscopy

Scanning electron microscopy was performed according to the **Section 3.3.8**.

4.3.9. Relative solubility of PPC-GA conjugates

Protein solubility was determined according to the **Section 3.3.7**.

4.3.10. Preparation of corn oil-in-water emulsion with PPC-GA conjugates

An emulsifier solution was prepared according the **Section 3.3.9**.

4.3.11. Particle size & zeta potential measurement

The emulsion particle size and size distributions were directly measured using a laser light scattering instrument (Mastersizer 3000, Malvern Instruments Ltd., Malvern, UK). The emulsion ζ -potential (mV) was measured using a micro-electrophoresis device (Nano-ZS, Malvern Instruments Ltd., Malvern, UK).

4.3.12. Physical stability of emulsions against environment stress

To evaluate the stability of emulsions across a range in pH, the emulsions were adjusted to different pH (2.0–8.0) with 1N HCl or NaOH, and left quiescently at room temperature for 30 min. To examine the stability of emulsions against thermal processing, emulsion samples (10 mL, pH 7.0) were transferred into glass test tubes, which were then incubated in a pre-heated incubator for 24 h at different temperatures (25, 37, and 72°C). After incubation, the emulsions were immediately cooled at room temperature. To assess the stability of emulsions against ionic stress (NaCl), the emulsions (10 mL, pH 7.0) were adjusted to various desired salt concentrations (0, 100, 300, and 500 mM), and left quiescently at room temperature for 30 min. Changes in particle size and ζ -potential of emulsions was recorded.

4.3.13. Volatile compounds measurements

Volatiles were analyzed by headspace solid phase microextraction in combination with gas chromatography coupled to mass spectrometry (HS-SPME-GC-MS). After 1 h of equilibrium at 30 °C, all uniform samples (0.20 g PPC/ 0.4 mL DI water, or 1.00 g conjugates/ 2 mL DI water) in 20 mL capped GC glass vials were preheated at 60 °C for 10 min in an auto-sampler heating block. A 50/30 μ m Divinylbenzene/Carboxen/ Polydimethylsiloxane solid-phase microextraction (SPME) fiber needle (Supelco, Bellefonte, PA) was injected into the vial absorbing volatiles for 50 min, and then was transferred to the injector port (250 °C) for 3 min. Splitless mode was selected for the injection port. GC-MS analyses were performed on GC 7697A coupled to an MSD 5977A (both Agilent, Palo Alto, CA), using a ZB-Wax column

(60 m × 0.25 mm × 0.25 μm, Agilent). After insertion of the SPME device into the injector, oven temperature program set as: the temperature raised at 45 °C/min from 40 to 85 °C, then at 9 °C/min from 85 to 200 °C, and at 45 °C/min from 200 to 250 °C and held for 3 min isothermally. Ultra-high purity helium was used as the carrier gas at the flow rate of 1.5 mL/min. Mass spectra in the electron impact mode (EI) was generated at 70 eV and at a scan range from m/z 28 to 350. The identification of volatile compounds was selected only if the match factor was greater than 80 according to the NIST 2.0 mass spectra libraries.

4.3.14. Statistical analysis

The experiment was conducted at least twice using the fresh prepared samples. Data were expressed as the mean ± standard deviation of at triplicate measurements. The data were statistically analyzed using statistical software, SAS version 9.4 (SAS institute Inc. Cary, NC). One-way analysis of variance (ANOVA) was conducted, and significant difference was defined at $p < 0.05$ by Tukey's test.

4.4. Results and Discussion

4.4.1. Structure characterization of PPC and PPC-GA conjugates

To confirm the occurrence of conjugation in PPC-GA system, SDS-PAGE and FTIR (**Fig. 4.1&4.2**) were applied to monitor both molecular weight and structural changes of the products over the course of incubation.

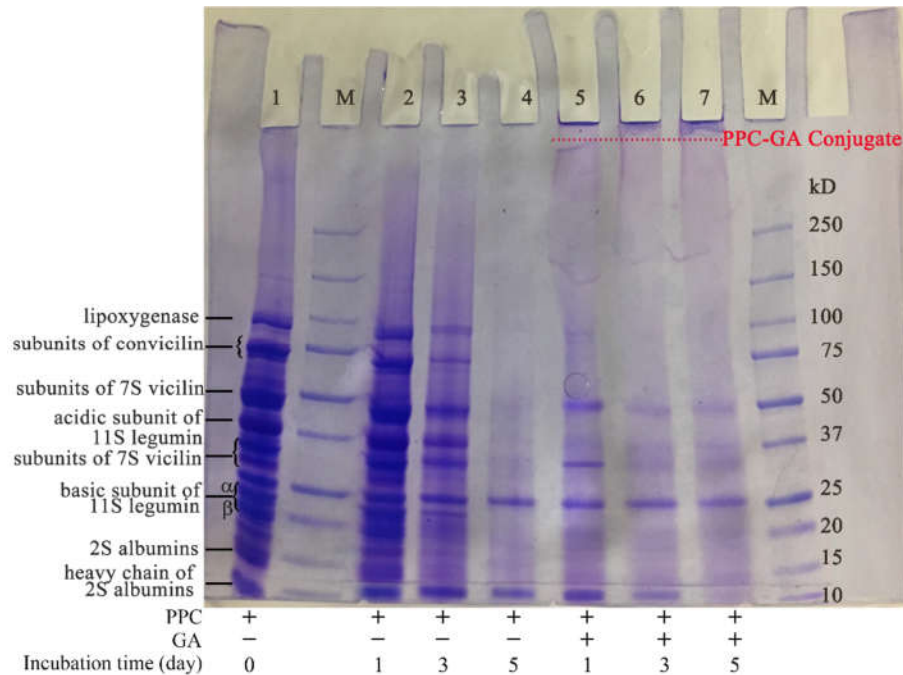


Figure 4.1. SDS-PAGE patterns for different PPC-GA conjugates: lane M for protein markers; lanes 1-7 for PPC-0 day, PPC-1 day, PPC-3 day, PPC-5 day, PPC-GA conjugates-1 day, PPC-GA conjugates-3 day, PPC-GA conjugates-5 day, respectively

It is well known that pea protein is mainly composed of albumins and globulins. Salt-soluble globulins can be further subdivided into primarily 11S legumin and 7S vicilin proteins, with a minor amount of a third type known as convicilin (Chéreau et al., 2016; Lam et al., 2018). One of the characteristic bands present in the initial PPC is the 2S albumin (**Fig. 4.1 lane 1**) that consists of both light (~4.5 kDa) and heavy (~10 kDa) polypeptide chains (Chéreau et al., 2016). Additionally, three (47.3, 33.3 and 28.7 kDa) subunits of 7S vicilin, two subunits of convicilin (77.9 and 72.4 kDa), as well as acidic (~40 kDa) and basic subunits (~20 kDa, α - β) constituting the monomers of 11S legumin were identified in lane 1 (Chéreau et al., 2016; Lam et al., 2018). Obviously, a newly formed band near the loading end of the gel concomitant with the disappearance of some of pea protein subunits was observed (**Fig. 4.1, lanes 5, 6 & 7**). The presence of large molecular weight biopolymers that could not migrate into the separating gel occurred presumably because of the large M.W. of GA (> 250 kDa) conjugating with PPC (Pirestani, Nasirpour, Keramat, Desobry, & Jasniewski, 2017). The intensity of the

band became stronger as incubation time increased. The absence of such band in PPC alone with the same treatment confirmed that the development of PPC-GA conjugates was responsible for the newly formed band (**Fig. 4.1, lanes 2, 3 & 4**). It was found that the characteristic bands associated with 2S primarily participated in the conjugation reaction. Remarkable changes were observed in the intensity of 2S bands as the reaction proceeded for 1 day, and then less changes in the intensity was found with the extension of incubation time. Surprisingly, a band at around 94 kDa (lane 1) that has previously been assigned to pea seeds lipoxygenase (LOX) also existed in the raw PPC (Barać et al., 2011; Szymanowska, Jakubczyk, Baraniak, & Kur, 2009). Lipoxygenase is one of the key contributors for the production of beany flavor compounds in pea proteins and the conjugation of PPC with GA seemed to be an efficient means to degrade LOX as indicated by the disappearance of the LOX band.

The conjugation of PPC to GA as reflected in the changes in chemical structure can also be characterized using FTIR-ATR (**Fig. 4.2**). The distinguished characteristic bands of amide I, II, and III in the spectrum of PPC were observed at 1635 cm^{-1} (C=O stretching), 1546 cm^{-1} (N-H deformation), and $1398\text{ & }1246\text{ cm}^{-1}$ (C-N stretching and N-H bending vibrations), respectively (Pirestani et al., 2018; Su, Huang, Yuan, Wang, & Li, 2010). The band at 1078 cm^{-1} was attributed to vibrations such as out-of-plane C-H bending (Su et al., 2010). The absorption band at 2925 cm^{-1} was due to the antisymmetric stretching of C-H in CH_2 and CH_3 groups (Pirestani et al., 2018). In terms of GA, the FTIR spectrum revealed that the bands in the region of $1500\text{-}800\text{ cm}^{-1}$ might be due to C-H deformation, C-O and C-C stretching (Pirestani et al., 2018).

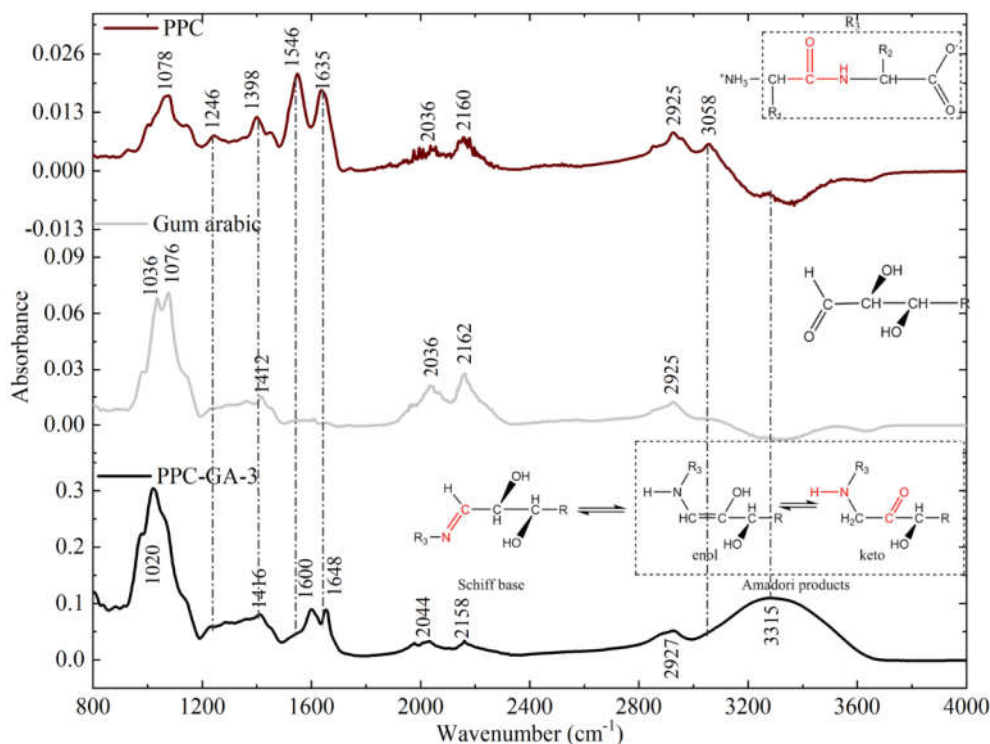


Figure 4.2. The characteristic structure of PPC-GA conjugate by Fourier transform infrared spectroscopy-attenuated total reflection (FTIR-ATR). PPC and GA represent pea protein concentrate and gum Arabic, respectively.

Upon structural modification by the Maillard reaction (3 days incubation), a newly appearing band (1600 cm^{-1}) located between the amide band I and II regions may be ascribed to Maillard reaction products such as carboxylate ion COO^- (antisym stretch, $1610\text{-}1560\text{ cm}^{-1}$), β -diketones ($\text{C}=\text{O}$ stretch, enol/keto form $1640\text{-}1580\text{ cm}^{-1}$), or pyridine derivatives (ring stretch, doublet, $1615\text{-}1565\text{ cm}^{-1}$) (Nursten, 2005). Moreover, another two new absorption bands at 1648 cm^{-1} and 3315 cm^{-1} indicated a $\text{C}=\text{N}$ stretching vibration deriving from the newly formed Schiff's base and a O-H & N-H groups stretching vibration, respectively (Su et al., 2010). The absorption bands identified above further confirmed the development of conjugation of PPC with GA.

4.4.2. Determination of degree of PPC-GA conjugation

The degree of conjugation between protein and polysaccharide has a substantial impact on the functionality of conjugates. The degree of conjugation is highly dependent on incubation

time under the given reaction temperature and PPC/GA ratio. Hence, in this section, the effect of incubation time on the degree of PPC-GA conjugations using three parameters including non-specific markers of Maillard reaction, the block of free amino groups, and color development (**Fig. 4.3-4.5**) was examined.

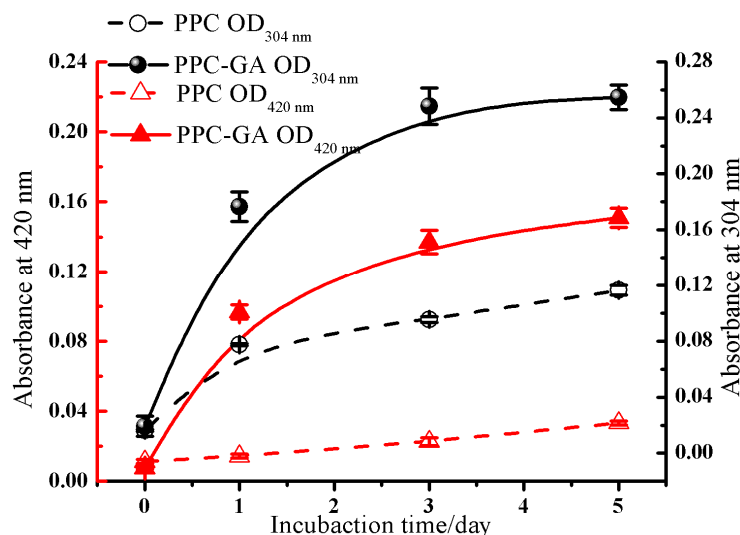


Figure 4.3. Changes in absorbance at 304 nm and 420 nm in mixture of PPC and GA incubated at 60°C and 79% relative humidity for 0-5 day.

Non-specific markers of Maillard reaction, as measured by the absorbance of conjugation solution at 304 nm and 420 nm (**Fig. 4.3**), have been widely used as the indicators for the degree of conjugation as they correspond to early-intermediate (e.g. Amadori compounds) and final Maillard reaction products (e.g. melanoidins), respectively (Wang & Ismail, 2012; Zhu et al., 2010). The absorbance of PPC-GA mixture at 304 nm increased sharply during the first 3 days of incubation ($p < 0.05$), after which was gradually leveled off with increasing incubation time up to 5 days. This result suggests that Amadori compounds were developed within 3 days of incubation. A parallel trend for the formation of colored melanoidins was seen based on the absorbance at 420 nm (**Fig. 4.3**). The values obtained at 304 nm were always higher than those obtained at 420 nm for all PPC-GA conjugates, which indicates a dominant early-intermediate Maillard reaction products in all conjugate (Delgado-Andrade et al., 2010; Pirestani, Nasirpour, Keramat, & Desobry, 2017). Meanwhile, a slight

increase in the non-specific markers, particularly the absorbance at 304 nm for PPC along was also observed during incubation, presumably because of the presence of carbohydrates with reducing carbonyl groups that can undergo Maillard reaction with PPC during incubation.

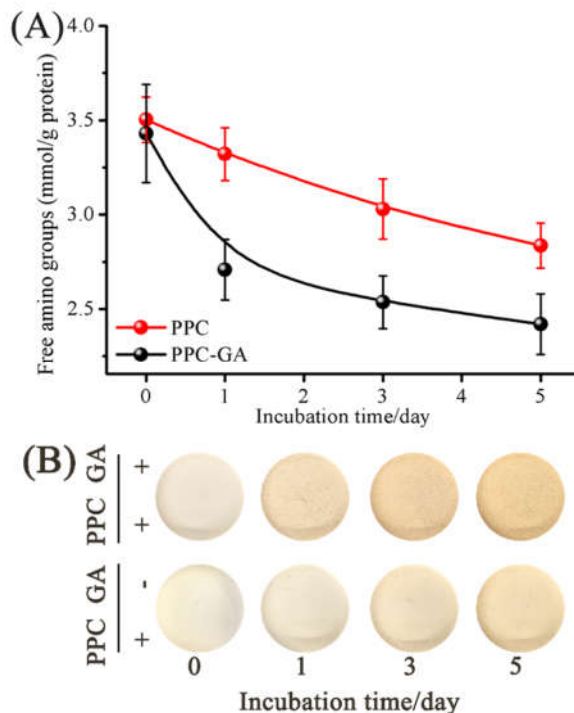


Figure 4.4. Changes of free amino groups (A) as a function of incubation time during glycation of PPC and GA at 60°C and 79% relative humidity; The real figures of samples (B).

Available free amino groups are another indicator of the degree of conjugation (**Fig. 4.4**). In PPC-GA system, available free amino groups dropped remarkable during the first 3 days of incubation, giving a reduction of nearly 25.9% percentage. It was deduced that the binding of PPC to GA contributed to the primary reduction of available amino groups in conjugates. A further decrease in free amino groups in PPC-GA system was noted after 3 days of incubation; this might be attributed to a reduction in the reactivity of saccharides (Laroque et al., 2008; Pirestani, Nasirpour, Keramat, & Desobry, 2017). Although available free amino groups in PPC alone (11.4 %) was two times less than that in PPC-GA system after 3 days incubation, the loss of free amino groups again suggests that Maillard reactions also existed in PPC alone and the greater extent of conjugation occurred after 1 day of incubation.

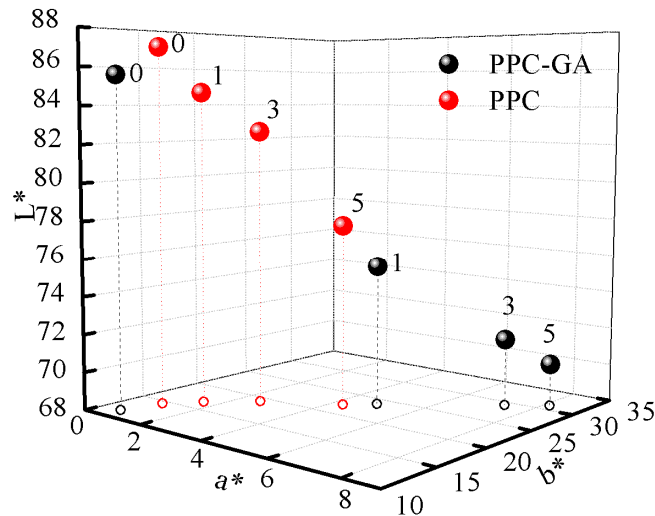


Figure 4.5. Color development in samples incubated at different times of 0, 1, 3, 5 day, respectively, under 60°C and 79% relative humidity conditions.

The extent of PPC-GA conjugation can also be determined using CIE Lab parameters as they associate with variations in the observed visual color after thermal treatment. In PPC-GA mixture systems, prominent increases in a^* (+red) and b^* (+yellow) values along with a decrease of L^* (+lightness) value were found with the extension of incubation time (**Fig. 4.5**). These changes were most remarkable at the end of 5 days incubation, allowing us to believe that the conjugation of PPC-GA is time dependent. However, smaller changes in CIE Lab parameters were observed in PPC alone, again implying the presence of both GA and PPC participating in Maillard reaction contribute to color development.

Statistical negative linear correlations were obtained between absorbance at 420 nm and L^* value or free amino groups ($r = -0.952$, $p=0.00027$; $r = -0.917$, $p =0.00132$, respectively). Such correlations are in agreement with the results from other researchers and can be explained by the progress of Maillard reaction (Ameur, Zude, Trystram, & Birlouez-Aragon, 2004; Martinez-Alvarenga et al., 2014).

4.4.3. Impact of incubation time on the solubility of PPC-GA conjugates

As aforementioned, low solubility is one of the biggest challenges to utilize pea protein as functional food ingredients as it is one of the most important functional properties. Due to

the hydrophilic nature of GA, one would expect that the solubility of PPC-GA conjugates may be determined by incubation time in the current system. **Figure 4.6** presents the changes in solubility of PPC and PPC-GA conjugates over the course of 5 days incubation. The solubility of PPC-GA mixture at day 0 was similar to that of PPC itself ($p > 0.05$) implying that no physicochemical interactions at a neutral pH. The solubility of PPC when conjugated with GA can be described as a parabolic pattern. It was significantly improved from 29.2 % to 36.4 % after 1 day incubation, and continued to 40.9 % at day 3. A sharp turnover was observed as incubation time exceeded to 5 days. A similar pattern in regard to the solubility of PPC was displayed except an earlier decrease with greater extent after 1 day incubation.

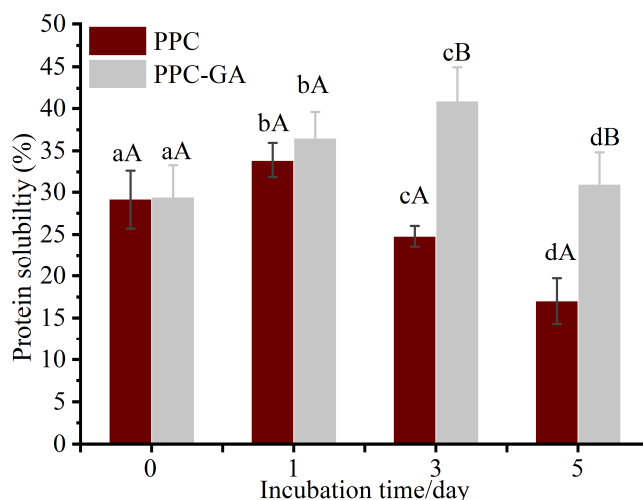


Figure 4.6. Relative protein solubility of different PPC-GA conjugates incubated at different times of 1, 3, 5 day, respectively; Note: the lowercase is for comparison in groups during different incubation time; the uppercase is for comparison among groups at the same incubation time. Different letters indicated significance at $p < 0.05$.

In order to gain better understanding on how incubation time impacts the solubility of PPC-GA conjugates, interfacial and morphological properties of PPC-GA conjugates were examined by scanning electron microscopy (**Fig. 4.7**). The microstructures of GA (**Fig. 4.7-1**) and PPC (**4.7-2**) primarily presented near spherical or irregular polygonal and indiscernible irregular form, respectively. The staggering pattern between irregular polygonal and irregular forms in the micrograph of PPC-GA mixture (**Fig. 4.7-3**) indicated that there was no chemical

bonded association between the two biopolymers but physical mixing. The attachment of PPC on the surface of GA via covalent bonds, as the conjugation proceeded for 1 day at 60°C gave rise to an inhomogeneous network structure accompanied by the disappearance of initial PPC microstructures (Fig. 4.7-4). Further extending the incubation to day 3 resulted in a greater inhomogeneity that may facilitate the interaction between conjugates and water and increase the solubility of conjugates. Similar morphologies were reported when a covalent linkage was obtained after conjugation of corn fiber gum with milk protein (Yadav, Strahan, Mukhopadhyay, Hotchkiss, & Hicks, 2012). The decline in the solubility of PPC-GA conjugates after 5 days incubation can be explained by their extensive conjugation as reflected by a whole chunk of compressed samples with a flattened surface morphology (Fig. 4.7-6). In consequence, overreaction of PPC-GA conjugation that occurs during thermal processing with prolonged time is a determinant factor to cause the loss of its solubility. Thus, controlling the incubation time is of great importance to achieve the optimum functional properties of PPC-GA conjugates.

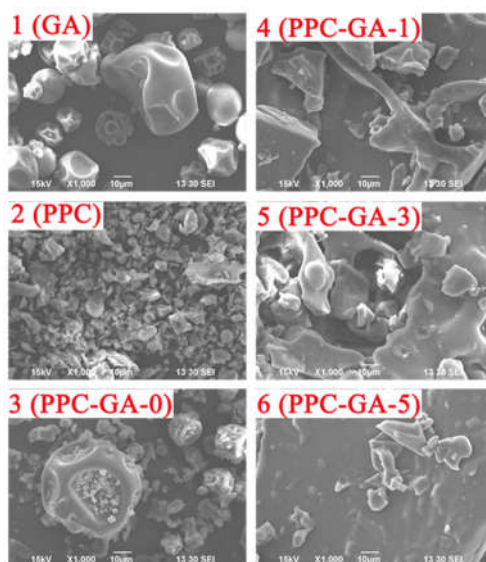


Figure 4.7. SEM for surface characters profiles of PPC-GA conjugates: 1-3 for GA, PPC, mixture of PPC and gum Arabic, 4-6 for PPC-GA conjugates incubated at different times of 1, 3, 5 day, respectively. Magnification 1000×; scale bar =10µm.

4.4.4. Impact of incubation time on the emulsifying property of PPC-GA conjugates

Emulsification is another important function of protein ingredient in the food industry. The emulsification property of PPC-GA conjugates with different incubation time was examined by measuring the particle size and size distributions of corn oil-in-water emulsion it stabilized (**Fig. 4.8**).

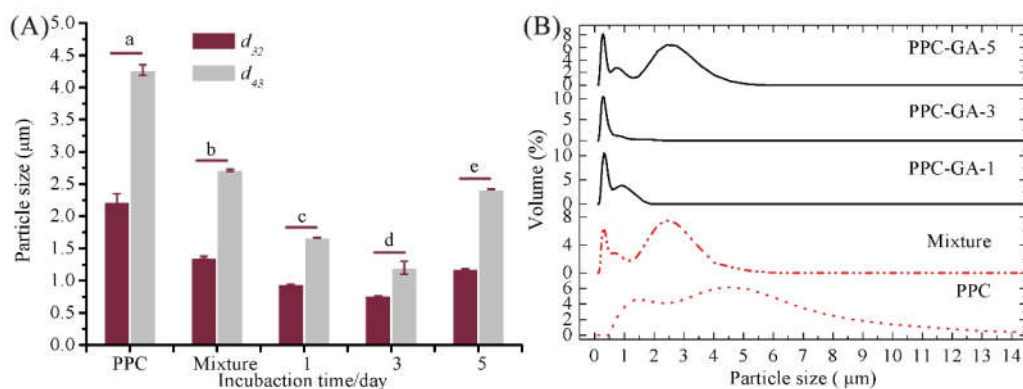


Figure 4.8. (A) Changes of particle size (d_{32} and d_{43}) at different incubation times for emulsions stabilized with PPC alone, mixture of PPC and gum Arabic and PPC-GA conjugates; (B) Changes of size distribution for emulsions stabilized with PPC alone, mixture of PPC and gum Arabic and PPC-GA conjugates. Note: for (A), the lowercase is for comparison among groups at different treatments; Different letters indicated significance at $p < 0.05$.

The surface-mean (d_{32}) and volume-mean droplet diameter (d_{43}) of PPC stabilized corn oil-in-water emulsions was 2.23 and 4.27 μm , respectively (**Fig. 4.8A**). Physically mixed PPC-GA reduced the volume-mean droplet diameter of emulsion to 2.72 μm , which might be due to the inherent emulsification property of GA. The size of emulsions prepared by PPC-GA conjugates with relatively shorter incubation time (1 and 3 days) significantly reduced the droplet size of the emulsion (d_{32}/d_{43} , 0.94/1.67 μm ; 0.77/1.20 μm , respectively). This result confirmed that enhanced emulsification property of PPC derived from the covalent bonding with GA via Maillard reaction, rather than physical mixing. Extending incubation time to 5 days, however, adversely affects its emulsification property as supported by the increased particle size of emulsions. The size distributions of the emulsions prepared from both PPC alone and the mixture of PPC-GA had broad multimodal distributions (**Fig. 4.8B**). Conversely,

a narrow monomodal distribution with a peak around 0.28 μm was observed in the emulsion prepared using PPC-GA conjugates after 3 days incubation. Interestingly, further extension of the incubation to 5 days resulted in the conjugates producing a trimodal distribution for the emulsion droplets it stabilized, which suggest that extensive reaction can reduce the emulsification property of conjugates.

4.4.5. Physical stability of oil-in-water emulsions stabilized by PPC-GA conjugates

The emulsion prepared using pea proteins is physically unstable against environmental stresses (Gumus, Decker, & McClements, 2017). To examine whether the physical stability of PPC-GA conjugate stabilized emulsions could be improved under environmental stresses, PPC-GA conjugate developed after 3 days incubation was selected to prepare corn oil-in-water emulsion for physical stability studies as it formed the smallest droplets with narrow size distribution.

4.4.5.1. Influence of pH on physical stability of emulsions

The impact of pH on the particle size and ζ -potential of the emulsions stabilized with PPC-GA conjugate (PPC and mixture as controls) was investigated (**Fig. 4.9A, B&C**). Serious phase separation was visualized in emulsions stabilized by PPC at pH 4-6, while the macroscopic instability was not observed in PPC-GA mixture and conjugate emulsions within the pH range (**Fig. 4.9B**). The results suggested that PPC alone stabilized emulsions were highly unstable to droplet aggregation at pH values near its isoelectric point (IEP \sim 4.5, **Fig. 4.9C**). The difference in stability was further supported by particle size measurements where the mean particle size of PPC stabilized emulsion was significantly larger than those prepared by PPC-GA conjugate and mixture under the whole pH range. The particle size of the emulsions prepared by PPC-GA conjugate and mixture was identical at pH 4–8. A remarkable size increase was recorded in PPC-GA mixture stabilized emulsion as pH adjusted to 3 and below, which can be explained by a deterioration effect of GA destabilizing emulsions at pH

lower than 3 (Nakauma et al., 2008). The well-maintained small particle size of emulsions prepared by PPC-GA conjugate across a broad pH range (2-8) suggested that the enhancement of the emulsions against pH was ascribed to the presence of GA that is covalent conjugated with PPC.

The ζ -potential of the emulsion droplets as a function of pH was displayed in **Fig. 4.9C**. For PPC stabilized emulsions, the ζ -potential was highly negative at pH 6 (-25 mV); however such strong electrostatic repulsion of emulsion droplets stabilized by PPC did not improve the physical stability, again suggesting the poor functionality of PPC alone. The IEP of PPC-GA conjugate was 2.0 (**Fig. 4.9C**), which was consistent with literature that IEP of protein was lowered after glycation due to the modification of available amino groups (Delahaije, Gruppen, Van Nieuwenhuijzen, Giuseppin, & Wierenga, 2013). When comparing the ζ -potential of the emulsion droplets stabilized by PPC-GA conjugate and PPC-GA mixture across the entire pH range, no significant difference was observed (**Fig. 4.9C**). Consequently, the difference in emulsion stability at acidic pH (2 & 3) between PPC-GA conjugate-based emulsions and PPC-GA mixture-based emulsions cannot be attributed to the differences in electrostatic interactions. Alternatively, the improved steric repulsion resulting from changes in conformation of glycoproteins might play a dominant role in the observed differences (Oliver et al., 2006). The strong steric repulsion could counter the prevailing van der Waals attraction between emulsion droplets at pH close to the IEP and thereby prevents flocculation and phase separation (Delahaije et al., 2013).

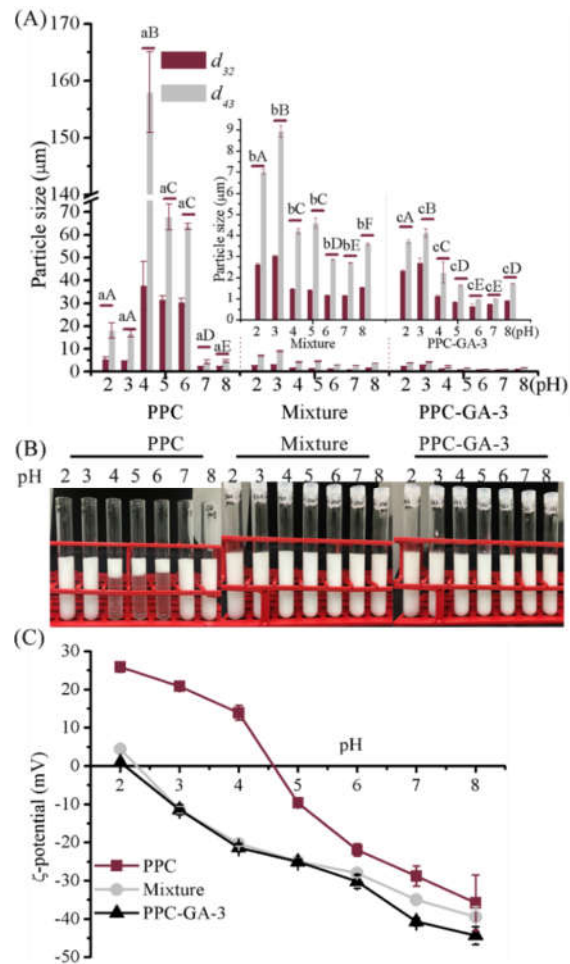


Figure 4.9. Changes of particle size (A), real figures (B) and ζ -potential (C) for emulsions stabilized with PPC alone, mixture of PPC with GA and PPC-GA conjugates against different pHs. Note: for (A), the lowercase is for comparison among groups at the same treatments; the uppercase is for comparison in groups at the different treatments. Different letters indicated significance at $p < 0.05$.

4.4.5.2. Influence of thermal processing on physical stability of emulsions

The impact of thermal treatment temperature (25, 37, and 72°C) on the stability of emulsions prepared by PPC-GA conjugate at pH 7.0 was investigated by measuring the particle size and ζ -potential (Fig. 4.10A, B&C).

A considerable ascending in mean particle size of emulsion prepared by PPC alone and PPC-GA mixture was observed upon the increase of thermal treatment temperature, which suggests the tendency of emulsion droplets to coalescence (Fig. 4.10A&B). The thermal processing may denature the protein anchored on the interface and cause the loss of surface

charge (**Fig. 4.10C**); and this, in return, allowed Van der Waals attractive interactions to dominate between oil droplets (Bi, Yang, Fang, Nishinari, & Phillips, 2017). Oil droplets stabilized by PPC-GA conjugate, on the other hand, presented the smallest particle size upon thermal treatments among all the emulsion, with d_{43} slightly increased from 1.20 μm at 25°C to 2.45 μm at 72°C. Meanwhile, the net ζ -potential of PPC-GA conjugate stabilized emulsions was much higher than the other two systems upon both 25 and 37°C thermal treatment (**Fig. 4.10C**). This can be explained by the loss of ionizable amine groups of PPC upon conjugating with GA which converts cationic amino groups to anionic GA residues. Consequently, the stronger electrostatic and steric repulsions stemmed from the increased net negative charges as well as the thicker layers of interface on emulsion droplets will improve the thermal stability (Oliver et al., 2006).

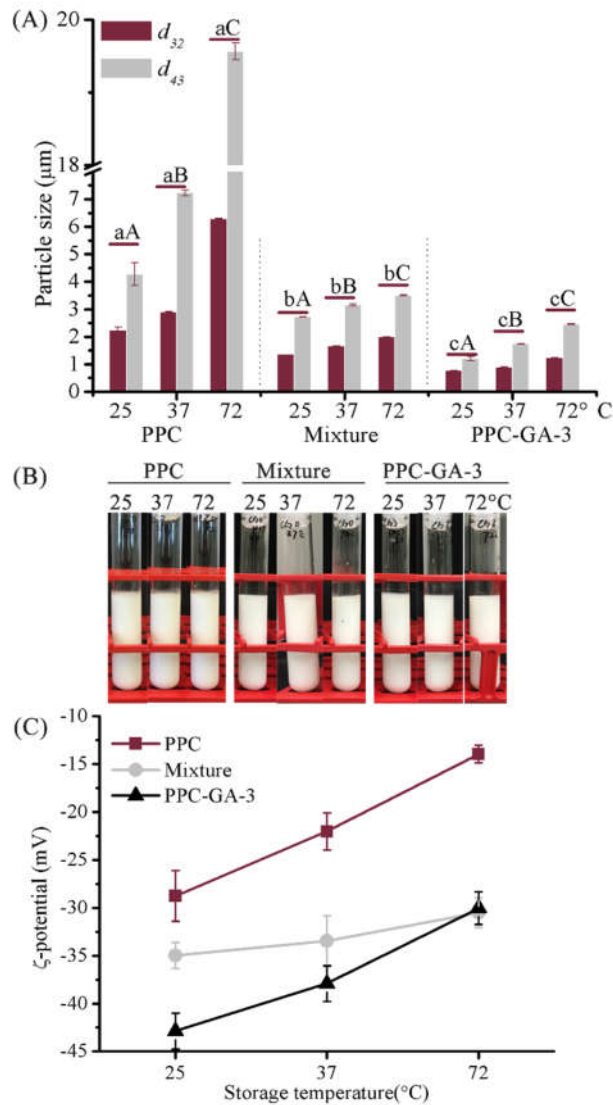


Figure 4.10. Changes of particle size (A), real figures (B) and ζ -potential (C) for emulsions stabilized with PPC alone, mixture of PPC with GA and PPC-GA conjugates against thermal temperature. PPC and GA represent pea protein concentrate and gum Arabic, respectively. Note: for (A), the lowercase letters are for comparison among groups at the same treatments; the uppercase letters are for comparison in groups at the different treatments. Different letters indicated significance at $p < 0.05$.

4.4.5.3. Influence of ionic strength on physical stability of emulsions

The impact of various salt concentrations (0, 100, 300, and 500 mM NaCl) on particle size and ζ -potential of emulsions stabilized by PPC-GA conjugate at pH 7.0 was monitored (Fig. 4.11A, B&C).

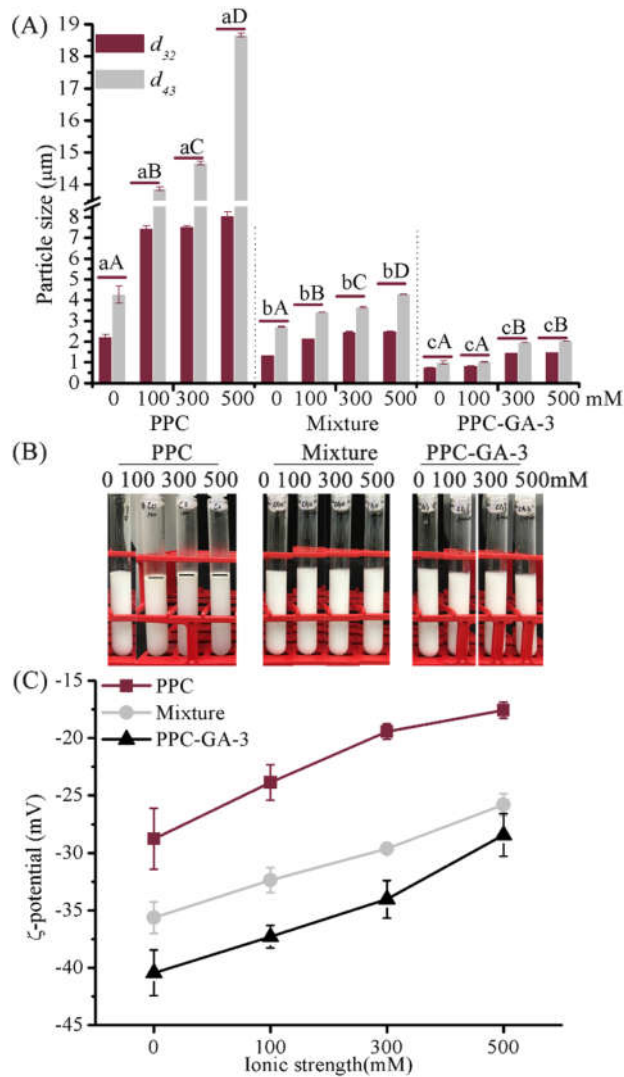


Figure 4.11. Changes of particle size (A), real figures (B) and ζ -potential (C) for emulsions stabilized with PPC alone, mixture of PPC with GA and PPC-GA conjugates against ionic strengths. PPC and GA represent pea protein concentrate and gum Arabic, respectively. Note: for (A), the lowercase letters are for comparison among groups at the same treatments; the uppercase letters are for comparison in groups at the different treatments. Different letters indicated significance at $p < 0.05$.

PPC stabilized emulsion was unstable upon NaCl addition as supported by an increase in d_{43} from 4.27 to 13.87 μm , and the formation of a cream layer (Fig. 4.11A). Further increase in the salt concentration accelerated the drastic increase of particle size and the decrease of ζ -potential. The electrostatic repulsions, the dominant force to stabilize the emulsion in this case, was screened at the interface at the presence of salt which increases Van der Waals attractive interactions between droplets and leads to the aggregation of emulsion (Bi et al., 2017). A

similar tendency, but to a lesser extent, was observed in the changes of both particle size and ζ -potential of the emulsions prepared by PPC-GA mixture. Nevertheless, no phase separation was observed which indicates greater emulsion stability than that of PPC. The emulsion stabilized by PPC-GA conjugate was still homogeneous with a relatively small particle size ($d_{43}=2.03 \mu\text{m}$) even upon the introduction of 500 mM salt. Since there was no difference of net ζ -potential between PPC-GA conjugate and PPC-GA mixture stabilized emulsion as 500 mM salt was introduced, it can be inferred that the enhanced steric hindrance of conjugate on the interface was responsible for the improvement.

4.4.6. Impact of conjugation on the flavor attributes of PPC

Based on HS-SPME-GC-MS analysis, a total of 129 volatiles were identified in the samples, including 36 alcohols, 19 aldehydes, 14 ketones, 5 acids, 8 ethers, 7 pyrazines, 2 furans, 11 phenols, 5 aromatics, 14 hydrocarbons, and 8 other compounds. Among them, 1-pentanol, 1-hexanol, 1-octen-3-ol, hexanal, nonanal, and 2-pentylfuran, which represent the core volatiles identified in PPC, are associated with the degradative oxidation products of unsaturated fatty acids through lipoxygenase catalytic action (Kobayashi, Tsuda, Hirata, Kubota, & Kitamura, 1995). Other potent unpleasant odorants such as 1-penten-3-ol, 2-heptanone, E-2-hexenal, E-2-heptenal, octanal, 2-octen-1-ol, benzaldehyde, and 3-methyl-1-butanol also were each detected in PPC (Samoto, Miyazaki, Kanamori, Akasaka, & Kawamura, 1998). Furthermore, some key aromatic compounds contributing to the aroma of Maillard reaction products such as pyrazines, thiophenes, ketones, and Strecker aldehydes were also identified in PPC-GA conjugates, and a sharp increase in these volatiles was observed with extended incubation time. In PPC-GA conjugate systems, 3-ethyl-2,5-dimethyl-pyrazine, 2-ethyl-3,6-dimethyl-pyrazine, 2-ethyl-3,5-dimethyl-pyrazine, and 3,5-dimethyl-pyrazine which are considered as potent aromatic compounds derived from the Strecker degradation and have very low odor thresholds and nutty and roast meat-like odorants were also identified (Adams, Polizzi, Van Boekel, & De

Kimpe, 2008; Van Lancker, Adams, & De Kimpe, 2012). Many sulfur-containing compounds, such as thiophenes and sulfur substituted furans, have been reported to act as aroma components and precursors in reactions producing more complex aroma compounds (Mottram, 1998). However, only 2,5-bis (2-methylpropyl)-thiophene was detected in all of PPC-GA conjugates, which indicates that the conjugation of PPC-GA via Maillard reaction could not generate sulfur-containing compounds with important odor impact. This is reasonable as pea proteins are abundant in lysine and arginine, but distinctly deficient in sulfur-containing amino acids such as cysteine and methionine (Zare & Pletch, 2010). Three Strecker aldehydes, 5-methyl-2-furancarboxaldehyde, 5-ethyl-2-furaldehyde, and phenylacetaldehyde, were identified in PPC-GA conjugates, and Strecker aldehydes were not only aroma-active compounds, but also important flavor precursors in Maillard reaction system. It was also found that acids and esters significantly increased in PPC-GA conjugates system compared to PPC alone. Acids are of considerable importance as starting materials in the manufacture of esters, and many of esters are valuable fragrance materials responsible for a particular fruity or floral aroma.

To better visualize the differences and similarities in the volatile compositions among the four samples (PPC alone, PPC-GA-1, PPC-GA-3, and PPC-GA-5), principal component analysis (PCA) can be employed by normalizing the relative content of each volatile using E-2-octenal as a standard (**Fig. 4.12A&B**). Based on the PCA result, two significant principal components (PCs) accounted for 58.57 % and 24.86 % of the variation, respectively. It can be clearly seen in **Fig. 4.12A** that PPC and PPC-GA-1 samples were in the positive part of PC2, while PPC-GA-3 and PPC-GA-5 samples appeared on the negative side. PC1 clearly differentiated PPC and PPC-GA conjugates of different incubation times. As indicated in **Fig. 4.12B**, 1-hexanol (A2), 1-octen-3-ol (A7), and hexanal (B1) were the dominant eigenvectors in PC1, whereas acetic acid (D1), hexanoic acid (D3), and 2,3-butanedione (C7) were dominant eigenvectors in PC2. Base on the above results, it was concluded that PPC and PPC-GA-1

present beany or grassy flavor, while PPC-GA-3 & PPC-GA-5 featured the non-specific aroma flavor.

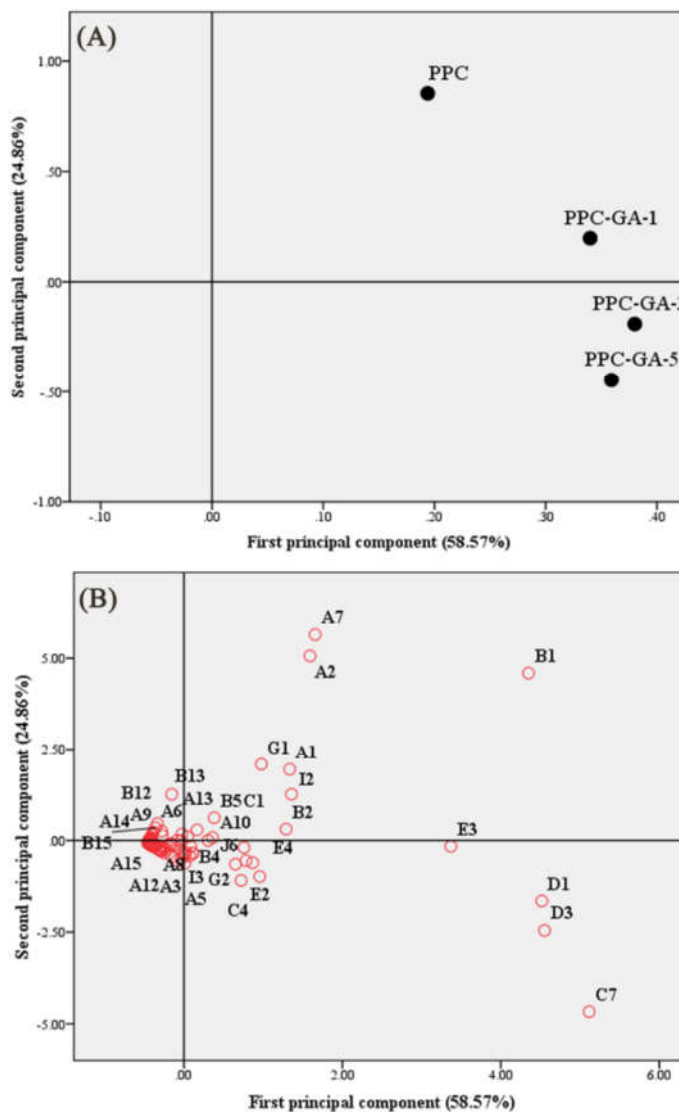


Figure 4.12. Principal component analysis (PCA) of identified flavor compositions by GC-MS, (A) the loadings of different PPC-GA conjugates; (B) the scores of various identified volatile compounds. Note: mixture represented the mixture of pea protein concentrate (PPC) and gum Arabic (GA); PPC-GA-1, PPC-GA-3 and PPC-GA-5 represented conjugation of PPC with GA for 1, 3, 5 day, respectively. A, alcohols; B, aldehydes; C, ketones; D, acids; E, esters; F, pyrazines; G, furans; H, phenols; I, aromatics; J, hydrocarbons; K, other compounds.

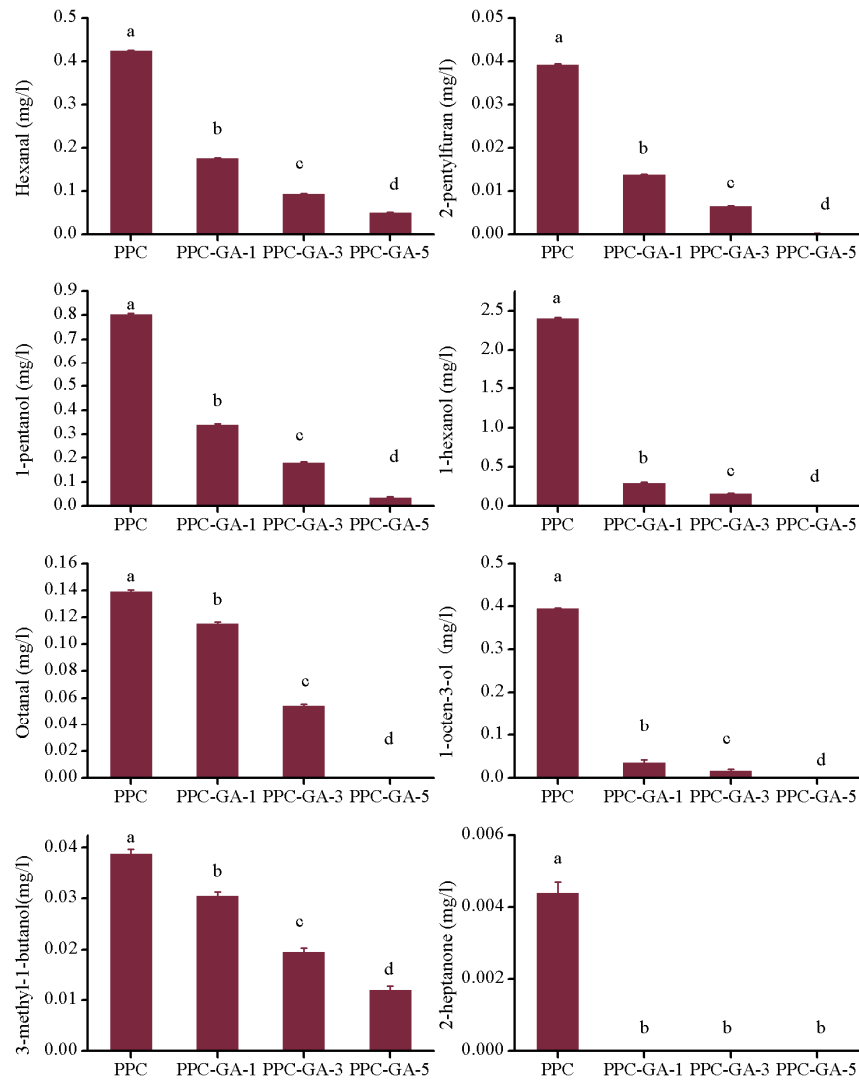


Figure 4.13. The impacts of incubation time on the selected off-flavors in different PPC-GA conjugates. Note: mixture represented the mixture of pea protein concentrate (PPC) and gum Arabic (GA); PPC-GA-1, PPC-GA-3 and PPC-GA-5 represented conjugation of PPC with GA for 1, 3, 5 day, respectively. Different letters indicated significance at $p < 0.05$.

To further confirm the effect of PPC-GA conjugation on the beany flavor mitigation, three distinctive markers (1-hexanol, 1-octen-3-ol, and hexanal) identified from PCA results as well as other 5 key beany flavor markers reported from pea sensory study of Bott and Chambers (Bott & Chambers IV, 2006) were quantified (Fig. 4.13). The initial concentration of the markers in PPC followed the order: 1-hexanol (2.14 ppm) > 1-pentanol (0.81 ppm) > hexanal (0.43) > 1-octen-3-ol (0.40 ppm) > octanal (0.14 ppm) > 3-methyl-1-butanol (0.04 ppm) = 2-pentylfuran (0.04 ppm) > 2-heptanone (0.004 ppm). These flavor markers have low beany

thresholds (1-10 ppm). Upon the conjugation between PPC and GC, the contents of all these beany flavor markers decreased significantly in PPC-GA conjugates and all of them were below 1 ppm even after 1 day incubation. Some of the beany flavors markers that exist in PPC were not detectable after 1 day incubation. Extending the incubation time could greatly mitigate the beany flavor markers with some of them even being vanished after 5 days incubation. The mitigation of beany flavor of PPC after conjugating with GA may be attributed to the structural reorientation and conformational change of PPC that releases beany flavors it tightly bond with. The incubation of PPC-GA at 60°C may also facilitate the migration of beany flavor volatiles to the headspace, thus long incubation time could remove the vast majority of beany flavor markers.

4.5. Conclusion

The successful covalent coupling of gum Arabic to pea protein concentrates at 60°C and 79% relative humidity was supported by SDS-PAGE and FTIR characterization. The absorbance of non-specific Maillard reaction markers in the PPC-GA conjugates that measured at 420 nm possess a statistical negative linear correlation with available free amino groups and can be used to determine the degree of conjugation and control the reaction. The solubility and emulsification properties of PPC-GA conjugates are sufficiently enhanced by controlling the incubation time to 3 days. The physical stabilities of corn oil-in-water emulsions against environmental stresses are improved which can be attributed to the increased electrostatic repulsions and/or steric hindrance effects. The unique Strecker aldehyde aromatic components associated with Maillard reaction are identified in PPC-GA conjugates via HS-SPME-GC-MS study. A remarkable beany flavor mitigation effect was also recorded in PPC-GA conjugates shortly after the 1 day incubation. A clean beany flavor profile in PPC-GA conjugate was achieved after 5 days of incubation as indicated by the disappearance of beany flavor markers. Considering the impact of incubation time on both functional properties and beany flavor

characteristics in PPC-GA conjugates, PPC-GA conjugates produced after 3 days of incubation will have a great potential in industrial applications.

4.6. References

- Abeyssekara, S., Chilibeck, P. D., Vatanparast, H., & Zello, G. A. (2012). A pulse-based diet is effective for reducing total and LDL-cholesterol in older adults. *British Journal of Nutrition*, *108*(S1), S103–S110. <https://doi.org/10.1017/S0007114512000748>
- Adams, A. N., Polizzi, V., Van Boekel, M., & De Kimpe, N. (2008). Formation of pyrazines and a novel pyrrole in Maillard model systems of 1,3-dihydroxyacetone and 2-oxopropanal. *Journal of Agricultural and Food Chemistry*, *56*(6), 2147–2153. <https://doi.org/10.1021/jf0726785>
- Ameur, L., Zude, M., Trystram, G., & Birlouez-Aragon, I. (2004). Hydroxymethylfurfural: An indicative parameter of heat damage in cereal products. *Czech Journal of Food Science*, *29*, 99–101.
- Barać, M., Čabrilo, S., Pešić, M., Stanojević, S., Pavličević, M., Maćej, O., & Ristić, N. (2011). Functional properties of pea (*Pisum sativum*, L.) protein isolates modified with chymosin. *International Journal of Molecular Sciences*, *12*(12), 8372–8387. <https://doi.org/10.3390/ijms12128372>
- Bi, B., Yang, H., Fang, Y., Nishinari, K., & Phillips, G. O. (2017). Characterization and emulsifying properties of β -lactoglobulin-gum Acacia Seyal conjugates prepared via the Maillard reaction. *Food Chemistry*, *214*, 614–621. <https://doi.org/10.1016/J.FOODCHEM.2016.07.112>
- Bott, L., & Chambers IV, E. (2006). Sensory characteristics of combinations of chemicals potentially associated with beany aroma in foods. *Journal of Sensory Studies*, *21*(3), 308–321. <https://doi.org/10.1111/j.1745-459X.2006.00067.x>

- Boye, J., Zare, F., & Pletch, A. (2010). Pulse proteins: Processing, characterization, functional properties and applications in food and feed. *Food Research International*, 43, 414–431. <https://doi.org/10.1016/j.foodres.2009.09.003>
- Chéreau, D., Videcoq, P., Ruffieux, C., Pichon, L., Motte, J.-C., Belaid, S., Ventureira, J. & Lopez, M. (2016). Combination of existing and alternative technologies to promote oilseeds and pulses proteins in food applications. *OCL*, 23(4), D406. <https://doi.org/10.1051/ocl/2016020>
- Christoph Cerny, A., & Davidek, T. (2003). Formation of aroma compounds from ribose and cysteine during the Maillard reaction. *Journal of Agricultural and Food Chemistry*, 51(9), 2714–2721. <https://doi.org/10.1021/JF026123F>
- Dahl, W. J., Foster, L. M., & Tyler, R. T. (2012). Review of the health benefits of peas (*Pisum sativum* L.). *British Journal of Nutrition*, 108(S1), S3–S10. <https://doi.org/10.1017/S0007114512000852>
- de Oliveira, F. C., Coimbra, J. S. dos R., de Oliveira, E. B., Zuñiga, A. D. G., & Rojas, E. E. G. (2016). Food protein-polysaccharide conjugates obtained via the Maillard reaction: A review. *Critical Reviews in Food Science and Nutrition*, 56, 1108–1125. <https://doi.org/10.1080/10408398.2012.755669>
- de Oliveira, F. C., dos Reis Coimbra, J. S., de Oliveira, E. B., Rodrigues, M. Q. R. B., Sabioni, R. C., de Souza, B. W. S., & Santos, I. J. B. (2015). Acacia gum as modifier of thermal stability, solubility and emulsifying properties of α -lactalbumin. *Carbohydrate Polymers*, 119, 210–218. <https://doi.org/10.1016/J.CARBPOL.2014.11.060>
- Delahaije, R. J. B. M., Gruppen, H., Van Nieuwenhuijzen, N. H., Giuseppin, M. L. F., & Wierenga, P. A. (2013). Effect of glycation on the flocculation behavior of protein-stabilized oil-in-water emulsions. *Langmuir*, 29(49), 15201–15208. <https://doi.org/10.1021/la403504f>

- Delgado-Andrade, C., Morales, F. J., Seiquer, I., & Pilar Navarro, M. (2010). Maillard reaction products profile and intake from Spanish typical dishes. *Food Research International*, *43*(5), 1304–1311. <https://doi.org/10.1016/j.foodres.2010.03.018>
- Gumus, C. E., Decker, E. A., & McClements, D. J. (2017). Impact of legume protein type and location on lipid oxidation in fish oil-in-water emulsions: Lentil, pea, and faba bean proteins. *Food Research International*, *100*, 175–185. <https://doi.org/10.1016/j.foodres.2017.08.029>
- Kobayashi, A., Tsuda, Y., Hirata, N., Kubota, K., & Kitamura, K. (1995). Aroma constituents of soybean [*Glycine max* (L.) Merrill] milk lacking lipoxygenase isozymes. *Journal of Agricultural and Food Chemistry*, *43*(9), 2449–2452. <https://doi.org/10.1021/jf00057a025>
- Lam, A. C. Y., Can Karaca, A., Tyler, R. T., & Nickerson, M. T. (2018). Pea protein isolates: Structure, extraction, and functionality. *Food Reviews International*, *34*, 126–147. <https://doi.org/10.1080/87559129.2016.1242135>
- Laroque, D., Inisan, C., Berger, C., Vouland, É., Dufossé, L., & Guérard, F. (2008). Kinetic study on the Maillard reaction. Consideration of sugar reactivity. *Food Chemistry*, *111*(4), 1032–1042. <https://doi.org/10.1016/J.FOODCHEM.2008.05.033>
- Liu, J., Liu, M., He, C., Song, H., & Chen, F. (2015). Effect of thermal treatment on the flavor generation from Maillard reaction of xylose and chicken peptide. *LWT - Food Science and Technology*, *64*(1), 316–325. <https://doi.org/10.1016/J.LWT.2015.05.061>
- Ma, Z., Boye, J. I., Simpson, B. K., Prasher, S. O., Monpetit, D., & Malcolmson, L. (2011). Thermal processing effects on the functional properties and microstructure of lentil, chickpea, and pea flours. *Food Research International*, *44*(8), 2534–2544. <https://doi.org/10.1016/j.foodres.2010.12.017>

- Martinez-Alvarenga, M., Martinez-Rodriguez, E. Y., Garcia-Amezquita, L. E., Olivas, G. I., Zamudio-Flores, P. B., Acosta-Muniz, C. H., & Sepulveda, D. R. (2013). Effect of Maillard reaction conditions on the degree of glycation and functional properties of whey protein isolate – Maltodextrin conjugates. *Food Hydrocolloids*, *38*, 110–118. <https://doi.org/10.1016/j.foodhyd.2013.11.006>
- Mottram D.S. (1998). Flavour formation in meat and meat products:a review. *Food Chemistry*, *62*(4), 415–424. [https://doi.org/10.1016/S0308-8146\(98\)00076-4](https://doi.org/10.1016/S0308-8146(98)00076-4)
- Nakauma, M., Funami, T., Noda, S., Ishihara, S., Al-Assaf, S., Nishinari, K., & Phillips, G. O. (2008). Comparison of sugar beet pectin, soybean soluble polysaccharide, and gum arabic as food emulsifiers. 1. Effect of concentration, pH, and salts on the emulsifying properties. *Food Hydrocolloids*, *22*(7), 1254–1267. <https://doi.org/10.1016/J.FOODHYD.2007.09.004>
- Nursten, H. (2005). *The Maillard Reaction: Chemistry, Biochemistry, and Implications*. Royal Society of Chemistry.
- Oliver, C. M., Melton, L. D., & Stanley, R. A. (2006). Creating proteins with novel functionality via the Maillard reaction: A review. *Critical Reviews in Food Science and Nutrition*, *46*(4), 337–350. <https://doi.org/10.1080/10408690590957250>
- Pirestani, S., Nasirpour, A., Keramat, J., & Desobry, S. (2017). Preparation of chemically modified canola protein isolate with gum Arabic by means of Maillard reaction under wet-heating conditions. *Carbohydrate Polymers*, *155*, 201–207. <https://doi.org/10.1016/j.carbpol.2016.08.054>
- Pirestani, S., Nasirpour, A., Keramat, J., Desobry, S., & Jasniewski, J. (2017). Effect of glycosylation with gum Arabic by Maillard reaction in a liquid system on the emulsifying properties of canola protein isolate. *Carbohydrate Polymers*, *157*, 1620–1627. <https://doi.org/10.1016/J.CARBPOL.2016.11.044>

- Pirestani, S., Nasirpour, A., Keramat, J., Desobry, S., & Jasniewski, J. (2018). Structural properties of canola protein isolate-gum Arabic Maillard conjugate in an aqueous model system. *Food Hydrocolloids*, *79*, 228–234.
<https://doi.org/10.1016/j.foodhyd.2018.01.001>
- Samoto, M., Miyazaki, C., Kanamori, J., Akasaka, T., & Kawamura, Y. (2005). Improvement of the off-flavor of soy protein isolate by removing oil-body associated proteins and polar lipids. *Bioscience, Biotechnology, and Biochemistry*, *62*(5), 935–940.
<https://doi.org/10.1271/bbb.62.935>
- Su, J. F., Huang, Z., Yuan, X. Y., Wang, X. Y., & Li, M. (2010). Structure and properties of carboxymethyl cellulose/soy protein isolate blend edible films crosslinked by Maillard reactions. *Carbohydrate Polymers*, *79*(1), 145–153.
<https://doi.org/10.1016/J.CARBPOL.2009.07.035>
- Szymanowska, U., Jakubczyk, A., Baraniak, B., & Kur, A. (2009). Characterisation of lipoxygenase from pea seeds (*Pisum sativum* var. Telephone L.). *Food Chemistry*, *116*(4), 906–910. <https://doi.org/10.1016/J.FOODCHEM.2009.03.045>
- U.S. Department of Health and Human Services. (2015). Dietary Guidelines for Americans 2015-2020. In *U.S. Department of Agriculture* (8th ed). Washington, DC: U.S. Government Printing Office.
- Van Boekel, M. A. J. S. (2006). Formation of flavour compounds in the Maillard reaction. *Biotechnology Advances*, *24*(2), 230–233.
<https://doi.org/10.1016/j.biotechadv.2005.11.004>
- Van Lancker, F., Adams, A., & De Kimpe, N. (2012). Impact of the N-terminal amino acid on the formation of pyrazines from peptides in maillard model systems. *Journal of Agricultural and Food Chemistry*, *60*(18), 4697–4708.
<https://doi.org/10.1021/jf301315b>

- Wang, Q., & Ismail, B. (2012). Effect of Maillard-induced glycosylation on the nutritional quality, solubility, thermal stability and molecular configuration of whey protein. *International Dairy Journal*, 25(2), 112–122.
<https://doi.org/10.1016/j.idairyj.2012.02.009>
- Yadav, M. P., Strahan, G. D., Mukhopadhyay, S., Hotchkiss, A. T., & Hicks, K. B. (2012). Formation of corn fiber gum–milk protein conjugates and their molecular characterization. *Food Hydrocolloids*, 26(2), 326–333.
<https://doi.org/10.1016/J.FOODHYD.2011.02.032>
- Zhu, D., Damodaran, S., & Lucey, J. A. (2010). Physicochemical and emulsifying properties of whey protein isolate (WPI)–dextran conjugates produced in aqueous solution. *Journal of Agricultural and Food Chemistry*, 58(5), 2988–2994.
<https://doi.org/10.1021/jf903643p>

5. GUM ARABIC-MEDIATED SYNTHESIS OF GLYCO-PEA PROTEIN HYDROLYSATE VIA MAILLARD REACTION IMPROVES SOLUBILITY, FLAVOR PROFILE, AND FUNCTIONALITY OF PEA PROTEIN³

5.1. Abstract

Pea protein hydrolysate (PPH) was successfully conjugated with gum Arabic (GA) through Maillard-driven chemistry. The effect of cross-linking conjugation on the structure, solubility, volatile substances, emulsification, and antioxidative activity of glyco-PPH was investigated, and found to improve all properties. The formation of glyco-PPH was confirmed by sodium dodecyl sulfate-polyacrylamide gel electrophoresis (SDS-PAGE), Fourier-transform infrared (FTIR), and scanning electron microscopy (SEM). Size exclusion chromatography-multi angle light scattering (SEC-MALS) unveiled that the maximum molecular mass of glyco-PPH occurred after 1 day conjugation and approximately 1.2 mole of gum Arabic conjugates on one mole of PPH. Headspace solid-phase microextraction gas chromatography-mass spectrometry (HS-SPME-GC-MS) revealed the odor changes of glycoprotein before and after cross-linking. Oil-in-water emulsions using glyco-PPH have enhanced physical stability against pH changes and chemical stability against lipid oxidation.

5.2. Introduction

Because of the combined characteristics of low allergens and lipids, as well as high versatility and abundance, plant-based pea protein has been breaking into the mainstream as a critical functional protein contender to supplant animal protein (Dahl, Foster, & Tyler, 2012).

³ Based on the article of Fengchao Zha, Zhongyu Yang, Jiajia Rao & Bingcan Chen published in *Journal of Agricultural and Food Chemistry* online Aug. 2019 (DOI:10.1021/acs.jafc.9b04099). Fengchao Zha was responsible for methodology, data collection and analysis, was the primary developer of the conclusions advanced here, and drafted and revised all versions of this chapter. Zhongyu Yang assisted with reviewing the draft. Jiajia Rao assisted with instruments. Bingcan Chen was primary responsible for resources, reviewing and editing, supervising.

Since the presence of certain anti-nutritional factors and high level of fibrous material in pea proteins can somehow be digestive discomfort (Chung Hyun Jung, Liu Qiang, & Hoover Ratnajothi, 2010; Roy, Boye, & Simpson, 2010), especially for people with sensitivity or poor tolerance to intact proteins. Commercially, pea proteins are often enzymatically hydrolyzed into peptides to enhance their digestibility and absorbability (Humiski & Aluko, 2007). The resulting pea protein hydrolysate (PPH) is able to deliver the optimal performance and allow for nutritional and simultaneously functional contribution to food, pharmaceutical, and cosmetic industry (Chao, He, Jung, & Aluko, 2013; Korhonen & Pihlanto, 2003). Like other plant proteins, several major obstacles restrict consumer acceptability of pea protein hydrolysate and the derived products. Off-flavors of plant proteins caused by oxidative deterioration of unsaturated fatty acid in protein-lipid complexes during the storage and processing of pea impose restrictions on their utilization (Humiski & Aluko, 2007; Ma et al., 2011). In addition, alkaline extraction followed by acid (isoelectric) precipitation is performed commercially to manufacture plant protein concentrates and isolates; this extraction process, however, can lower the solubility of final products (Lam, Can Karaca, Tyler, & Nickerson, 2018). Other functionalities including emulsification, foaming, and gelation, are impaired accordingly, as they are highly associated with protein solubility (Chéreau et al., 2016; Lam et al., 2018). Consequently, there is a tremendous demand for plant protein that is high in solubility and low in off-flavors.

Conjugation of polysaccharide with plant proteins through Maillard-driven reaction, a so-called cooking chemistry, has turned out to be a promising green chemistry to ameliorate the general functionality of proteins (de Oliveira, Coimbra, de Oliveira, Zuñiga, & Rojas, 2016; Oliver, Melton, & Stanley, 2006; Román & Wilker, 2019). The formation of glycoprotein conjugates via Maillard-driven reaction involves the Amadori rearrangement of Schiff base adducts of carbonyl-containing polysaccharides with protein ϵ -amino groups at the initial stage

(Martinez-Alvarenga et al., 2013; Pirestani, Nasirpour, Keramat, Desobry, & Jasniewski, 2018). Unfortunately, most protein-polysaccharide conjugation studies via Maillard-driven reactions were conducted on animal-based proteins focusing primarily on characterizing the functionality of the conjugates; only a few studies have been done on the formation mechanisms. Our recent research has shown that Maillard-driven reaction allows plant-based protein, pea proteins concentrate (PPC) or isolate (PPI) with low initial solubility to be covalently linked with gum Arabic (GA) in a dry state, thus enhancing their emulsification and solubility particularly around the isoelectric point of the protein. Equally important, conformational changes of pea proteins after conjugation could potentially impact the level of off-flavors, as well as the formation of some pleasant aroma-active volatiles derived from the Amadori rearrangement and Strecker degradation (Cerny & Davidek, 2003; Zha, Dong, Rao, & Chen, 2019b).

Leveraging on the exceptional functionality (e.g., hydrophilicity, steric hindrance, and viscosity) offered by polysaccharides, and coupling the unique volatile aroma of glycoprotein mediated by polysaccharides could provide enhanced functionality and flavor profile of plant-based proteins. However, the use of protein hydrolysate for glycoprotein synthesis via Maillard-driven reaction is not well explored. In this work, pea protein hydrolysate (PPH), for the first time, was selected to conjugate with gum Arabic via Maillard-driven chemistry. As compared to animal proteins pea protein has the advantages of environmental sustainability, cultural acceptability, and low-cost accessibility (Mohammadinejad et al., 2019), while as compared to PPC or PPI, PPH has the advantages of greater nutritional efficacy (digestibility and absorbability). Gum Arabic was selected because it is a natural polysaccharide with high biocompatibility and biodegradability as compared to synthetic organic compounds. Therefore, a mild Maillard-driven green chemistry method is effective at improving plant protein functionality. The goals of this research were to systematically understand the cross-linking

mechanisms and the relationship between glyco-PPH structure and functionality. Gum Arabic-mediated synthesis of glyco-PPH was controlled by conjugation time. Thus, the structural characteristics of glyco-PPH was fully characterized and compared to those of the raw PPH. Additionally the functionality of glyco-PPH, including volatile substances, solubility, and physicochemical stability of the emulsion it prepared, was evaluated.

5.3. Materials and Methods

5.3.1. Materials

Both PURIS™ pea protein 870 (PPI) and PURIS™ pea protein 870H (PPH, the hydrolysates of PPI; protein ~80%, moisture ~6%, ash ~5%, carbohydrate ~6%, lipid ~ 8%) were obtained from Cargill. TIC Pretested® gum Arabic Spray Dry Powder (GA, moisture ~6.7%, polysaccharide ~90%, protein ~3.2%, and minerals ~ 0.2%) was kindly offered by TIC Gums (Belcamp, MD). Mazola® Corn oil (saturated fatty acid ~14.3%, monounsaturated fatty acid ~28.6%, polyunsaturated fatty acid ~57.1%) was purchased locally. All other chemicals were of analytical grade. All bulk samples were used as received.

5.3.2. Gum Arabic-mediated synthesis of glyco-pea protein hydrolysate

The glycoprotein was synthesized as described by Zha and co-workers with a slight modification (Zha et al., 2019b; Zha, Dong, Rao, & Chen, 2019a). Briefly, PPH and gum Arabic (GA) were first mixed at a mass ratio of 1:4, followed by hydration in deionized water (1:2, w/v) for 24 h on a stir plate operating at 300 rpm and room temperature (22 °C). The pH of the hydrated mixture was adjusted to 7.0, which was lyophilized to dryness (Lyophilizer, SP scientific, Gardiner, New York). Five grams of lyophilized mixture was transferred into a VWR clear glass straight-sided jar (60 mL). The jar was uncovered and set on a perforated porcelain plate in a desiccator. The relative humidity and temperature of the desiccator were maintained at 79% by saturated KBr solution and 60 °C by a pre-heated incubator (Heratherm IMH180,

Thermo Fisher Scientific, Inc., USA), respectively. Maillard-driven conjugation was performed with variable time (0, 1, 3, and 5 day) to prepare glyco-PPH with different structures.

5.3.3. Characterization of structure and degree of conjugation

The structure of PPH-GA and degree of conjugation were characterized following our previous studies (Zha et al., 2019b, 2019a). Briefly, for Amadori compounds and melanoidins formation, free amino groups in PPH were recorded using a Shimadzu UV-1100 spectrophotometer (Shimadzu Corp., Kyoto, Japan). Color development (L^* , a^* , b^*) was measured with a Minolta CR-310 chroma meter (Osaka, Japan). Sodium dodecyl sulfate-polyacrylamide gel electrophoresis (SDSPAGE) was performed with a Bio-Rad Mini-Protein apparatus III (Bio-Rad Laboratories Inc., Richmond, CA). Fourier Transform infrared spectroscopy-attenuated total reflection (FTIR-ATR) was applied on a Varian 600-IR series spectrometer (Varian, Palo Alto, CA), and scanning electron microscopy (SEM) of glyco-PPH was characterized with a Cressington 108 auto sputter (Ted Pella Inc., Redding, CA) coupled with a JEOL JSM-6490LV scanning electron microscope (JEOL USA, Peabody, MA).

5.3.4. Determination of molecular weight by size exclusion chromatography with multiangle laser light scattering (SEC-MALLS) detector

Glyco-PPH (0.10 g) was dissolved in 10 mL PBS (10 mM, pH 7.0). The sample solution was hydrated for 2 h, followed by centrifugation at 2,000 x g for 30 min. The supernatant was then filtered through a 0.45 μm nylon filter to remove any insoluble precipitation or dust. Glyco-PPH solution was separated by an Agilent 1200 HPLC using a tandem array of a polySep-GFC-P (35 \times 7.8mm) and polySep-GFC-P linear (300 \times 7.8mm) columns (Phenomenex, Torrance, CA, USA). One hundred microliter of sample was injected and eluted using PBS buffer (10 mM, pH 7.0) at a flow rate 0.3 mL/min. Elution from columns was monitored sequentially with a DAD detector (280 nm), with a refractive index detector (Agilent 1362 A), and a DAWN HELEOS II multiangle laser light scattering detector (Wyatt

Technology, Santa Barbara, CA, USA) equipped with a helium-neon laser ($\lambda = 661 \text{ nm}$). The gum Arabic refractive index increment (dn/dc) was set at 0.141 mL/g according to the previous study (Al-Assaf, Phillips, & Williams, 2005). A known dn/dc (0.174 mL/g) of NaCl was used to calibrate the refractive index detector (RI). Data accumulated by the UV, RI, and MALLS detectors were analyzed by the ASTRA 7.1.2.5 software (Wyatt Technology). The SEC-MALLS measurement was carried out at room temperature (22°C). The number of gum Arabic molecules (N) attached to each PPH molecule was calculated using the following formula (Liu & Zhong, 2013);

$$N = (\overline{M}_{w2} - \overline{M}_{w1}) / \overline{M}_{w3} \quad (5.1)$$

$$\overline{M}_{wi} = [\sum (F_i M_i) / \sum F_i] \quad (5.2)$$

Where \overline{M}_{w1} , \overline{M}_{w2} , and \overline{M}_{w3} are the average molecular masses of monomeric PPH, glyco-PPH, and gum Arabic, respectively; F_i is the proportion of fraction, and M_i is the molecular mass of the fraction.

5.3.5. Volatile substances in glyco-pea protein hydrolysate

The volatile substances in glyco-PPH were sampled by headspace solid phase microextraction (CTC Analytics, Zwingen, Switzerland), separated by an Agilent 7890B gas chromatograph, and identified by an Agilent 5977A mass spectrometer on the basis of the NIST database. The detailed parameters can be found in our previous work (Zha et al., 2019b).

5.3.6. Relative solubility of glyco-pea protein hydrolysate

Protein solubility was determined according to our previous work without any modification (Zha et al., 2019b), and protein concentration was determined following the method of Bradford (Bradford, 1976). The solubility was expressed as the percentage of the initial PPH concentration.

5.3.7. Corn oil-in-water emulsion prepared by glyco-PPH

A coarse corn oil-in-water emulsion was prepared by mixing 2 wt % corn oil with 98 wt % emulsifier solution (0.20 wt % glyco-PPH in 10 mM, pH 7.0 PBS buffer) using a high-speed blender (M133/128-0, Biospec Products, Inc., ESGC, Switzerland) for 2 min. A fine emulsion with reduced particle size was prepared by passing the coarse emulsion through a two-stage high-pressure valve homogenizer (LAB 2000, APV-Gaulin, Wilmington, MA) at first and second stage pressures of 5,000 and 500 psi, respectively, three times. To prevent microbial growth during the emulsion storage, 0.04% of sodium azide was added to the final emulsions. The emulsions prepared by the same amounts of PPH or the mixture of PPH and GA were used as controls.

5.3.8. Physical stability of emulsions against pH changes

The stability of emulsions against pH (2.0–8.0) changes was determined by measuring the particle size and ζ -potential of emulsions after 30 min storage at room temperature (22 °C). The particle size was directly determined using a Mastersizer 3000 from Malvern (Malvern Instruments Ltd., UK) and reported as the volume-weight mean diameter ($d_{43} = \sum n_i d_i^4 / \sum n_i d_i^3$), where n_i was the number of droplets of diameter d_i . The ζ -potential (mV) of droplets was measured using a Malvern Nano-ZS (Malvern Instruments Ltd., UK).

5.3.9. Lipid oxidation kinetics of emulsions

Primary oxidation marker lipid hydroperoxides were quantified using a method adapted from Chen, McClements, and Decker without any modification (Chen, McClements, & Decker, 2010). Secondary oxidation product marker hexanal was determined using the methods described by Zha and co-workers without any modification (Zha et al., 2019a). The concentration of hexanal was quantified using a calibration curve prepared from an authentic standard (LOD: 7.89 ng/mL). The lag phase is defined as the time at which a sudden increase of hexanal formation is observed.

5.3.10. Statistical analysis

At least two independent experiments were conducted to prepare the fresh samples. All measurements were performed with triplicate samples. The values reported herein were means \pm standard deviation (SD) of triplicates from fresh samples. The data were analyzed using SAS version 9.4 (SAS institute Inc. Cary, NC). One-way analysis of variance (ANOVA) was conducted, and significant difference was defined at $p < 0.05$ by Tukey's test.

5.4. Results and Discussion

5.4.1. Structure characterization of glyco-pea protein hydrolysate

To confirm the formation of glyco-PPH, SDS-PAGE, FT-IR and SEM (**Fig. 5.1-5.3**) were applied to monitor both molecular weight and structure changes of the products at different conjugation time.

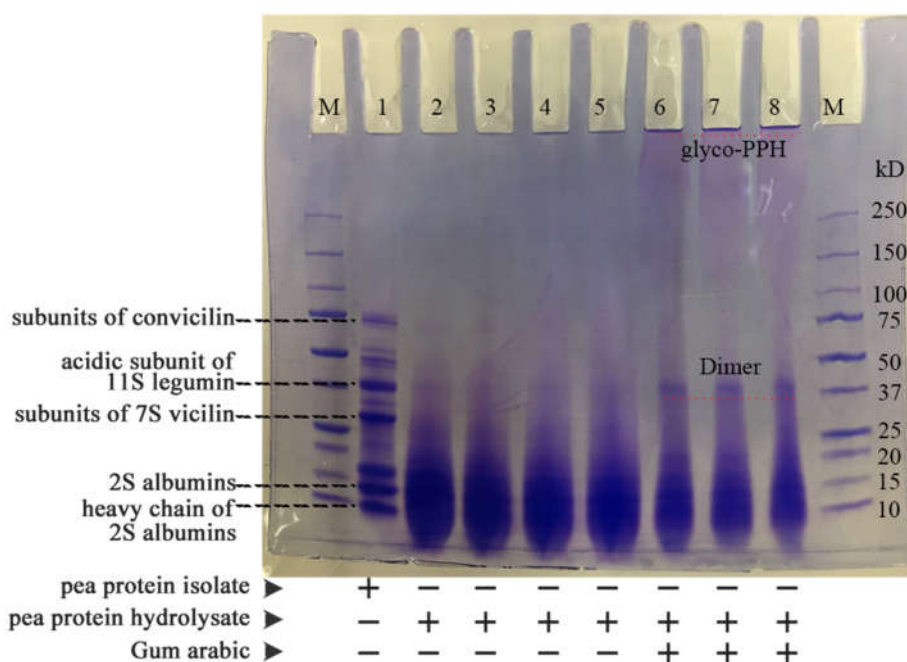


Figure 5.1. SDS-PAGE patterns for different glyco-PPH: lane M for protein markers; lanes 1-8 for pea protein isolate (PPI), PPH-0 day, PPH-1 day, PPH-3 day, PPH-5 day, glyco-PPH-1 day, glyco-PPH-3 day, and glyco-PPH-5 day, respectively.

One of the characteristic bands presenting in raw PPI is the 2S albumin (**Fig. 5.1, lane 1**) that consists of both light (~4.5 kDa) and heavy (~10 kDa) polypeptide chains (Chéreau et al., 2016). Additionally, one subunit of convicilin (~72.4 kDa), one (~28.7 kDa) subunit of 7S

vicilin, as well as acidic (~40 kDa) constituting the monomers of 11S legumin were identified in lane 1 (Chéreau et al., 2016; Lam et al., 2018). Our former research has indicated that the globulin and albumin are the primary constituents in pea protein that involved in the conjugation with GA (Zha et al., 2019a). After enzymatic hydrolysis, it was clear that these large proteins were cleaved into small peptides (<20 kDa), especially peptides with molecular weight lower than 10 kDa (**Fig. 5.1, lane 2**). One serious issue of hydrolyzed protein is the formation of undesirable low molecular weight hydrophobic bitter peptides (Humiski & Aluko, 2007). Cho et al. reported the bitterness of fractionated peptides from soy protein hydrolysates was closely related to molecular mass of peptides (Cho, Unklesbay, Hsieh, & Clarke, 2004). Obviously, these corresponding bands (<20 kDa) of bitter peptides significantly narrowed down and became shallow as compared to PPH alone with conjugation time from 1 to 5 days (**Fig. 5.1, lane 6-8**). This might be partly due to the disappearance of 2S albumin that has been proven to be primarily involved in conjugating with GA. Still it cannot rule out the participation of newly formed hydrolysates in Maillard-driven reaction where both of them would result in the decrease of corresponding bands. A newly formed characteristic band (~37 kDa) of PPH dimers was exclusively identified in glyco-PPH. The formation of PPH dimers might be attributed to the heat-induced dimerization of PPH which was promoted by the physical complexes of PPH with GA. Apparently, a newly formed band near the loading boundary of the gel concomitant with the elimination or reduction of certain PPH subunits was observed (**Fig. 5.1, lanes 6-8**). The large molecule was unable to migrate into the separating gel (Pirestani, Nasirpour, Keramat, & Desobry, 2017). The SDS-PAGE pattern confirms that the newly formed band is responsible for the development of glyco-PPH.

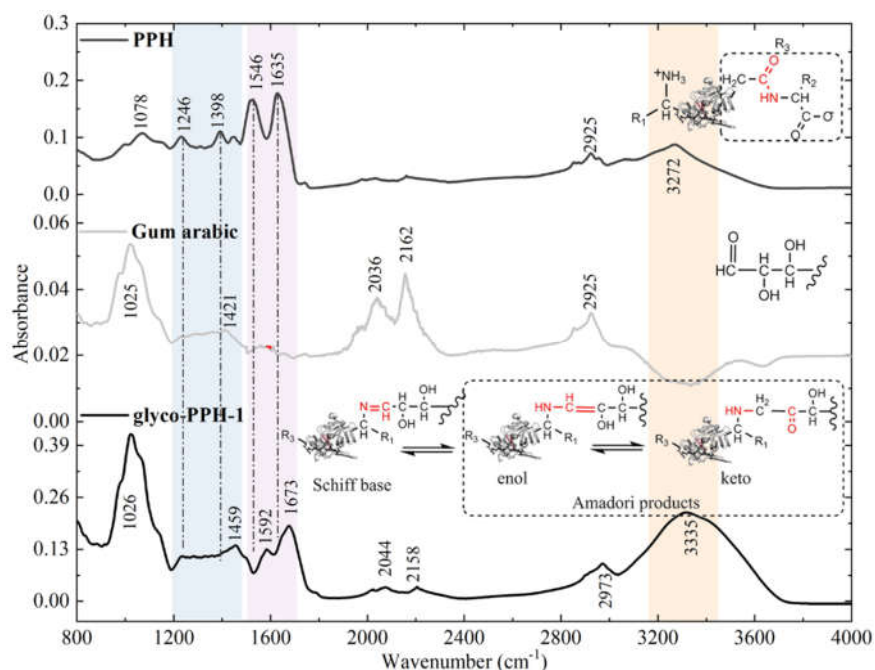


Figure 5.2. The characteristic structure of glyco-PPH (1 day) by Fourier transform infrared spectroscopy-attenuated total reflection (FTIR-ATR).

The formation of glyco-PPH was further characterized by FTIR-ATR (**Fig. 5.2**). The distinguished characteristic bands of amide I, II, and III in the spectrum of PPH were identified at 1635 cm^{-1} (C=O stretching), 1546 cm^{-1} (N-H deformation), and 1398 & 1246 cm^{-1} (C-N stretching and N-H bending vibrations), respectively (Pirestani et al., 2018; Su, Huang, Yuan, Wang, & Li, 2010; Yue, Cui, Shuttleworth, & Clark, 2012; Zha et al., 2019b). The band at 1078 cm^{-1} was due to vibrations such as out-of-plane C-H bending vibration (Su et al., 2010). The absorption band at 2925 cm^{-1} represented the antisymmetric stretching of C-H in CH_2 and CH_3 groups (Pirestani et al., 2018). The FTIR spectrum illuminated that the bands in the region of $1500\text{-}800\text{ cm}^{-1}$ might be ascribed to C-H deformation, C-O and C-C stretching. Upon conjugation right after 1 day, a newly appearing band (1592 cm^{-1}) of glyco-PPH located between the amide band I and II regions may be attributed to Maillard reaction products such as carboxylate ion COO^- (antisym stretch, $1610\text{-}1560\text{ cm}^{-1}$), β -diketones (C=O stretch, enol/keto form $1640\text{-}1580\text{ cm}^{-1}$), or pyridine derivatives (ring stretch, doublet, $1615\text{-}1565\text{ cm}^{-1}$) (Pirestani et al., 2018; Zha et al., 2019b). Furthermore, another two new absorption bands at

1673 cm^{-1} and 3335 cm^{-1} exhibited a C=N stretching vibration deriving from the newly formed Schiff's base and a O-H & N-H groups stretching vibration, respectively (Su et al., 2010). The FTIR spectrum further confirmed the development of glyco-PPH.

The interfacial and morphological properties of glyco-PPH monitored by scanning electron microscopy (SEM) are shown in **Figure 5.3**. The microstructures of PPH (**Fig. 5.3-1**) and GA (**Fig. 5.3-2**) mainly displayed indiscernible irregular and near spherical or irregular polygonal form, respectively. The staggering pattern between irregular polygonal and irregular forms in the micrograph of PPH-GA mixture (**Fig. 5.3-3**) indicated that there was no chemical bonded association between the two biopolymers but physical mixing. The attachment of GA on the surface PPH of via covalent bond as Maillard-driven reaction proceeded for 1 day at 60°C gave rise to a heterogeneous network structure accompanied by the disappearance of initial PPH microstructures (**Fig. 5.3-4**). Further preceding the reaction to 3 days produced a greater heterogeneity in the glyco-PPH. Similar changes in the morphologies of milk protein were reported when conjugating of corn fiber gum via covalent linkage (Yadav, Strahan, Mukhopadhyay, Hotchkiss, & Hicks, 2012). A whole chunk of compressed products with a flattened surface morphology occurred after 5 days of conjugation (**Fig. 5.3-6**). The observed morphological changes of PPH induced by covalent cross-linking with GA via Maillard reaction could provide further insights on the functionality of glyco-PPH.

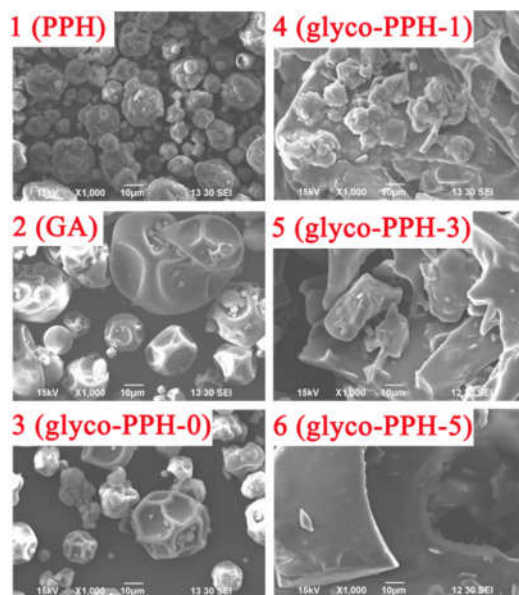


Figure 5.3. SEM for surface characters profiles of glyco-PPH: 1-3 for PPH, GA, mixture of PPH and gum arabic, 4-6 for glyco-PPH with different times of 1, 3, 5 day, respectively. Magnification 1000 \times ; scale bar =10 μ m. PPH and GA represent pea protein hydrolysate and gum Arabic, respectively.

The interfacial and morphological properties of glyco-PPH monitored by scanning electron microscopy (SEM) are shown in **Figure 5.3**. The microstructures of PPH (**Fig. 5.3-1**) and GA (**Fig. 5.3-2**) mainly displayed indiscernible irregular and near spherical or irregular polygonal form, respectively. The staggering pattern between irregular polygonal and irregular forms in the micrograph of PPH-GA mixture (**Fig. 5.3-3**) indicated that there was no chemical bonded association between the two biopolymers but physical mixing. The attachment of GA on the surface PPH of via covalent bond as Maillard-driven reaction proceeded for 1 day at 60 $^{\circ}$ C gave rise to a heterogeneous network structure accompanied by the disappearance of initial PPH microstructures (**Fig. 5.3-4**). Further preceding the reaction to 3 days produced a greater heterogeneity in the glyco-PPH. Similar changes in the morphologies of milk protein were reported when conjugating of corn fiber gum via covalent linkage (Yadav, Strahan, Mukhopadhyay, Hotchkiss, & Hicks, 2012). A whole chunk of compressed products with a flattened surface morphology occurred after 5 days of conjugation (**Fig. 5.3-6**). The observed

morphological changes of PPH induced by covalent cross-linking with GA via Maillard reaction could provide further insights on the functionality of glyco-PPH.

5.4.2. Molecular parameters of glyco-pea protein hydrolysate

Representative differential refractive index (dRI), UV and molar mass signals of SEC elution profiles of glyco-PPH at different conjugation time are presented in **Figure 5.4**, and the calculated specific molecular parameters were shown in **Table 5.1**.

PPI was separated into three different fractions in SEC profiles where they closely correspond to the typical quaternary conformation of pea protein (**Fig. 5.4A**): hexameric (~340 kDa) for 11S legumin, trimeric (~160 kDa) for 7S vicilin, and dimeric (~15 kDa) for 2S albumin (Klost & Drusch, 2019; Shevkani, Singh, Kaur, & Rana, 2015). After hydrolysis (degree of hydrolysis 12% in PPH), convicilin, legumin, and vicilin were no longer detectable in PPH on the basis of SDS-PAGE; instead, a variety of smaller peptides appeared. In terms of SEC, PPH was separated into three similar fractions of ~254, ~158 and ~13 kDa (**Fig. 5.4B**). It was reported that 11S legumin maintained a nearly intact tertiary structure (M.W. = 200±50 kDa) and showed enhanced functional properties when subjected to limited hydrolysis (Klost & Drusch, 2019). The similar fraction (MW ≈ 280 kDa, **Fig. 5.4B**) of PPH in SEC profiles was also observed after hydrolysis.

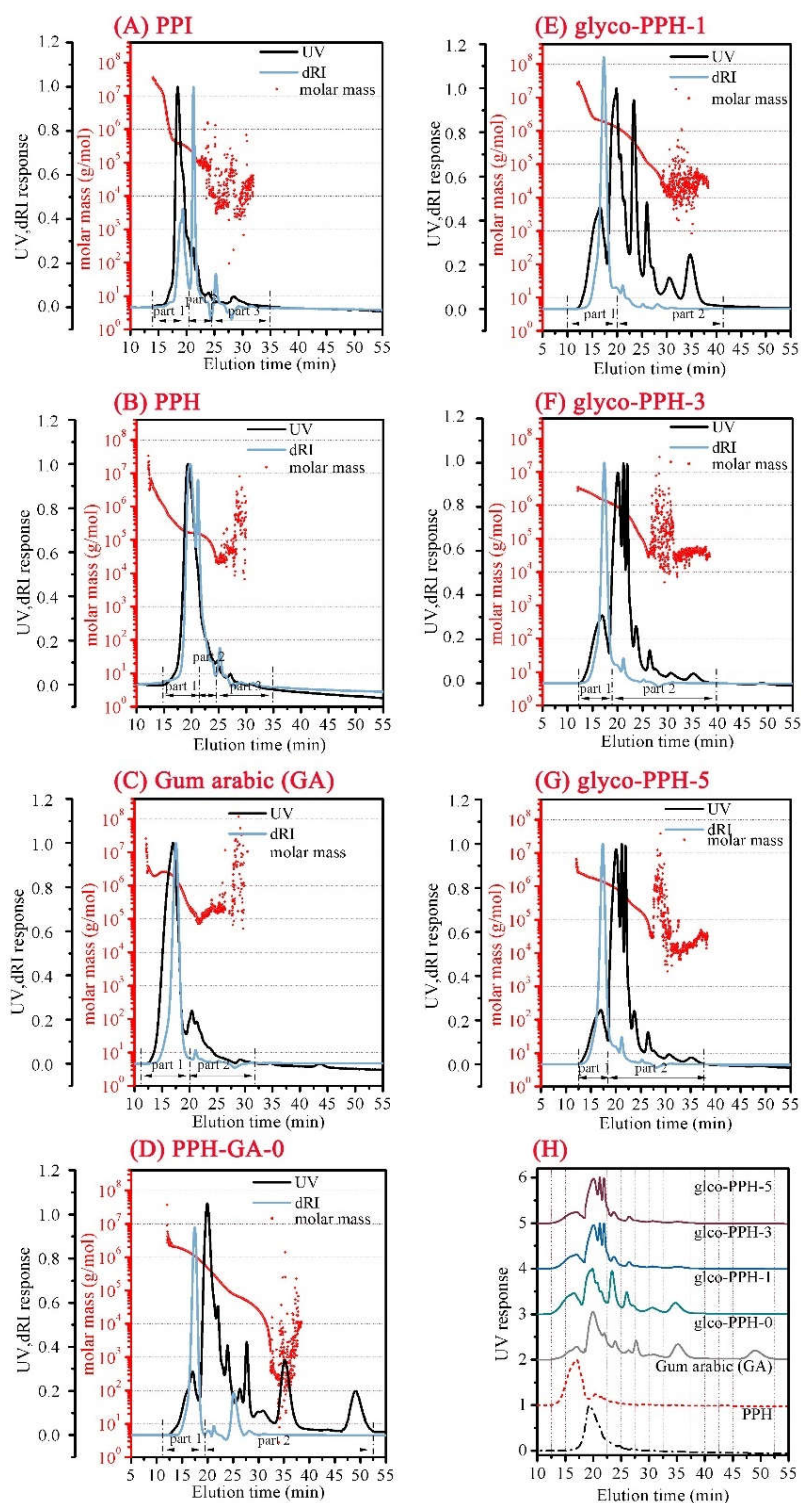


Figure 5.4. (A-H) A range of selected samples were characterized by a size-exclusion chromatography with multiangle laser light scattering (SEC-MALLS). Molar mass, UV and differential refractive index (dRI) as a function of retention time of various glyco-PPH. (H) Comparison of the elution profiles monitored by UV at 280 nm for different glyco-PPH.

With respect to GA, two distinct fractions in SEC profiles of GA were identified (**Fig. 5.4C**). The first fraction representing about 80% of the GA, had a high \bar{M}_w of $\sim 2.17 \times 10^6$ g/mol and was the representative of the highly branched arabinogalactan (AG) units. The second fraction represents the heterogeneous arabinogalactan-protein complex (AGP), the minor part ($\sim 20\%$) of the GA, and gave an \bar{M}_w of $\sim 2.64 \times 10^5$ g/mol (**Table 5.1**). All these results agree well with the literature (Picton, Bataille, & Muller, 2000). The average radius of gyration (\bar{R}_g) value confirmed the spherical conformation of GA and overall was 30.5 nm for the AG components, and 27.7 nm when the AGP fraction was taken as a reference. Even though the broad range of eluted fraction of AG showed a higher polydispersity index ($\bar{M}_w / \bar{M}_n = 1.26$) than that of AGP ($\bar{M}_w / \bar{M}_n = 1.08$), the polydispersity index of both fractions of GA was close to 1, indicating both of them owned a narrow range of molecular weight (Philip, 1993).

Prior to cross-linking, the mixture of PPH and GA showed multiple fractions in the SEC profiles (**Fig. 5.4D**). The overall elution profile was divided into two parts. The first fraction that represents $\sim 31.5\%$ of the mixture had a \bar{M}_w of $\sim 2.48 \times 10^6$ g/mol while the rest (fraction 2, $\sim 68.5\%$) of the mixture had a relatively low \bar{M}_w of $\sim 3.23 \times 10^5$ g/mol. As Maillard-driven conjugation time increased up to 1 day, the similarity in elution profile between glyco-PPH and PPH-GA mixture manifested the limited progress of cross-linking (Pirestani et al., 2017). However, a larger proportion (47.4%) of the first fraction in glyco-PPH eluted earlier with an increase in the size of the peak at 16.6 min of eluting time when compared to that in mixture (31.5%, 17.2 mL), which indicates an increase in molecular mass (**Table 5.1**). In terms of fraction 2 in glyco-PPH after 1 day conjugation, some small peaks gradually merged with the larger peak and shifted to a shorter eluting time compared to that in PPH-GA mixture. Accordingly, the formation of glyco-PPH was supported through the conjugation between PPH

and GA, and the number of GA molecules conjugated to each PPH molecule was approximately 1.2 based on **Eq. 5.1&5.2**.

The proportion of fraction 1 in glyco-PPH decreased to 40% and 37%, respectively, after conjugation up to 3 and 5 days (**Table 5.1**). The intensity of the dRI signal in fraction 1 also weakened (**Fig. 5.4F&G**). This may be ascribed to the progress of Maillard-driven reaction into advanced or late stage, resulting in decomposition of glycoprotein into other relevant compounds through retro-aldolization or Strecker degradation (Boekel, 2006). Furthermore, the peaks belonging to fraction 2 of glyco-PPH shifted leftward and almost merged in a single peak compared to the glyco-PPH after 3 days of conjugation. Meanwhile, no changes were observed in the elution patterns in fraction 2 of glyco-PPH after 3 or 5 days cross-linking indicating the kinetics of Maillard-driven reaction was relatively constant when subjected to 3 to 5 days conjugation.

Table 5.1. Molecular mass parameters of various glyco-PPH determined by SEC-MALLS.

Samples	Fraction	Mass fraction (%)	\bar{M}_w (g/mol)	\bar{M}_n (g/mol)	\bar{R}_g (nm)	$I = \bar{M}_w / \bar{M}_n$	Mass recovery (%)
PPI	1	48.7	$3.59 \times 10^5 \pm 12.6\%$	$1.29 \times 10^5 \pm 6.41\%$	$34.0 \pm 0.81\%$	$2.76 \pm 14.2\%$	98.2
	2	44.6	$1.72 \times 10^5 \pm 8.42\%$	$5.95 \times 10^4 \pm 8.60\%$	$28.6 \pm 1.82\%$	$2.89 \pm 2.14\%$	11
	3	6.70	$6.01 \times 10^4 \pm 3.41\%$	$2.54 \times 10^4 \pm 4.11\%$	$22.4 \pm 0.90\%$	$2.36 \pm 3.07\%$	7.1
PPH	1	58.9	$2.81 \times 10^5 \pm 5.20\%$	$8.19 \times 10^4 \pm 6.60\%$	$32.8 \pm 0.10\%$	$3.43 \pm 8.37\%$	94.1
	2	34.2	$1.52 \times 10^5 \pm 0.82\%$	$4.16 \times 10^4 \pm 8.60\%$	$22.6 \pm 1.80\%$	$3.69 \pm 28.8\%$	34
	3	6.90	$5.61 \times 10^4 \pm 1.11\%$	$1.98 \times 10^4 \pm 4.12\%$	$20.4 \pm 1.93\%$	$2.83 \pm 7.36\%$	12.1
GA	1	80.1	$2.17 \times 10^6 \pm 0.48\%$	$1.72 \times 10^6 \pm 0.43\%$	$30.5 \pm 0.15\%$	$1.26 \pm 0.64\%$	86.3
PPH-GA-0	1	31.5	$2.48 \times 10^6 \pm 0.39\%$	$2.41 \times 10^6 \pm 0.38\%$	$36.8 \pm 1.19\%$	$1.03 \pm 0.54\%$	92.5
	2	68.5	$3.23 \times 10^5 \pm 1.34\%$	$5.18 \times 10^4 \pm 0.80\%$	$26.3 \pm 1.52\%$	$6.34 \pm 1.56\%$	89.5
glyco-PPH-1	1	47.4	$4.17 \times 10^6 \pm 0.38\%$	$2.87 \times 10^6 \pm 0.36\%$	$38.8 \pm 0.18\%$	$1.45 \pm 0.52\%$	99.1
	2	52.6	$6.22 \times 10^5 \pm 5.37\%$	$1.31 \times 10^5 \pm 1.39\%$	$34.2 \pm 0.21\%$	$4.75 \pm 5.55\%$	90.1
glyco-PPH-3	1	39.9	$3.66 \times 10^6 \pm 1.19\%$	$3.27 \times 10^6 \pm 0.39\%$	$32.2 \pm 0.18\%$	$1.14 \pm 0.61\%$	99.4
	2	60.1	$7.75 \times 10^5 \pm 7.29\%$	$3.97 \times 10^5 \pm 6.67\%$	$28.5 \pm 0.33\%$	$1.95 \pm 9.88\%$	68.7
glyco-PPH-5	1	36.9	$3.36 \times 10^6 \pm 0.38\%$	$3.33 \times 10^6 \pm 0.35\%$	$36.7 \pm 0.14\%$	$1.01 \pm 0.52\%$	98.1
	2	63.1	$7.96 \times 10^5 \pm 6.64\%$	$4.68 \times 10^5 \pm 5.33\%$	$26.8 \pm 0.25\%$	$1.70 \pm 8.52\%$	78.6

¹ \bar{M}_w , weight-average molecular weight; \bar{M}_n , number-average molecular weight; \bar{R}_g , radius of gyration; I , polydispersity

² PPI, pea protein isolate; PPH, pea protein hydrolysate; GA, gum Arabic;

5.4.3. Degree of conjugation in glyco-PPH

The degree of covalent cross-linking between protein and polysaccharide has a significant impact on the functionality of glycoproteins, which is highly dependent on conjugation time. Hence, the effect of reaction time on the degree of PPH-GA conjugation was examined using variable parameters including non-specific markers of Maillard-driven reaction, the block of free amino groups in PPH, and color development of glyco-PPH (Figs. 5.5-5.7)

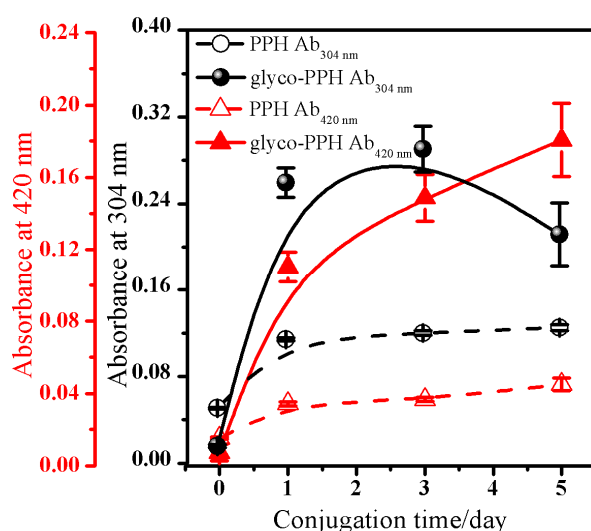


Figure 5.5. Changes in absorbance at 304 nm and 420 nm in the mixture of PPH and GA reacted at 60°C and 79% relative humidity for 0-5 day.

The formation of Amadori compounds and melanoidins was determined by measuring the absorbance of glyco-PPH solution at 304 and 420 nm, respectively (Fig. 5.5) (Zha et al., 2019b; Zhu, Damodaran, & Lucey, 2010). The Ab_{304nm} of glyco-PPH increased sharply after 1 day of conjugation ($p < 0.05$), after which it gradually leveled off and even declined with prolonged conjugation toward 5 days. This result indicated that Amadori compounds were produced after 1 day reaction between PPH and GA. The formation of melanoidin colorants increased continuously with conjugation time in light of the increment of Ab_{420nm} (Fig. 5.5). The Ab_{304nm} values were higher than Ab_{420nm} after 3 days of conjugation for all glyco-PPH, indicating the dominance of early intermediate Maillard reaction products in all glycoproteins

(Delgado-Andrade, Morales, Seiquer, & Pilar Navarro, 2010). Meanwhile, a slight increase of Ab304nm for PPH alone was also observed after the same conjugation time. This can be explained by the presence of substances with carbonyl groups that can react with PPH via Maillard reaction.

The quantity of free amino groups in Maillard reaction products is another common indicator of the degree of conjugation (**Fig. 5.6**). In the PPH-GA system, the crosslinking of GA to PPH after 3 days reduced the amount of free amino groups by $\sim 26.5\%$. A decrease was steady afterward, which might be due to a reduction in the reactivity of GA (Laroque et al., 2008). The depleted free amino groups in PPH alone (9.8%) were about 3 times less than that in glyco-PPH after 3 days of conjugation. Such loss again implied that Maillard reactions may also exist in PPH in the absence of other reactants carrying carbonyl groups, and the greater extent of crosslinking occurred after 1 day.

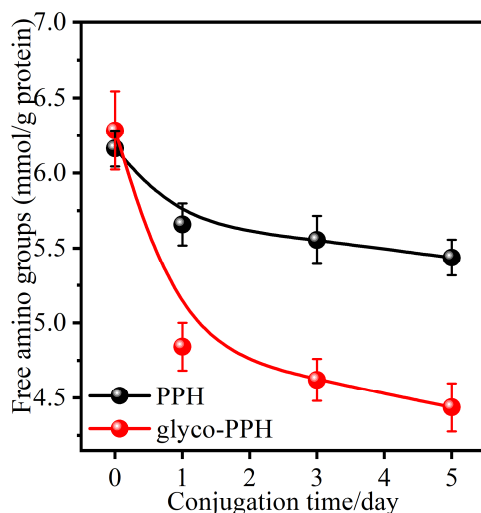


Figure 5.6. Changes of free amino groups as a function of reaction time during cross-linking of PPH and GA at 60°C and 79% relative humidity.

Color development of glyco-PPH was detected over the course of Maillard reaction. The extension of conjugation time from 1 to 5 days increased both a^* (+redness) and b^* (+yellowness) values, but decreased the L^* (+lightness) value (**Fig. 5.7**). The changes of conjugates confirmed that the cross-linking between PPH and GA was time dependent.

However, smaller changes in color parameters were recorded in PPH alone during incubation, which again suggested that the Maillard reaction between GA and PPH aided the color development of glyco-PPH.

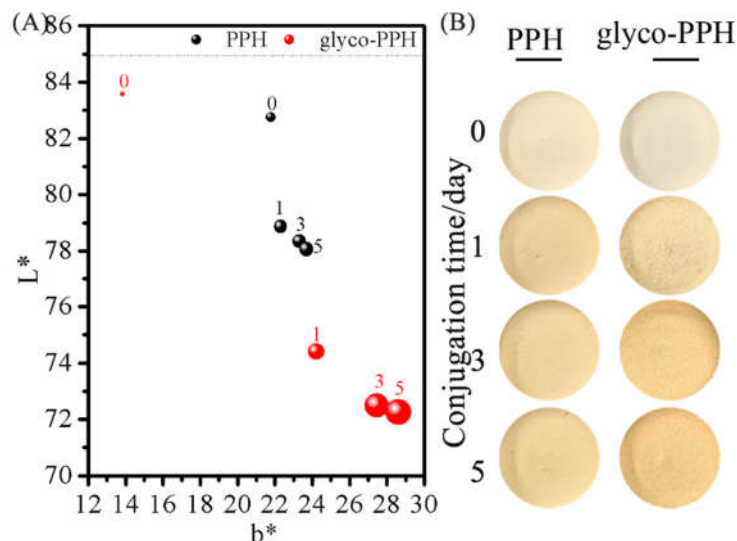


Figure 5.7. Color development (A) and real figures (B) of samples reacted at 0, 1, 3, and 5 days, respectively. The size of bubble is related to redness (a^*) value; PPH and GA represent pea protein hydrolysate and gum Arabic, respectively.

5.4.4. Volatile substances in glycoprotein

To identify volatile substances in glyco-PPH, analysis by HS-SPME-GC-MS was performed. A total of 95 volatiles were isolated and identified in the glycoproteins, including 24 alcohols, 11 aldehydes, 13 ketones, 5 acids, 6 esters, 7 pyrazines, 1 furan, 2 phenols, 1 aromatic, 15 hydrocarbons, and 10 other compounds. Numerically, alcohols (25%) and hydrocarbons (16%) were the most abundant chemical classes.

Roughly, the number and concentration of volatiles identified in GA was much less in comparison with glycoproteins. Among the volatiles identified in PPH, 1-octen-3-ol, 1-hexanol, 1-pentanol, hexanal, nonanal, 2-pentylfuran, 1-octen-3-one, 3-methyl-1-butanol were the major and characteristic contributors to the beany flavor of PPH, all of which are associated with lipoxygenase initiated lipid oxidation products (Kobayashi, Tsuda, Hirata, Kubota, & Kitamura, 1995). Hexanal (63%) was the major constituent among the aldehydes in PPH,

which, altogether, accounted for 14% of the identified chemical constituents in PPH. Other potent unpleasant odorants such as (Z)-2-octen-1-ol, 3-methyl-1-butanol, 1-penten-3-ol, octanal, and acetophenone were also detected in PPH (Samoto, Miyazaki, Kanamori, Akasaka, & Kawamura, 2005).

With respect to the volatiles identified in glyco-PPH, some key volatile compounds contributing to the aroma of Maillard-driven reaction products such as pyrazines, thiophenes, ketones, and Strecker aldehydes were detected. Pyrazines possess a unique organoleptic characteristic described as baked cereal products notes, roast, and meat-like odorants that can notably impact the sensory aspects of plant protein based food (Maga, 1992). The proposed formation pathway is the reaction of α -dicarbonyl fragments with amine group of amino acids in the Strecker degradation mechanism, producing α -amino carbonyl intermediate and condensed pyrazines. In addition, a variety of alkylation pyrazines-related compounds were identified in glyco-PPH, including 2,5-diethyl-pyrazine, 3-ethyl-2,5-dimethyl-pyrazine, 2-ethyl-3,6-dimethyl-pyrazine, 2-ethyl-3,5-dimethyl-pyrazine, and 3,5-dimethyl-pyrazine, all being considered as potent aromatic compounds derived from the Strecker degradation with low odor thresholds (Adams, Polizzi, Van Boekel, & De Kimpe, 2008; Van Lancker, Adams, & De Kimpe, 2012).

Sulfur-containing aromatic compounds (e.g., thiophenes and sulfur substituted furans) act as active components and precursors in reactions to produce other aroma compounds (Mottram, 1998). In all glyco-PPH, only two sulfur-containing compounds, 2-methylthiophene and 2-ethylthiophene, were detected. This is consistent with the fact that pea proteins are distinctly deficient in sulfur-containing amino acids cysteine and methionine (Boye, Zare, & Pletch, 2010). A variety of Strecker aldehydes-related compounds, such as benzaldehyde, 5-methyl-2-furancarboxaldehyde, furfural, and 3,5-di-butyl-4-hydroxybenzaldehyde, were also detected in all glyco-PPH. These aldehydes were not only aroma-active compounds, but

characteristic flavor precursors representing a “fingerprint” of Maillard-driven chemistry. The concentration of all these Strecker aldehydes in glyco-PPH presented a rising trend with the extension of conjugation time. However, two furanone-related compounds (4,5-dihydro-5-propyl-2(3H)-furanone & 4,5-dihydro-5-butyl-2(3H)-furanone) were also detected and identified in glyco-PPH after 5 days of conjugation, and both imparted potent unpleasant odorous, i.e. fatty, pungent, roasty, and caramel-like flavors (Specht & Baltes, 1994). In conclusion, it is critical to control the conjugation time to a certain degree of cross-linking to achieve the desirable flavor profiles that fulfill the organoleptic requirements. Overall, all of the glyco-PPH conjugates could recede or eliminate the characteristic beany flavors of plant proteins, and produce aroma flavors as compared to a mixture of PPH-GA, but overreaction such as glyco-PPH-5 will negatively impact the flavors and develop other unpleasant odors.

The changes of volatile compounds during Maillard-driven cross-linking PPH with GA were examined by principal component analysis (PCA), and the relative content of each volatile was normalized using E-2-octenal as an internal standard (**Fig. 5.8A&B**). In general, three significant principal components (PCs) accounted for 51 %, 24% and 13 % of the total variation. PC1 mainly integrated the variation of alcohols (A1-18), ketones (C), furans (G), aromatics (I), hydrocarbons (J), and other compounds (K). Analogously, the variation of chemical classes (alcohols (A19-24), aldehydes (B), acids (D), pyrazines (F) and phenols (H)) was primarily summarized by PC2, and the variation of esters (E) was represented in PC3. Based on the 3-D spatially relative location in **Figure 5.8A**, Glyco-PPH produced after 1, 3, and 5 days of conjugation can be grouped into a category; whereas GA, PPH, and the mixture of PPH-GA were significantly different from each other. In the plane of PC1 and PC2, GA and PPH-GA mixture that located in the positive part of PC2 were clearly differentiated with PPH and glyco-PPH in the negative part of PC2; whereas the differences between PPH and glyco-PPH were clearly visualized by PC1. Accordingly, as indicated in **Figure 5.8B**, Strecker

aldehydes (B2,4,7), furanones (C12,13), Pyrazines (F1,2,3,4,5,6), and thiophenes (K8,9) were the dominant eigenvectors that were responsible for the volatiles in glyco-PPH. On the basis of above results, it is concluded that both PPH and PPH-GA mixture present beany or grassy flavor, while glyco-PPH formed after 1 day of conjugation features the non-specific aroma odors. Glyco-PPH produced after 3 or 5 days of conjugation not only possesses the non-specific aroma flavor, but has slight off-flavors resulting from the formation of furanones.

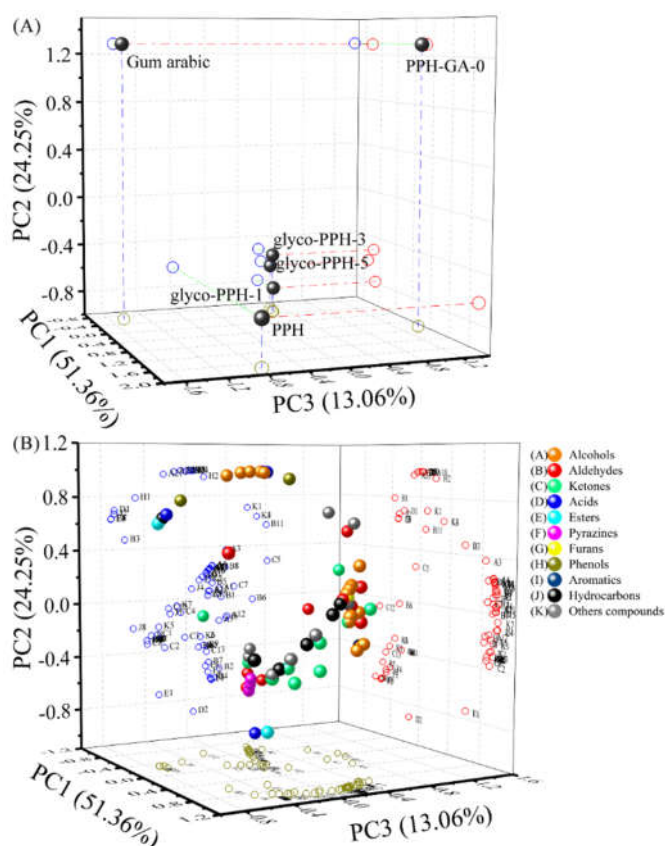


Figure 5.8. Principal component analysis (PCA) (A) loading plot (B) score plot of identified flavor compositions in different glyco-PPH. Note: PPH-GA-0 represented the mixture of pea protein hydrolysate (PPH) and gum arabic (GA); glyco-PPH-1, glyco-PPH-3 and glyco-PPH-5 represented glyco-PPH cross-linked between PPH and GA for 1, 3, 5 day, respectively.

To further confirm the effect of covalent cross-linking between PPH and GA on the beany flavor mitigation, six distinctive markers identified from PPH and reported from pea sensory study (Bott & Chambers IV, 2006), were quantified (**Table 5.2**). The eluting profiles of selected characteristic beany flavors were shown in **Figure 5.9**. A decrease tendency in the

elution profiles of these markers, which is consistent with the qualitative data (Table 5.2). According to the qualitative analyses performed, the initial concentration of these identified volatiles followed the order: hexanal (3.54 ppm) > 1-octen-3-ol (1.10 ppm) > 1-octen-3-one (1.07 ppm) > 3-methyl-1-butanol (0.45 ppm) > acetophenone (0.40 ppm) > 2-pentylfuran (0.19 ppm). Based on the thresholds of these volatiles (40-164 ppb) (Burdock, 2004), it is concluded that the odor activity value (OAV) of these volatiles was above 1, and hence were considered as the main flavor-active components. Upon covalent crosslinking between PPH and GA, the concentration of the beany flavor markers in glyco-PPH was reduced significantly, and was more than 2-fold less than in PPH even after 1 day of conjugation. Extending the conjugation time could greatly reduce the beany flavors in glyco-PPH. The reduction of beany flavor compounds in glyco-PPH might be related to structural reorientation and conformational change of PPH (SEM results) upon conjugation, resulting in the release of hydrophobic beany flavors compounds

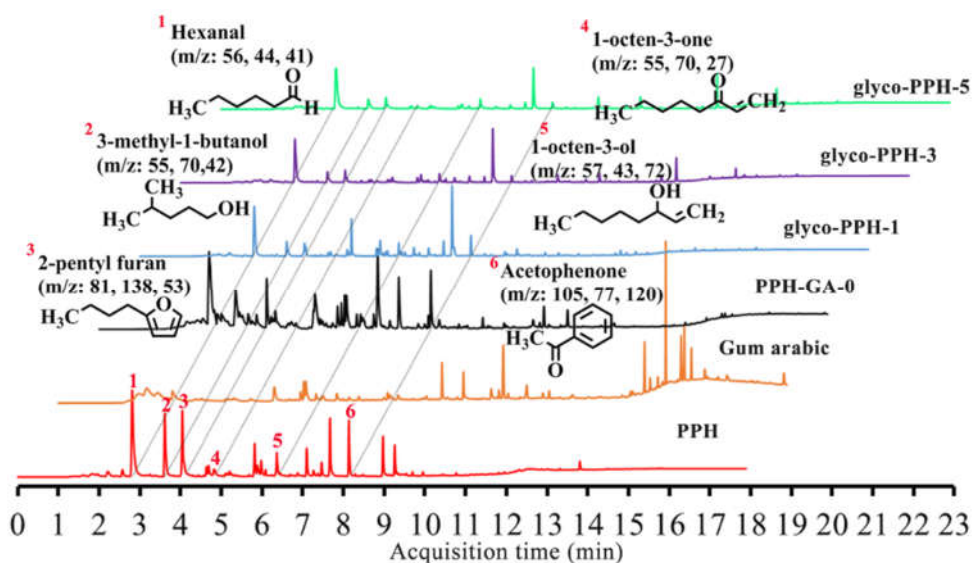


Figure 5.9. Chromatograms of beany flavor markers. Note: PPH-GA-0 represented the mixture of pea protein hydrolysate (PPH) and gum arabic (GA); glyco-PPH-1, glyco-PPH-3 and glyco-PPH-5 represented glyco-PPH cross-linked between PPH and GA for 1, 3, 5 day, respectively.

Table 5.2. The level of selected off-flavor volatiles in various glyco-PPH conjugates (n = 3)

no.	compound	Identification method			sample						LOD (mg·L ⁻¹)	Recovery (%)	RSD%
		qualitative ion (m/z)	quantitative ion (m/z)		PPH	GA	glyco-PPH-0	glyco-PPH-1	Glyco-PPH-3	Glyco-PPH-5			
1	hexanal	St	56, 44, 41	56	3.54 ± 0.04a	nd	3.17 ± 0.06a	1.28 ± 0.07b	0.78 ± 0.02c	0.42 ± 0.04d	0.025	92.59	4.68
2	3-methyl-1-butanol	St	55, 70, 42	55	0.45 ± 0.02a	nd	0.36 ± 0.01b	0.12 ± 0.01c	0.05 ± 0.01c	0.03 ± 0.01c	0.023	96.40	1.64
3	2-pentyl furan	St	81, 138, 53	81	0.19 ± 0.04a	nd	0.16 ± 0.02a	0.05 ± 0.01b	0.02 ± 0.01c	0.01 ± 0.00c	0.008	91.83	2.61
4	1-octen-3-one	St	55, 70, 27	55	1.07 ± 0.01a	nd	0.82 ± 0.02a	0.33 ± 0.01b	0.09 ± 0.01c	0.04 ± 0.02d	0.015	97.97	7.12
5	1-octen-3-ol	St	57, 72, 43	57	1.10 ± 0.03a	nd	0.95 ± 0.02a	0.34 ± 0.02b	0.19 ± 0.01c	0.11 ± 0.01d	0.016	95.86	0.12
6	acetophenone	St	105, 120, 77	105	0.40 ± 0.07a	nd	0.45 ± 0.03a	0.17 ± 0.04b	0.13 ± 0.01b	0.07 ± 0.01c	0.012	94.83	6.14

¹ Units of milligrams per gram of dry weight;

² Number (no.) corresponds to the elution order by GC-MS analysis in Figure 5.9;

³ St, standard; nd, not detected; PPH, pea protein hydrolysate; GA, gum Arabic; 0, 1, 3, 5, different reaction time (day) at 60°C and 79% relative humidity; LOD, limit of quantitation; RSD, relative standard deviation;

⁴ Different lowercases present significant difference at $p < 0.05$.

5.4.5. Solubility and emulsification properties of glyco-PPH

As aforementioned, low solubility is one of the biggest challenges to utilize pea protein as functional materials. The solubility of PPH and glyco-PPH with different conjugation time was measured (Fig. 5.10).

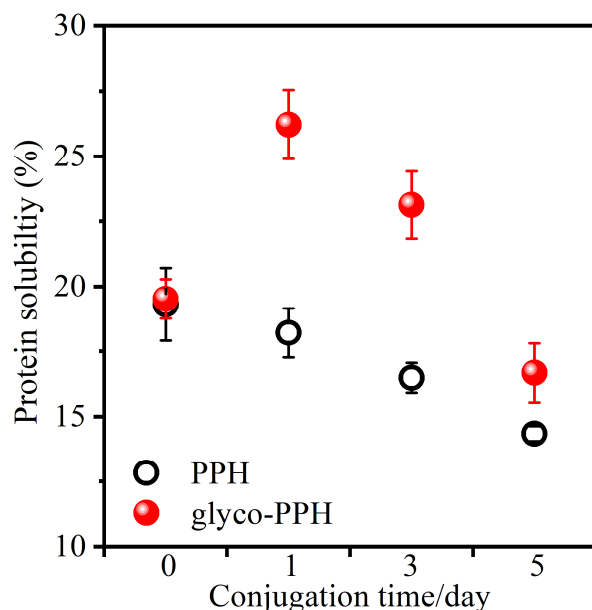


Figure 5.10. Relative protein solubility of different glyco-PPH cross-linked at 1, 3, and 5 days, respectively. PPH and GA represent pea protein hydrolysate and gum Arabic, respectively.

The solubility of PPH-GA mixture was similar to that of PPH itself ($p>0.05$) implying that no physicochemical interactions between PPH and GA at a neutral pH. The solubility of PPH after cross-linking with GA followed a parabolic pattern. It was significantly improved from 19.4 % to 26.2 % after 1 day of conjugation. A sudden turnover was observed as conjugation time exceeded 3 days. In terms of the solubility of PPH alone, a consistently downward trend was exhibited as PPH subjected to the same conjugation time. Clearly, overreaction of crosslinking that occurs during Maillard-driven reaction under prolonged time is a determinant factor to the loss of its solubility. Thus, modulating conjugation time is of great importance to synthesize glyco-PPH with desirable solubility.

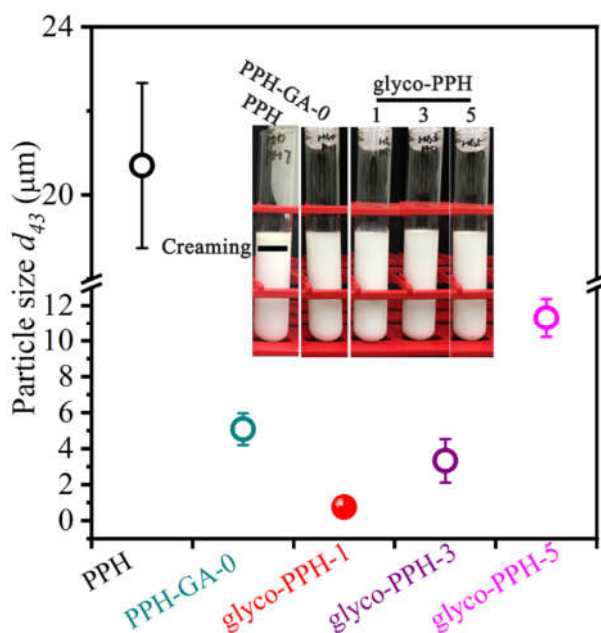


Figure 5.11. Changes of particle size (d_{43}) for emulsions stabilized with pea protein hydrolysate (PPH) alone, mixture of PPH and gum Arabic (GA), and various glyco-PPH.

The emulsification property of glyco-PPH with different conjugation time was examined by measuring the particle size of corn oil-in-water emulsion (Fig. 5.11). A U pattern for the changes of particle size in emulsion stabilized by glyco-PPH was observed. An initial improvement of emulsifying properties, followed by a decline when cross-linking was carried out too extensively. The volume-mean droplet diameter (d_{43}) of PPH stabilized corn oil-in-water emulsions was 20.7 μm (Fig. 5.11), which was far bigger than other particle size in emulsions stabilized either by PPH-GA mixture or glyco-PPH. A layer of creaming was observed in PPH stabilized emulsions compared to others (Fig. 5.11 inserted image). The mixture of PPH-GA was able to reduce the particle size of emulsion to 5.08 μm , presumably because of the inherent emulsification property of GA. The emulsion droplet size (d_{43}) stabilized by glyco-PPH with 1 day of conjugation was significantly reduced to 0.75 μm , which suggested that the emulsification property of PPH can be substantially enhanced upon covalent cross-linking with GA via the Maillard reaction. However, such enhancement vanished in

emulsion stabilized by the glyco-PPH with 3 or 5 days of conjugation, which resulted in the increased particle size of emulsions.

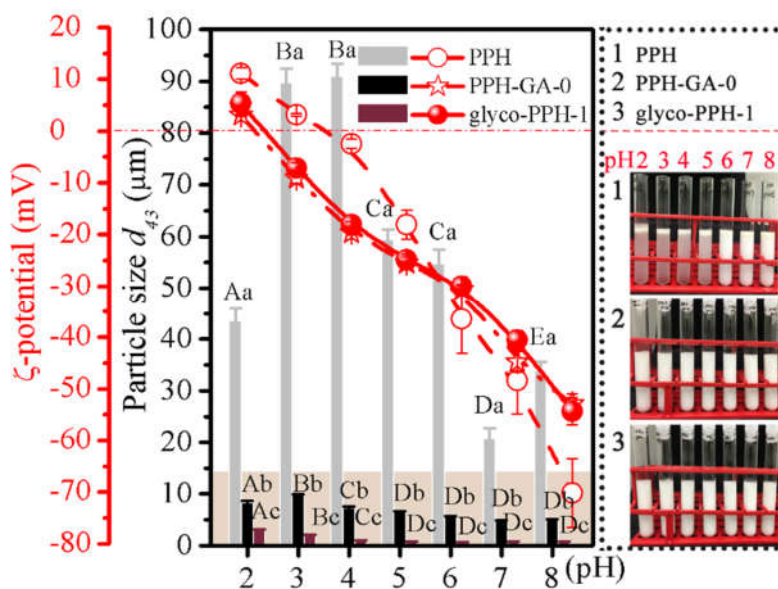


Figure 5.12. Changes of particle size (d_{43}) and ζ -potential for emulsions stabilized with pea protein hydrolysate (PPH) alone, mixture of PPH with gum Arabic (GA), and glyco-PPH with 1 day reaction against different pHs. Note: the lowercase letters are for comparison among groups at the same pH values; the uppercase letters are for comparison in groups at the different pH values. Different letters indicated significance at $p < 0.05$.

In general, the emulsion stabilized by pea proteins is unstable against pH changes (Gumus, Decker, & McClements, 2017). To examine if glyco-PPH could improve the physical stability of emulsion under various pH values (2–8), glyco-PPH synthesized after 1 day of conjugation was used to prepare a corn oil-in-water emulsion as it can form the smallest droplets ($0.75 \mu\text{m}$). The impact of pH on the physical stability of the emulsions (PPH and mixture as controls) was investigated by measuring the particle size (d_{43}) and ζ -potential (Fig. 5.12). As can be seen, serious phase separation was visualized in PPH stabilized emulsions across at pH 2–5, whereas macroscopic stable emulsions were observed in both PPH-GA mixture and glyco-PPH stabilized emulsions at pH 2–8 (Fig. 5.12). In addition, the particle size of PPH stabilized emulsion was significantly larger than those prepared by glyco-PPH or PPH-GA mixture at the same pH. A similar particle size of the emulsions prepared by glyco-

PPH or mixture was detected at pH 5–8 ($p > 0.05$). The particle size (d_{43}) of emulsions stabilized by PPH-GA mixture was considerably increased at pH 3 or below, corresponded to a reduced emulsification effect of GA at an acidic condition (Nakauma et al., 2008). By contrast, particle size of emulsions prepared by glyco-PPH remained steady across a broad pH range (2–8), suggesting that the presence of GA covalently cross-linked with PPH can effectively enhance the physical stability of emulsions against pH.

To elucidate the mechanism of the enhanced physical stability of emulsion stabilized by glyco-PPH, the ζ -potential of the emulsions under different pH values were compared (**Fig. 5.12**). PPH stabilized emulsions exhibited a high ζ -potential (-36.5 mV) at pH 6, indicating a strong electrostatic repulsion between emulsion droplets; this, however, did not warrant a greater physical stability, again denoting the poor emulsification property of PPH. The IEP of PPH was ~ 3.5 , and the conjugation with GA lowered it to 2.5 (**Fig. 5.12**). The modification of available amino groups in protein might be responsible for the lowered IEP of glyco-PPH (Delahaije, Gruppen, Van Nieuwenhuijzen, Giuseppin, & Wierenga, 2013). The ζ -potential of the emulsion stabilized by glyco-PPH or PPH-GA mixture had no significant difference across the entire pH range ($p > 0.05$) (**Fig. 5.12**). Consequently, the similarity in electrostatic interactions cannot be the cause of the difference in physical stability between glyco-PPH and PPH-GA mixture-based emulsions at acidic pH (2 and 3). Alternatively, the attachment of GA on PPH could improve the steric hindrance in emulsion droplets covered by glyco-PPH. The enhanced steric repulsion could prevent emulsion droplets from flocculation and phase separation by counteracting the van der Waals force between emulsion droplets at pH close to the IEP.

5.4.6. Oxidative stability of oil-in-water emulsions stabilized by glyco-PPH

The iron binding capacity of anionic polysaccharides may exert a preventive effect against emulsion oxidation. However, when they are coated on emulsion droplets, negative

surface charge of droplets has the potential to bring transition metals (e.g., Fe^{2+}) into close proximity to hydroperoxides (LOOH), thus accelerating emulsion oxidation by decomposing LOOH and producing rancid flavors. This was a particular concern in glyco-PPH stabilized emulsions as it had the highest negative surface charge at pH 6–8. Hence, the oxidative stability of emulsions stabilized by glyco-PPH after 1 day of conjugation was examined by measuring the formation of LOOH and hexanal in emulsion during storage at 37 °C (**Fig. 5.13A&B**).

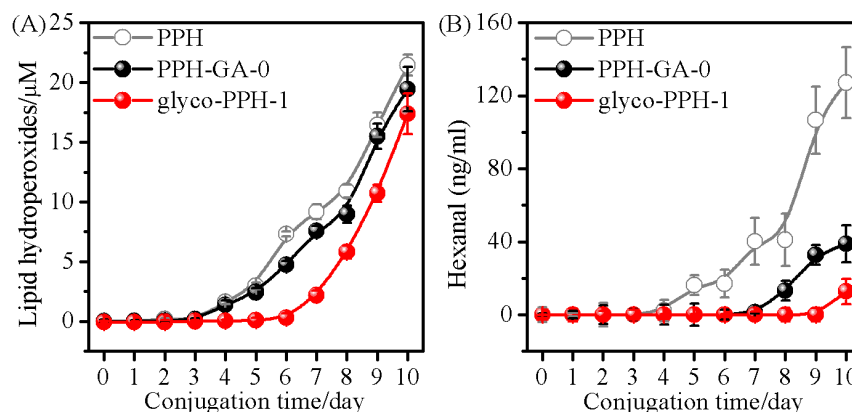


Figure 5.13. The formation of (A) lipid hydroperoxides and (B) hexanal in corn oil-in-water emulsions (pH 7.0) stabilized by pea protein hydrolysate (PPH), mixture of PPH with gum Arabic (GA), and glyco-PPH for 1 day during storage at 37 °C.

LOOH in PPH stabilized emulsion increased slightly after 3 days of storage, as did the generation of hexanal (**Fig. 5.13A&B**). Similarly, the development of LOOH in emulsion prepared by PPH-GA mixture was boosted after 3 days of storage; however, a significant increase in hexanal occurred after 7 days of storage. This result suggested that the presence of GA in PPH–GA mixture stabilized emulsion extended the lag phase of the emulsion in terms of hexanal formation. In terms of glyco-PPH-based emulsion, the level of LOOH remained constant after 5 days of storage, while a considerable increase tendency appeared after 6 days of storage. That indicated the glyco-PPH synthesized by 1 day of conjugation could delay the development of LOOH in the emulsion it stabilized. Surprisingly, the concentration of hexanal in the glyco-PPH stabilized emulsion was still lower than LOD even after 9 days of storage. This result implied that glyco-PPH can considerably prevent the formation of hexanal. We

attributed the improved oxidative stability of emulsion to the stronger steric hindrance derived from the thicker layer of glyco-PPH on the emulsion droplet surface, which hindered the transition metals from getting into close proximity to the core lipids.

5.5. Conclusion

The successful covalent crosslinking of gum Arabic to pea protein hydrolysates via a mild Maillard reaction at 60 °C and 79% relative humidity was confirmed by SDS-PAGE, FTIR-ATR, and SEM characterizations. SEC-MALLS indicated that approximately 1.2 mol of GA was covalently linked to 1 mol of PPH after 1 day of conjugation. The degree of conjugation between GA and PPH can be predicted by measuring the development of nonspecific Maillard reaction marker (A_{b420nm}) and the available free amino groups in glyco-PPH. The characteristic Strecker degradation products, aldehyde and pyrazines aromatic components associated with Maillard reaction, were identified in glyco-PPH via SPME-GC-MS. A remarkable beany flavor mitigation effect occurred in glyco-PPH with 1 day of conjugation. Extending the conjugation time greatly diminished the formation of beany flavor markers. The solubility and emulsification properties of glyco-PPH were sufficiently improved by controlling the conjugation time to 1 day. The physical stability of corn oil-in-water emulsions stabilized by glyco-PPH with 1 day of conjugation was improved, particularly at pH's close to IEP. Emulsions stabilized by glyco-PPH with 1 day of conjugation also exhibited superior chemical stability against lipid oxidation. The improved physicochemical stability of the emulsion was attributed to the increased steric hindrance of the emulsion droplet surface. The remarkable functionality and antioxidant activity of glyco-PPH with 1 day of conjugation gives it great potential for use as a natural plant protein-based functional material.

5.6. References

Adams, A. N., Polizzi, V., Van Boekel, M., & De Kimpe, N. (2008). Formation of pyrazines and a novel pyrrole in Maillard model systems of 1,3-dihydroxyacetone and 2-

- oxopropanal. *Journal of Agricultural and Food Chemistry*, 56(6), 2147–2153.
<https://doi.org/10.1021/jf0726785>
- Al-Assaf, S., Phillips, G. O., & Williams, P. A. (2005). Studies on acacia exudate gums. Part I: The molecular weight of Acacia senegal gum exudate. *Food Hydrocolloids*, 19(4), 647–660. <https://doi.org/10.1016/j.foodhyd.2004.09.002>
- Boekel, M. A. J. S. van. (2006). Formation of flavour compounds in the Maillard reaction. *Biotechnology Advances*, 24(2), 230–233.
<https://doi.org/10.1016/j.biotechadv.2005.11.004>
- Bott, L., & Chambers IV, E. (2006). Sensory characteristics of combinations of chemicals potentially associated with beany aroma in foods. *Journal of Sensory Studies*, 21(3), 308–321. <https://doi.org/10.1111/j.1745-459X.2006.00067.x>
- Boye, J., Zare, F., & Pletch, A. (2010). Pulse proteins: Processing, characterization, functional properties and applications in food and feed. *Food Research International*, 43, 414–431. <https://doi.org/10.1016/j.foodres.2009.09.003>
- Bradford, M. M. (1976). A rapid and sensitive method for the quantitation of microgram quantities of protein utilizing the principle of protein-dye binding. *Analytical Biochemistry*, 72(1–2), 248–254. [https://doi.org/10.1016/0003-2697\(76\)90527-3](https://doi.org/10.1016/0003-2697(76)90527-3)
- Burdock, G. A. (2004). Fenaroli's Handbook of Flavor Ingredients. In *Fenaroli's Handbook of Flavor Ingredients*. <https://doi.org/10.1201/9781420037876>
- Cerny, C., & Davidek, T. (2003). Formation of aroma compounds from ribose and cysteine during the Maillard reaction. *Journal of Agricultural and Food Chemistry*, 51(9), 2714–2721. <https://doi.org/10.1021/jf026123f>
- Chao, D. F., He, R., Jung, S., & Aluko, R. E. (2013). Effect of pressure or temperature pretreatment of isolated pea protein on properties of the enzymatic hydrolysates. *Food*

Research International, 54(2), 1528–1534.

<https://doi.org/10.1016/j.foodres.2013.09.020>

Chen, B., McClements, D. J., & Decker, E. A. (2010). Role of continuous phase anionic polysaccharides on the oxidative stability of menhaden oil-in-water emulsions. *Journal of Agricultural and Food Chemistry*, 58(6), 3779–3784.

<https://doi.org/10.1021/jf9037166>

Chéreau, D., Videcoq, P., Ruffieux, C., Pichon, L., Motte, J.-C., Belaid, S., Ventureira, J., & Lopez, M. (2016). Combination of existing and alternative technologies to promote oilseeds and pulses proteins in food applications. *OCL*, 23(4), D406.

<https://doi.org/10.1051/ocl/2016020>

Cho, M. J., Unklesbay, N., Hsieh, F. H., & Clarke, A. D. (2004). Hydrophobicity of bitter peptides from soy protein hydrolysates. *Journal of Agricultural and Food Chemistry*, 52(19), 5895–5901. <https://doi.org/10.1021/jf0495035>

Chung, H. J., Liu, Q., & Hoover, R. (2010). Effect of single and dual hydrothermal treatments on the crystalline structure, thermal properties, and nutritional fractions of pea, lentil, and navy bean starches. *Food Research International*, 43(2), 501–508.

<https://doi.org/10.1016/j.foodres.2009.07.030>

Dahl, W. J., Foster, L. M., & Tyler, R. T. (2012). Review of the health benefits of peas (*Pisum sativum* L.). *British Journal of Nutrition*, 108(S1), S3–S10.

<https://doi.org/10.1017/S0007114512000852>

de Oliveira, F. C., Coimbra, J. S. dos R., de Oliveira, E. B., Zuñiga, A. D. G., & Rojas, E. E. G. (2016). Food protein-polysaccharide conjugates obtained via the Maillard reaction: A review. *Critical Reviews in Food Science and Nutrition*, 56, 1108–1125.

<https://doi.org/10.1080/10408398.2012.755669>

- Delahaije, R. J. B. M., Gruppen, H., Van Nieuwenhuijzen, N. H., Giuseppin, M. L. F., & Wierenga, P. A. (2013). Effect of glycation on the flocculation behavior of protein-stabilized oil-in-water emulsions. *Langmuir*, *29*(49), 15201–15208.
<https://doi.org/10.1021/la403504f>
- Delgado-Andrade, C., Morales, F. J., Seiquer, I., & Pilar Navarro, M. (2010). Maillard reaction products profile and intake from Spanish typical dishes. *Food Research International*, *43*(5), 1304–1311. <https://doi.org/10.1016/j.foodres.2010.03.018>
- Gumus, C. E., Decker, E. A., & McClements, D. J. (2017). Impact of legume protein type and location on lipid oxidation in fish oil-in-water emulsions: Lentil, pea, and faba bean proteins. *Food Research International*, *100*, 175–185.
<https://doi.org/10.1016/j.foodres.2017.08.029>
- Humiski, L. M., & Aluko, R. E. (2007). Physicochemical and bitterness properties of enzymatic pea protein hydrolysates. *Journal of Food Science*, *72*(8), S605–S611.
<https://doi.org/10.1111/j.1750-3841.2007.00475.x>
- Klost, M., & Drusch, S. (2019). Functionalisation of pea protein by tryptic hydrolysis – Characterisation of interfacial and functional properties. *Food Hydrocolloids*, *86*, 134–140. <https://doi.org/10.1016/j.foodhyd.2018.03.013>
- Kobayashi, A., Tsuda, Y., Hirata, N., Kubota, K., & Kitamura, K. (1995). Aroma constituents of soybean [*Glycine max* (L.) Merrill] milk lacking lipoxygenase isozymes. *Journal of Agricultural and Food Chemistry*, *43*(9), 2449–2452.
<https://doi.org/10.1021/jf00057a025>
- Korhonen, H., & Pihlanto, A. (2003). Food-derived bioactive peptides--opportunities for designing future foods. *Current Pharmaceutical Design*, *9*(16), 1297–1308.

- Lam, A. C. Y., Can Karaca, A., Tyler, R. T., & Nickerson, M. T. (2018). Pea protein isolates: Structure, extraction, and functionality. *Food Reviews International*, *34*, 126–147.
<https://doi.org/10.1080/87559129.2016.1242135>
- Laroque, D., Inisan, C., Berger, C., Vouland, É., Dufossé, L., & Guérard, F. (2008). Kinetic study on the Maillard reaction. Consideration of sugar reactivity. *Food Chemistry*, *111*(4), 1032–1042. <https://doi.org/10.1016/j.foodchem.2008.05.033>
- Liu, G., & Zhong, Q. (2013). Thermal aggregation properties of whey protein glycated with various saccharides. *Food Hydrocolloids*, *32*(1), 87–96.
<https://doi.org/10.1016/j.foodhyd.2012.12.008>
- Ma, Z., Boye, J. I., Simpson, B. K., Prasher, S. O., Monpetit, D., & Malcolmson, L. (2011). Thermal processing effects on the functional properties and microstructure of lentil, chickpea, and pea flours. *Food Research International*, *44*(8), 2534–2544.
<https://doi.org/10.1016/j.foodres.2010.12.017>
- Maga, J. A. (1992). Pyrazine update. *Food Reviews International*, *8*(4), 479–558.
<https://doi.org/10.1080/87559129209540951>
- Martinez-Alvarenga, M., Martinez-Rodriguez, E. Y., Garcia-Amezquita, L. E., Olivas, G. I., Zamudio-Flores, P. B., Acosta-Muniz, C. H., & Sepulveda, D. R. (2013). Effect of Maillard reaction conditions on the degree of glycation and functional properties of whey protein isolate – Maltodextrin conjugates. *Food Hydrocolloids*, *38*, 110–118.
<https://doi.org/10.1016/j.foodhyd.2013.11.006>
- Mohammadinejad, R., Shavandi, A., Raie, D. S., Sangeetha, J., Soleimani, M., Hajibehzad, S.S., Thangadurai, D., Hospet, R., Popoola, J. O., Arzani, A., & Gómez-Lim, M.A. (2019). Plant molecular farming: Production of metallic nanoparticles and therapeutic proteins using green factories. *Green Chemistry*. <https://doi.org/10.1039/c9gc00335e>

- Mottram, D. S. (1998). Flavour formation in meat and meat products: a review. *Food Chemistry*, 62(4), 415–424. [https://doi.org/10.1016/S0308-8146\(98\)00076-4](https://doi.org/10.1016/S0308-8146(98)00076-4)
- Nakauma, M., Funami, T., Noda, S., Ishihara, S., Al-Assaf, S., Nishinari, K., & Phillips, G. O. (2008). Comparison of sugar beet pectin, soybean soluble polysaccharide, and gum arabic as food emulsifiers. 1. Effect of concentration, pH, and salts on the emulsifying properties. *Food Hydrocolloids*, 22(7), 1254–1267. <https://doi.org/10.1016/j.foodhyd.2007.09.004>
- Oliver, C. M., Melton, L. D., & Stanley, R. A. (2006). Creating proteins with novel functionality via the Maillard reaction: A review. *Critical Reviews in Food Science and Nutrition*, 46(4), 337–350. <https://doi.org/10.1080/10408690590957250>
- Philip J, W. (1993). Light scattering and the absolute characterization of macromolecules. *Analytica Chimica Acta*, 272(1), 1–40. [https://doi.org/10.1016/0003-2670\(93\)80373-s](https://doi.org/10.1016/0003-2670(93)80373-s)
- Picton, L., Bataille, I., & Muller, G. (2000). Analysis of a complex polysaccharide (gum arabic) by multi-angle laser light scattering coupled on-line to size exclusion chromatography and flow field flow fractionation. *Carbohydrate Polymers*, 42(1), 23–31. [https://doi.org/10.1016/S0144-8617\(99\)00139-3](https://doi.org/10.1016/S0144-8617(99)00139-3)
- Pirestani, S., Nasirpour, A., Keramat, J., & Desobry, S. (2017). Preparation of chemically modified canola protein isolate with gum Arabic by means of Maillard reaction under wet-heating conditions. *Carbohydrate Polymers*, 155, 201–207. <https://doi.org/10.1016/j.carbpol.2016.08.054>
- Pirestani, S., Nasirpour, A., Keramat, J., Desobry, S., & Jasniewski, J. (2018). Structural properties of canola protein isolate-gum Arabic Maillard conjugate in an aqueous model system. *Food Hydrocolloids*, 79, 228–234. <https://doi.org/10.1016/j.foodhyd.2018.01.001>

- Román, J. K., & Wilker, J. J. (2019). Cooking chemistry transforms proteins into high-strength adhesives. *Journal of the American Chemical Society*, *141*(3), 1359–1365.
<https://doi.org/10.1021/jacs.8b12150>
- Roy, F., Boye, J. I., & Simpson, B. K. (2010). Bioactive proteins and peptides in pulse crops: Pea, chickpea and lentil. *Food Research International*, *43*, 432–442.
<https://doi.org/10.1016/j.foodres.2009.09.002>
- Samoto, M., Miyazaki, C., Kanamori, J., Akasaka, T., & Kawamura, Y. (2005). Improvement of the off-flavor of soy protein isolate by removing oil-body associated proteins and polar lipids. *Bioscience, Biotechnology, and Biochemistry*, *62*(5), 935–940.
<https://doi.org/10.1271/bbb.62.935>
- Shevkani, K., Singh, N., Kaur, A., & Rana, J. C. (2015). Structural and functional characterization of kidney bean and field pea protein isolates; a comparative study. *Food Hydrocolloids*. *43*, 679–689. Retrieved from
<https://www.sciencedirect.com/science/article/pii/S0268005X14002677>
- Specht, K., & Baltes, W. (1994). Identification of volatile flavor compounds with high aroma values from shallow-fried beef. *Journal of Agricultural and Food Chemistry*, *42*(10), 2246–2253. <https://doi.org/10.1021/jf00046a031>
- Su, J. F., Huang, Z., Yuan, X. Y., Wang, X. Y., & Li, M. (2010). Structure and properties of carboxymethyl cellulose/soy protein isolate blend edible films crosslinked by Maillard reactions. *Carbohydrate Polymers*, *79*(1), 145–153.
<https://doi.org/10.1016/j.carbpol.2009.07.035>
- Van Lancker, F., Adams, A., & De Kimpe, N. (2012). Impact of the N-terminal amino acid on the formation of pyrazines from peptides in maillard model systems. *Journal of Agricultural and Food Chemistry*, *60*(18), 4697–4708.
<https://doi.org/10.1021/jf301315b>

- Yadav, M. P., Strahan, G. D., Mukhopadhyay, S., Hotchkiss, A. T., & Hicks, K. B. (2012). Formation of corn fiber gum–milk protein conjugates and their molecular characterization. *Food Hydrocolloids*, *26*(2), 326–333.
<https://doi.org/10.1016/j.foodhyd.2011.02.032>
- Yue, H. B., Cui, Y. D., Shuttleworth, P. S., & Clark, J. H. (2012). Preparation and characterisation of bioplastics made from cottonseed protein. *Green Chemistry*, *14*(7), 2009–2016. <https://doi.org/10.1039/c2gc35509d>
- Zha, F., Dong, S., Rao, J., & Chen, B. (2019a). Pea protein isolate-gum Arabic Maillard conjugates improves physical and oxidative stability of oil-in-water emulsions. *Food Chemistry*, *285*, 130–138. <https://doi.org/10.1016/j.foodchem.2019.01.151>
- Zha, F., Dong, S., Rao, J., & Chen, B. (2019b). The structural modification of pea protein concentrate with gum Arabic by controlled Maillard reaction enhances its functional properties and flavor attributes. *Food Hydrocolloids*, *92*, 30–40.
<https://doi.org/10.1016/j.foodhyd.2019.01.046>
- Zhu, D. A. N., Damodaran, S., & Lucey, J. A. (2010). Physicochemical and emulsifying properties of whey protein isolate (WPI)-dextran conjugates produced in aqueous solution. *Journal of Agricultural and Food Chemistry*, *58*(5), 2988–2994.
<https://doi.org/10.1021/jf903643p>

6. CONJUGATION OF PEA PROTEIN ISOLATE VIA MAILLARD-DRIVEN CHEMISTRY WITH SACCHARIDES OF DIVERSE MOLECULAR MASS: MOLECULAR INTERACTIONS CAUSING AGGREGATION OR GLYCATION?

6.1. Abstract

Diverse saccharides are effectively grafted to pea protein isolate (PPI) through Maillard-driven chemistry. The development of conjugates (glyco-PPI) was validated by ultraviolet-visible (UV-Vis) spectrum, sodium dodecyl sulfate-polyacrylamide gel electrophoresis (SDS-PAGE) and size exclusion chromatography-high performance liquid chromatography (SEC-HPLC). The impact of covalent conjugation on color development, structural modification, solubility, thermal stability, and volatiles of glycoprotein was examined. The protein solubility was improved while its thermal stability seemed to be negatively influenced. The principle proposed involves Maillard-driven generation of the conjugates which enhanced the surface hydrophilicity and unfolding of protein architecture of glyco-PPI. Additionally, molecular mass and the grafted number of saccharides played a vital role in determining the function of glyco-PPI. Protein tends to denature at reaction conditions (80°C, pH 10.0) and its cross-linkage occurred in aqueous system. The two potential routes of molecular interactions between PPI and saccharides were: (i) denaturation, and (ii) glycation or self-cross-linkage. Flavor profile alteration of glycoprotein before and after conjugation was depicted and relevant off-odors were quantified via headspace solid-phase microextraction gas chromatography-mass spectrometry (HS-SPME-GC-MS).

6.2. Introduction

Plant-based proteins have earned a reputable status as natural, biodegradable functional biomaterials, getting substantial interest in numerous environmentally sensitive sectors like agriculture, packaging and biomedical fields (Mohammadinejad et al., 2019; Silva et al., 2014; Yue, Cui, Shuttleworth, & Clark, 2012). Owing to scalable versatility and high abundance, eco-

friendly pea protein (*Pisum sativum* L.) has become a serious contender to other proteins, of which the dominant position on the global market has been gradually counterbalanced (Mession, Sok, Assifaoui, & Saurel, 2013; Zha, Yang, Rao, & Chen, 2019).

In spite of the advantages associated with pea protein, its prominent off-odors lower consumer acceptability (Rackis, Sessa, & Honig, 1979; Zha, Yang, et al., 2019) and its inferior solubility, ascribed to the alkaline extraction and acid precipitation process, places a major stumbling block for its down-stream application in food systems (Lam, Can Karaca, Tyler, & Nickerson, 2018; Zha, Yang, et al., 2019). Other functions concerned with solubility including gelling, emulsifying and foaming are likewise diminished (Zha, Dong, Rao, & Chen, 2019b; Zha, Yang, et al., 2019). It has been well-documented that protein–polysaccharide interactions via Maillard-driven chemistry is a potential means to overcome these challenges (de Oliveira, Coimbra, de Oliveira, Zuñiga, & Rojas, 2016; Oliver, Melton, & Stanley, 2006). Our recent researchers have supported pea protein glycation with gum Arabic via Maillard-driven chemistry as an effective antioxidant, emulsifier and solubility enhancer, especially approximate to the isoelectric point of the protein (Zha, Dong, et al., 2019b; Zha, Dong, Rao, & Chen, 2019a; Zha, Yang, et al., 2019) and that conformational alterations of pea proteins after glycation could mitigate off-odors, and potentially trigger the development of non-specific aroma-active volatiles during the Amadori rearrangement and Strecker degradation (Zha, Dong, et al., 2019b; Zha, Yang, et al., 2019).

Whereas polysaccharides are a good candidate in light of controlling the extent of Maillard reaction, its low reactivity and steric hindrance limit the level of polysaccharides to be grafted onto proteins (de Oliveira et al., 2016; Jiménez-Castaño, Villamiel, & López-Fandiño, 2007). It is inferred that factors including the quantity of saccharides grafted to the amino acid residues, chain length, and structural characteristics of reacting saccharides profoundly impact the functionality of resultant glyco-protein (de Oliveira et al., 2016; Oliver

et al., 2006). Previous research noted that only ~1.2 mole of gum Arabic was able to be attached to one mole of pea protein hydrolysate under dry-heating condition (Zha, Yang, et al., 2019). Nevertheless, the majority of the researches applied a massive amount of saccharides in hopes to enhance the reaction rate with proteins via Maillard-drive chemistry (de Oliveira et al., 2016; Oliver et al., 2006). Currently, synthesis of protein–saccharide conjugates can be primarily achieved under controlled wet- or dry-heating conditions (de Oliveira et al., 2016; Oliver et al., 2006). Wet-heating appears to be superior to dry-heating with respect to the incubation time. It is worthy of note that solvent parameters (i.e., pH, temperature, and ionic strength) contribute largely to the altered conformational characteristics and physicochemical properties of proteins (Klupšaitė & Juodeikienė, 2015; Messio et al., 2013). Solvent modifications could potentially bring about destabilization of protein native architecture and reversible or irreversible molecular rearrangements (Messio et al., 2013). Conditions enabling the compact globular structure of pea proteins pre-unfold are of primary interest, since more available active sites exposure to reactive systems would help stimulate the number of bonds between the amines and carbonyl groups. It has been reported that denatured proteins with more available lysine residues might bind to more carbohydrates than protein in its native state (de Oliveira et al., 2016).

To continue the research regarding dictating pea protein functions via Maillard-driven chemistry, it herein aims to synthesize glyco-protein conjugates in an aqueous system (pH 10.0, 80°C), by employing a handful of saccharides with diverse molecular mass and structural characteristics. It was hypothesized that more numbers of saccharides will be grafted to pea proteins under such reactive conditions, and that the solubility and thermal stability of resultant conjugates get enhanced accordingly.

6.3. Materials and Methods

6.3.1. Extraction of pea protein isolate

Glucose and lactose were purchased from MilliporeSigma (St. Louis, MO, USA). Maltodextrins of three different dextrose equivalents (DE 5, 10, 18) were a gift from Cargill (Minneapolis, MN). The average molecular weight (Mw) of DE 5, 10, 18 is 30,000, 15,000, and 10,000 g/mol, respectively. Pea protein isolate (PPI) was extracted from defatted yellow pea flour (Harvest Innovations LLC, Indianola, Iowa, USA) using isoelectric precipitation techniques as previously described (Boye et al., 2010; Stone, Karalash, Tyler, Warkentin, & Nickerson, 2015). The in-house prepared PPI contained 84.90% protein ($\%N \times 6.25$), ~5.25% moisture, ~4.36% ash, ~4.84% carbohydrate, and 0.65% lipid. All other reagents and chemicals were procured from MilliporeSigma (St. Louis, MO, USA) and were of analytical grade. All chemicals were used as received.

6.3.2. Saccharides-mediated synthesis of glyco-pea protein isolate

Five diverse saccharides were employed in the synthesis, namely, glucose, lactose, and maltodextrin with three different dextrose equivalents (DE 5, 10, or 18). The PPI powder and each individual saccharide were mixed at a mass ratio of 5:1, and then dissolved in carbonate buffer solution (pH 10.0, 10 mM; 1:2, w/v) for 12 h on a stir plate operating at 300 rpm and room temperature (RT, 22 °C) until obtaining relatively homogenous-dispersed mixture. The aim of applying alkaline environment (pH 10.0) was to transform protein molecules into an unfolded state (Cao, Fu, & He, 2007; Gao et al., 2020; Su, Huang, Yuan, Wang, & Li, 2010). Then, 100 mL of dispersion mixture was transferred into a glass jar (200 mL) hermetically sealed, kept continuous stirring, and then placed into an 80 °C pre-heated incubator (Heratherm IMH180, Thermo Fisher Scientific, Inc., USA), where Maillard-driven glycation was carried out. Glyco-PPI with different structure was synthesized depending on a series of conjugation time. The resultant solution was freeze-dried for 48 h (Lyophilizer, SP scientific, Gardiner,

New York), and was named PG, PL, PDE5, PDE10, PDE18 in regard to the applied saccharides, respectively.

6.3.3. Characterization and degree of glycosylated proteins

Color development, Amadori compounds formation, free amino groups, and sodium dodecyl sulphate-polyacrylamide gel electrophoresis (SDS-PAGE) of glyco-PPI were characterized following our previous studies (Zha, Dong, et al., 2019a, 2019b; Zha, Yang, et al., 2019).

6.3.4. Size exclusion-high performance liquid chromatography (SEC-HPLC)

Glyco-PPI (0.10 g) was precisely weighed and dispersed into 10 mL SPB (10 mM, pH 7.0). The resultant solution was incubated for 2 h at RT, centrifuged at 2,000 x g for 30 min, and then filtered through a 0.45 µm nylon filter prior to analysis. The separation of glyco-PPI solution was achieved using an Agilent 1200 HPLC system coupled with a Securityguard™ cartridges (AJ0-4489) and Yarra™ SEC-4000 LC (3µm, 300×7.8 mm; 00H-4514-K0) column (Phenomenex, Torrance, CA, USA). Aliquots of 5 µL were injected into the HPLC system with an Agilent autosampler (G1329A), and eluted using SPB (10 mM, pH 7.0) at a flow rate 0.5 mL/min. Elution from columns was monitored at 280 nm with a DAD detector (Agilent 1315D). The size exclusion chromatographic columns were pre-calibrated with a gel filtration Markers kit (catalog No. MWGF1000, Sigma-Aldrich) containing a set of wide Mw protein standards (29–700 kDa). The number of saccharide molecules (*N*) grafted to a PPI molecule was determined with the following equations (Liu & Zhong, 2013; Zha, Yang, et al., 2019);

$$N = (\overline{M}_{w2} - \overline{M}_{w1}) / \overline{M}_{w3} \quad (6.1)$$

$$\overline{M}_{wi} = [\sum (F_i M_i) / \sum F_i] \quad (6.2)$$

Where \bar{M}_{w1} , \bar{M}_{w2} , and \bar{M}_{w3} is the average molecular mass of PPI, glyco-PPI, and saccharides, respectively; F_i is the proportion of fraction, and M_i is the molecular mass of the fraction.

6.3.5. Relative solubility of glyco-pea protein isolate

Protein solubility was determined by measuring the concentration of soluble protein at pH 7.0 using PierceTM BCA Protein Assay Kit (Thermo Fisher scientific). Protein solubility was expressed as the percentage of the initial PPI concentration.

6.3.6. Differential scanning calorimetry (DSC)

Thermal stability of PPI and glyco-PPI was assessed by DSC Q2000 calorimeter (TA instruments Ltd., New Castle, DE, USA), as previously described with some modifications (Pirestani, Nasirpour, Keramat, Desobry, & Jasniewski, 2018). Briefly, sample (10%, w/v) was dissolved in sodium phosphate buffer (SPB, pH 7.0, 10 mM). The resultant dispersions (10 μ L) were precisely weighed into an aluminum pan, which was hermetically sealed and heated from 25 to 140 °C at the temperature ramping rate of 10 °C/min. Onset temperature (T_{on}), denaturation temperature (T_d), and enthalpy changes of denaturation (ΔH) of each sample were computed with the TA Universal Analysis Program.

6.3.7. Volatile substances in glyco-pea protein isolate

The aromatic profile in glyco-PPI was examined by headspace solid-phase microextraction in combination with gas chromatography coupled with mass spectrometry (HS-SPME-GC-MS), as previously described with some modifications (Zha, Dong, et al., 2019b; Zha, Yang, et al., 2019). Briefly, 1.0 g of sample powder was hydrated with 2 mL SPB (pH 7.0, 10mM) in a 20 mL GC vial capped with PTFE/silicone septa, and subsequently equilibrated for 1 h at RT. The samples were then loaded into an PAL RSI 120 autosampler and incubated at 60 °C for 10 min (CTC Analytics, Zwingen, Switzerland). A 50/30 μ m DVB/CAR/PDMS solid-phase microextraction (SPME) fiber needle (Supelco, Bellefonte, PA)

was applied to adsorb volatiles for 50 min, which was then transferred to the injector port (250 °C) for 3 min desorption in splitless mode. Volatile compounds were separated by a ZB-Wax column (60 m × 0.25 mm × 0.25 μm, Agilent) on an Agilent GC 7697A. The MS profile was recorded utilizing an Agilent MSD 5977A (Agilent, Palo Alto, CA) in the electron impact mode (EI) at 230°C and 70 eV, scanning from m/z 28 to 350.

6.3.8. Statistical analysis

All measurements were conducted with triplicate samples unless otherwise specified, and values were shown as means ± SD of triplicates from each of two independent experiments. One-way analysis of variance (ANOVA) was performed by SAS software (version 9.4, SAS institute Inc. Cary, NC), and the differences between means were assessed using Tukey's test with a significance level of $p < 0.05$.

6.4. Results and Discussion

6.4.1. Characterization of formation and conjugation extent in glyco-PPI

Non-enzymatic color development, non-specific markers of Maillard-driven chemistry, SDS-PAGE and available amino groups were employed to validate the formation of glyco-PPI and glycation extent, respectively (**Fig. 6.1**).

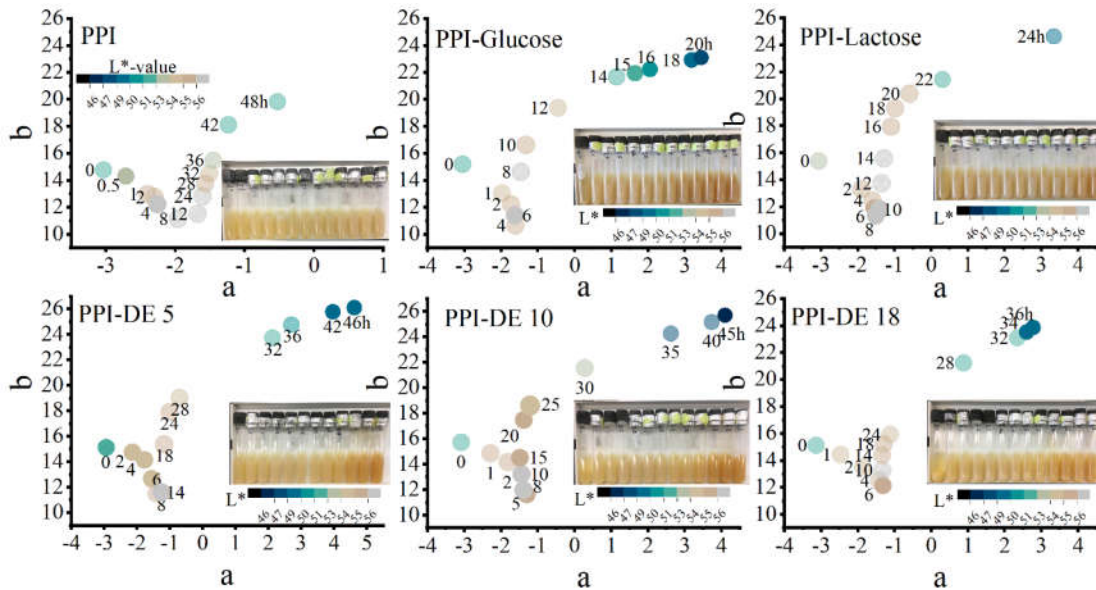


Figure 6.1. Color development in samples incubated for various time, where a and b-value mean redness and yellowness, respectively. The bubble size and color map is related to the lightness (L^*) value; PPI and DE 5, 10, 18 represent pea protein isolate and Maltodextrin DE5, 10, 18, respectively.

Color is normally served as an organoleptic characteristic and is associated with hedonic responses by the consumer (Bustos, Rocha-Parra, Sampedro, De Pascual-Teresa, & León, 2018; Delgado-Andrade, Morales, Seiquer, & Pilar Navarro, 2010). CIE $L^*a^*b^*$ parameters, including L^* (+luminosity), a^* (+redness) and b^* -value (+yellowness), were utilized to quantify the visual color of glyco-PPI so as to indirectly reflect the course of Maillard-driven chemistry (Zha, Yang, et al., 2019). Statistical analysis revealed that the heat-induced color development of glyco-PPI was not only reaction time dependent ($p < 0.001$), it was also affected by the components of the reactants as well as their interactions. Apparently, the a^* -value detected in the reactants slowly rose in the beginning, which was surprisingly kept relative constant in a short window ($\approx 6\text{--}10$ h), but continued to increase throughout the incubation (**Fig. 6.1**). The L^* value of all the samples was subjected to a similar pattern in which it started with an uptick and then dropped after a period of incubation time; yet the b^* -value displayed a completely reverse trend, albeit the turning-point varied in different saccharides-containing systems (**Fig. 6.1**).

Schematic illustration of the macroscopic kinetic phenomena including three different phases was presented in **Figure 6.2**, namely, denaturation, Maillard reaction, and crosslinking of protein. It is of note that three-dimensional secondary to quaternary architectures of native proteins generally were stabilized by supramolecular interactions, such as hydrogen bonds, ionic, van der Waals, and hydrophobic interactions, with the exception of disulfide bonds and peptide bonds (Silva et al., 2014). These non-covalent bonds responsible for the folding of protein structures could be actively influenced by several elements like temperature, pH, and organic solvents (Silva et al., 2014). The alterations in protein architectures would take place as their exposure to specified conditions assigned for denaturation, where only the primary structure constructed through peptide bonds still remained unchanged (Silva et al., 2014). Herein, 80°C, which is close to the thermal denaturation temperature of PPI ($\approx 84^\circ\text{C}$), and pH 10.0 were applied to achieve the protein expanding and unfolding state ($\approx 8\text{h}$). As a result, more potential active side chain residues, such as lysine (pKa 10.67), arginine (pKa 12.10), and histidine (pKa 6.04) residues, were exposed to environment. Two possible routes followed by the denaturation step were proposed, i.e., Maillard reaction (MR) and protein crosslinking. It was speculated that Maillard-driven reaction dominated the molecular interactions in the saccharides-containing system, while protein crosslinking was major in PPI alone even though MR also occurred in such aqueous systems. This can be verified by observing development of browning color after critical time point ($\sim 8\text{h}$) in real product photos, which implied the presence of saccharides participating in Maillard-driven reaction with PPI.

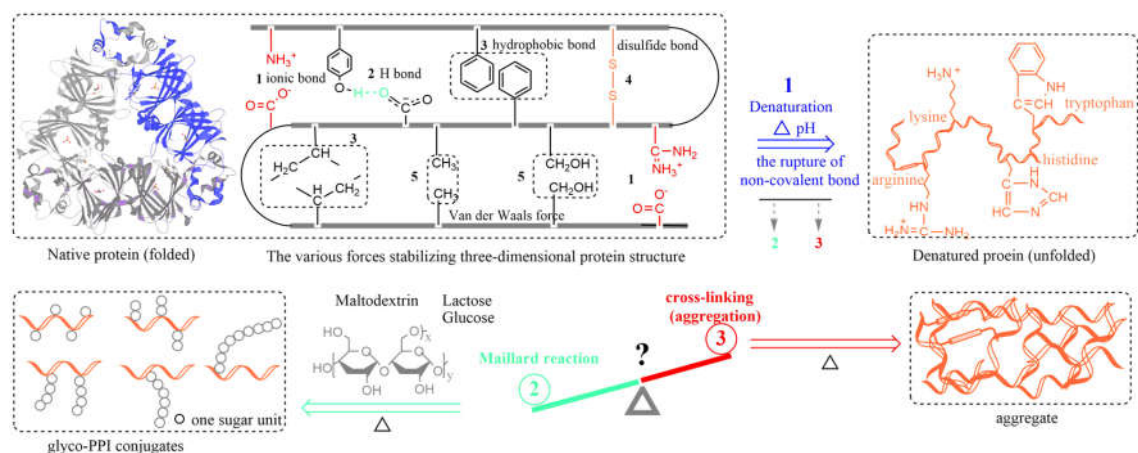


Figure 6.2. Schematic illustration of heat induced pea protein isolate denaturation and aggregation and of the Maillard-driven glycation reaction.

The absorbance of resultant products at 304 nm (**Fig. 6.3**), turned out to be a non-specific marker of Maillard-driven reaction, served to characterize the formation of glyco-PPI and reaction extent as it accords with the development of Amadori compounds (Zha, Dong, et al., 2019b; Zha, Yang, et al., 2019). The Ab_{304nm} of all heated samples increased continuously ($p < 0.05$), and then gradually leveled off with the extension of incubation time. The results clearly showed the higher Ab_{304nm} obtained in the cases of PPI heated in the presence of glucose, lactose, and maltodextrin DE5, 10, 18, compared to PPI alone. These kinetic curves also indicated that the development rate of Amadori compounds in all glycosylated proteins complied with the sequences: $Glu > Lac > DE18 > DE10 > DE5$, which were consistent with the rule of color development. A proven track record that a higher rate constant value for the loss of lysine in casein-glucose models was statistically calculated compared to that in lactose-containing system (Naranjo, Gonzales, Leiva, & Malec, 2013). In light of the maltodextrins with various DE, the higher DE value signified more active carbonyl groups were available in MR. Laroque et al. (2008) noted reducing sugars with less steric hindrance and higher proportion of acyclic form enhanced the sugar reactivity, further positively impacting the kinetics of MR. Stationary point of each reaction system can be extrapolated on the basis of the

plotted kinetic curves (**Fig. 6.3**), which was 12 h for glucose and lactose, and 24 h for maltodextrins, respectively.

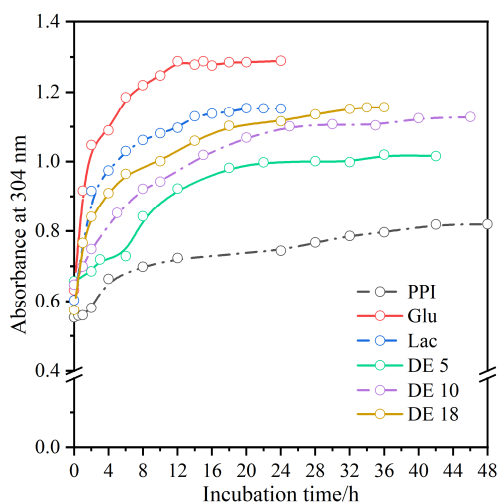


Figure 6.3. Changes in absorbance at 304 nm in the mixture of PPI and diverse saccharides reacted at 80°C, which is associated with Amadori compounds development. PPI, pea protein isolate; Glu, glucose; Lac, lactose; DE 5, 10, 18 are maltodextrin DE 5, 10, 18, respectively.

To further elucidate the development of glyco-PPI, SDS-PAGE (**Fig. 6.4**) was employed to examine molecular weight changes of the resultant products at selected incubation time. Pea proteins primarily are composed of 2S albumin (ca. 20%) and globulins (ca. 70%), i.e., 11S legumin and 7S vicilin/convicilin (Chéreau et al., 2016; Messin et al., 2013). The 2S albumin (**Fig. 6.4-left, lane 1**), as one characteristic band of PPI consisting of two polypeptide chains (light ca. 4.5 kDa and heavy ca. 10 kDa), are compact globular proteins with conserved cysteine residues (Chéreau et al., 2016). In addition, one subunit of convicilin (ca. 72.4 kDa), three (ca. 47.5, 33.3, 28.7 kDa) subunits of 7S vicilin, as well as one acidic (ca. 40 kDa) and one basic (ca. 19–23 kDa) polypeptide assembling one monomer of 11S legumin were detected in lane 1 (Chéreau et al., 2016; Lam et al., 2018; Zha, Dong, et al., 2019b; Zha, Yang, et al., 2019). The band with Mw of about 94 kDa was deemed as lipoxygenase (LOX, lane 1), which has already been characterized from pea seeds (Szymanowska, Jakubczyk, Baraniak, & Kur, 2009; Zha, Dong, et al., 2019b). Lipoxygenase is closely associated with the formation of beany flavors in plant-based proteins, glycosylating PPI with saccharides appeared to eliminate LOX as

displayed by the vanishing of LOX band. Our earlier studies revealed that the 11S/7S globulin and 2S albumin mainly engaged in the glycation of pea proteins with gum Arabic under dry heating conditions (Zha, Dong, et al., 2019a; Zha, Yang, et al., 2019). Apart from the above-mentioned protein constituents, convicilin herein, was also involved in the glycation which was corroborated by the fading convicilin band in such an aqueous system. A newly emerged characteristic band in proximity to the loading boundary of the gel was noticed (**Fig. 6.4, left, lanes 4–7; right, lanes 4–9**), which corresponded to the heated PPI in the presence of various saccharides at different conjugation time. It was speculated that this band was the glyco-PPI (> 250 kDa) that formed via Maillard-driven chemistry. Interestingly, a similar newly formed band in heated PPI alone for 24h (**Fig. 6.4, right, lane1**) was also observed. This may be attributed to the aggregation of denatured proteins, resulting in the development of high Mw crosslinked polymers. It seems to again confirm that the schematic illustration of potential reaction routes of denatured PPI that was proposed above. Still there is a possibility that the formation of glyco-PPI was concomitant with protein cross-linking in the mixture of PPI and saccharide after 24h incubation, although the latter may have less potency. But one thing is certain, that is, the glyco-PPI was inevitably produced, which can be mutually authenticated through color development.

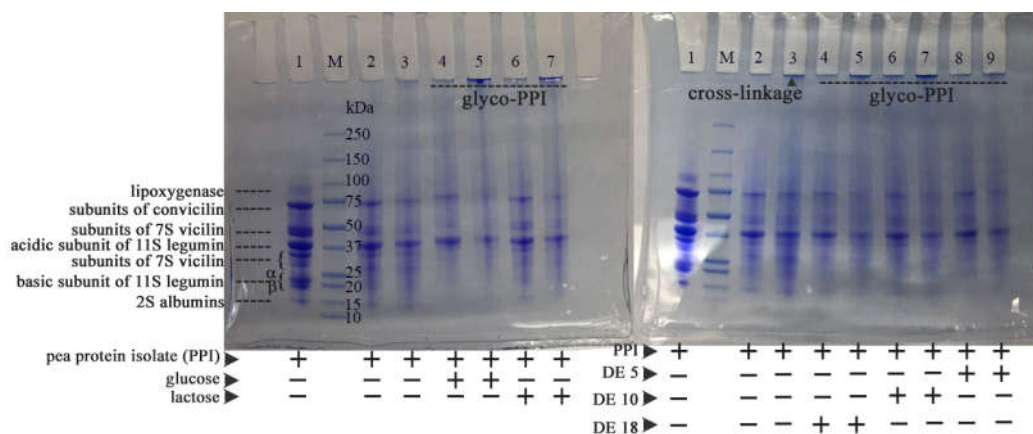


Figure 6.4. SDS-PAGE patterns for different glyco-PPI. Lane M for protein markers; lanes 1-7 of left figure are PPI-0 hour, PPI-6 hour, PPI-12 hour, PPI-glucose-6 hour, PPI-glucose-12 hour, PPI-lactose-6 hour, and PPI-lactose-12 hour, respectively; Lanes 1-9 of right figure are PPI-0 hour, PPI-12 hour, PPI-24 hour, PPI-DE 5-12 hour, PPI-DE 5-24 hour, PPI-DE 10-12 hour, PPI-DE 10-24 hour, PPI-DE 18-12 hour and PPI-DE 18-24 hour, respectively; The “+ & -” mean “included and non-included” respectively; glyco-PPI indicates the conjugates that pea protein isolate (PPI) glycosylated with diverse saccharides.

In order to reconfirm the hypothesis, available amino groups were analyzed to determine the extent of glycation (Fig. 6.5). The degree of covalently conjugated protein with saccharides remarkably influenced the functionality of glycoproteins (Zha, Yang, et al., 2019). In PPI-saccharides system, available free amino groups were reduced substantially after conjugating for 12 and 24h, respectively. It was clear that glucose-glycated PPI gave the highest reduction (~59.6%) after 12h conjugation when compared to that of other saccharide-containing systems. The results were in line with the kinetic analysis at Ab304nm involving the development of Amadori compounds. Assuming that protein crosslinking dominated the reaction process in saccharides-containing system, almost the same amount of available free amino groups should be blocked in heated PPI alone compared to that in PPI-saccharides systems. However, the opposite was observed. The depleted available amino groups in PPI alone (~14.7%) were far less than that in glyco-PPI, and the blocked amino groups in PPI-DE 5, 10, 18 were about 33%, 38%, and 45%, respectively, after 24h incubation. It was thus concluded that the grafting of various saccharides to PPI via Maillard-driven chemistry was responsible for the major decline of free amino groups in glycoproteins.

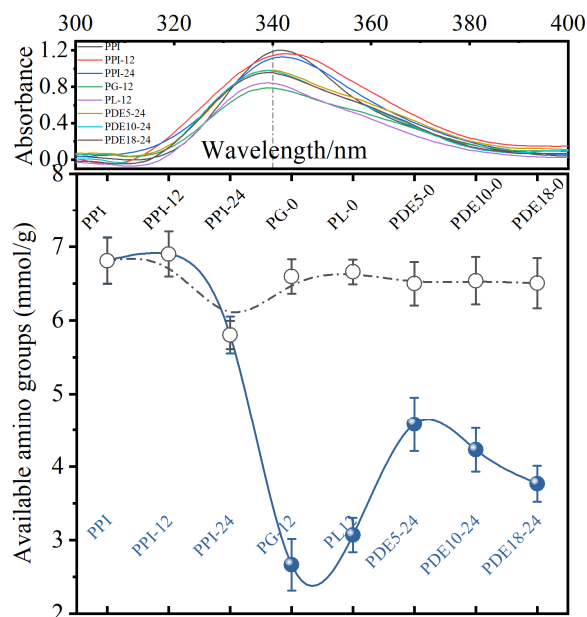


Figure 6.5. Changes of free amino groups as a function of reaction time during glycation of PPI with saccharides at 80°C. PPI, pea protein isolate; PG, PPI and Glucose; PL, PPI and Lactose; PDE5, 10, 18 are PPI and maltodextrin DE 5, 10, 18, respectively; the number behind “-” means incubation time (hour).

6.4.2. Molecular parameters of glyco-pea protein isolate

SEC-HPLC elution profiles of glyco-PPI prepared with diverse saccharides are shown in **Figure 6.6**, and the computed specific molecular parameters was presented in **Table 6.1** using the typical calibration curve in **Figure 6.7**.

The SEC elution profiles of all samples were approximately divided into ten fractions. Fraction-1 in PPI-saccharides systems was attributed to glyco-PPI identified in SDS-PAGE pattern. Apparently, the fraction-2 which was exclusively discovered in PPI, was primarily responsible for the conjugation with diverse saccharides via Maillard-driven chemistry. Although fraction-1 occurred in PPI-12 and PPI-24, protein crosslinking, as aforementioned, would be scarce in heated PPI when various saccharide was presented. Thus, it was speculated that Maillard reaction (carbohydrate residues exist in PPI) and protein crosslinking collectively contributed to its emerging in heated PPI alone.

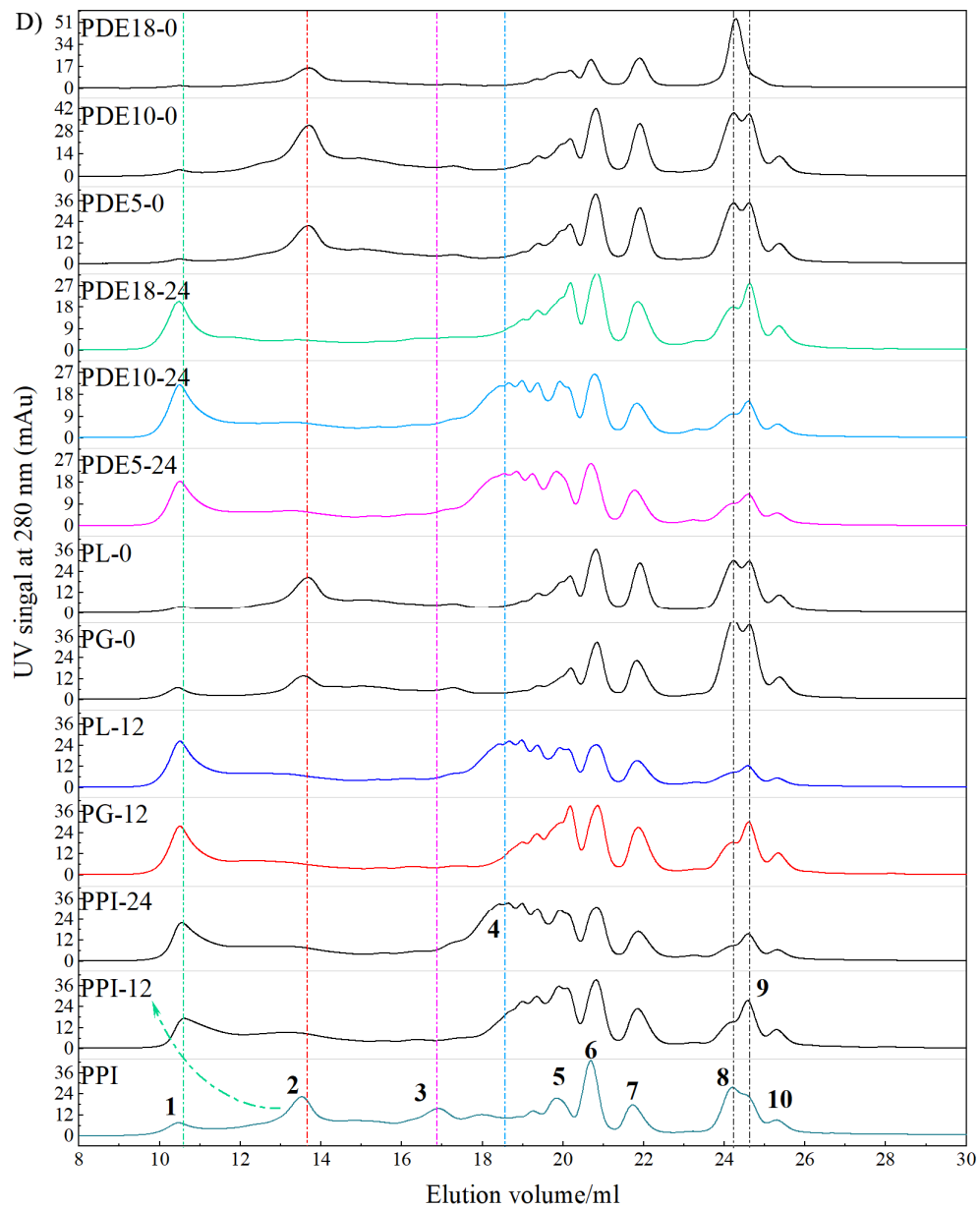


Figure 6.6. The elution profiles monitored by UV at 280 nm for a range of selected samples, characterized by a size-exclusion chromatography (SEC-HPLC). PPI, pea protein isolate; PG, PPI and Glucose; PL, PPI and Lactose; PDE5, 10, 18 are PPI and maltodextrin DE 5, 10, 18, respectively; the number behind “-” means incubation time (hour).

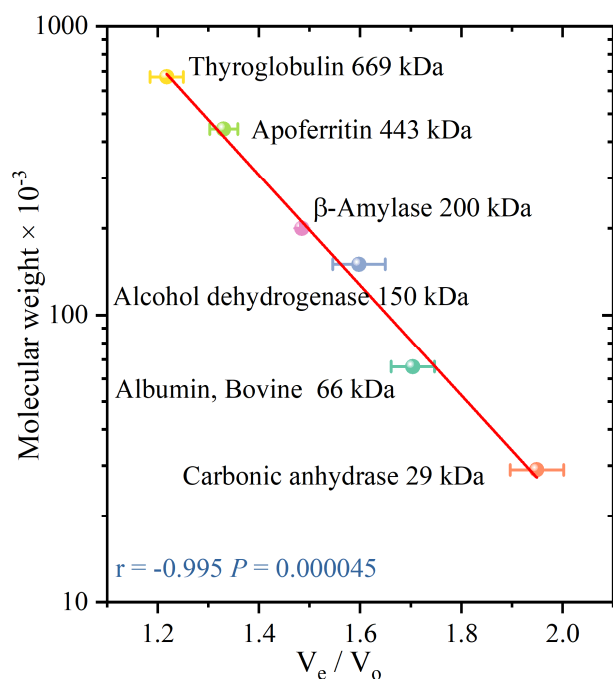


Figure 6.7. Typical calibration curve obtained with proteins from the MWGF1000 Kit run on Yarra™ SEC-4000 LC column; V_e and V_o mean elution volume and void volume, respectively.

To better analyze the constituents in each fraction corresponding to the pea protein architectures, it should be noted that the theoretical Mw of hexameric 11S legumin, trimeric 7S vicilin, and 2S albumin would be 336 ($\sim 6 \times 56$), 156 ($\sim 3 \times 52$), and 15 kDa, respectively (Mession et al., 2013; Tandang-Silvas, Tecson-Mendoza, Mikami, Utsumi, & Maruyama, 2011; Zha, Yang, et al., 2019). The Mw of each fraction was calculated based on the calibration curve, and the relative content of each fraction was statistically computed providing the total spectrum integrated area was 100% (**Table 6.1**).

Table 6.1. Percentage of integrated area from SEC-HPLC spectra at 280 nm, of glyco-PPI conjugates incubated in an aqueous system (80°C, pH 10.0).

Elution volume (ml)	10.47-10.55	13.48	16.91	17.98-19.25	19.83-20.16	20.68	21.72	24.19	24.61	25.29
\bar{M}_w (kDa)	> 669	669-29				< 29				
Protein fraction (n)	1	2	3	4	5	6	7	8	9	10
Sample	Relative percentage of protein fraction (%)									
PPI	4.09	15.02	5.98	3.47	9.20	20.44	9.33	27.73		4.76
PPI-12	16.07			26.40	9.77	14.18	9.79		20.36	3.41
PPI-24	19.19			28.05	12.42	13.71	10.31		12.39	3.94
PG-0	1.56	8.53			10.88	14.12	10.56	27.59	20.09	6.66
PG-12	41.42			19.09	7.44	12.40	9.52		8.79	1.32
PL-0	1.85	14.44		5.05	12.66	17.37	13.13	17.39	14.56	5.41
PL-12	33.37			18.84	8.50	14.89	11.72		11.13	1.55
PDE5-0	1.01	14.50		4.32	11.94	17.01	13.04	18.33	15.40	5.45
PDE5-24	20.21			33.95	13.77	12.12	8.11		10.48	1.36
PDE10-0	1.17	18.76		4.02	10.64	15.55	11.65	18.22	14.84	5.16
PDE10-24	21.23			30.24	13.09	12.66	8.46		12.77	1.57
PDE18-0	0.99	15.13		4.01	18.06	13.77	17.41	30.76		
PDE18-24	25.48			10.48	18.46	15.90	13.25		14.95	1.48

¹ Protein relative fraction (%) was calculated by the ratio with the total integrated area (summed fractions taken as 100%).

² Number (no.) corresponds to the elution order by SEC-HPLC analysis in Figure 6.6;

³ PPI, pea protein isolate; PG, PPI and Glucose; PL, PPI and Lactose; PDE5, 10, 18 are PPI and maltodextrin DE 5, 10, 18, respectively; the number behind “-” means incubation time (hour).

⁴ The results that beyond the range of linear curve ($M_w \sim 669\text{-}29$ kDa) are only for reference.

The elution volume of fraction-2 was approximate 13.48 mL and statistically calculated Mw was 491.8 kDa. Interestingly, this seemed not to match with any individual protein constituent like 7S/11S globulins. In fact, it was deduced that 11S legumin and 7S vicilin (total Mw~492 kDa) of native PPI were collectively responsible for fraction-2. And the outcomes in SDS-PAGE pattern also indicated that 11S/7S globulin and 2S albumin of pea protein were mainly engaged in the glycation with various saccharide, which appeared to indirectly prove this hypothesis. Additionally, Mession et al also noted that legumin and vicilin of pea proteins coeluted in SEC-HPLC elution profiles (Mession et al., 2013). As for the elution fraction-4 of native PPI (Mw~ 73.3–42.8 kDa), it was speculated that the fraction contained the subunits of convicilin, which have been characterized by SDS-PAGE pattern. Analogously, fraction-5, 6, and 7 of native PPI was attributed to the subunits of 7S vicilin, basic subunit of 11S legumin, and 2S albumin, respectively, which was consistent with the characteristic bands in SDS-PAGE.

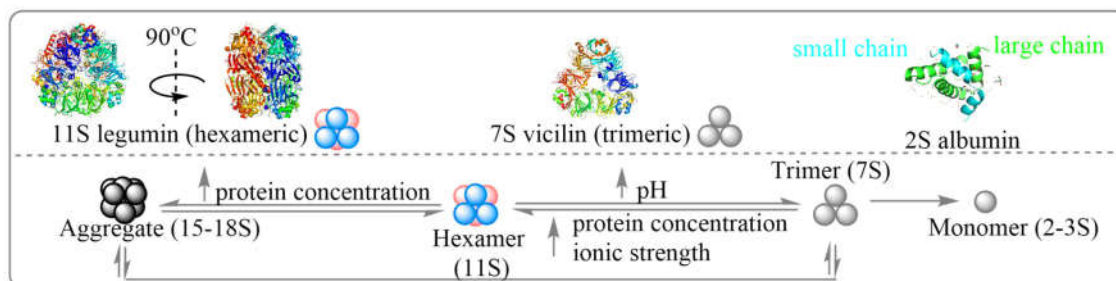


Figure 6.8. Schematic ribbon diagram of the 11S globulin (PDB entry: 3FZ3); 7S globulin-1 (PDB entry: 2EA7), and 2S albumin (PDB entry: 6S3F), and the association-dissociation phenomena of legumin- and vicilin-type globulins.

The elution profiles of native PPI could be closely involved in the association–disassociation phenomena of pea protein (**Fig. 6.8**). The reversible and irreversible associated–dissociation phenomena of 7S vicilin and 11S legumin quaternary conformation could be modulated by protein concentration, ionic strength and pH (González-Pérez & Arellano, 2009; Murthy & Rao, 1984; Schwenke & Linow, 1982). That rendered their complexity of isolation and characterization. Most 7S globulins originated from plant seeds

could associate into larger Mw aggregates (9–12S) at a low ionic strength ($I = 0.1$ M) (González-Pérez & Arellano, 2009). It was also reported that dissociation of 11S globulin from soybean into 7S globulin when the I was lowered from 0.5 to below 0.1 M at a neutral pH (González-Pérez & Arellano, 2009) and the 7S globulin can be reversibly dissociated into a 2–3s and 5–6s fraction under certain conditions (pH 2–5, $I < 0.1$ M) (González-Pérez & Arellano, 2009). Actually, the non-covalent interactions among these subunits (i.e. hydrogen bonds, electrostatic, hydrophobic, and van der Waals), dominate such association–dissociation state of proteins. What is noteworthy is that the number of saccharide molecules (glucose, lactose, and maltodextrin DE5, 10, 18) grafted to each PPI molecule via Maillard-driven chemistry was approximately 4.5, 3.7, 2.1, 2.3 and 2.8, respectively, according to **Eq. 6.1 & 6.2**. It was of note that the particular characteristics of saccharides, like molecular mass and structural characteristics that are highly associated with steric hindrance and reactivity, would determine the number of saccharides attached to PPI (de Oliveira et al., 2016; Oliver et al., 2006).

6.4.3. Solubility and thermal stability of glyco-pea protein isolate

Alterations in protein architectures necessarily impact its functionalities (Tandang-Silvas et al., 2011). Inferior solubility of pea proteins has blocked its application for biomedical and pharmaceutical purposes. Therefore, the solubility of PPI and conjugates by glycosylating PPI with different saccharides was examined (**Fig. 6.9**).

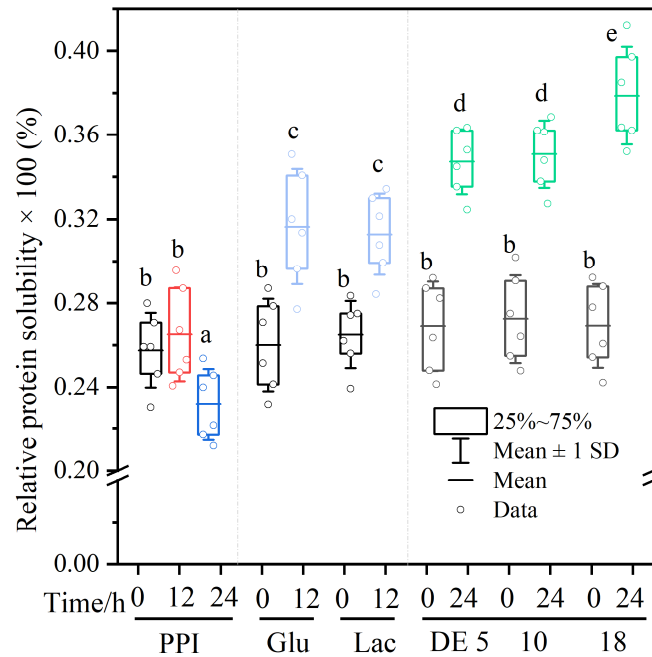


Figure 6.9. Relative protein solubility of different glyco-PPI conjugates at 12 and 24 hour (n = 6), respectively, at neutral pH (7.0). Different letters indicated significance at $p < 0.05$.

No statistically significant difference was obtained between solubility of PPI–saccharides physical mixture and that of PPI itself ($p > 0.05$), suggesting that physical molecular interactions between PPI and various saccharides did not affect the solubility at a neutral pH. A slight increase in solubility was exhibited as PPI was incubated alone for 12h, even if not significant, which may be ascribed to the partial denaturation of PPI (Kester & Richardson, 1984). A significant decrease ($p < 0.05$) was observed when PPI alone was subjected to 24h incubation compared to native PPI. These results are reasonable since complete denaturation induces the exposure of more buried hydrophobic residues and enhances protein–protein interactions that usually result in a loss of solubility (Kester & Richardson, 1984). In the case of glyco-PPI solubility, a consistent incremental trend was obtained as PPI glycosylated with various saccharides for 12h and 24h. Maltodextrin seemed to exert a greater positive impact on the protein solubility than that of glucose and lactose, especially, DE18–PPI conjugates which gave rise to the maximum increment in solubility from 25.7% to 37.8%. It was thus deduced that molecular mass of saccharides and the number of saccharides covalently

attached to PPI synergistically determined the solubility of glycated protein. Protein solubility usually depends on the balance between hydrophobic–hydrophilic groups on the protein surfaces (Yin, Tang, Wen, Yang, & Yuan, 2010). The enhanced protein solubility of glyco-PPI can be attributed to the introduced hydrophilic saccharide groups and its steric hindrance, which restrained the protein–protein interactions. In addition, glycation via Maillard-driven chemistry would loosen the protein structures, facilitating protein–water interactions (Zha, Dong, et al., 2019b).

Thermal behavior of glyco-PPI was examined by DSC at 10 °C/min temperature ramping rate (**Fig. 6.10**), and the thermal parameters were shown in **Table 6.2**. T_{on} and T_d provide critical information on heat-induced protein unfolding and protein thermal stability, respectively. The enthalpy changes (ΔH) respond to the energy requirement for the ordered structure of proteins to be transformed from native compact architectures to an unfold state. The measured T_{on} and T_d values of PPI were about 78°C and 85°C, respectively, implying that the set experimental temperature (80°C) would gradually unfold pea protein architectures. Thermograms exhibited only one broad endothermic peak, which was in accordance with the overlapping denaturation of 7S/11S globulin and 2S albumin fractions (Mession et al., 2013). In terms of heated PPI alone, it was found that T_{on} and T_d of PPI-12 & PPI-24 significantly decreased ($p < 0.05$). By contrast, it was observed a significant increment in T_{on} and T_d values of PPI–saccharides mixtures compared to that of native PPI ($p < 0.05$), which implied that the physical mixture appeared to interfere with the process of protein unfolding. Furthermore, maltodextrins were more capable of enhancing the thermal stability of PPI than glucose and lactose. The thermograms of glyco-PPI demonstrated a flat line (**Fig. 6.10**), which was in agreement with the previously reported results of conjugating whey protein isolate with dextran in aqueous solution (Zhu, Damodaran, & Lucey, 2010). This is because that glycation via Maillard-driven chemistry caused the PPI to unfold and expand (Zhu et al., 2010). It was noted

that glycation of β -lactoglobulin with ribose or arabinose rendered the protein with extensive unfolding as verified by non-thermal transition in DSC thermograms of the conjugates (Chevalier, Chobert, Dalgalarondo, Choiset, & Haertlé, 2002). Likewise, Hattori et al. noticed that the ΔH for β -lactoglobulin–carboxymethyl dextran conjugates decreased to $\sim 40\%$ compared to that for β -lactoglobulin alone (Hattori, Nagasawa, Ametani, Kaminogawa, & Takahashi, 1994). That was attributed to a decline in the level of secondary structure in β -lactoglobulin as a consequence of glycation with dextran.

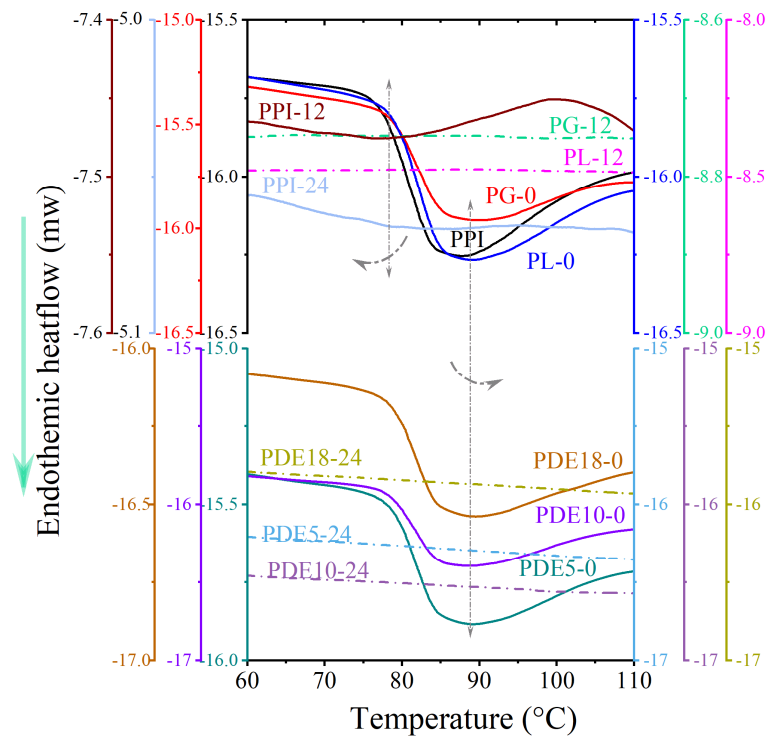


Figure 6.10. DSC thermograms of glyco-PPI conjugates incubating pea protein isolate with diverse saccharides at a scan rate $10^{\circ}\text{C}/\text{min}$.

Table 6.2. Thermal parameters of various heat-treated glyco-PPI conjugates (n = 3)

sample	Heating Rate 10°C/min		
	T_{on} (°C)	T_d (°C)	ΔH (J/g protein)
PPI	78.37 ± 0.06c	84.94 ± 0.10c	9.08 ± 0.12c
PPI-12	62.22 ± 0.02b	78.53 ± 0.12b	1.47 ± 0.10b
PPI-24	61.45 ± 0.01a	76.37 ± 0.08a	0.86 ± 0.05a
PG-0	78.89 ± 0.01d	86.32 ± 0.10d	9.24 ± 0.20d
PL-0	79.05 ± 0.02d	86.59 ± 0.10d	9.46 ± 0.10d
PDE5-0	79.24 ± 0.03f	87.67 ± 0.10f	10.4 ± 0.20f
PDE10-0	79.19 ± 0.02ef	87.42 ± 0.15ef	9.86 ± 0.22ef
PDE18-0	79.14 ± 0.02e	87.22 ± 0.05e	9.64 ± 0.09e
Glyco-PPI	not determined		

¹ T_{on} , onset temperature; T_d , denaturation temperature; ΔH , enthalpy of denaturation

² PPI, pea protein isolate; PG, PPI and Glucose; PL, PPI and Lactose; PDE5, 10, 18 are PPI and maltodextrin DE 5, 10, 18, respectively; the number behind “-” means reaction time (hour).

³ Glyco-PPI indicated that the conjugates of pea protein isolate glycosylated with five diverse saccharides, glucose, lactose, maltodextrin DE 5, 10, 18. The detail can follow the Figure 2(B).

⁴ Different lowercases in a column present significant difference at $p < 0.05$.

6.4.4. Volatile substances in glycoprotein

The volatiles in native PPI and glyco-PPI were identified using HS-SPME-GC-MS, and the elution profiles of volatile substrates were shown in **Figure 6.11**. These results clearly showed a relatively decline in the abundance of volatiles presented in elution spectrum of glyco-PPI compared to native PPI. A total of 82 flavor substrates were isolated and identified, including 10 alcohols, 22 aldehydes, 16 ketones, 5 acids, 5 esters, 5 furan, 9 hydrocarbons, 7 N-containing compounds and 3 phenols. Arithmetically, aldehydes were the most abundant chemical category accounting for 27% of total volatiles.

Roughly, the abundance and number of volatile compounds detected in various saccharides were far less than any conjugates. Among the flavor constituents identified in PPI, hexanal, 2-pentylfuran, octanal, 1-octen-3-ol, and acetophenone were associated with the off-flavor of PPI, which stem from the degradative oxidation of unsaturated fatty acids by lipoxygenase catalysis (Kobayashi, Tsuda, Hirata, Kubota, & Kitamura, 1995; Samoto, Miyazaki, Kanamori, Akasaka, & Kawamura, 2005). Some volatiles such as ketones, Strecker aldehydes and N-containing compounds were originated from Maillard-driven chemistry, and

served as characteristic contributors to the aroma of resultant products identified in glyco-PPI (Zha, Yang, et al., 2019). Pyrazine derivatives, tagged as baked cereal products notes, roast and meat-like odorants, could give a markedly effect on the organoleptic quality of protein-based foodstuffs (Zha, Yang, et al., 2019). These compounds could serve as characteristic flavor precursors depicting a “fingerprint” of Maillard-driven chemistry (Zha, Yang, et al., 2019).

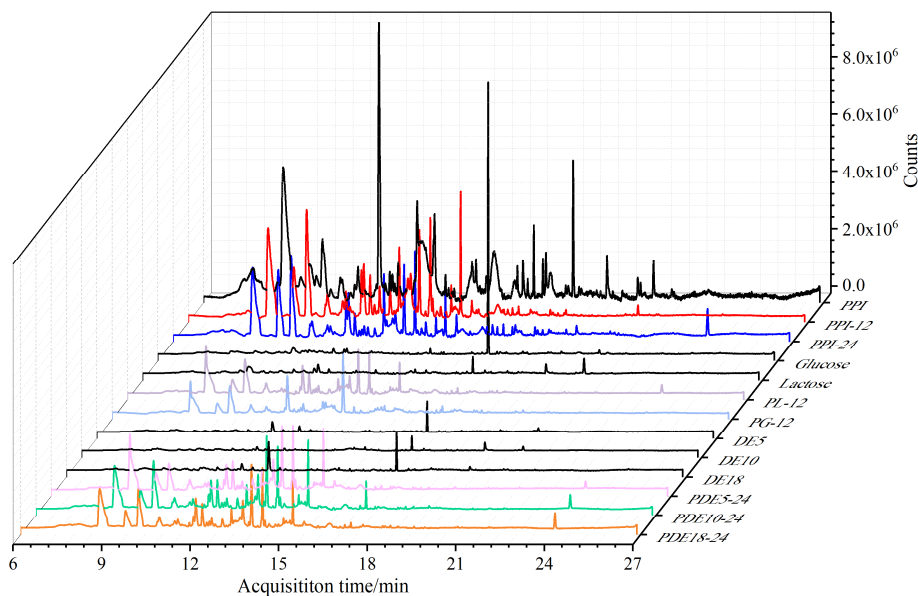


Figure 6.11. Gas chromatograms of a set of selected samples.

The differences in volatile flavor profile between PPI and the conjugates achieved via Maillard-driven glycation of PPI with various saccharides were analyzed by hierarchical cluster analysis (HCA) and principal component analysis (PCA), where the abundance of volatiles was normalized employing E-2-octenal as an internal standard (**Fig. 6.12&6.13**). HCA analysis of 82 volatiles clustered various samples based on their similarities. Apparently, the examined samples were divided into two prime clusters: saccharides alone and PPI-containing systems, the latter of which was further divided into two groups: PPI alone and glyco-PPI. The heat map indicated that most of the variations among different reaction systems were derived from volatiles in cluster 2 & 3 for PPI-containing systems and in cluster 1 for saccharides.

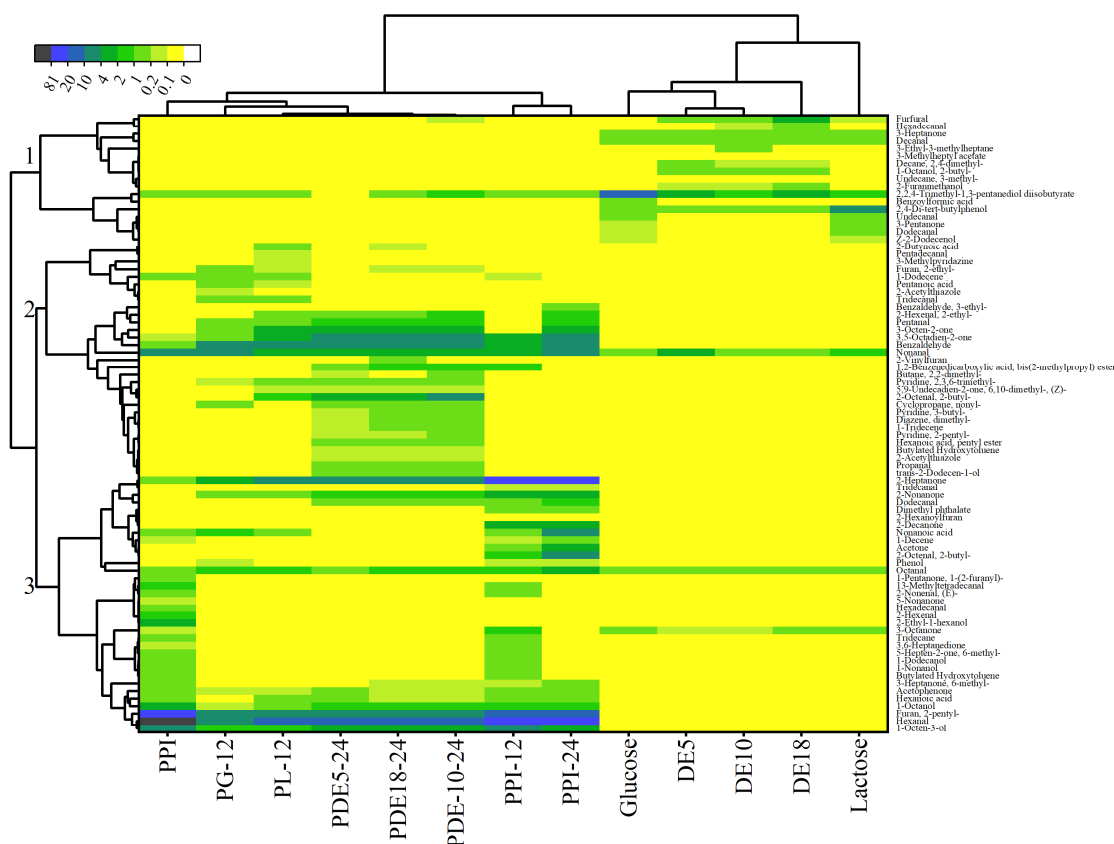


Figure 6.12. Hierarchical cluster analysis and heat map of various glyco-PPI conjugates. The color map indicated the level of identified volatiles

As shown in PCA score plot (**Fig. 6.13A**), two significant principal components PC1 and PC2 accounted for 29.04 % and 23.27% of the total variation, respectively. According to the relative position of samples located in the plane of PC1 and PC2, glyco-PPI generated via Maillard-driven chemistry can be grouped into a category, whereas native PPI and PPI incubated alone for 12h & 24 h belonged to another group. The results were in line with that of HCA analysis. Both native PPI and PPI incubated alone for 12h & 24h located in the positive part of PC2. They were evidently differentiated with saccharides and glyco-PPI that resided in the negative part of PC2. The aromatic profile differences between saccharides and glyco-PPI were definitely visualized by PC1. Accordingly, as shown in **Figure 6.13B**, aldehydes (B3, 7, 13–15, 19, 21), furans (F3, 4), and N-containing compounds (H2, 3, 4, 5, 6) were the main eigenvectors that contributed to the volatiles in glyco-PPI.

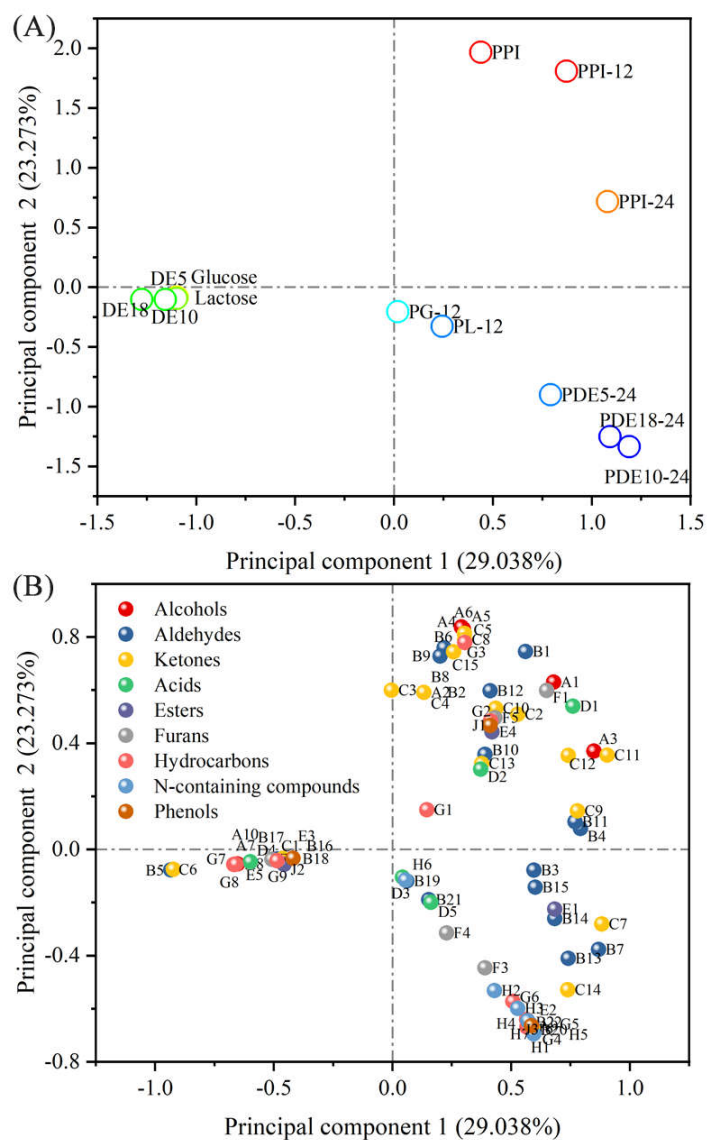


Figure 6.13. Principal component analysis (PCA) (A) loading plot (B) score plot of identified flavor compositions in different glyco-PPI. Note: PPI, pea protein isolate; PG, PPI and Glucose; PL, PPI and Lactose; PDE5, 10, 18 are PPI and maltodextrin DE 5, 10, 18, respectively; the number behind “-” means incubation time (hour).

In order to examine the impact of glycation between PPI and various saccharides on distinct beany odor mitigation, five characteristic markers detected from PPI and identified from pea sensory study (Bott & Chambers IV, 2006) were quantified (Fig. 6.14).

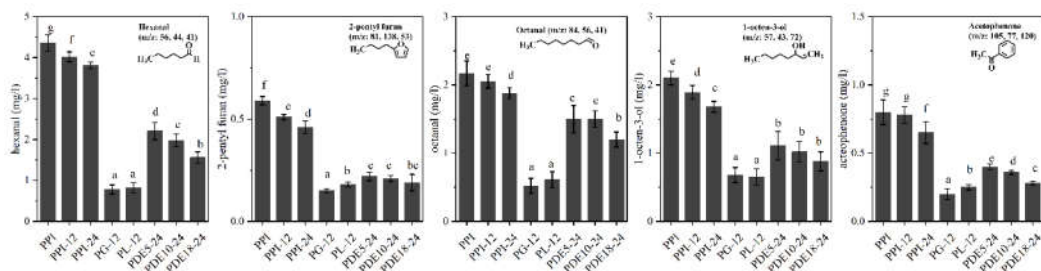


Figure 6.14. The level of selected off-flavor volatiles in various heat-treated glyco-PPI conjugates (n = 3). Note: Different letters indicated significant at $p < 0.05$; Volatiles are identified by mass spectrum comparison with NIST 14 library, reference standards, and retention index comparison with NIST database; limit of quantitation (LOD) ≈ 0.016 - 0.025 mg/l; relative standard deviation (RSD) ≈ 1.12 - 6.24% ; and recovery ≈ 91.8 - 96.0% .

According to the qualitative analyses performed, the initial concentration of these identified volatiles followed the order: hexanal (4.4 ppm) > octanal (2.2 ppm) > 1-octen-3-ol (2.1 ppm) > acetophenone (0.8 ppm) > 2-pentylfuran (0.6 ppm). Previously, John (2010) reported that these volatiles were major flavor-active components as all of their odor activity value (OAV) was above 1 on the basis of the thresholds of these volatiles (40–164 ppb). Upon glycation between PPI and various saccharides, the level of these selected markers in glyco-PPI diminished remarkably ($p < 0.05$), and it seemed that glucose and lactose imposed a greater impact on the mitigation of these beany odors compared to maltodextrins, presumably because of their stronger extent of glycation. The mitigation of beany odor in PPI after glycation with various saccharides may be due to the reoriented structure and altered conformation of PPI that facilitated the release of off-flavors it is tightly bond with (Zha, Yang, et al., 2019).

6.5. Conclusion

Pre-unfolding protein structure under set certain conditions can facilitate covalent bonding of saccharides to protein. The extent of denaturation should be strictly monitored by controlling incubation time for fear of the occurrence of protein aggregation. The development of glyco-PPI was characterized by SDS-PAGE, and both the absorbance (304 nm) of non-specific Maillard-driven reaction markers and the available free amino groups in glyco-PPI was found to predict the degree of conjugation. SEC-HPLC indicated that the number of

glucose, lactose, and maltodextrin DE5, DE10, DE18 grafted to 1 mole of PPI in an aqueous system (80°C, pH 10.0) was approximately 4.5, 3.7, 2.1, 2.3, and 2.8, respectively. The molecular mass and structural characteristics of saccharides and the number of saccharides attached to protein synergistically modulated protein function. The solubility of glyco-PPI was sufficiently improved after glycation, while thermal stability was lowered. The pyrazines aromatic components associated with Maillard-driven reaction were identified in glyco-PPI via HS-SPME-GC-MS. A remarkable beany flavor mitigation effect was also recorded after glycation, especially for glucose mediated Maillard reaction.

6.6. References

- Bott, L., & Chambers IV, E. (2006). Sensory characteristics of combinations of chemicals potentially associated with beany aroma in foods. *Journal of Sensory Studies*, 21(3), 308–321. <https://doi.org/10.1111/j.1745-459X.2006.00067.x>
- Boye, J. I., Aksay, S., Roufik, S., Ribéreau, S., Mondor, M., Farnworth, E., & Rajamohamed, S. H. (2010). Comparison of the functional properties of pea, chickpea and lentil protein concentrates processed using ultrafiltration and isoelectric precipitation techniques. *Food Research International*, 43(2), 537–546. <https://doi.org/10.1016/j.foodres.2009.07.021>
- Bustos, M. C., Rocha-Parra, D., Sampedro, I., De Pascual-Teresa, S., & León, A. E. (2018). The influence of different air-drying conditions on bioactive compounds and antioxidant activity of berries. *Journal of Agricultural and Food Chemistry*, 66(11), 2714–2723. <https://doi.org/10.1021/acs.jafc.7b05395>
- Cao, N., Fu, Y., & He, J. (2007). Preparation and physical properties of soy protein isolate and gelatin composite films. *Food Hydrocolloids*, 21(7), 1153–1162. <https://doi.org/10.1016/j.foodhyd.2006.09.001>

- Chéreau, D., Videcoq, P., Ruffieux, C., Pichon, L., Motte, J. C., Belaid, S., Ventureira, J., & Lopez, M. (2016). Combination of existing and alternative technologies to promote oilseeds and pulses proteins in food applications. *OCL - Oilseeds and Fats, Crops and Lipids*, 41(1). <https://doi.org/10.1051/ocl/2016020>
- Chevalier, F., Chobert, J. M., Dalgalarondo, M., Choiset, Y., & Haertlé, T. (2002). Maillard glycation of β -lactoglobulin induces conformation changes. *Nahrung - Food*, 46(2), 58–63. [https://doi.org/10.1002/1521-3803\(20020301\)46:2<58::AID-FOOD58>3.0.CO;2-Y](https://doi.org/10.1002/1521-3803(20020301)46:2<58::AID-FOOD58>3.0.CO;2-Y)
- de Oliveira, F. C., Coimbra, J. S. dos R., de Oliveira, E. B., Zuñiga, A. D. G., & Rojas, E. E. G. (2016). Food protein-polysaccharide conjugates obtained via the Maillard reaction: A review. *Critical Reviews in Food Science and Nutrition*, 56, 1108–1125. <https://doi.org/10.1080/10408398.2012.755669>
- Delgado-Andrade, C., Morales, F. J., Seiquer, I., & Pilar Navarro, M. (2010). Maillard reaction products profile and intake from Spanish typical dishes. *Food Research International*, 43(5), 1304–1311. <https://doi.org/10.1016/j.foodres.2010.03.018>
- Gao, Z., Shen, P., Lan, Y., Cui, L., Ohm, J. B., Chen, B., & Rao, J. (2020). Effect of alkaline extraction pH on structure properties, solubility, and beany flavor of yellow pea protein isolate. *Food Research International*, 131, 109045. <https://doi.org/10.1016/j.foodres.2020.109045>
- González-Pérez, S., & Arellano, J. B. (2009). Vegetable protein isolates. In *Handbook of Hydrocolloids: Second Edition* (383–419). <https://doi.org/10.1533/9781845695873.383>
- Hattori, M., Nagasawa, K., Ametani, A., Kaminogawa, S., & Takahashi, K. (1994). Functional changes in β -lactoglobulin by conjugation with carboxymethyl dextran. *Journal of Agricultural and Food Chemistry*, 42(10), 2120–2125. <https://doi.org/10.1021/jf00046a009>

- Jiménez-Castaño, L., Villamiel, M., & López-Fandiño, R. (2007). Glycosylation of individual whey proteins by Maillard reaction using dextran of different molecular mass. *Food Hydrocolloids*, 21(3), 433–443. <https://doi.org/10.1016/j.foodhyd.2006.05.006>
- John, C. (2010). Flavor-base 2001 (Demo) [DB]. *Leffingwell & Associates*. Retrieved from <http://www.leffingwell.com/download/olfaction2.pdf>
- Kester, J. J., & Richardson, T. (1984). Modification of whey proteins to improve functionality. *Journal of Dairy Science*, 67(11), 2757–2774. [https://doi.org/10.3168/jds.S0022-0302\(84\)81633-1](https://doi.org/10.3168/jds.S0022-0302(84)81633-1)
- Klupšaitė, D., & Juodeikienė, G. (2015). Legume: composition, protein extraction and functional properties. A review. *Chemical Technology*, 66(1). <https://doi.org/10.5755/j01.ct.66.1.12355>
- Kobayashi, A., Tsuda, Y., Hirata, N., Kubota, K., & Kitamura, K. (1995). Aroma constituents of soybean [*Glycine max* (L.) Merrill] milk lacking lipoxygenase isozymes. *Journal of Agricultural and Food Chemistry*, 43(9), 2449–2452. <https://doi.org/10.1021/jf00057a025>
- Lam, A. C. Y., Can Karaca, A., Tyler, R. T., & Nickerson, M. T. (2018). Pea protein isolates: Structure, extraction, and functionality. *Food Reviews International*, 34, 126–147. <https://doi.org/10.1080/87559129.2016.1242135>
- Laroque, D., Inisan, C., Berger, C., Vouland, É., Dufossé, L., & Guérard, F. (2008). Kinetic study on the Maillard reaction. Consideration of sugar reactivity. *Food Chemistry*, 111(4), 1032–1042. <https://doi.org/10.1016/J.FOODCHEM.2008.05.033>
- Liu, G., & Zhong, Q. (2013). Thermal aggregation properties of whey protein glycosylated with various saccharides. *Food Hydrocolloids*, 32(1), 87–96. <https://doi.org/10.1016/j.foodhyd.2012.12.008>

- Mession, J. L., Sok, N., Assifaoui, A., & Saurel, R. (2013). Thermal denaturation of pea globulins (*Pisum sativum* L.) - Molecular interactions leading to heat-induced protein aggregation. *Journal of Agricultural and Food Chemistry*, *61*(6), 1196–1204.
<https://doi.org/10.1021/jf303739n>
- Mohammadinejad, R., Shavandi, A., Raie, D. S., Sangeetha, J., Soleimani, M., Hajibehzad, S.S., Thangadurai, D., Hospet, R., Popoola, J. O., Arzani, A., & Gómez-Lim, M.A. (2019). Plant molecular farming: Production of metallic nanoparticles and therapeutic proteins using green factories. *Green Chemistry*. <https://doi.org/10.1039/c9gc00335e>
- Murthy, N. V. K. K., & Rao, M. S. N. (1984). Acid denaturation of mustard 12S protein. *International Journal of Peptide and Protein Research*, *23*(1), 94–103.
<https://doi.org/10.1111/j.1399-3011.1984.tb02697.x>
- Naranjo, G. B., Gonzales, A. S. P., Leiva, G. E., & Malec, L. S. (2013). The kinetics of Maillard reaction in lactose-hydrolysed milk powder and related systems containing carbohydrate mixtures. *Food Chemistry*, *141*(4), 3790–3795.
<https://doi.org/10.1016/j.foodchem.2013.06.093>
- Oliver, C. M., Melton, L. D., & Stanley, R. A. (2006). Creating proteins with novel functionality via the maillard reaction: A review. *Critical Reviews in Food Science and Nutrition*, *46*(4), 337–350. <https://doi.org/10.1080/10408690590957250>
- Pirestani, S., Nasirpour, A., Keramat, J., Desobry, S., & Jasniewski, J. (2018). Structural properties of canola protein isolate-gum Arabic Maillard conjugate in an aqueous model system. *Food Hydrocolloids*, *79*, 228–234.
<https://doi.org/10.1016/j.foodhyd.2018.01.001>
- Rackis, J. J., Sessa, D. J., & Honig, D. H. (1979). Flavor problems of vegetable food proteins. *Journal of the American Oil Chemists' Society*, *56*(3), 262–271.
<https://doi.org/10.1007/BF02671470>

- Samoto, M., Miyazaki, C., Kanamori, J., Akasaka, T., & Kawamura, Y. (2005). Improvement of the off-flavor of soy protein isolate by removing oil-body associated proteins and polar lipids. *Bioscience, Biotechnology, and Biochemistry*, 62(5), 935–940.
<https://doi.org/10.1271/bbb.62.935>
- Schwenke, K. D., & Linow, K. J. (1982). A reversible dissociation of the 12 S globulin from rapeseed (*Brassica napus* L.) depending on ionic strength. *Food / Nahrung*, 26(1), K5–K6. <https://doi.org/10.1002/food.19820260139>
- Silva, N. H. C. S., Vilela, C., Marrucho, I. M., Freire, C. S. R., Pascoal Neto, C., & Silvestre, A. J. D. (2014). Protein-based materials: From sources to innovative sustainable materials for biomedical applications. *Journal of Materials Chemistry B*, 2(24), 3715–3740. <https://doi.org/10.1039/c4tb00168k>
- Stone, A. K., Karalash, A., Tyler, R. T., Warkentin, T. D., & Nickerson, M. T. (2015). Functional attributes of pea protein isolates prepared using different extraction methods and cultivars. *Food Research International*, 76(P1), 31–38.
<https://doi.org/10.1016/j.foodres.2014.11.017>
- Su, J. F., Huang, Z., Yuan, X. Y., Wang, X. Y., & Li, M. (2010). Structure and properties of carboxymethyl cellulose/soy protein isolate blend edible films crosslinked by Maillard reactions. *Carbohydrate Polymers*, 79(1), 145–153.
<https://doi.org/10.1016/j.carbpol.2009.07.035>
- Szymanowska, U., Jakubczyk, A., Baraniak, B., & Kur, A. (2009). Characterisation of lipoxygenase from pea seeds (*Pisum sativum* var. Telephone L.). *Food Chemistry*, 116(4), 906–910. <https://doi.org/10.1016/j.foodchem.2009.03.045>
- Tandang-Silvas, M. R. G., Tecson-Mendoza, E. M., Mikami, B., Utsumi, S., & Maruyama, N. (2011). Molecular design of seed storage proteins for enhanced food physicochemical

properties. *Annual Review of Food Science and Technology*, 2(1), 59–73.

<https://doi.org/10.1146/annurev-food-022510-133718>

Yin, S. W., Tang, C. H., Wen, Q. B., Yang, X. Q., & Yuan, D. B. (2010). The relationships between physicochemical properties and conformational features of succinylated and acetylated kidney bean (*Phaseolus vulgaris* L.) protein isolates. *Food Research International*, 43(3), 730–738. <https://doi.org/10.1016/j.foodres.2009.11.007>

Yue, H. B., Cui, Y. D., Shuttleworth, P. S., & Clark, J. H. (2012). Preparation and characterisation of bioplastics made from cottonseed protein. *Green Chemistry*, 14(7), 2009–2016. <https://doi.org/10.1039/c2gc35509d>

Zha, F., Dong, S., Rao, J., & Chen, B. (2019a). Pea protein isolate-gum Arabic Maillard conjugates improves physical and oxidative stability of oil-in-water emulsions. *Food Chemistry*, 285, 130–138. <https://doi.org/10.1016/j.foodchem.2019.01.151>

Zha, F., Dong, S., Rao, J., & Chen, B. (2019b). The structural modification of pea protein concentrate with gum Arabic by controlled Maillard reaction enhances its functional properties and flavor attributes. *Food Hydrocolloids*, 92, 30–40. <https://doi.org/10.1016/j.foodhyd.2019.01.046>

Zha, F., Yang, Z., Rao, J., & Chen, B. (2019). Gum Arabic-mediated synthesis of glyco-pea protein hydrolysate via Maillard reaction improves solubility, flavor profile, and functionality of plant protein. *Journal of Agricultural and Food Chemistry*, 67(36), 10195–10206. <https://doi.org/10.1021/acs.jafc.9b04099>

Zhu, D., Damodaran, S., & Lucey, J. A. (2010). Physicochemical and emulsifying properties of whey protein isolate (WPI)–dextran conjugates produced in aqueous solution. *Journal of Agricultural and Food Chemistry*, 58(5), 2988–2994. <https://doi.org/10.1021/jf903643p>

7. OVERALL SUMMARY AND CONCLUSION

7.1. Conclusions

Glycation via Maillard-driven chemistry has turned out to be a potential eco-friendly method to assemble value-added protein derivatives, expanding their application as functional materials. Conjugates were assembled by glycating with PPI, PPC, or PPH with gum Arabic via Maillard mediated reaction at a ratio of 1:4 (protein/GA, w/w) under dry heating conditions (60°C, 79% relative humidity, pH 7.0). The resulting conjugates were characterized by SDS-PAGE, FTIR-ATR and SEM. The absorbance of non-specific Maillard reaction markers in the protein-GA conjugates that measured at 304 nm and 420 nm, visual color development, and the available free amino groups can be used to determine the degree of conjugation and control the reaction. The solubility at a neutral pH was improved for PPI from 10.1% to 15.5% after 1 day incubation, for PPC from 29.2% to 40.9% after 3 day incubation, and for PPH from 19.4% to 26.2% after 1 day incubation, respectively. The physical stabilities of corn oil-in-water emulsions stabilized by protein-GA conjugates against environmental stresses were enhanced, particularly at a pH close to IEP, which can be attributed to the increased electrostatic repulsions and/or steric hindrance effects. Emulsions stabilized by these conjugates also exhibited superior chemical stability against lipid oxidation. The characteristic Strecker degradation products, including aldehyde and pyrazines aromatic components, were identified in glyco-PPC and glyco-PPH via HS-SPME-GC-MS. Glycation of pea protein with gum Arabic presented a remarkable beany flavor mitigation effect.

SEC-MALLS indicated that approximately 1.2 mol of GA was covalently linked to 1 mol of PPH after 1 day of conjugation under dry heating conditions. SEC-HPLC revealed that the number of glucose, lactose, maltodextrin DE5, DE10, and DE18 grafting to 1 mole of PPI in an aqueous system (80°C, pH 10.0), was approximately 4.5, 3.7, 2.1, 2.3, and 2.8, respectively. The solubility of glyco-PPI was sufficiently improved after glycation, with a

maximum elevation be observed from maltodextrin DE18-mediated glycation. However, thermal stability of PPI was lowered after glycation in such aqueous systems. These outcomes could provide valuable in-depth information for tailoring the functions of glycoproteins via Maillard-driven chemistry between protein and saccharides.

7.2. Future Research

Whereas the functionality of pea protein was proved to be improved after glycating with saccharides in this research, the fundamental mechanisms on how Maillard-driven chemistry modifies the protein architectures have yet to be addressed. In the future, several relevant topics are worth exploiting: i) how does pea protein subunit impact/participate in Maillard-driven glycation. This can be addressed by isolating protein subunits, like 11S or 7S globulin, which are then applied to glycate with saccharides, with the binding sites being characterized by ESI-TOF-MS; ii) elucidating the Maillard reaction site on protein by purifying the resulting products. Isolation and purification of Maillard-driven conjugates can be achieved by dialysis coupling with HPLC based on the molecular mass of conjugates; iii) exploiting novel and emerging strategies by coupling glycation with other physical means such as high pressure and extrusion to modify protein functions; iv) producing innovative sustainable adhesive depend on protein gelling and filming via Maillard-driven chemistry; and v) the nutritional profile of resultant conjugates generated via glycation should be assessed. This can be achieved by conducting animal experiments to evaluate its safety, and antioxidant activity, and digestibility.